



DESIGN OF A FRONT AERODYNAMIC PACKAGE

Final Design Report

Team Members (Team 20 – KHAB Design & Engineering):

Nishant Balakrishnan

Mohamed Alnouri

Mohammad Heiranian

Waldemar Koos

Sponsored By UMSAE | Advisor: Dr. Paul Labossiere

Submission Date: December 5, 2011

2011-12-05

Professor P. E. Labossiere
Department of Mechanical Engineering
Faculty of Engineering
University of Manitoba
Winnipeg, Manitoba
R3T 2N2

Dear Professor Labossiere,

Please find attached our final design report titled "*Design of a Front Aerodynamic Package.*" The report was submitted on December 5, 2011 by Team 20 of Section A01 of the MECH 4860 course. Team 20 consists of Nishant Balakrishnan, Mohamed Alnouri, Mohammad Heiranian, and Waldemar Koos.

The purpose of the report is to present the final design of an active aerodynamic system developed for the UMSAE Electric vehicle, aimed at being implemented for the 2012 SAE Design Competition.

The report includes a detailed presentation of the design, highlighting the key features of the design as well as an overall cost analysis. The team demonstrates how the proposed design meets the client's needs, by describing the mode of operation of the design and its intended effect on the performance of the UMSAE Electric vehicle. In conclusion, the report presents the final design for further development into a working prototype.

Sincerely,

Waldemar Koos
Team 20 Leader

Enclosure

Abstract

Aerodynamic devices are utilized in higher levels of motorsport such as Formula-1 to increase the traction of the tires by generating down force. This increase in traction increases the performance envelope of the race car since cornering can be performed at higher speeds without a loss of control. However, the aerodynamic device that provides the down force also increases drag. The additional drag is especially detrimental on straight sections of the track. As higher speeds are attained, the increased drag leads to a decrease in lap-times and the drive force required is increased. An ideal solution is a dynamically adjustable aerodynamic device which offers the ability to change the relative amount of down force and drag. Such devices have been used in many forms of motorsport in the past.

The **Society of Automotive Engineers (SAE)** Collegiate Design Series is an engineering competition wherein university students compete in the design, building and racing of an open-wheel race car. The Formula Electric team has requested a design of an adjustable aerodynamic device. The device is to be mounted to the front of the vehicle such that the wing mount is integrated into the carbon fibre monocoque. Furthermore, the nose cone is to be designed such that there is absolutely no lift experienced by it. The dimensions of the vehicle were provided. The goal of the design is to decrease the team's lap times during the autocross event at the SAE competition.

In this report, the details of the design are presented. When the car is on a straight away, the device positions itself such that it has minimal detrimental aerodynamic effect, as requested by the client. During cornering, the functional position is assumed, which creates down force. The variable down force is accomplished by an active wing section that was optimized to create as much down force as possible given that the car would be banking a turn at approximately 50 km/h. In addition to the active wing, another wing section is fixed in close proximity to the ground. The bottom wing accomplishes several tasks. Firstly, it is used as a structural member supporting the endplates to which the active wing is mounted. Secondly, it houses the actuators and microcontroller responsible for the adjustment of the active wing.

The developed design was used in a simulation of the current SAE Electric race car. At a representative speed of 50 km/h, the use of the active front wing was found to improve steady state cornering by 6% to 1.89g (active wing @ 13°). Alternatively, the car's straight-line braking could be improved by 8% to 2.04g (active wing @ 28°). With the wing in the low-drag position (active wing @ +6°), the additional power requirement is only 19.45W.



Nomenclature

AoA, α	angle of attack relative to chord line
C_D	airfoil drag coefficient for finite wing
C_{D0}	airfoil drag coefficient for infinite wing
C_{Di}	airfoil induced drag coefficient
C_{D90}	drag coefficient at 90° AoA
C_l	airfoil lift coefficient for infinite wing
$C_{l,max}$	airfoil maximum lift coefficient for infinite wing
$C_{m,c/4}$	airfoil pitching-moment coefficient about the quarter-chord point for infinite wing
c	airfoil chord which extends from the leading to the trailing edge
CFD	computational fluid dynamics
CG	centre of gravity
DAQ	data acquisition system
PLU	programmable logic unit
PMW	pulse width modulation
SAE	Society of Automotive Engineers
UMSAE	University of Manitoba Society of Automotive Engineers
V	free stream velocity
x	airfoil x coordinate



Table of Contents

1	Introduction	1
1.1	Problem Description	1
1.1.1	Background	2
1.1.2	Customer Needs.....	2
1.1.3	Target Specifications	4
1.2	Project Objectives	5
2	Details of the Design	6
2.1	Analysis Methodology and Assumptions	8
2.2	Aerodynamic Features	9
2.2.1	Nose Cone	11
2.2.2	Motor Cowling	16
2.2.3	Airfoil Selection	18
2.2.4	Wing Shape	21
2.2.5	Drag Characteristics	25
2.2.6	Operation	26
2.2.7	Summary	29
2.3	Airfoil Actuation System	31
2.3.1	Design and Analysis of Actuation Mechanism	37
2.3.2	Summary	45



2.4	Control System.....	46
2.4.1	Design and Analysis of Control System	47
2.4.2	Operation and Components of the Control System	50
2.4.3	Summary	57
3	Conclusion.....	59
4	References	61
5	Appendix	64



List of Figures

Figure 1. 2012 Formula Electric– No Aero Package vs. Aero Package (bottom)	10
Figure 2. 2012 Formula Electric– Standard Nose cone vs. Nose cone Redesign	11
Figure 3. 2012 Formula Electric– Standard Nose cone vs. Nose cone Redesign	12
Figure 4. Velocities across Current Nose Cone Design.....	13
Figure 5. Velocities across New Nose Cone Design.....	14
Figure 6. Velocities across Nose Cone with the Fixed Symmetric Airfoil.....	15
Figure 7. Velocities across New Nose Cone Design.....	15
Figure 8. 2012 Formula Electric – No Cowling vs Cowling, Separated From Chassis.....	17
Figure 9. S1223 (11.93%) for high Lift at slow Flight.....	20
Figure 10. Symmetric Airfoil, As Used in Design	20
Figure 11. Typical Wing Shapes.....	21
Figure 12. Volumetric Design Boundary	22
Figure 13. Aerodynamic requirements when cornering on the SAE Autocross Circuit.	27
Figure 14. Flow Trajectories Velocity Plot in Low Drag Configuration	27
Figure 15. Flow Trajectories Velocity Plot in Airbrake Configuration.....	28
Figure 16. Flow Trajectories Velocity Plot in Maximum Down Force Configuration	29
Figure 17. Vehicle Velocity vs Down Force / Drag.	31
Figure 18. Four-Bar Linkage Setup on Movable Wing.	32
Figure 19. Active Airfoil Positioning – Cornering Configuration.	33
Figure 20. Active Airfoil Positioning – Straight Line Configuration.	34
Figure 21. Active Airfoil Positioning – Air-Brake Configuration.	35
Figure 22.Torxis i00600 servo-motor.....	36
Figure 23. The actuated four-bar linkage and its main components.....	38



Figure 24. Vector representation of the four-bar linkage.	39
Figure 25. The plot of rocker angle vs input angle.....	40
Figure 26. The plot of coupler angle vs. input angle.....	41
Figure 27. The required torque for different velocities and crank angles.....	43
Figure 28. The amount of down force for different velocities and crank angles.	44
Figure 29. The amount of drag for different velocities and crank angles.....	44
Figure 30. Overall Control Layout for Active Aerodynamic Control	46
Figure 31. Logical Flow – Active Aerodynamic Controller	47
Figure 32. Chosen Control System Topology	48
Figure 33. Updated System Layout – Black Box Motor Controller	51
Figure 34. Parker PK3 Stepper Motor Drive – 6.5”x7.0”x3.0”	52
Figure 35. Attachment points for the feedback system.	53
Figure 36. Non-Linear Transfer Function for Feedback Element.....	54
Figure 37. Updated System Layout – Feedback System	55
Figure 38. System Operation Flow Chart – Arduino Uno.....	56
Figure 39. Finalized Overall System Layout	58



List of Tables

TABLE I: CUSTOMER NEEDS.....	3
TABLE II: TARGET SPECIFICATIONS	4
TABLE III: OPTIONS FOR SUITABLE AIRFOIL.....	19
TABLE IV: PERFORMANCE CHARACTERISTICS OF AIRFOILS TYPICALLY USED FOR SLOW FLYING UAV....	19
TABLE V: MAXIMUM ALLOWABLE DIMENSIONS FOR FRONT AERODYNAMIC PACKAGE (PER SIDE).	22
TABLE VI: PROPOSED DIMENSIONS OF FRONT WINGS AND END PLATE (PER SIDE).	23
TABLE VII: SUMMARY OF DOWN FORCE AND DRAG GENERATED AT 50 KM/H.....	30
TABLE VIII: LENGTHS OF LINKS AND LOCATIONS OF FIXED JOINTS.	38
TABLE IX: SUMMARY OF POSITION AND FORCE ANALYSIS FOR THE FOUR-BAR MECHANISM.	45



1 Introduction

The following final design report outlines a proposed adjustable front wing that can be implemented on the **University of Manitoba Society of Automotive Engineers (UMSAE)** 2012 Formula Electric race car. The Formula Electric team has asked for a design with the objective of providing down force applied to the front of the vehicle to increase the overall track performance of their vehicle. The report includes a detailed description of the chosen design, as well as the methodology used to develop a solution that meets the constraints of Formula Electric as well as the **Society of Automotive Engineers (SAE)** Collegiate Design Series. A recommendation on how the adjustable device should be implemented into the current vehicle configuration is included, along with relevant manufacturing principles.

1.1 Problem Description

The goal of both the Formula Hybrid and the Formula Electric design competition is to produce a car that is designed for performance. The natural progression of the design is to make the car both light and powerful by optimizing the mechanical and structural efficiency of all aspects of the vehicle. This type of design development leads to a contradiction in that a lightweight vehicle is limited in its cornering ability by the weight over wheels, and cannot utilize an increase in power if the traction limits are exceeded.

To mitigate these problems, teams turn to aerodynamic features to produce down force as well as to minimize the aerodynamic drag on the car. For the 2012 competition, KHAB Engineering & Design has been contracted to produce a front aerodynamic package for the UMSAE Electric team, to be compatible with the 2012 Formula Electric vehicle. The overall objective is to provide a detailed design of a front aerodynamic package for the 2012 Formula Electric Vehicle that improves the overall performance of the vehicle and meets the needs of the UMSAE Electric team.



1.1.1 Background

Since its foundation in 2009, the Formula Electric team has utilized aerodynamic systems on its vehicles to improve the weight distribution of the car during the dynamic events. To date, the systems have always consisted of a single fixed wing placed at both the front and the rear.

For the upcoming SAE design competition, the Formula Electric Team has adopted a carbon fibre monocoque chassis from the UMSAE Formula team. This chassis was developed by the UMSAE Formula team during the previous season. Adopting a proven design presented a considerable means of saving both time and resources, since tooling and materials were already on hand to manufacture the chassis. The Formula Electric team could therefore focus its efforts on optimizing the existing design and make the necessary alterations to accommodate its electric drive train. The chassis had initially been designed in conjunction with a complete aerodynamic package. However, due to unforeseen resource limitations, the aerodynamic package was never implemented in its entirety.

As part of the design optimization, the UMSAE Electric team plans to implement an aerodynamic system which provides superior aerodynamic performance compared to the aerodynamic package that was designed in conjunction with the composite chassis. In the pursuit of the most efficient use of their resources, the UMSAE Electric team has decided to outsource the design of the adjustable aerodynamic system. The system is to be mounted at the front of the vehicle and aimed at providing selected amounts of down force during specified dynamic conditions, such as cornering, braking, and straight-line acceleration.

1.1.2 Customer Needs

The UMSAE Formula Electric team would like to increase the cornering ability of their vehicle. Specifically, the team intends to accomplish this performance increase by gaining additional traction on the vehicle's tires through the use of an active front wing. While providing a significant amount of down force during cornering, the device must not have an adverse effect on straight-line performance.



Considering that UMSAE is a student group which designs, manufactures, and assembles their race car in a shop provided by the Faculty of Engineering, the design should be implementable within the resources available to UMSAE. For repair, inspection, and evaluation purposes the design should facilitate access to interchangeable components and be easy to detach and replace as a whole.

TABLE I: CUSTOMER NEEDS [1]

Category	Need	Priority
<i>I. Aerodynamic Performance</i>		
A	provides significant down force during cornering	high
B	has no adverse effect on straight-line performance	high
C	improves cornering performance	medium
<i>II. Manufacturability</i>		
A	is light	high
B	is easy to manufacture	medium
C	can be mounted to the nose cone	low
<i>III. Assembly</i>		
A	provides ready access to interchangeable components	medium
B	is easily detached and replaced	medium
<i>IV. Structural Requirements</i>		
A	Is capable of impacting cones without damage	high
B	is not damaged by suspension movement	high
C	withstands repeated abrasion against the road surface	medium
D	is rigid	medium
<i>V. Functionality</i>		
A	can be set to the maximum down force created	high
B	can be manually locked in position	high

In order to provide several modes of operation and make the system more versatile, any active components should provide the option to lock the part into one of numerous positions. The



positions can then be selected prior to competing in an event at competition, should a malfunction with the control system or actuation mechanism occur. A condensed list of the client's needs is provided in TABLE I.

1.1.3 Target Specifications

The following specifications were developed in cooperation with the client. The importance of a given specification is equal to that of the corresponding need, which can be obtained from the relevant category in TABLE II.

TABLE II: TARGET SPECIFICATIONS [2]

Category	Specification
I. Aerodynamic Performance	A Provides a minimum of 100 N of down force at 50 km/h. B Provides a maximum straight line drag less than the 2011 wing. C Increases the lateral acceleration by 0.1 g.
II. Manufacturability	A Is lighter than 5.0 kg. B Will have an estimated build time of 2 months. C Can be mounted to the nose cone.
III. Assembly	A Is replaceable/modifiable by field replacement and modification must be possible using hand tools. B Is capable of removal within 10 minutes of normal work.
IV. Structural Requirements	A Provides performance without permanent deformation. B Has a ground clearance of the suspension travel as well as design deflection. C Is able to withstand abrasion against the ground without damage to other design components. D Has a maximum vertical deflection lower than the total ground clearance of the design.
V. Functionality	A Provides adjustable down force. B Can be locked into a position capable of holding the down force.



1.2 Project Objectives

The overall objectives stem from the preceding needs and corresponding specifications. The objectives of the design project are to employ an open ended approach to solving the problem given by the client and to develop a design that meets the customer's needs as well as possible. The client requires a design that complies with their overall mission, namely the design of a light, high performance race car. Specifically, the design should improve the overall cornering performance of the vehicle.

The customer's needs translate to a specific objective of designing a front aerodynamic system compatible with the chassis of the 2012 competition vehicle. The aerodynamic features of this system must be able to provide variable amounts of down force, with the purpose of minimizing the effects of drag. Moreover, the package must be designed to be light, rigid, and rugged. The plan is to have the UMSAE Electric team present the design at the 2012 Formula Electric Competition. It should therefore be able to withstand the rigours of the competition environment.

From the client's requests, latent objectives were determined which would add value to the final product. However, these requests are not critical. The ability of the device to function as an air-brake that slows the car down, to provide varying degrees of static down force, and to provide lift on the straight sections of track to minimize the rolling resistance of the car are latent objectives.



2 Details of the Design

The primary intention of race car aerodynamics is to generate a desired intensity of down force for the least possible amount of drag. Nonetheless, the balance of the forces under all circumstances due to speed and acceleration is equally important. The modeling was performed using SolidWorks [3] and the analysis was done both analytically and by means of **computational fluid dynamics (CFD)** using a flow simulation integrated with SolidWorks.

An overall system layout was developed for the aerodynamic package. The overall layout has been refined by the evaluation and scoring of each individual component, leading to a design that meets all of the client's needs on a subsystem level. Further details on the concept evaluation and scoring can be found in the appendix.

The method of generating down force was chosen to be a standard airfoil type wing. A linkage was added such that the wing is actuatable. The actuation is further extended by the idea of "path motion" where the wing can undergo rigid-body curvilinear motion, allowing the wing to not only rotate, but also translate under the actuation motion.

The individual links form a four-bar linkage, such that a rotary input causes the driving link to move in curvilinear motion. The differences between the individual link lengths, known as the motion ratio, allows the design to have a variable path which can be determined in the detailed design phase such that the design can be optimized for performance. The airfoil profile was chosen such that the design provides the target specification of lift, and also minimizes the drag on the design. In order to optimize the airfoil design, numerical methods were implemented in the detailed design phase. In addition, a digital control system was implemented to control this design.

The digital control system design that was chosen through the concept development process was a control system that utilized vehicle dynamics to control the wing actuation. The use of vehicle dynamics is easily possible through the **data acquisition system (DAQ)** on the 2011/2012 Formula Electric vehicle. The DAQ monitors the acceleration, braking, cornering forces, and dynamic loading on the vehicle. This data can be used in conjunction with a digital



controller, such as the 32-bit ATMEL AVR. A controller such as the ATMEL AVR is sophisticated enough to decode the DAQ outputs, but can also be programmed with logic that is simple enough that the overall complexity of such a system is reasonable to implement. The proposed control scheme is to use the vehicle dynamics to respond to major driver inputs, such as steering, acceleration, and braking, and supplement a driver actuated down force reduction. Thereby, a system wherein the driver can press a button on the straight sections of the track, which reduces the down force produced by the wing and provides an increase in straight line performance, is achieved. This system is supplemented by automatic control in situations of extreme acceleration and significant braking, whereby the wing would actuate to provide more/less down force in accordance with a preset control scheme. This control system is to be used with an actuation system, where the overall position of the front wing can be controlled through the use of an electric motor.

The electric motor actuation system was designed to actuate the path motion wing design and is capable of providing the required rotary input to move the wing along its predetermined path. The system offers proportional control, whereby the position of the wing can be shifted along a specific path with high accuracy. The motion control aspect was tested experimentally via physical prototyping as well as numerically via MATLAB [4] and SolidWorks motion analysis to optimize the path dependant control parameters of the system. This type of analysis allows the client to dictate the specific power and motion profile curves for the actuator, and allow a great degree of actuation flexibility.

The formal design represents a somewhat radical design for the 2012 Formula Electric Front Aerodynamic Package, but at the same time it also represents a formal design that was designed with the needs and capabilities of the team kept in mind. Although the design is complex, each individual component is simple and within the implementation scope of the client. The following sections cover the overall formal design that is the outcome of the project that KHAB Engineering & Design was contracted to complete for the UMSAE Formula Electric team. The main aspects of the design are the aerodynamic components, airfoil actuation



system, and the control system. The first major components to be presented are the aerodynamic features.

2.1 Analysis Methodology and Assumptions

Several different approaches can be taken in terms of analysis of a given design. Analytical, numerical, and experimental methods each have their advantages and disadvantages. Therefore, the most efficient scenario would be to employ all three of these methods in sequential iteration to guarantee validity of the obtained results while minimizing the cost. Initial hand calculation can be validated by a CFD simulation. However, in order to accurately analyze the performance of the developed design, an experiment should be conducted that accurately reflects the designs field of operation. Experimental analysis of the design was ruled out based on two reasons. Firstly, due to the limited time frame given to complete the design, the large number of tests required to fully evaluate all configurations of the active element and its effect on the rest of the vehicle, were beyond the scope of the project. Secondly and more importantly, neither the facilities nor the vehicle for which the design was intended were available at the time of development. Further study could include experimental work to provide a means of verification and validation of the numerical results presented in this report.

It was necessary to make an assumption regarding the interaction of flows between the wings and the car body, since a full model of the vehicle was not available at the time of the project. Ideally, the aerodynamic characteristic of the complete vehicle would be investigated for wing each setting. Due to the tight design space and the fact that it is placed very close to the rotating wheels will result in flow interaction between the wings and the wheels. This interaction tends to increase the down force generated by the wing if the wing location is chosen appropriately. Additionally, the total drag acting on the vehicle can be decreased by proper channelling of the air flow around the wheels and car body. Finally, the front wing will have significant effects on a potential rear wing. Obviously, all of these variables could not be accounted for within the resources available for this project as the process is very complex. A fully detailed analysis was therefore deemed beyond the scope of this project. To assess the



performance increase due to fitting the Formula Electric vehicle with a front wing, the interaction effects will be neglected.

2.2 Aerodynamic Features

The aerodynamic design is the key element of front wing since it is the most critical factor with respect to achieving the desired performance characteristics of the vehicle. Aerodynamic design is therefore often the first step when an inverse system design is employed to complete a project. Inverse system design describes the methodology whereby one starts with the overall design goals and works backward to determine the component characteristics that accomplish the goals. In this case, the goal was to design an active front wing which is capable of successfully producing 100 N of down force at a speed of 50 km/h while producing the least amount of drag possible. In order to accomplish this goal, the key elements, i.e. airfoil, wing dimensions, and nose cone, were varied parametrically along with other component parameters to accomplish the overall design goal.

The aerodynamic design for the project was done with a combination of numerical analysis and CFD, and was focused on optimizing the design of the front wing and related components to increase cornering ability. The increase in cornering ability can come from two major aspects: an increase in the aerodynamic down force and a decrease in the aerodynamic lift of the vehicle. Shown in Figure 1 is the formal design presented for the 2012 Front Aerodynamic Package. For comparison, the front chassis prior to the aerodynamic package design is also shown in Figure 1. The design, as can be seen from the images, encompasses changes to all of the major aerodynamic components, such as the bottom of the chassis, the nose cone and the front aerodynamic area of the car.

The individual components each provide some form of positive aerodynamic improvement, and the overall solution ultimately provides a high performance platform for the Formula Electric Team. The first of these major components that underwent a redesign was the nose cone which is discussed in the following section.

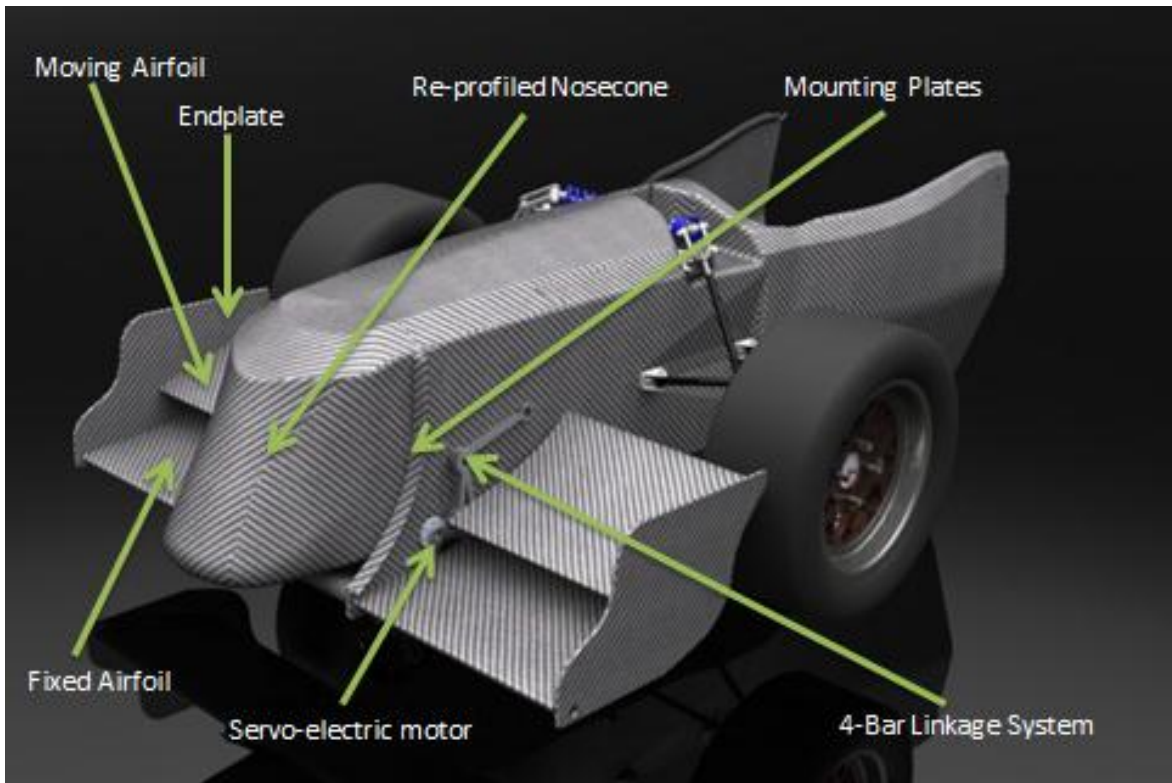
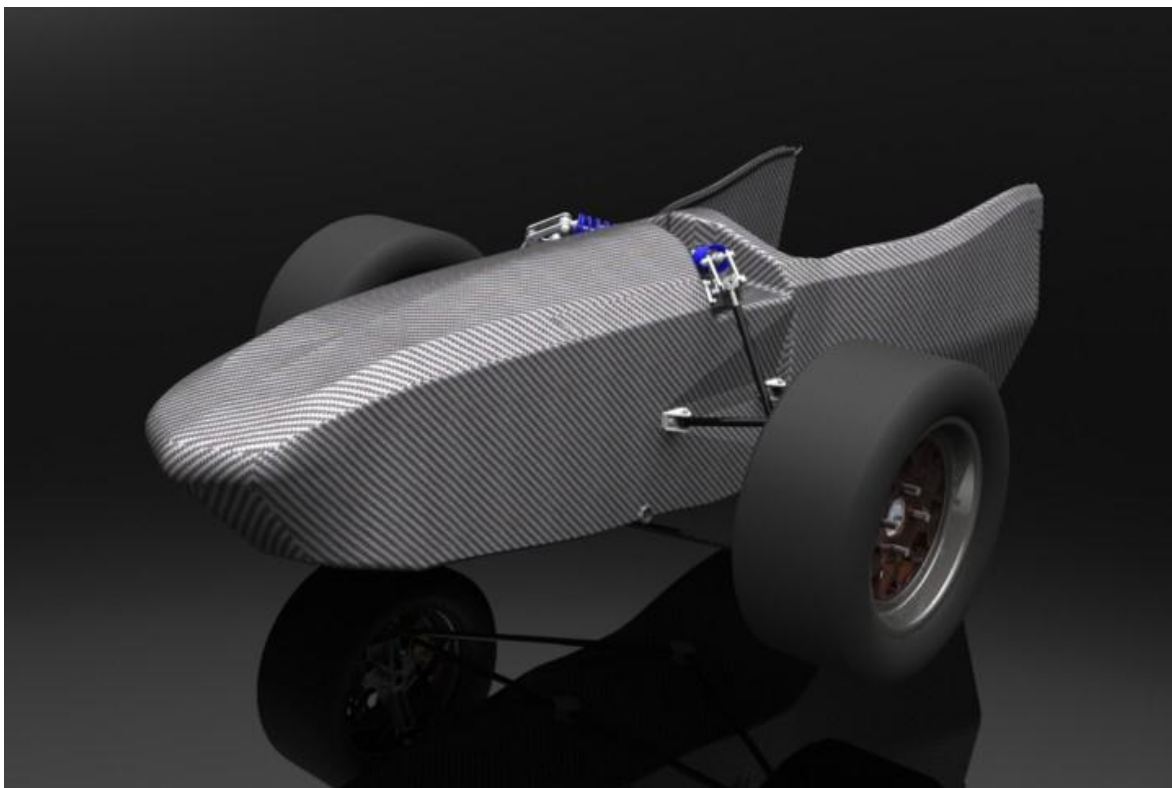


Figure 1. 2012 Formula Electric – No Aero Package (top) vs. 2012 Formula Electric – Aero Package (bottom) [5].



2.2.1 Nose Cone

The existing nose cone for the Formula Electric team was a significant source of aerodynamic issues for the client, primarily due to the aerodynamic lift associated with the design of the nose cone. The production of lift counters the desire for the car to produce down force, and adversely affects the cornering potential of the vehicle. The introduction of lift at low speeds can cause significant decreases in tractive forces during cornering, as well as a decrease in net steering stability in straight line acceleration [6]. Since the overall goal of the design was to increase the amount of available down force, the redesign of the front nose cone was initially considered as a method to increase the net down force by minimizing lift. Shown in the figure below is the current formula electric 2012 nose cone, alongside the proposed redesign.

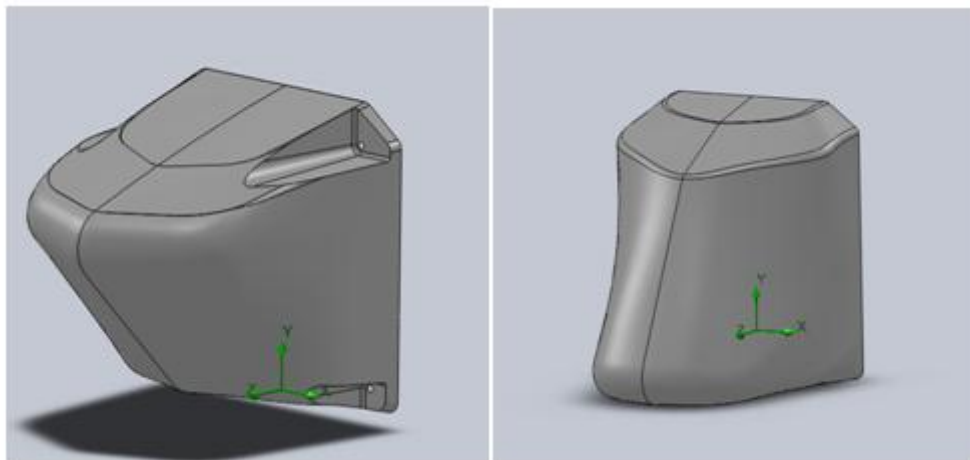


Figure 2. 2012 Formula Electric– Standard Nose cone (left) vs. 2012 Formula Electric – Nose cone Redesign (right) [5].

In order to make a significant improvement on the nose cone's performance, the height of the nose cone was lowered as much as possible. This change had the effect of decreasing the net lift produced by the nose cone, and also prevented some of the high speed stall issues that were noted with the existing design [1]. The difference between the profiles is shown in Figure 3, with the motor cowling also added to the redesigned nose cone. Another aspect of the nose cone redesign was the incorporation of the drop to the overall nose cone profile. Dropping the profile was done to facilitate the mounting of the actuators for the active aerodynamic wing system proposed in this design, and to allow the mounting method to pass the Formula electric



rules [7]. The redesign of the nose cone was performed in conjunction with modifications to the impact attenuator required to meet the Formula Electric rules.

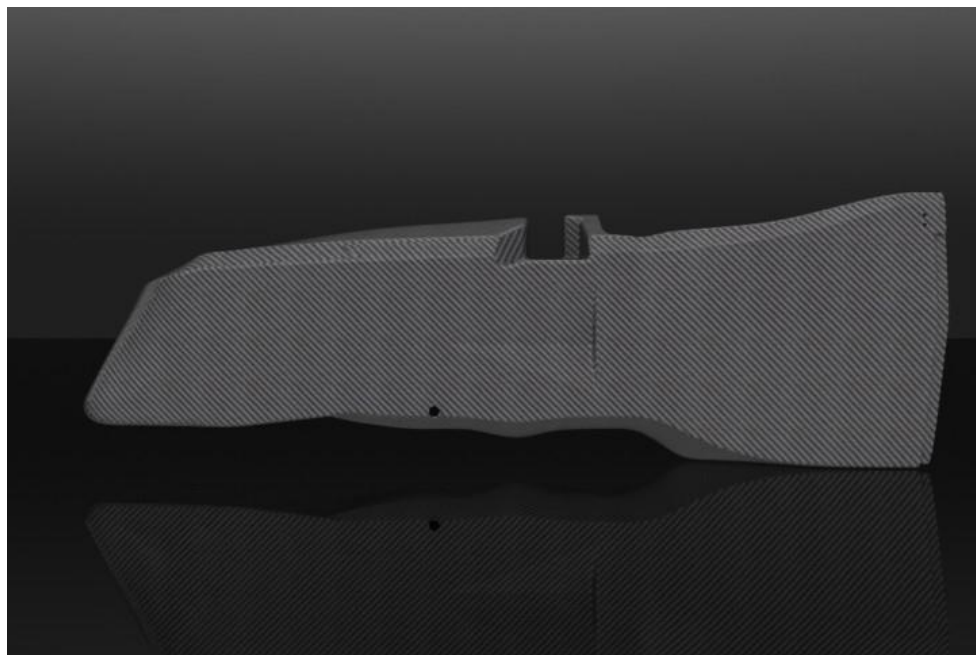
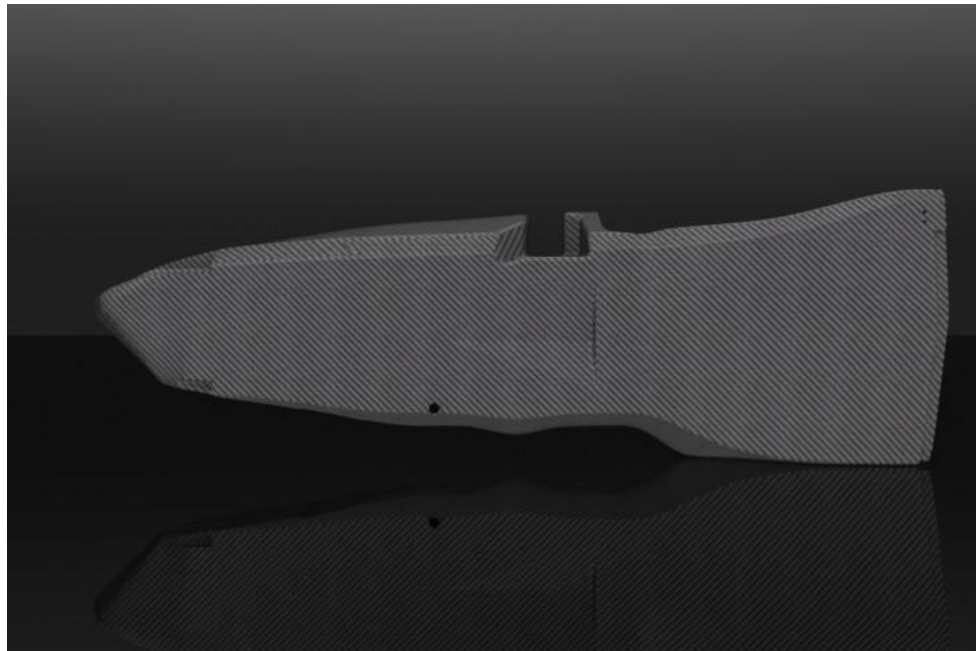


Figure 3. 2012 Formula Electric– Standard Nose cone (top) vs. 2012 Formula Electric – Nose cone Redesign (bottom) [5].



The nose cone is an important aspect to be considered aerodynamically as it is the foremost component of the vehicle. Thus, it has the benefit of dealing with clean undisrupted airflow. This benefit results in a high aerodynamic efficiency, meaning considerable amounts of lift or down force can be produced with minimal shape modifications.

The nose cone for the 2010 Formula vehicle was designed based on aesthetics, and reducing any drag effects. While the nose cone reduced drag, when implemented in the 2010 Formula vehicle, it also introduced lift. The vehicle already had little frontend weight. The imbalance combined with lift forces resulted in an unstable vehicle at high speeds and in low grip when cornering. Additionally, the lift forces counteracted greatly with any down force to be provided by the proposed front wing design. Thus, a new design for the nose cone was considered.

The current side profile of the nose cone is slanted upwards. By intuition, this slant should result in having lift forces. Figure 4 shows the current nose cone design in CFD. The green signifies regions of low velocity, while the yellow signifies regions of high velocity. The green under the nose cone shows a big region with low velocities, while having a high velocity region on top of the nose. Therefore, the difference in dynamic pressure on the nose cone results in lift forces.

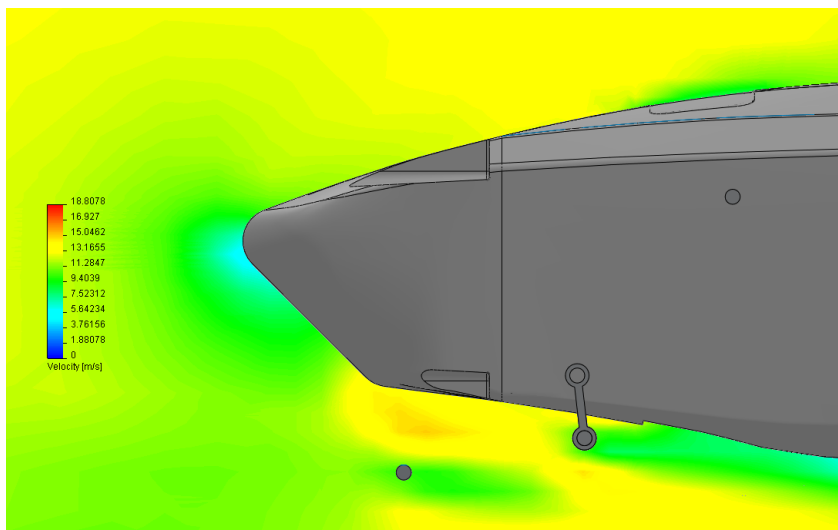


Figure 4. Velocities across Current Nose Cone Design [8].



A nose cone redesign is needed as it would greatly improve the vehicle's stability and handling characteristics. The new design features the same concept of having a pointed profile, but differs in that it is slanted downwards. Figure 5 shows the new nose cone design in CFD. The green region is now transitioned to the top side of the nose cone as a result of the nose cone being slanted downwards. The difference in dynamic pressure results in producing down force on the vehicle's frontend. This down force contributes significantly to the overall effect of the proposed front aerodynamic package. Additionally, the aerodynamic effect of having the motor cowling can be seen in Figure 5.

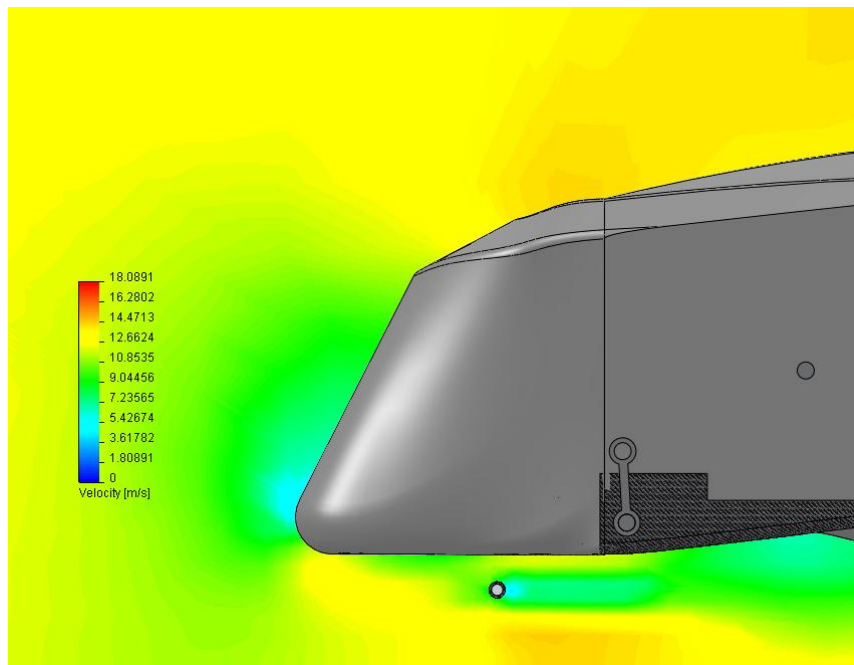


Figure 5. Velocities across New Nose Cone Design [9].

The addition of a fixed airfoil in the middle, covering the connecting rod, is a great use of available space to contribute to the down force produced. Figure 6 shows the velocity plot of the nose cone with the addition of the fixed symmetric wing. A high velocity region is present under the wing, along with a low velocity pressure on top of the wing. The dynamic pressure difference between the top and bottom will result in a considerable amount of down force that would not have been exploited without implementing the symmetric airfoil.

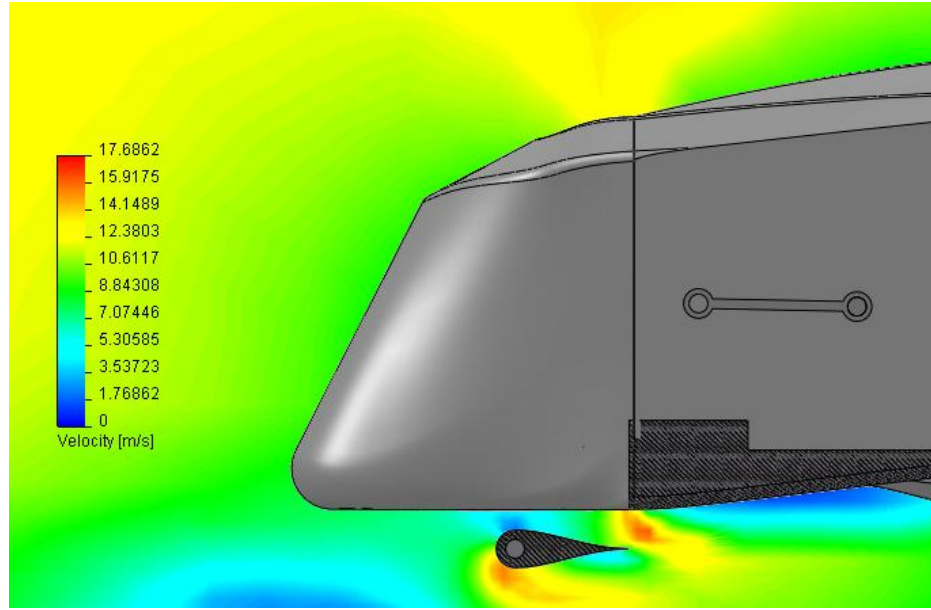


Figure 6. Velocities across Nose Cone with the Fixed Symmetric Airfoil [10].

The addition of the motor cowling is crucial to negate any disruptive airflow. Figure 7 displays the velocity plot without the cowling. The disruptive effects are clearly present. The red coloured regions are widespread indicating the presence of vortices resulting in significant drag forces.

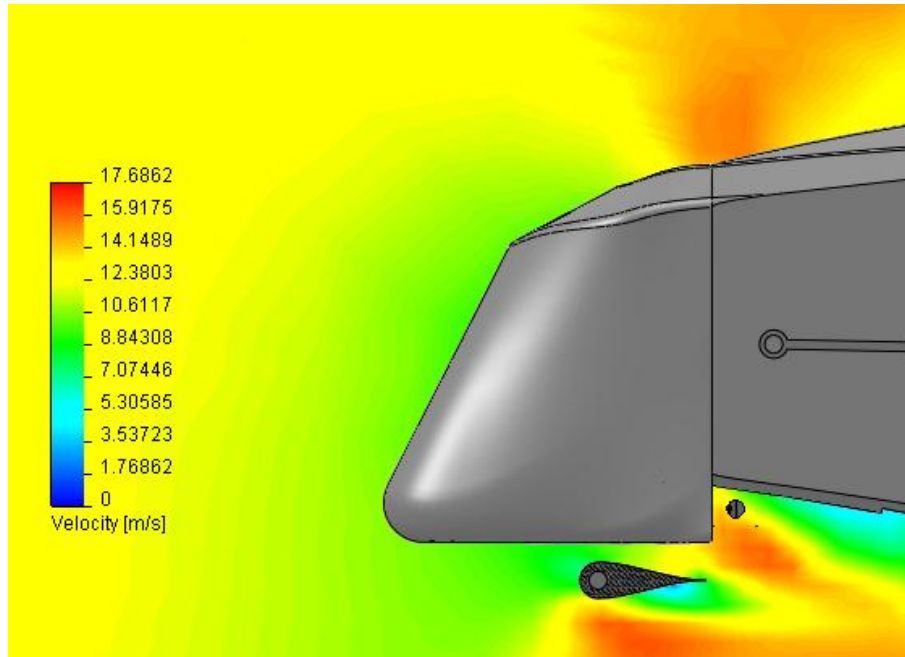


Figure 7. Velocities across New Nose Cone Design [11].



The final aspect of the nose cone design was to facilitate the mounting of the motor cowling. The cowling acts as a shroud for the motors to protect them from road debris and other objects that may damage them, but also acts to flatten the bottom of the chassis of the vehicle. The overall profile difference between the cowling bearing and non-cowling bearing chassis is significant, and provides a further increase in overall aerodynamic performance. However, to determine the specific performance increase, the entire chassis should be studied in a wind tunnel. Such experimentation, as previously mentioned, is beyond the scope of this project.

2.2.2 Motor Cowling

In order to accommodate an active aerodynamic system in the Formula Electric vehicle, one of the most difficult aspects that is encountered is the placement of the actuators. In a typical active aero implementation, such as what is found in conventional race cars, the active aerodynamic features are found at the back of the vehicle [12], [13]. This placement provides a lot of space to mount actuators and other motion control items, such that the control of the movement of the wing, and the mechanism does not stall under the air pressure that is present on a wing. The front wing however, adds a very interesting challenge; in that the overall wing design must incorporate a significant amount of clearance for the tires as well as the suspension travel and its effect on the tire movement [14]. This challenge is compounded significantly on open wheel race cars, where the aerodynamics around the wheels proves to be a significant challenge [13].

For the formula electric competition, this problem is also further compounded by the need to comply with a set of template rules [7]. Template rules are a strict fitting guide that determines the internal clearance that the driver has in the seating space. Since that space extends all the way to the front nose cone, the room that is available for items such as actuators is supremely limited. As such, a cowling was designed such that the actuators could sit outside of the chassis, which ensures the template rules can be met, but the actuators do not interfere with flow. Shown in Fig.8 is the cowling that was designed to fit the chassis, and view of the chassis without the cowling in place to demonstrate its location.



UNIVERSITY
OF MANITOBA

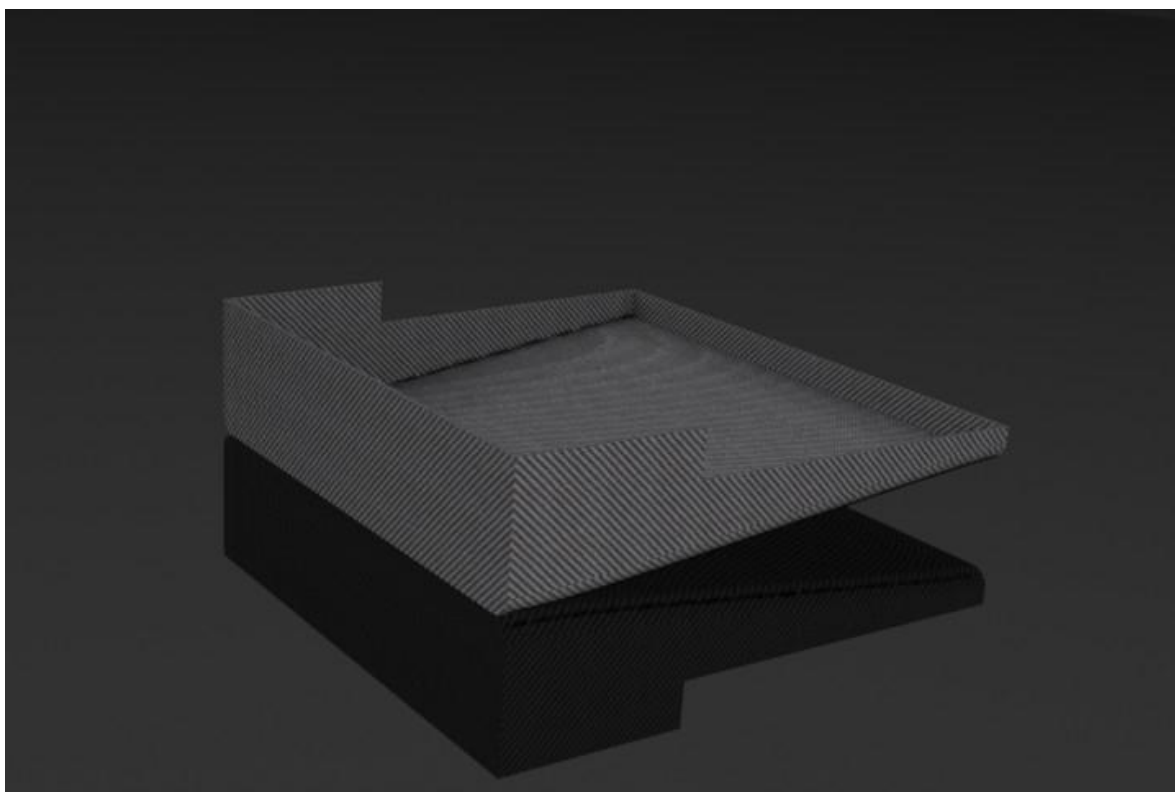
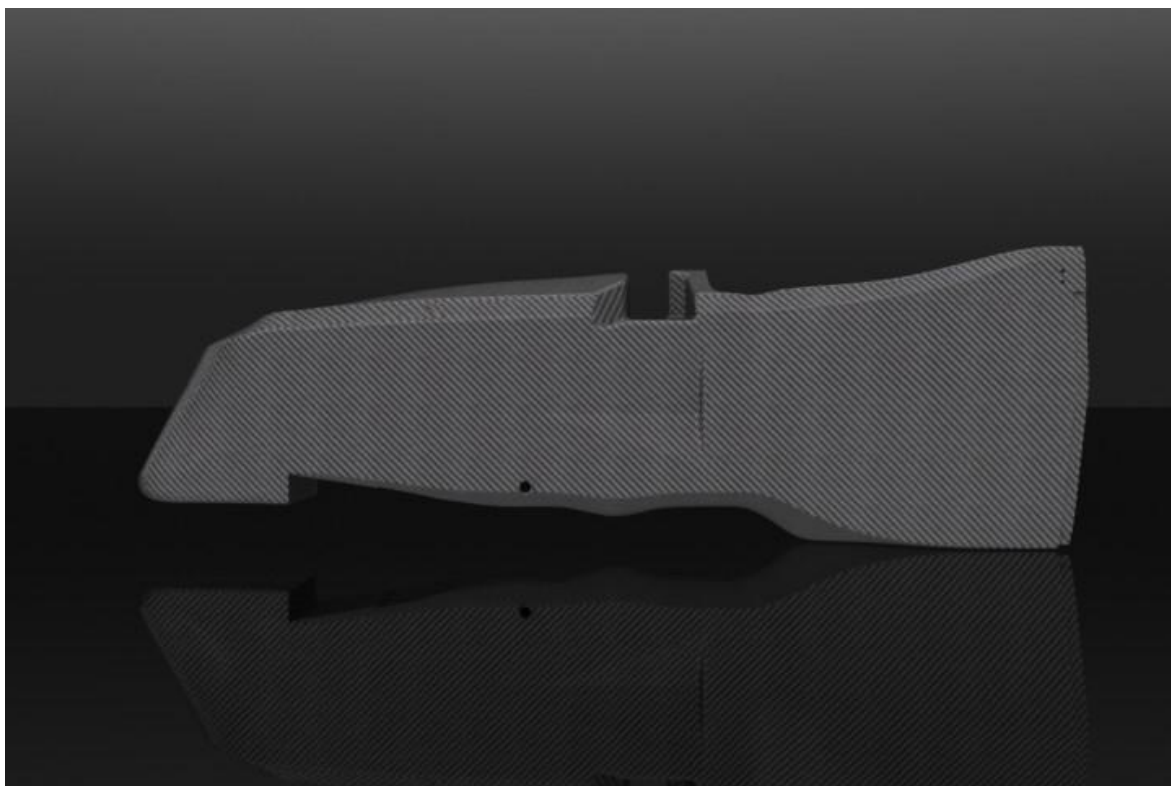


Figure 8. 2012 Formula Electric – No Cowling (top) Cowling, Separated From Chassis (bottom) [5].



The incorporation of the cowling provides a significant advantage to the team, in that it serves the purposes of reducing the front ground clearance in areas where the clearance is much higher than what is required by the suspension, providing room to mount the motors without intruding into the chassis. Moreover, the suspension provides a solid mounting location for the motors, such that the aerodynamic forces are coupled into the chassis, and to provide smoother flow on the under-chassis area of the vehicle.

2.2.3 Airfoil Selection

In order to implement the desired aerodynamic package, an airfoil with a predefined profile was selected. The main factor that limits the selection of an airfoil is its effectiveness at low velocities. Several airfoils suitable for low velocity applications were considered.

As previously mentioned, the airfoil is one of the main components influencing the characteristics of the design. The behaviour of different airfoils varies greatly as they are often tailored and optimized for specific applications. Consequently, the conditions that will be experienced by the vehicle, especially flow speed, need to be well understood before a selection can be made. Based on this knowledge, an airfoil can then be chosen, which excels at the given application.

Airfoils were initially developed for aircraft applications and were consequently characterized by their lift capabilities. A reliable measure of their performance is the coefficient of lift, which is a non-dimensional parameter used to characterize airfoils. Throughout the discussion on aerodynamics in this report, the terms lift and down force are used interchangeably. An airfoil that provides a large amount of lift will produce the same amount of down force when it is inverted and subjected to the same flow as before. The following table shows several options for a suitable airfoil.



TABLE III: OPTIONS FOR SUITABLE AIRFOIL

Airfoil Profile	Characteristics	Optimal Speed
Thin low cambered	Low drag	High
Thick deep cambered	High lift	Low
Thin deep cambered	High lift	Low
Symmetrical	Good stall properties	Medium

The requirement for high down force and minimal structural weight of the front wing, in addition to the fact that the speeds generally attained at competition are relatively low, makes the thin deep cambered airfoil the ideal choice for this application.

Extensive research was conducted to determine the optimum profile of the wing. A number of airfoils commonly used for motorsport applications with similar characteristics as required for the SAE Design Competition were researched to determine which of them would be most suitable for the purpose of this project. To determine which of the airfoil shapes would provide the highest down force performance, the maximum coefficient of lift, C_l , was found for each one. The results of this investigation are presented below.

TABLE IV: PERFORMANCE CHARACTERISTICS OF AIRFOILS TYPICALLY USED FOR SLOW FLYING UAV [15]

Airfoil	C_l , max	$C_m, c/4$	Re
E214	1.25	-0.11	2×10^5
E423	2.00	-0.25	2×10^5
FX 63-137	1.75	-0.17	2×10^5
M06-13-128	1.52	0.00	2×10^5
LA2573A	1.86	0.02	2.5×10^5
LNV109A	1.87	-0.02	2.5×10^5
S1223	2.23	-0.29	2×10^5
S3021	1.17	-0.07	2×10^5



TABLE IV facilitated the airfoil selection greatly. It is obvious that S1223 airfoil is the best option for the desired design based on its premier lift coefficient. The Selig 1223 airfoil was therefore, chosen for the aircraft. In comparison to other airfoils, it provides much higher lift in the Reynolds number range of 200,000 – 300,000, which represents the flow conditions encountered during the autocross event at competition. Figure 9 shows a plot of the Selig 1223.

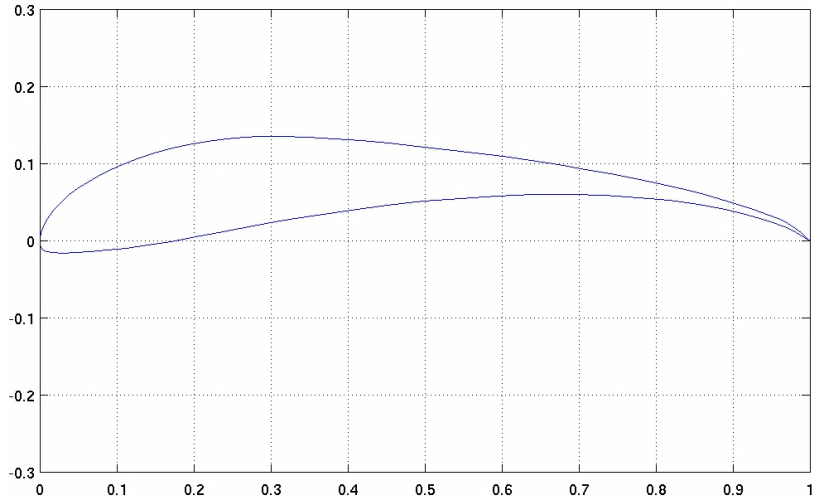


Figure 9. S1223 (11.93%) for high Lift at slow Flight [16]. Used with Permission.

A simple symmetric airfoil as shown in Figure 10 was designed to cover the rod connecting the fixed wings to reduce any occurring drag in that area, as well as to add to the overall down force generated by the package.

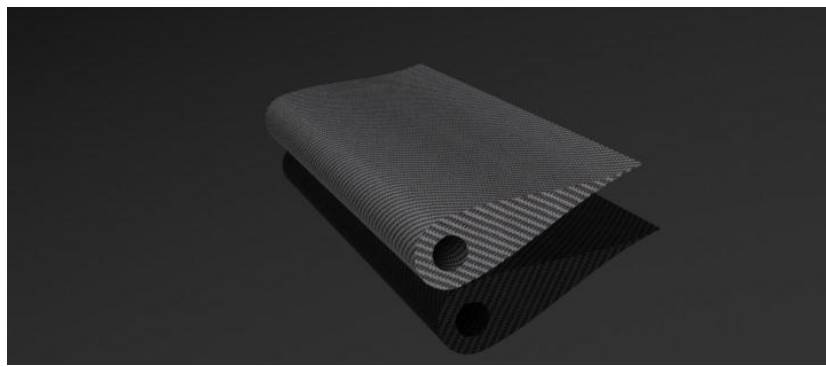


Figure 10. Symmetric Airfoil, As Used in Design [5].



2.2.4 Wing Shape

Another important characteristic that affects the design of the front wing is its plan form shape. There are three different options for wing shapes, each with different advantages and disadvantages. The design options are shown in Figure 11.

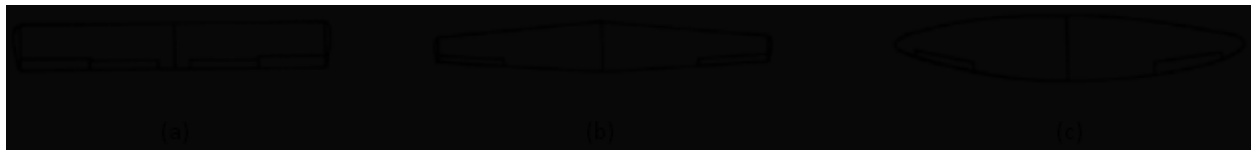


Figure 11. Typical Wing Shapes: (a) rectangular; (b) tapered; (c) elliptical [17]. *Permission pending.*

The rectangular design is well suited for control and easy to manufacture. However, it has the lowest wing efficiency in terms of stall and drag due to the greatest amount of induced drag. The tapered design is more efficient in comparison to the rectangular in terms of drag and lift but it is more difficult to construct. Finally, the elliptical wing is most efficient as it has the lowest amount of induced drag. Unfortunately, it is also the most difficult to construct and there additional difficulties with respect to control.

For this project, a rectangular wing was selected. It was found that the effect of the lower wing efficiency can be sufficiently reduced by attaching vertical end plates to the wing tip, which effectively reduce the induced drag. The effect of endplates can only be utilized with rectangular wings, as their effect on the other two wing shapes is negligible due to the variation in air flow pattern over the airfoil.

The 2012 Formula Hybrid Rules impose a number of restrictions on the placement and size of any aerodynamic device mounted to the car. The rules pertaining to this project can be found in the appendix. In addition to these, the Formula Electric team provided further dimensional requirements that would have to be taken into account to ensure that the design would not adversely affect the performance of the vehicle on the autocross track. To gain a better grasp of the available space for placement of the device, a volumetric design boundary was placed into a 3D model of the vehicle, as shown in Figure 12.



Figure 12. Volumetric Design Boundary resulting from SAE rules and Clearances specified by the UMSAE Electric Team [5].

The physical size of the wing was therefore limited to the following:

TABLE V: MAXIMUM ALLOWABLE DIMENSIONS FOR FRONT AERODYNAMIC PACKAGE (PER SIDE)

Width, w [m]	Length, l [m]	Height, h [m]
0.4064	0.4572	0.4206

From the above dimensions, the maximum allowable plan form area for a device was determined as follows:

$$S = w \times l = (0.4064)(0.4572) = 0.1858 \text{ m}^2$$

As specified by the client, a down force of 100 N was to be achieved at 50 km/h. Using the following equation, the necessary coefficient of lift that ensures that the specification is met, can be determined.

$$C_L = \frac{2L}{\rho V^2 S} = \frac{2(100)}{1.225 \left(\frac{70}{3.6}\right)^2 0.1858} = 1.16$$



The chosen airfoil must therefore provide a C_L of 1.16 in order to meet the client's specifications. The following sections describe the airfoil and wing shape and dimensions of the proposed design.

2.2.4.1 Wing Shape and Dimensions

The proposed design consists of two staggered airfoils arranged within the design boundary to optimize the ratio of produced down force and drag. The dimensions of the wings are as follows:

TABLE VI: PROPOSED DIMENSIONS OF FRONT WINGS AND END PLATE (PER SIDE)

Wings		End Plates
Span, b [m]	Chord, c [m]	Height, h [m]
0.4064	0.3018	0.4206

The end plates are designed to span the entire chord of the wing. The dimensions are therefore equal. The wings have a rectangular shape. The basic definition of AR for rectangular wings is as follows:

$$AR_{Actual} = \frac{b^2}{S} = \frac{b}{c}$$

Applying this relationship while considering the dimensions of the proposed, an AR in the order of around 1.5 would be expected. However, this relationship does not take into account the effect of the end plates. End plates tend to reduce unwanted 3D effects at the wing tips, thereby increasing the effective AR of the wing. To account for the beneficial effect of the end plates and obtain the effective AR , the following relationship between AR and end plate size was used:

$$AR_{effective} = AR_{Actual} * (1 + 1.9 \frac{h}{b})$$

Therefore, the effective AR is around three times the actual AR , which substantially decreases the induced drag of the device. The low ground clearance on the front will also have the effect of reducing 3D effects.



$$AR_{Actual} = \frac{0.4064}{0.3018} = 1.35$$

$$AR_{effective} = 1.35 * \left(1 + 1.9 \frac{0.4206}{0.4064}\right) = 4.00$$

Lift coefficient for a finite 3D wing before stall is defined as:

$$C_L = a(\alpha + \alpha_0)$$

Lift coefficient slope for wings with an $AR < 4$:

$$a = \frac{2\pi^2}{180 \left[\sqrt{1 + (2/AR)^2} + 2/(AR) \right]} = \frac{2\pi^2}{180 \left[\sqrt{1 + (2/4.00)^2} + 2/(4.00) \right]} = 0.06778$$

A basic way to account for the ground effect is the addition of a correction as follows for the fixed bottom wing:

$$a_{bw} = a + \frac{\pi}{180} \left(\frac{\frac{1}{(h/c)^2} - \frac{1}{4}}{5} \right) = 0.06778 + \frac{\pi}{180} \left(\frac{\frac{1}{(0.075/0.3018)^2} - \frac{1}{4}}{5} \right) = 0.12343$$

Similarly, for the active top wing:

$$a_{tw} = a + \frac{\frac{1}{(h/c)^2} - \frac{1}{4}}{5} = 0.06778 + \frac{\pi}{180} \left(\frac{\frac{1}{(0.177/0.3018)^2} - \frac{1}{4}}{5} \right) = 0.07706$$

The angle of attack where the Selig 1223 airfoil produces zero lift is $\alpha_0 = -6^\circ$. If the wing is inverted to produce down force, the sign on the values for angles of attack would change to positive. The fixed bottom wing is set to an AoA of $\alpha = -13^\circ$. The maximum C_L would be obtained at an AoA of $\alpha = -16^\circ$. However, to account for suspension movement, it was decided to reduce the angle, which leaves a margin of safety to prevent wing stall during braking, when the nose of the car pitches down. Accounting for the ground effect using the foregoing values for the lift slope, the maximum obtainable C_L for each wing of the proposed design becomes:



$$C_{L,bw} = a_{bw}(\alpha + \alpha_0) = 0.12343 \times |-13 - 6| = 2.34$$

$$C_{L,tw} = a_{tw}(\alpha + \alpha_0) = 0.07706 \times |-13 - 6| = 1.46$$

By erudite placement of the wings within the design space, the required value of C_L was successfully achieved for both wings.

2.2.5 Drag Characteristics

Reducing drag is critical to the feasibility of an aerodynamic device in order to warrant its application. In addition to the drag inherent to the selected airfoil, additional drag is induced as a result of the lift produced by the wing. Induced drag is created by the pressure differential acting on the surfaces of the wing. There is a migration of airflow to the wingtips of the aircraft along both top and bottom, causing a vortex at the wing tip when the two flows mix. With an increased angle of attack, the induced drag is increased proportionally until the wing stalls. Stall describes the condition when the wing ceases to produce lift. At this point, the airflow over the wing is similar to a bluff body as the drag is several orders of magnitude higher compared to a streamlined body. In order to reduce the wing's chance of stalling with high AoA at slow speeds, the wing for the Formula Electric vehicle has been designed to make use of endplates. Endplates are used to reduce drag associated with those vortices at the tips of the wing as they aid in keeping the flows separate.

The coefficient of drag prior to stall consists of the viscous drag and the lift-induced drag as defined by:

$$C_D = C_{D0} + C_{Di}$$

$$C_{Di} = \frac{C_L^2}{\pi \times AR}$$



2.2.5.1 Airbrake

The airbrake function takes advantage of the wing drag characteristics after the wing has stalled. As previously mentioned, the lift produced by a stalled wing is negligible. In order to supplement the vehicles hydraulic breaking system, the wing should produce the maximum amount of drag possible when in the airbrake configuration. For wings with an $AR < 10$, the lift and drag coefficients for a stalled wing can be found from the following relationships:

$$C_L = C_{D90} \cos(\alpha)$$

$$C_D = C_{D90} \sin(\alpha)$$

where C_{D90} = Drag coefficient at 90° AoA. For the wings proposed in this design, $C_{D90} = 1.23$ [18]. Moreover, research has shown that the ground clearance of the front wings reduces the initial value by approximately 20%, resulting in $C_{D90} = 0.984$ [18]. In order to stall the wing, it needs to be placed at an angle of less than $\alpha = -16^\circ$.

2.2.6 Operation

Figure 13 illustrates the different stages of desired aerodynamic effects along a simple corner on a racetrack. As the vehicle is on a straightaway (stage 1), minimal drag and down force are the goal aerodynamic effects. Having drag forces acting against the vehicle results in slower acceleration and a lower top speed. Figure 14 shows the trajectories velocity plot of the wing setup in the minimum drag configuration. The AoA for the wing in this configuration is -6° . In this configuration, the linkages are setup in such a way that as the wing is being moved to that angle, the gap between the top and bottom wings is increased in height. The airflow between the wings is somewhat unrestricted, resulting in relatively unrestricted airflow, thus reducing drag effects greatly. It should be noted that the vortex occurring behind the top wing in Figure 15 is not present in experimental data for the S1223 airfoil at this angle. The AoA recommendation is based on gathered experimental data which proves to be more accurate in most cases. More details on the CFD setup and accuracy are provided in the appendix.

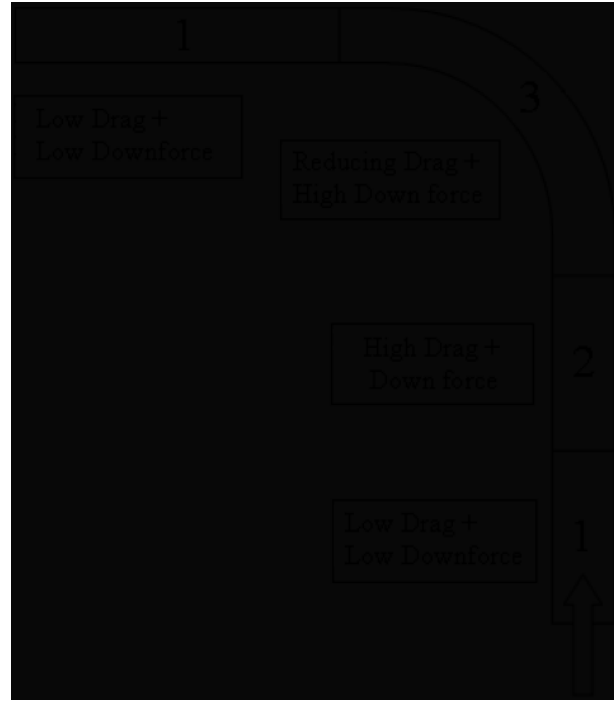


Figure 13. Aerodynamic requirements when cornering on the SAE Autocross Circuit [14]. *Permission pending.*

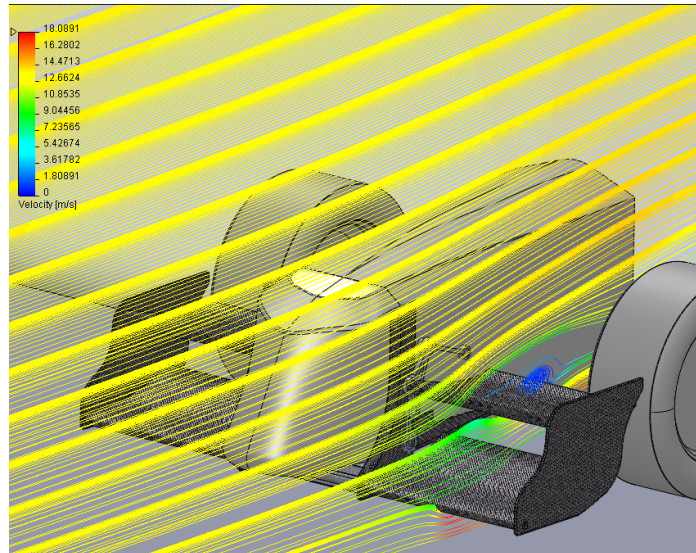


Figure 14. Flow Trajectories Velocity Plot in Low Drag Configuration [19].

As the vehicle is reaching a corner and begins braking; maximum amounts of drag are needed (stage 2) to help the vehicle break as fast as possible by reducing the vehicle's speed through the drag forces counteracting the motion of the car. Figure 15. Flow Trajectories Velocity Plot in Airbrake Configuration [20] shows the trajectories velocity plot for the wing at the airbrake

configuration. The AoA for the wing in this configuration is 28° . It can be seen that vortices are taking place in the blue region which results in low velocities and high dynamic pressure, thus drag, causing the vehicle to decelerate faster. Another aerodynamic effect that was not captured in the simulation is the low velocity region occurring between the top and bottom wing. Vortices are developed in this region, adding to the drag forces occurring.

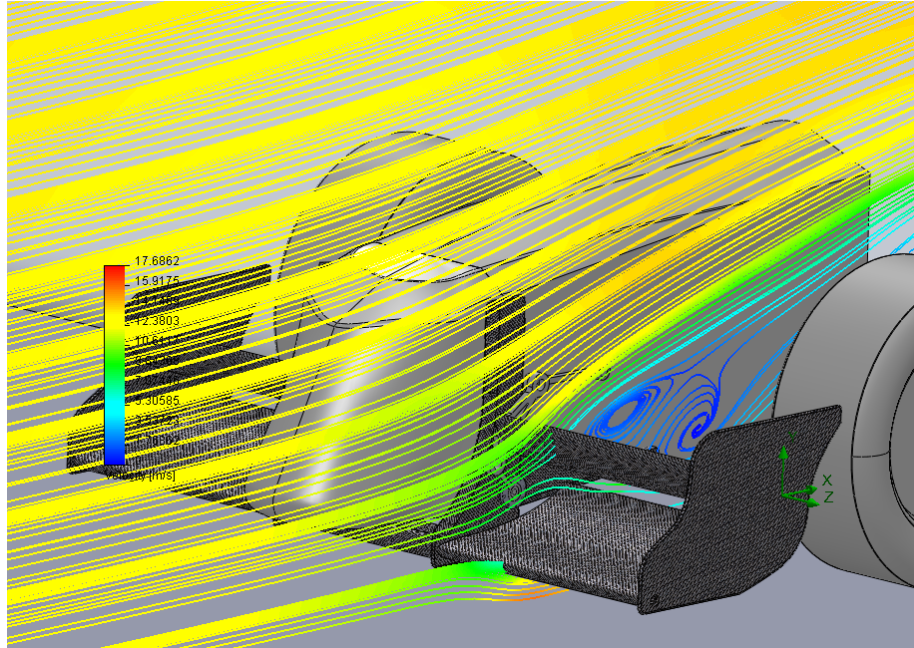


Figure 15. Flow Trajectories Velocity Plot in Airbrake Configuration [20].

As the car starts turning along the corner (stage 3), the transfer of momentum throws the weight of the car to the outward side of the corner, which causes the vehicle to slide away from the desired racing line. Most open wheel race cars such as the UMSAE Formula Electric vehicle have the tendency to be light at the frontend due to their design. This weight distribution causes the transfer of momentum while in a corner to the outward front tyre causing an understeering effect. Thus, at this stage, maximum amount of down force is needed to act as artificial weight pushing the frontend of the car to the ground, adding to the available grip, thus maximum cornering speed. Figure 16 shows the trajectories velocity plot for the wing at the down force configuration. The AoA for the wing in this configuration is 13° . It can be seen that laminar flow is present throughout the wing profile. The laminar flow contributes greatly to producing the maximum possible down force. Additionally, the red region below the fixed wing



signifies the high velocities due to the wing shape combined with ground effect due to the proximity to the ground. The combination of these effects results in highly efficient down force generation.

Using CFD, the behaviour of 3D wings was calculated for the S1223 profile. The results are shown in the appendix. In addition to the CFD analysis, a discussion on how the gained down force and the drag would affect the performance of the vehicle is provided.

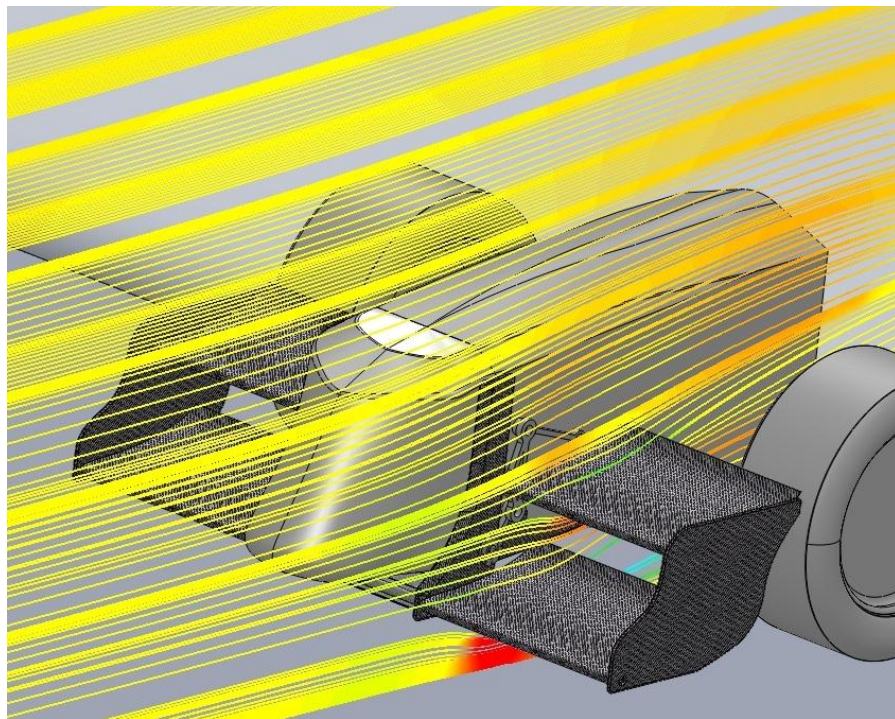


Figure 16. Flow Trajectories Velocity Plot in Maximum Down Force Configuration [21].

2.2.7 Summary

An estimate was made regarding the minimum coefficient of lift C_L required to meet the client specification. The estimate was then used to gage the down force that an active wing would be able to generate. In order to complete the analysis, the effect of ground proximity on both the lift and drag coefficients for both pre-stall and stalled configurations of the proposed rectangular wings was taken into account. TABLE VII shows four wing positions that would be suitable in different sections of the track to enhance the performance of the UMSAE vehicle. No information could be provided regarding the performance of the airbrake at this point as the



interaction between the airflow over the two wings is too complex to be analyzed accurately by means of simple hand calculations. As a result, this setup was studied using CFD. The results are presented in the appendix.

Figure 17 shows the combined down force and drag gained at the maximum down force positions from all four wings as a function of velocity of the vehicle.

TABLE VII: SUMMARY OF DOWN FORCE AND DRAG GENERATED AT 50 KM/H BY THE PROPOSED DESIGN

AoA	Fixed bottom Wing				Active top Wing				Total	
	C _L	C _D	Down Force [N]	Drag [N]	C _L	C _D	Down Force [N]	Drag [N]	Down Force [N]	Drag [N]
28°	Airbrake									
6°	0	0.024	0	0.35	0	0.24	0	0.35	0	1.4
-13°	2.34	1.736	-34.51	25.20	1.360	0.765	-21.72	11.10	-112.44	72.40
-28°	0.869	0.462	-12.81	6.71	1.086	0.577	-17.34	8.372	-60.3	30.16

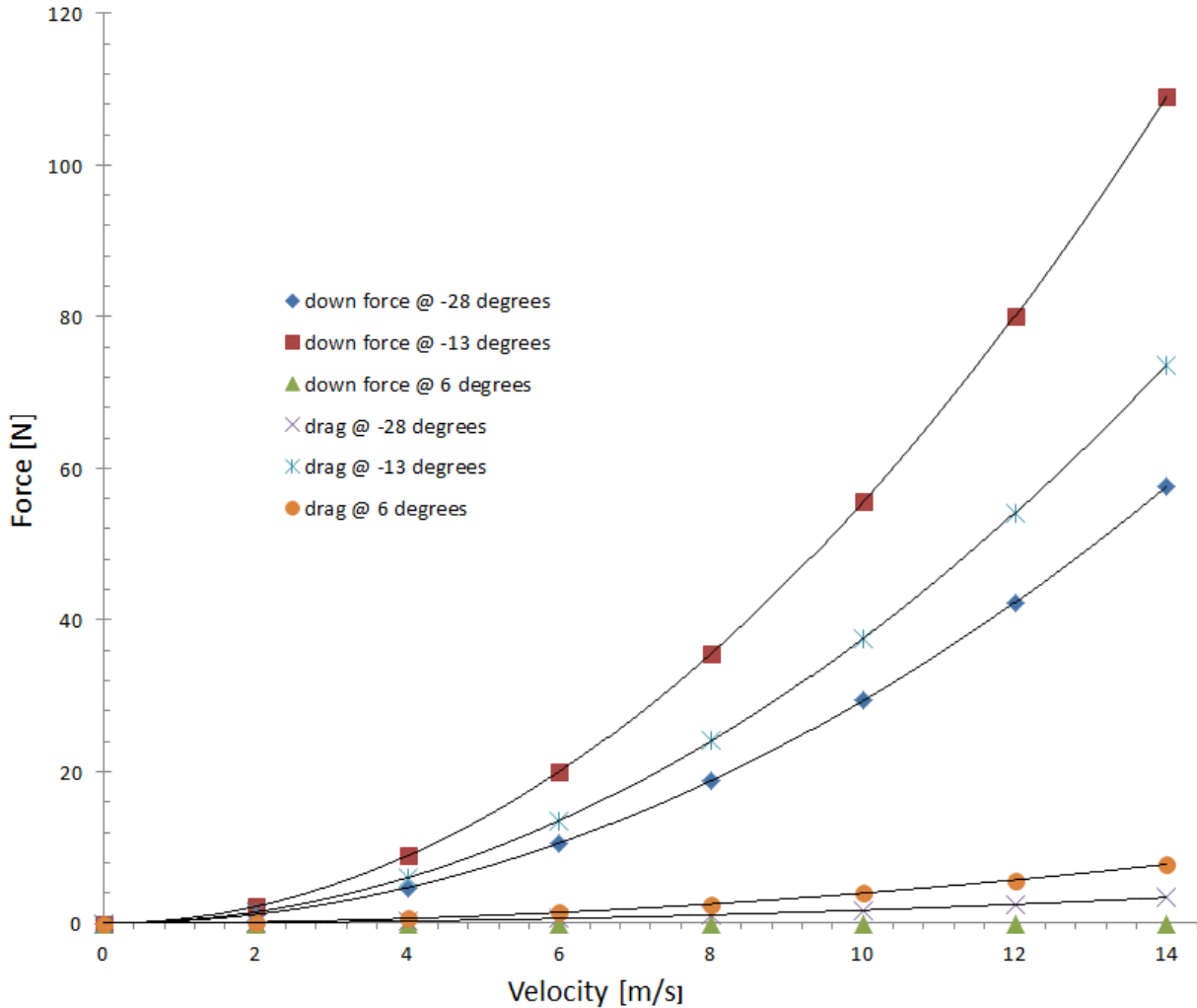


Figure 17. Vehicle Velocity vs Down Force / Drag.

2.3 Airfoil Actuation System

The design for the linkage system was one of the items that was evaluated in the conceptual design phase of the project, and is one of the few items that smoothly transitioned from conceptual design to a formal design. The idea behind the four bar linkage based wing concept, known as the path motion wing, was to produce a swept curvilinear path for the driven wing. The rationale behind the use of this type of motion was based on an optimization of the design space. Considering that the design could only occupy the previously described volumetric space, the ability to rotate the wings was severely limited as the chord sizes of the wings increased. By using a curvilinear motion path, the wing space could be maximized, since



each wing could rotate and translate within the specified design space. Shown below is the overall layout of the four bar linkage. This linkage setup is connected to one wing, such that the middle bi-planar mobile link is connected to the wing, allowing the wing to undergo path motion. This motion is done with respect to the fixed wing at the bottom.

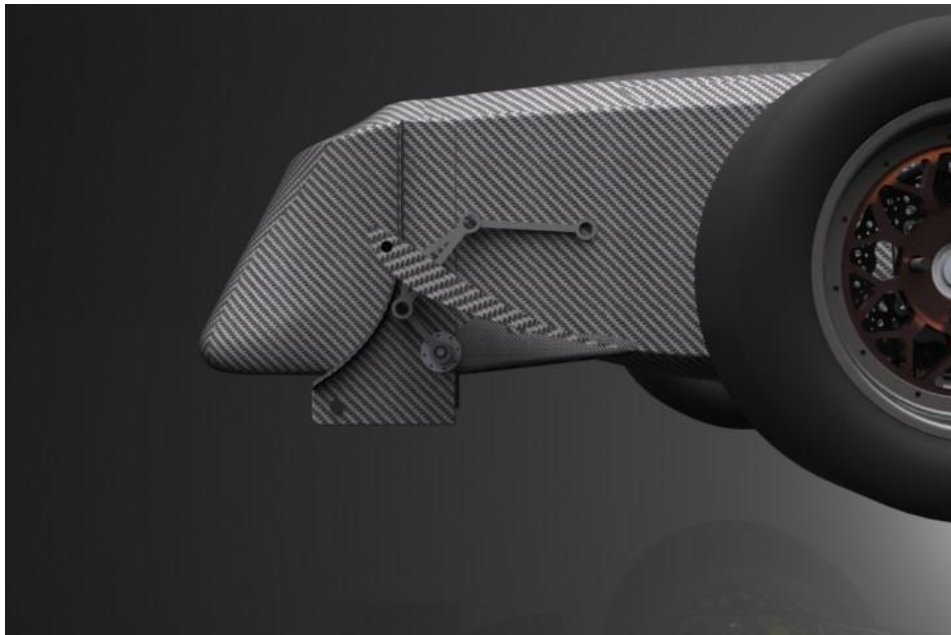


Figure 18. Four-Bar Linkage Setup on Movable Wing [5].

From the four bar linkage, three distinct motion patterns are possible, whereby the wing arrangement provides a very desirable aerodynamic motion. The possible profiles are cornering, braking, and straight line performance.

The simplest of the three profiles is the cornering profile, which involves the placement of both wings with the chord lines parallel. This arrangement provides a significant amount of lift, as both of the wings are at their maximum possible angle of attack. As an added bonus, the layout of the path motion linkage creates a much defined airflow channel between the wings. This channel provides a momentum flux based down force generation effect that also aids in the total amount of down force generated. As part of the design of the linkage, the upper wing can “tighten” or “loosen” this channel, by adjusting the separation, but at the same time utilize a nearly vertical wing motion. This motion path works well for the design because it allows a



great range of versatility at the edge of the usable design space. Shown below is the cornering configuration, with both wings brought together as close as possible.

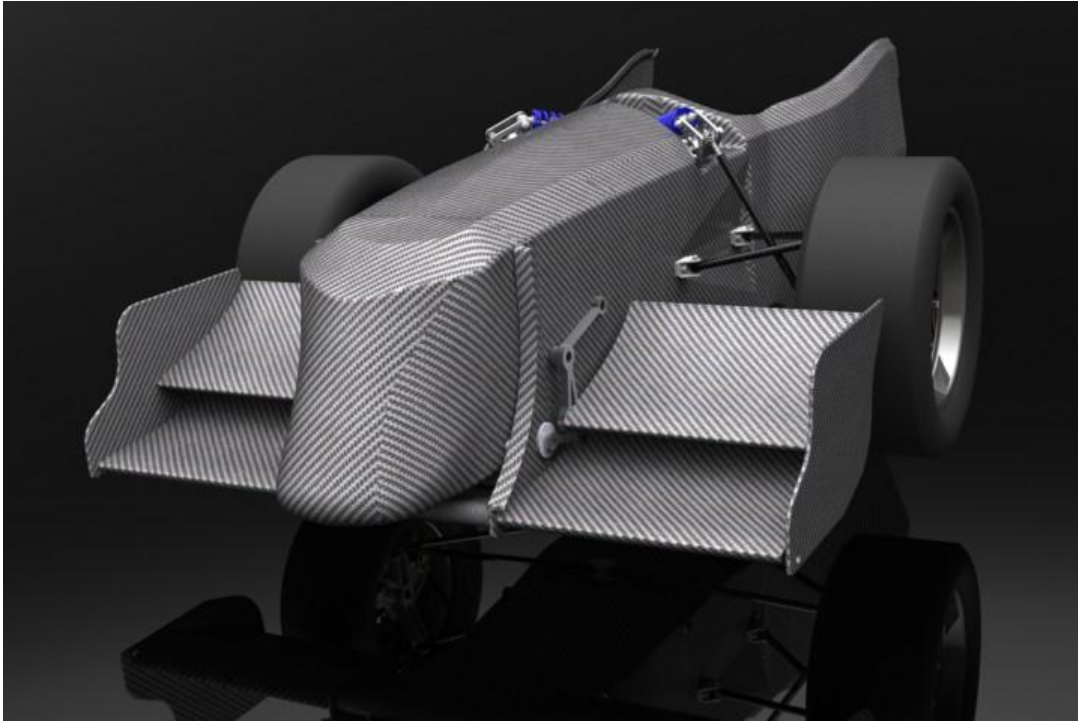


Figure 19. Active Airfoil Positioning – Cornering Configuration [5].

The second configuration that was specified by the client as a highly desirable aerodynamic function is a straight line profile, which minimizes the lift force from the airfoils. The straight line profile places the upper wing in its neutral state, which is the state where it produces no lift or down force. This absence means that the natural balance of the car is not upset during acceleration and straight line performance. Normally, a slight bit of lift is desirable [6], and as such, the amount of force can be tuned by slightly changing the angle of attack. Shown in Fig. 20 is the straight line configuration, with the second wing set at the neutral angle for the wing. This setup provides a static amount of down force, due to the angle of attack of this lower wing, which is non-adjustable.

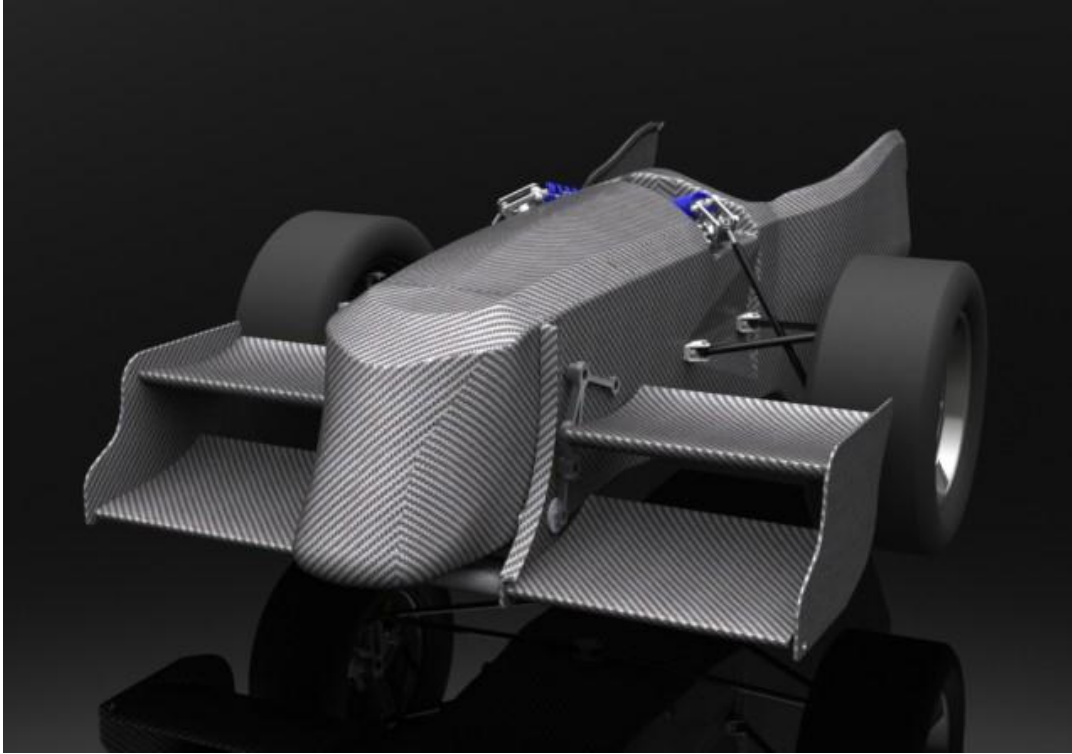


Figure 20. Active Airfoil Positioning – Straight Line Configuration [5].

The final configuration that was specified as a desirable configuration by the client is the airbrake profile. This configuration is very useful for two reasons: the increase in dynamic brake force and the increase in brake bias. The increase in drag caused by this arrangement of the wings comes from the large V-plow shape that the wings take. The large entrance area forces air through the narrow gap between the wings. Air that makes it through this gap has high relative viscous drag [22], and is also forced against the rotating tires at high speed. This drag causes a global deceleration on the vehicle, which helps slow down the vehicle quickly, and without causing additional stress on the braking system. The second critical aspect of this wing arrangement is the resulting pitching moment on the car. Since the centroid of the aerodynamic drag acts at a point above the **centre of gravity (CG)** of the car, the car is subject to a net tipping moment backwards. This moment is excellent under heavy braking, because it counteracts and minimizes the brake dive normally experienced [12], [13], [23]. The addition of a rear weight bias will increase the maximum tractive force from the rear tires under braking, which correspondingly means that more of the brake force can be utilized using regenerative



braking. Shown below is the most aggressive airbrake position, where the trailing edge of the top wing falls below the vertical position of the trailing edge of the bottom wing.

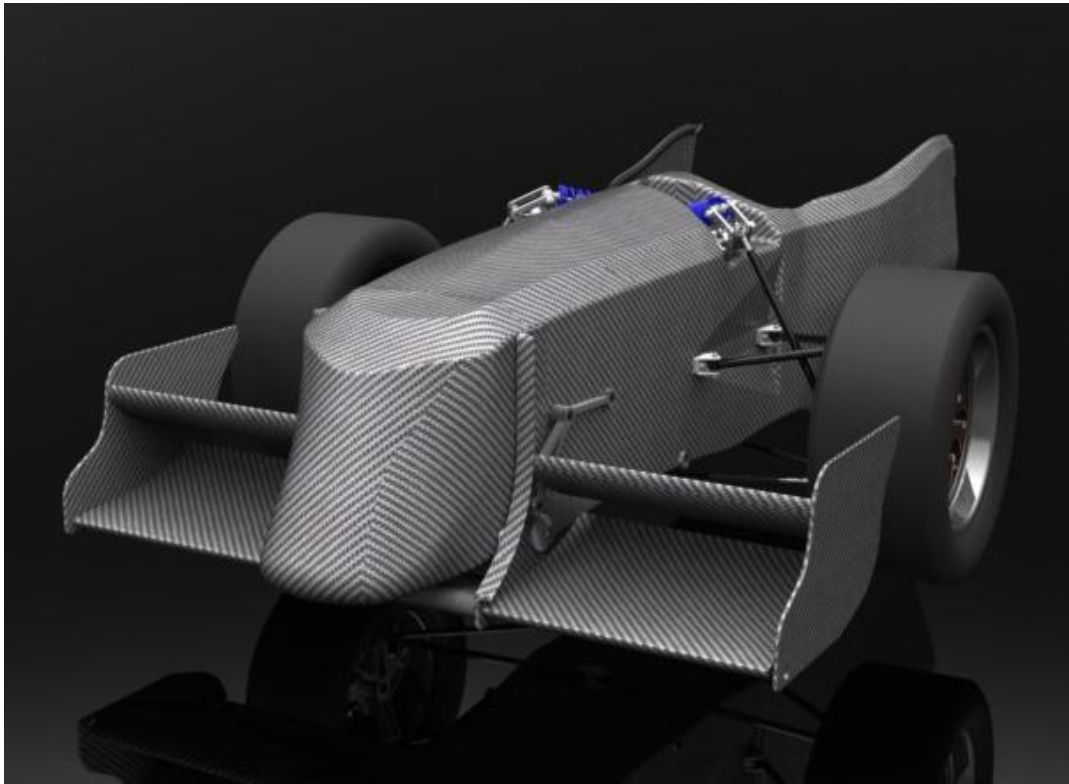


Figure 21. Active Airfoil Positioning – Air-Brake Configuration. [5]

In summary, the overall wing arrangement produced a high performance design that balances the weight requirements of the team with the gains in cornering performance that were desired. In the next section, the various actuation methods are examined.

The design of the actuation system was one of the trickiest aspects of the mechanical system due to the need for an exceptionally high torque based on the severely limited design space. The use of a path motion wing design meant that the torque that was delivered to the wing would act at a significant moment arm from the motor. This moment arm meant that the overall force that the wing could produce would be strongly dependant on the capacity of the motors that were there, because if the wing produced more force than the motors could take, the motors would back drive rather than move the wing forward. Comparisons were made between many different types of closed and open loop motor systems, and in the end a design decision was made to use a closed loop position feedback servo-electric actuator.



Part of the overall justification for the use of the servo-motors is their exceptional torque capability, which means that there are no foreseeable situations where the motor would stall during operation. The high torque capability is coupled with a very accurate closed loop system, which significantly simplifies the design compared to an open loop system. The selected servo motor is a heavily modified hobby type servo, the Torxis i00600, which was selected for its rated working torque of two times the expected aerodynamic load. This motor is shown below, encased in an aluminum housing for cooling. The size of the motors is substantial, considering they are 5.5" x 3.9" x 2.4", but it was deemed to be an acceptable trade-off for the performance.

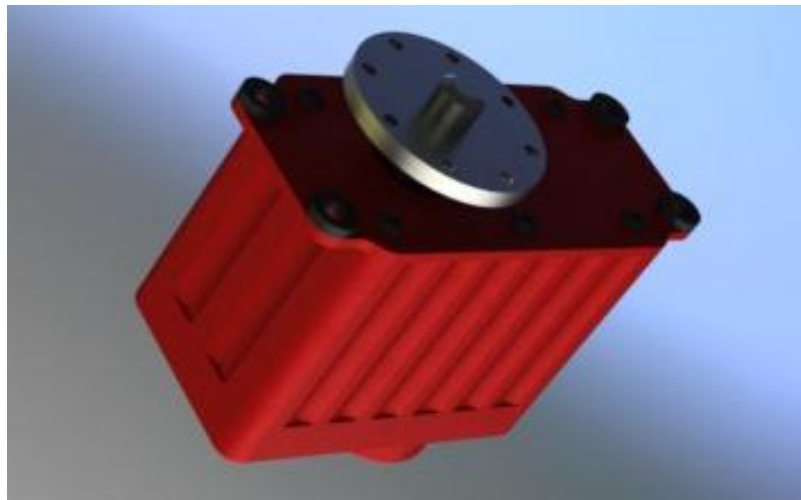


Figure 22.Torxis i00600 servo-motor [5].

The motors were mounted such that they directly drove the four bar linkage and the overall dimensions of each motor were deemed acceptable with the inclusion of a motor cowling, which covers them and blends their large size into the chassis.

Since these motors have their own black box control system built into them, the control aspect of the actuation system was significantly simplified. The instructions from the main control elements could easily be sent to the motor via **pulse width modulation (PWM)** signals, which could be instrumented through a variety of communication protocols.



2.3.1 Design and Analysis of Actuation Mechanism

The actuation mechanism is an important component of the design which controls and moves the aerodynamic front wing system. For the operation of the actuation system, the actuator needs an external power supply. This power source provides the actuation system with the energy needed for any movements and motion of the system. The goal was to design and implement an actuated four bar linkage that is capable of controlling, moving and holding the aerodynamic front wings with a minimum power input. In addition, the four bar linkage positions and configuration which correspond to the airbrake, down force generation and neutral state were identified. In order to achieve these features of the actuation design, the position and the force analyses of the four bar linkage have been carried out using Maple [24]. The details and results of these analyses are presented in the following sections.

Based on the latest Formula SAE rules and the aerodynamic front wing dimensional requirements and limitations, the geometric locations and lengths of the four-bar links were specified. Basically, a four-bar mechanism comprises a frame, a crank, a coupler and a rocker which are shown in Figure 23 [25]. These links, except for the frame, are interconnected in a way that each link is free to rotate. The frame is a virtual link connecting the prismatic joint 1 on the chassis to the crank joint 2. The wing, as shown, is attached to the coupler which determines the angle of attack and the corresponding aerodynamic forces and moments. The coupler is connected to the crank and the rocker using revolute joints 3 and 4. For the purpose of the analysis, the links and joints are numbered as illustrated in Figure 23.

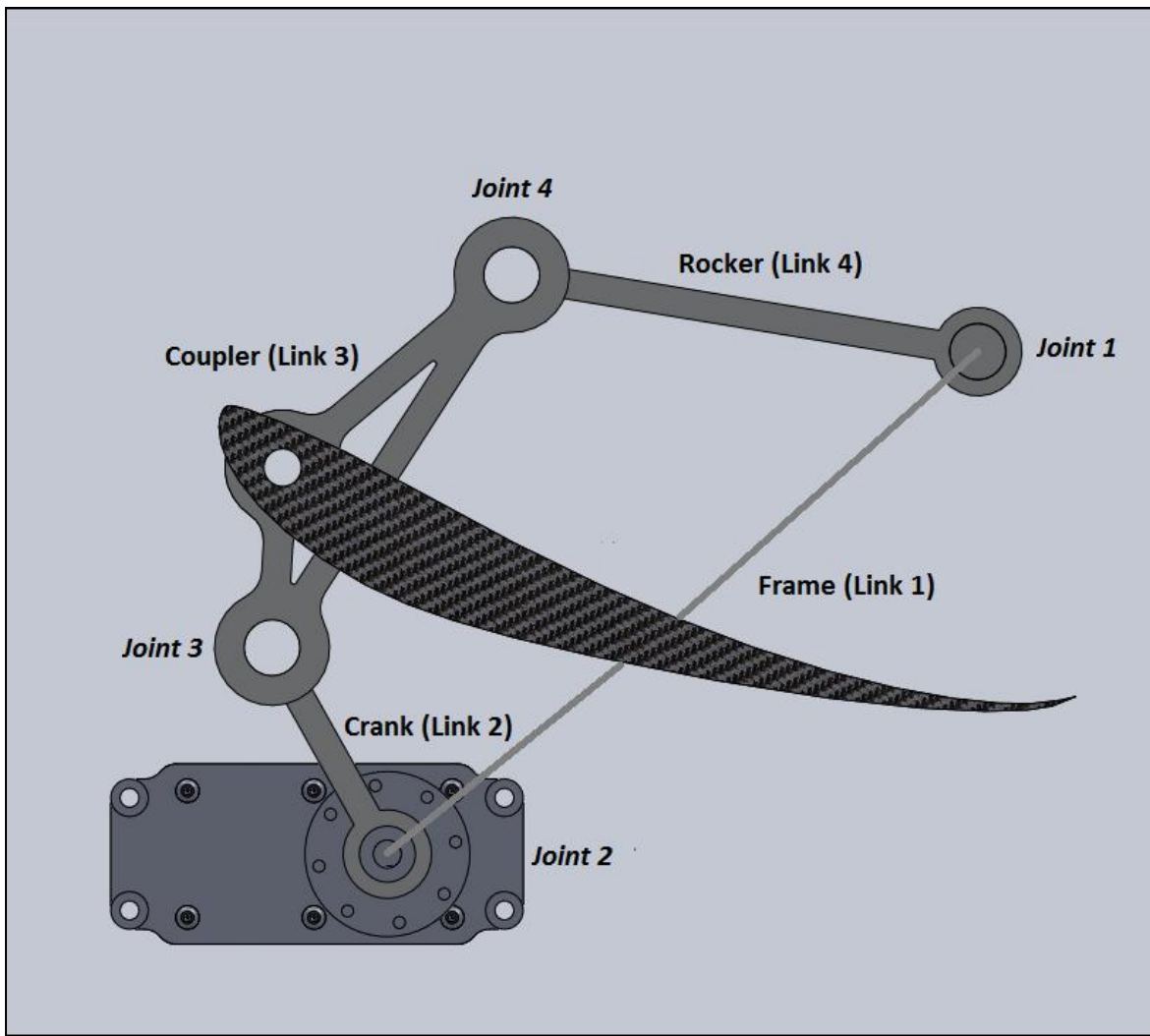


Figure 23. The actuated four-bar linkage and its main components [26].

According to the dimensional limitations, the links' lengths and the locations of fixed joints 1 and 2 were specified. The results are outlined in TABLE VIII.

TABLE VIII: LENGTHS OF LINKS AND LOCATIONS OF FIXED JOINTS.

Link 1, L ₁ [mm]	Link 2, L ₂ [mm]	Link 3, L ₃ [mm]	Link 4, L ₄ [mm]	Joints 1-2 vertical distance [mm]	Joints 1-2 horizontal distance [mm]
262.50	81.00	150.00	160.50	170.00	200.00

Once the geometry and configuration of the four-bar linkage were defined, the position and force analyses of the mechanism had to be performed in order to find the required angle and torque inputs of the motor. The next sections of the report present the results of these analyses.



2.3.1.1 Position Analysis

There are several methods that the position analysis can be approached. In this report, however, a mathematical vector approach is used in which a vector is assigned to each link. As known, a vector has a magnitude and a direction so the magnitude is simply the length of the link and the direction is defined as the angle the tail of the vector makes with the horizontal. These vectors are illustrated in Figure 24. Note that vectors are presented by letter R and the angles are shown as θ . According to fundamentals of vectors, the sum of all vectors in a loop must be equal to zero which can be shown as follows:

$$\sum_{i=1}^4 R_i = R_1 + R_2 + R_3 + R_4 = 0$$

This equation is known as the Loop-Closure Equation [25]. Since it is a vector equation, there are two scalar equations to solve and eight possible unknowns for a four-bar linkage. These unknowns include both the magnitude and angle of each vector or link.

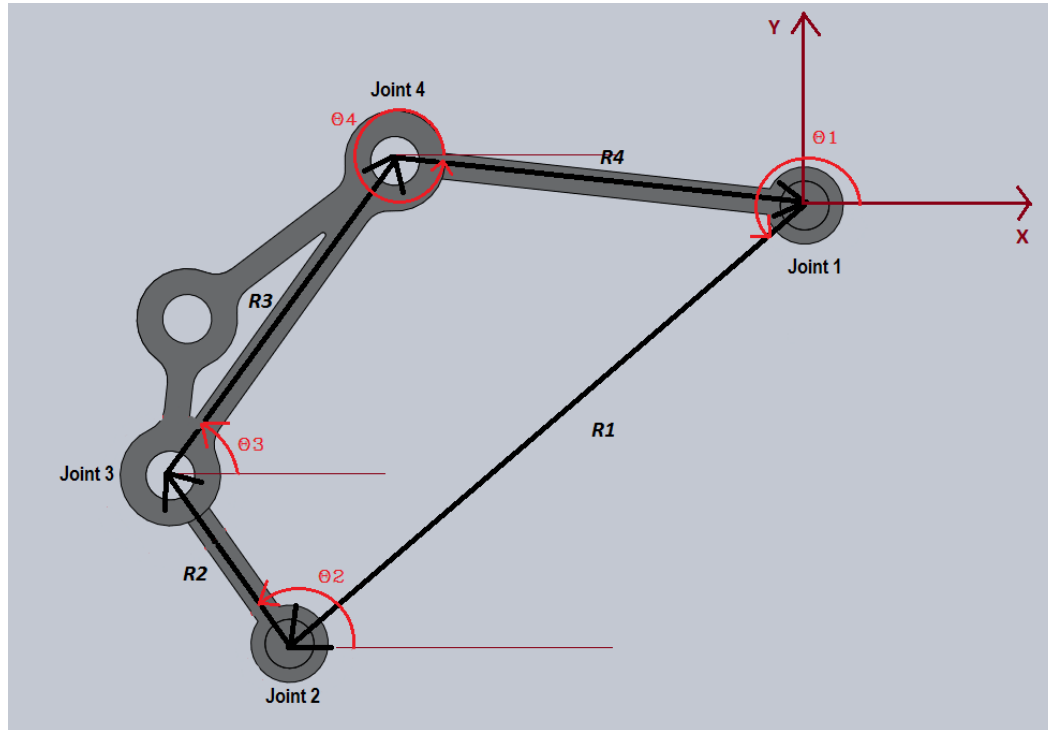


Figure 24. Vector representation of the four-bar linkage [26].



The magnitudes of all vectors are known. Also the angle of the link 1, θ_1 , is constant and is calculated to be 229.647 degrees based on the geometry. θ_2 which is the input angle is also considered to be known as the unknowns can be written in terms of θ_2 . Therefore, the two unknowns, in this four-bar linkage, are the angles of links 3 and 4 (θ_3 and θ_4). By solving the Loop-Closure Equation, one of these angles can be obtained from the following relation [25]:

$$L_3 \sqrt{1 - \left(\frac{L_4}{L_3}\right)^2 \sin^2(\beta - \theta_4)} = -L_4 \cos(\beta - \theta_4) + b$$

where b and β are the magnitude and the angle of the resultant known vectors. The equation above was solved in Maple and θ_4 was plotted in terms of the input angle θ_2 . The plot is shown in Figure 253 and the detailed calculations are presented in the appendix.

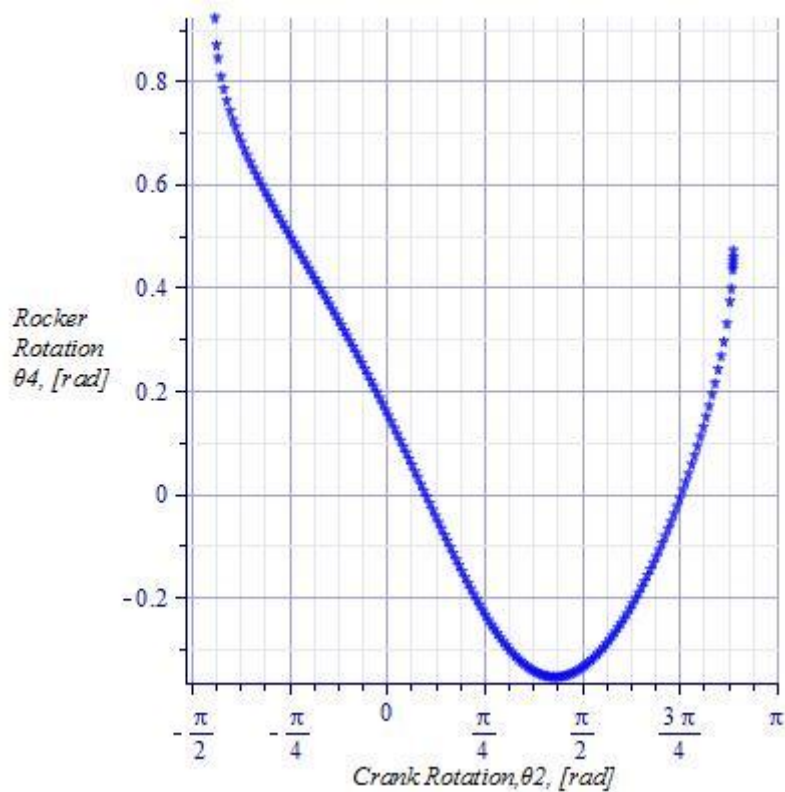


Figure 25. The plot of rocker angle vs input angle [27].



The other angle, θ_3 , which is related to the angle of attack of the top wings, can be obtained solving these two relations [25]:

$$\cos(\beta - \theta_3) = \frac{b - L_4 A}{L_3}$$

$$\sin(\beta - \theta_3) = \pm \frac{L_4}{L_3} \sqrt{1 - A^2}$$

where A is found from the following relation:

$$A = \frac{b^2 - L_3^2 + L_4^2}{2bL_4}$$

The plus and minus sign in the second equation above suggests that there are two possible physical configurations or solutions. Therefore, the configuration which corresponds to the design was chosen in the Maple analysis. The detailed calculations and Maple codes are presented in the appendix. The above equations were solved in Maple, and θ_3 was plotted in terms of the input angle θ_2 which is illustrated in Figure 26.

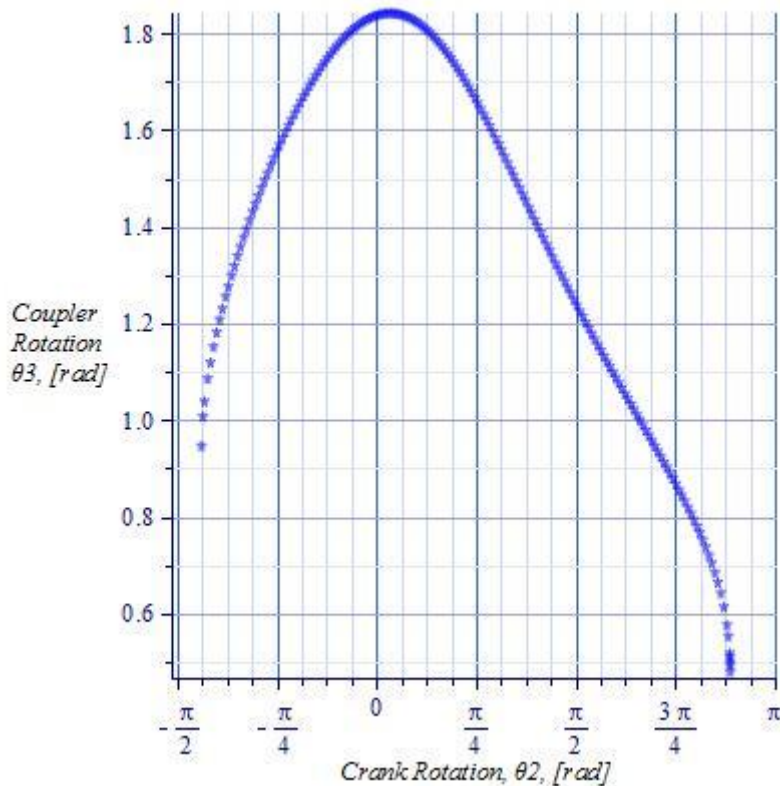


Figure 26. The plot of coupler angle vs. input angle [27].



Using this graph, the input angle can be easily found for the airbrake, down force generation and the neutral state. Basically, these critical input angles or positions serve as the requirements for the control system.

2.3.1.2 Force Analysis

The force analysis is a key element of design in order to determine the amount of torque needed to move and hold the wing in position at different angles and car speeds. Basically, the external power or torque input to the crank flows through the links. The flow of forces within the mechanism is dependent on the position and type of mechanism. In other words, these forces are a function of position or input angle (θ_2) to the crank. The other external forces and moments that are applied to the mechanism are the aerodynamic forces and moments. As mentioned in the aerodynamic design section of this report, Section 2.1, these forces and moments depend on the car's velocity and the wing's angle of attack. Therefore, the torque required to move and control the mechanism can be written in terms of velocity, V , and the angle of attack, α [28].

In this report, the inverse dynamics method is applied to solve for forces and moments. In this method, it is assumed that the motion is known so the velocity and acceleration of the links can be obtained from the known motion. Knowing the acceleration, the inertial forces can be found and considered as external forces. As a result, the force analysis can be solved by applying equilibrium equations at any given position or time. The vector equilibrium equations of the inverse dynamics can be written as [25]:

$$\sum_{i=1}^n F_i = 0 \quad \& \quad \sum_{j=1}^m M_j = 0$$

where n and m are the number of forces (F_i) and moments (M_j) respectively. For the force analysis in this report, the inertial forces are ignored since they are relatively negligible. The equilibrium equations were applied to the four-bar linkage in Maple (Detailed analysis and Maple codes are presented in the appendix. The input torque, T , was plotted against both the crank angle and the car's velocity. This three-dimensional plot is shown in Figure 27 in two

different view configurations. As expected, the minimum amount torque required occurs when the crank angle is approximately 90 degrees with respect to the horizontal. This crank angle corresponds to the wing's neutral position. On the other hand, the maximum torque of 0.7 N.m must be applied to hold the wing in position to produce the maximum amount of down force while cornering and about 2.1 N.m to provide the airbrake.

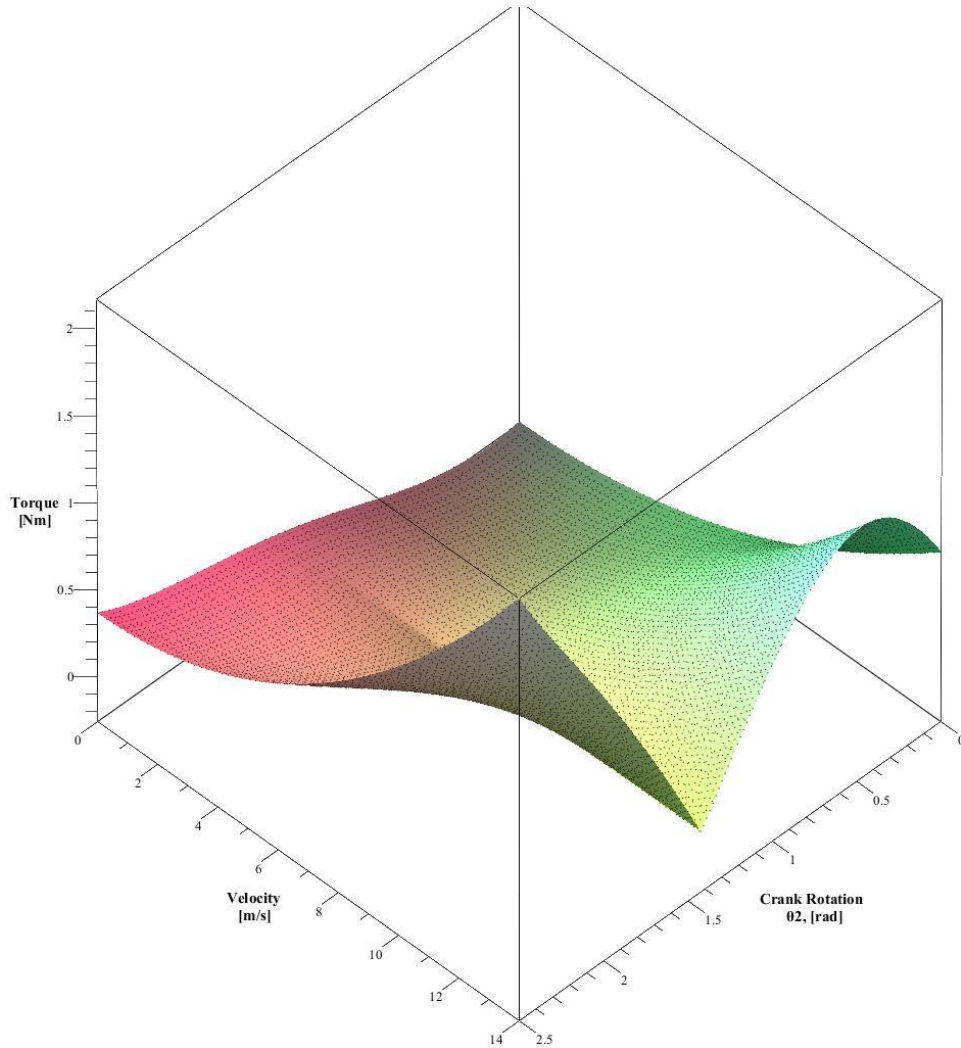


Figure 27. The required torque for different velocities and crank angles [28].

For a better and clearer understanding how the driving input crank affects the aerodynamic down force and drag at different vehicle velocities, plots of these forces in terms of the actuator input angle and vehicle speeds are shown in Figure 28 and Figure 29 . Down force, F , and drag, D , are in units of Newtons.

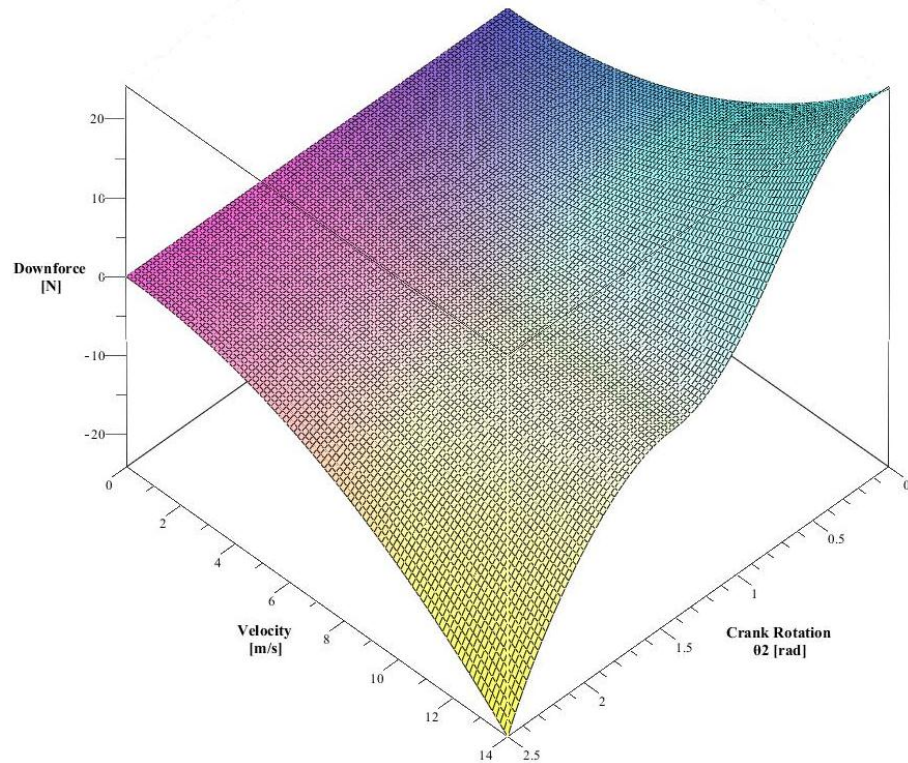


Figure 28. The amount of down force for different velocities and crank angles [28].

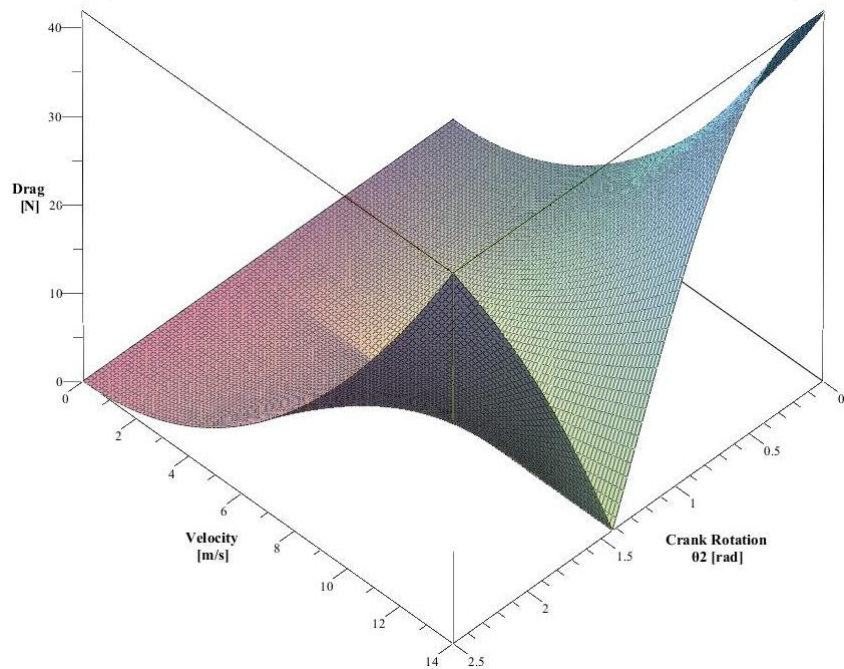


Figure 29. The amount of drag for different velocities and crank angles [28].



2.3.2 Summary

The geometry and dimensions of the actuated four-bar linkage were determined in accordance with the space limitation and the latest Formula SAE rules. These dimensions are outlined in TABLE VIII. A position analysis, based on the Loop-Closure vector equation, was carried out using Maple software to find the three input crank angles corresponding to the cornering, braking, and straight line profiles. These crank positions are required to perform the control analysis of the design.

An inverse dynamic force analysis was used to determine the amount of torque needed to hold and move the four-bar linkage at different wing positions and car velocities. The effect of inertia forces were ignored as they were negligible compared to aerodynamic forces. The force analysis required implementing a 3-D plot of torque as functions of the input crank angle and the car velocity. In addition, plots of aerodynamic forces as functions of the driving crank rotation and vehicle velocity were plotted to illustrate the effect of the actuator input on the aerodynamic performance of the vehicle. The results of this four-bar linkage actuation analysis are summarized in TABLE IX.

TABLE IX: SUMMARY OF POSITION AND FORCE ANALYSIS FOR THE ACTUATED FOUR-BAR MECHANISM

Wing Setup	Crank angle [degrees]	Coupler angle [degrees]	Rocker angle [degrees]	Required crank torque at 50 km/h [N.m]
Cornering	57.38	88.51	-17.54	0.7
Braking	139.18	47.51	2.93	2.1
Straight line	91.95	69.51	-18.52	0.35



2.4 Control System

After extensive discussion with the client [23], it was decided that the control system must be compatible with the current electrical systems on the formula electric vehicle, but should also be simple enough that a simple driver controlled system can be implemented.

Therefore, the approach taken to the control systems portion of the design was to create a simple design that is capable of quickly and adaptively adjusting the performance of the aerodynamic package. The control system includes the control of rather high order semi-linear motor systems, as well as the effects of air damping and viscous drag on the actuation mechanism. These effects are not insignificant [29], as have been seen in other cases, and as such the approach was to produce a system that minimized computational cost by utilizing existing systems on the car and off the shelf items for high order data processing. Shown below is the overall block diagram of the system.

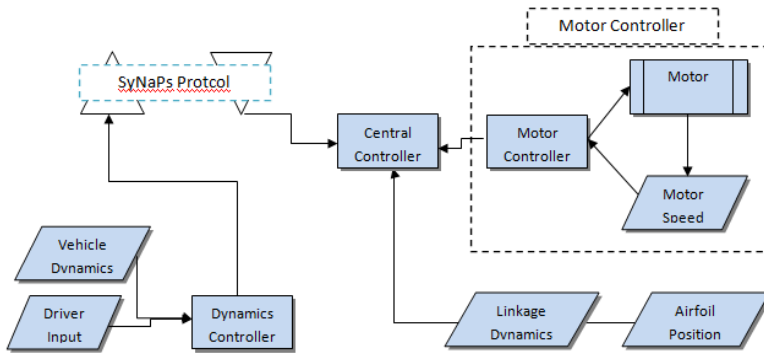


Figure 30. Overall Control Layout for Active Aerodynamic Control [30].

The overall layout of the control system corresponds to a closed loop position control for the wing, with higher order feedback driving the actuation signal. This closed loop control was possible through the use of the vehicle dynamics controller present on the vehicle, and through the use of the SyNaPs protocol, which is being implemented on the Formula Electric 2012 vehicle. The SyNaPs simplifies the overall control structure of the central wing controller significantly, resulting in a very simple control algorithm for the wing, which is discussed in detail in the appendix. Shown in Fig.31 is the logic flow of the system, from the perspective of the wing controller.

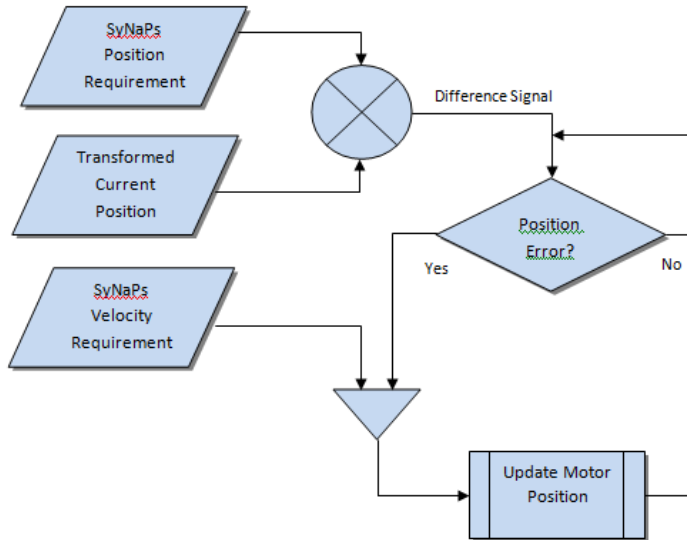


Figure 31. Logical Flow – Active Aerodynamic Controller [30].

The use of this type of a layout eliminates the need for a powerful processor to handle the control elements of the active aerodynamic features, provided that a link with the vehicle dynamics controller can be established using SyNPs. If this link is not present, the option exists in the developed code to allow for manual control of the wing for position and velocity.

2.4.1 Design and Analysis of Control System

In order to meet the requirements of the design, the overall actuation system was designed to utilize a full featured control system. The control circuitry, as detailed previously, is a multi-component digital system that provides a dynamic control capability to the overall design. The main components of the system are: the motor controller, the feedback system, and the programmable logic unit used for instrumenting the system. In the following sections of the report, each of these subsystems is discussed in detail.

2.4.1.1 Motor Controller

The control system associated with the motor is what is known as a ‘black box’ style controller. The meaning of these terms comes down the concept of computational domains, and the understanding that each system in the vehicle only requires a very select amount of information from the rest of the vehicle, and only needs to provide a select amount of the



implementation chosen for the system, as shown in Figure 32, was to utilize a black box system around the motor controller in order to deal with oscillatory behaviour of the motor system, actively track higher order statistics of the motor controller, and to be able to provide higher motion control.

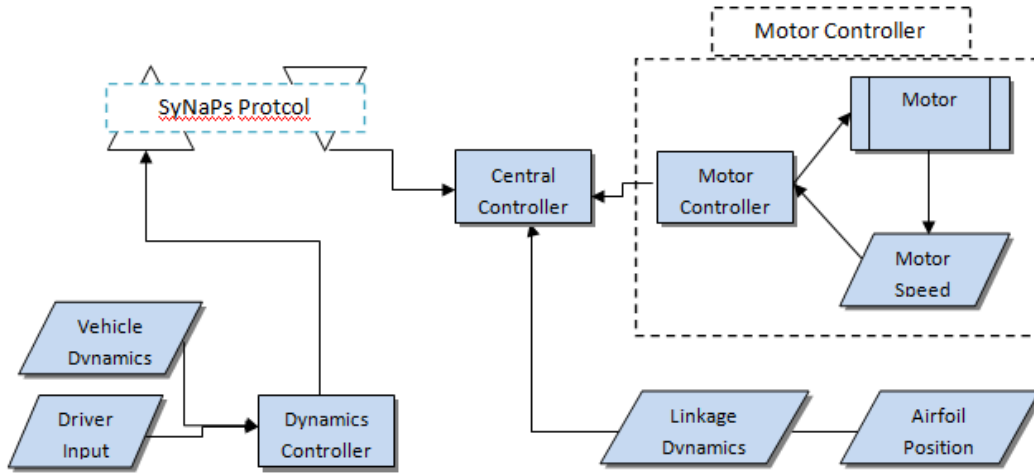


Figure 32. Chosen Control System Topology [30].

The importance of oscillatory response control is critical in the aero design field, as the vibrational response of air is significant and where stability control is required due to the effectively low stiffness of a fluid medium system. The ability for the system to cope with oscillatory behaviour comes from a high pulse rate correction system, and the ability for the system to provide micro corrections to motion.

The importance of higher order tracking is combined strongly with the need to provide higher order motion. The addition of down force provides a complicated interaction with the vehicle, due to the points of application of the aerodynamic force. The application of a force such as an aerodynamic load acts at a sufficiently large distance from the centre of gravity of the car, and therefore, causes a shift in the weight of the car by changing the effective weight distribution of the car [31]. The shift in weight from front to rear has a tendency to upset the balance of the car, and often causes significant and potentially catastrophic side effects if it is applied too quickly [31]. A first order control system is only able to linearly apply this force,



which is not ideal, because the need for aerodynamic force does not translate into a linear requirement. With the need for higher order control, the issue becomes the bandwidth of data required. For a system to process all of the actuation feedback such as driver input, vehicle dynamics, etc., the bandwidth is already rather high. With the addition of the motor feedback, and position feedback, the overhead of the system increases greatly, and it becomes necessary to look at increasingly complex systems. By replacing the more complex aspects of motor control with a single pre-controlled unit, the complexity drastically decreases, and the overall performance of the system can increase.

2.4.1.2 Feedback System

The feedback system for the active aerodynamic project was chosen to be a closed loop linear velocity feedback system. The need for a feedback system stems from the requirement to know where the wing is during actuation, and the requirement to have smooth motion control of the wing.

Since the wing is controlled using high gain motors, a proportional response is to be expected from the wing from a systems perspective. This response can be modelled such that the overall response of the wing is a function of the corrective gain of the motors. Since the motors only have local feedback through potentiometers inside the servo-electric drive elements, the requirement exists for a more global approach to feedback where the overall position of the wing is tracked. The addition of this feedback translates to a second order system, where a microcontroller can be used to provide a tuned PID control topology over the system.

For the feedback system, two different types of systems were looked at: rotary encoders and linear encoders. The use of rotary encoders was immediately ruled out, due to the requirement that the rotary output for these devices must be taken off the linkages. Since the linkages are moving elements, mounting the encoders would be very difficult and much care would need to be taken to place the encoders such that they do not foul the airstream. As such, the feedback component was chosen to be a linear encoder.



2.4.1.3 Programmable Logic Unit

The **programmable logic unit (PLU)** forms a cornerstone to the design, in that it is the overarching control element that all the inputs and outputs feed to. The choice of PLU was largely based on the design team's experience with various programmable controllers, and the ease at which a solid solution could be implemented. The solution that was chosen such that is:

- Compatible with the SyNaPs protocol that is proposed for the 2011/2012 vehicle
- Compatible with the existing power systems of the vehicle
- Able to perform first order control and feedback systems
- Able to control the servo-electric actuators that were chosen

Based on these tasks, the overall system was chosen as an Arduino based ATmega controller, due to its small size, and high level control capability. This system was checked for compatibility with the low voltage system [32] on the 2012 formula electric vehicle, as well as the SyNaPs control protocol [33].

2.4.2 Operation and Components of the Control System

From the preceding discussion, it can be seen that the overall control system of the car acts as a single unit from the interaction of several independent systems. The main components of the overall control system are the motor controller, the feedback system, and the programmable logic unit. The solutions presented in this section were developed in conjunction with the client's electrical specialists, such that the overall solutions were reasonable and general enough that they form baseline solutions. The solutions presented are therefore a minimum system requirement to ensure adequate performance of the system.

2.4.2.1 Motor Controller

The aforementioned motor control topology was used as a baseline for the selection process behind the control system. The overall requirements for the system are to provide a closed loop feedback system for the individual motors used. A Torxis i00600 actuator is recommended. This actuator represents a prepackaged servo-electric configuration where the



internals of the servo operate as a closed loop position control system. The internal controller for the servo is a high speed digital control system, which actuates an internal motor that is driven with a 1044:1 reduction. This internal motor is driven at high speed, and through a resistive feedback system, the overall position is controlled.

This type of controller is sufficiently suitable for the design, as the overall specifications of the controller meet the desired design requirements. The main points that were looked at, when compared to other alternatives, is the relative ease of integrating the built in traxis controller to the control topology. The simplified system diagram with the Torxis controller is shown in Figure 33, where the motor control element can be simplified to a simple off the shelf black box control element.

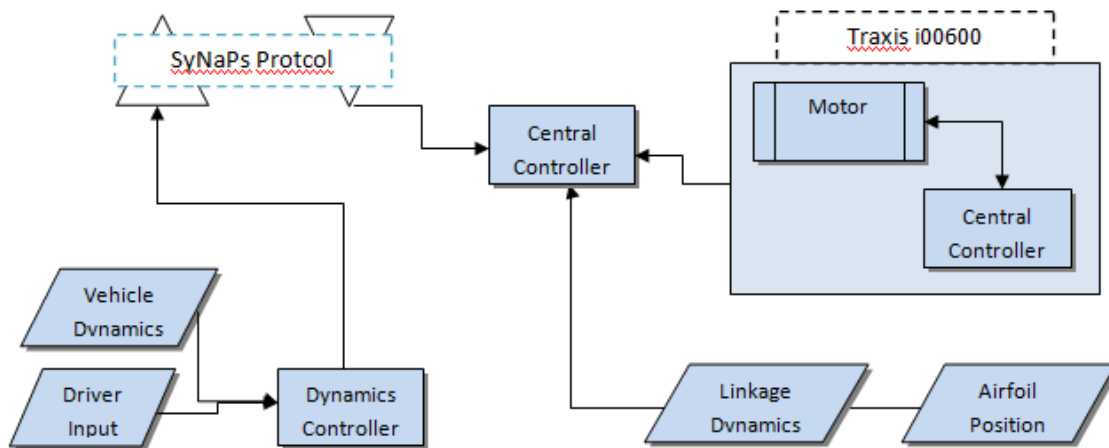


Figure 33. Updated System Layout – Black Box Motor Controller [30].

This simplification poses a strong design solution, in that the overall weight of the design significantly decreases in comparison with similar designs. A comparison to an equivalent drive design is a Parker Digiplan controller which also provides closed loop position feedback, but for stepper based systems. The advantage to the prepackaged system is that the overall footprint is significantly smaller, and that the heat dissipation capabilities are shared between the motor and the controller through the machined aluminum housing of the i00600. The overall size difference of the controllers is significant, as can be seen in Figure 34, where the parker stepper drive is approximately 6.5"x7.0"x3.0", which is compared to 5.9"x3.9"x2.4" size of the i00600.



This comparison indicates that the i00600 motor and controller is 40% of the size of just a similar capacity motor controller.



Figure 34. Parker PK3 Stepper Motor Drive – 6.5”x7.0”x3.0” [34].

Overall, the solution presented by i00600 integrated controller is one that captures the initial design intent, providing a solution that is compact, powerful, and accurate. The integration of a full closed loop motor controller in a pre-tested and off the shelf package represents a design that can easily be implemented to a high performance point, and does not require significant effort in terms of design or effort.

2.4.2.2 Feedback System

In order to gauge the overall performance of the control system and verify that the control parameters can be accurately judged and controlled, a closed loop position feedback system was chosen to be employed on the actual airfoil itself. In a global view, this feedback system is a redundant system that does not technically provide the system with any additional feedback as to the performance of the wing or the position of the wing. The purpose of this redundant feedback system is to account for the black box control element, which does not receive feedback from the overall wing position, and instead only receives data in regards to the angular position of the motors.

The attachment points for the feedback system were taken to be joint 2 and 4 on the linkage analysis as shown in Figure 35 , and as such the linkage dynamics can be calculated for



the system in relation to the angle of the wing itself. Shown in Figure 36 is a graph of the string pot extension as a function of crank rotation.

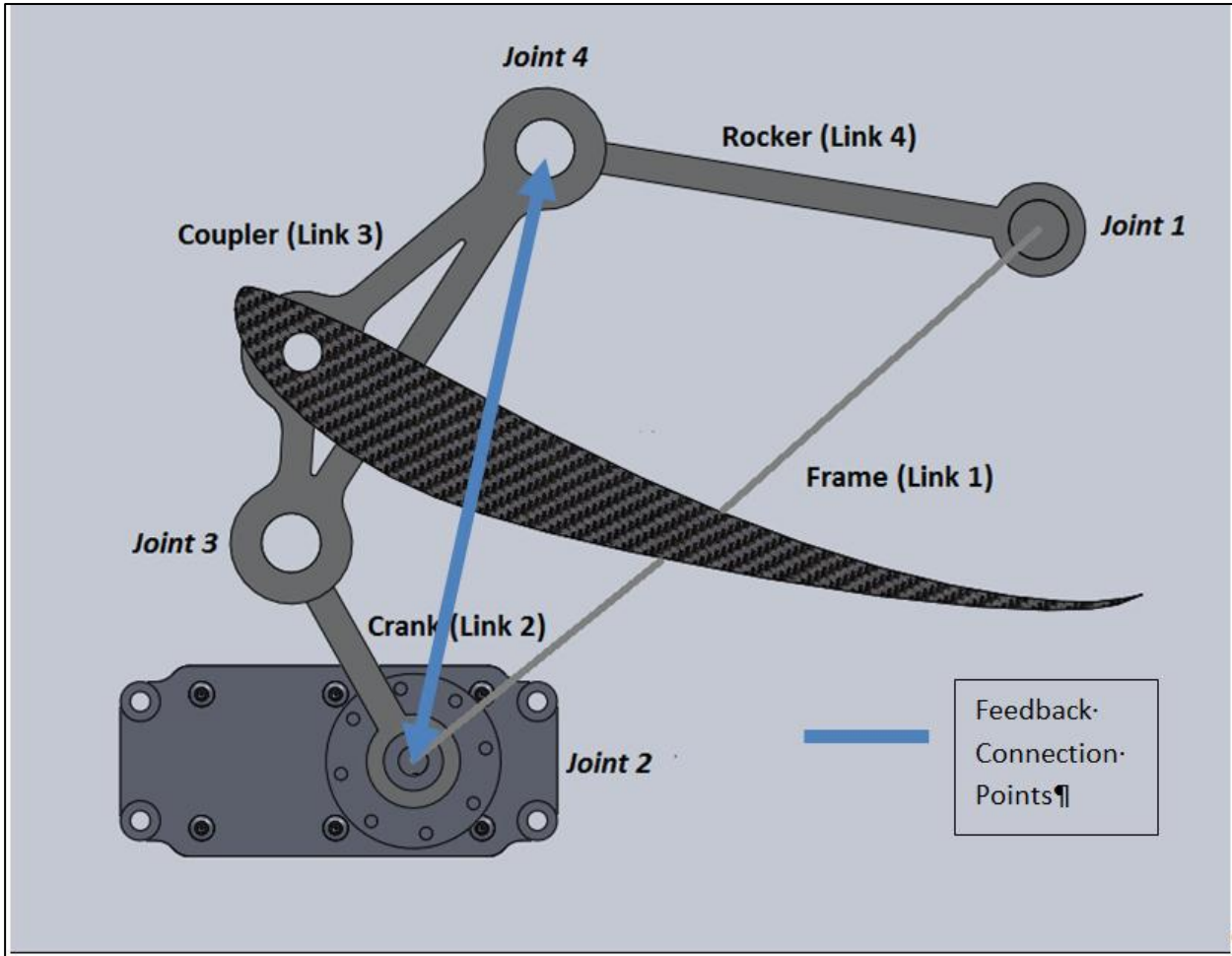


Figure 35. Attachment points for the feedback system [27].

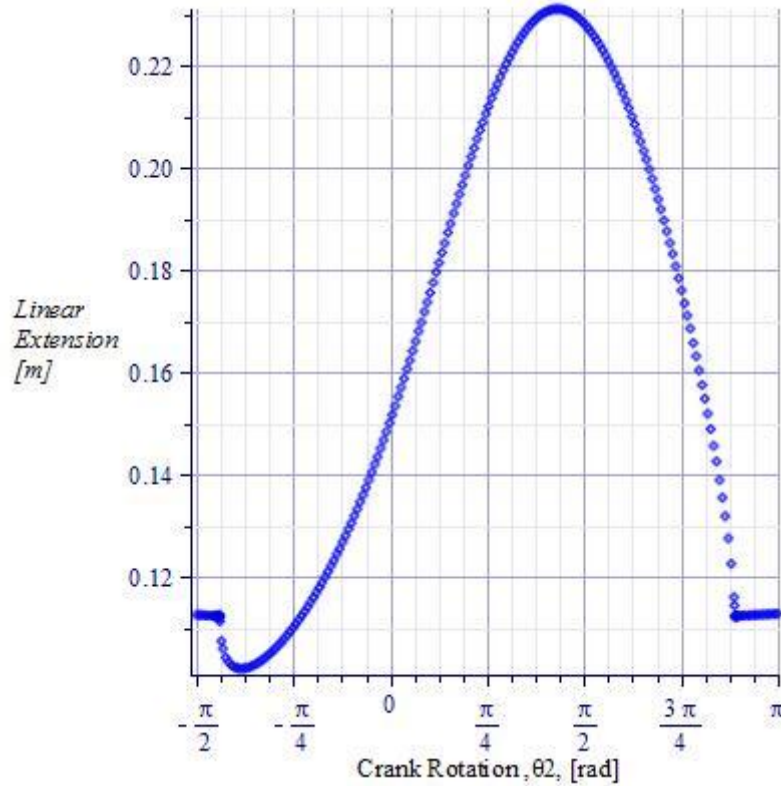


Figure 36. Non-Linear Transfer Function for Feedback Element [27].

The design recommendation for the feedback system is a linear string potentiometer, which measures linear changes in wing position, in a non-linear reference frame. The data from this system can be processed through the SyNaPs system, onboard the 2012 Formula Electric Vehicle, to provide a linear feedback on the position of the wing in relation to a measured linear deflection. Since the system is not necessarily required for implementation, it is only suggested here as a recommendation, and as such is not a fully developed solution. Therefore, three commercial designs are compared in the appendix, and the overall best system was found to be a linear string pot system. The recommended system, being one of the lightest commercially available systems, is a Celeesco SM-2.

The non-linear transfer function from the linkage analysis is well within the capabilities of the vehicle dynamics controller on-board the vehicle [33], and as such the system can feed only the required information to the programmable logic unit. Thus, the system topology can be updated to shift the burden of linkage dynamics conversion from the programmable logic unit



and shift that to the vehicle dynamics controller (SyNaPs node) that is present on the 2011 Formula Electric vehicle as shown below.

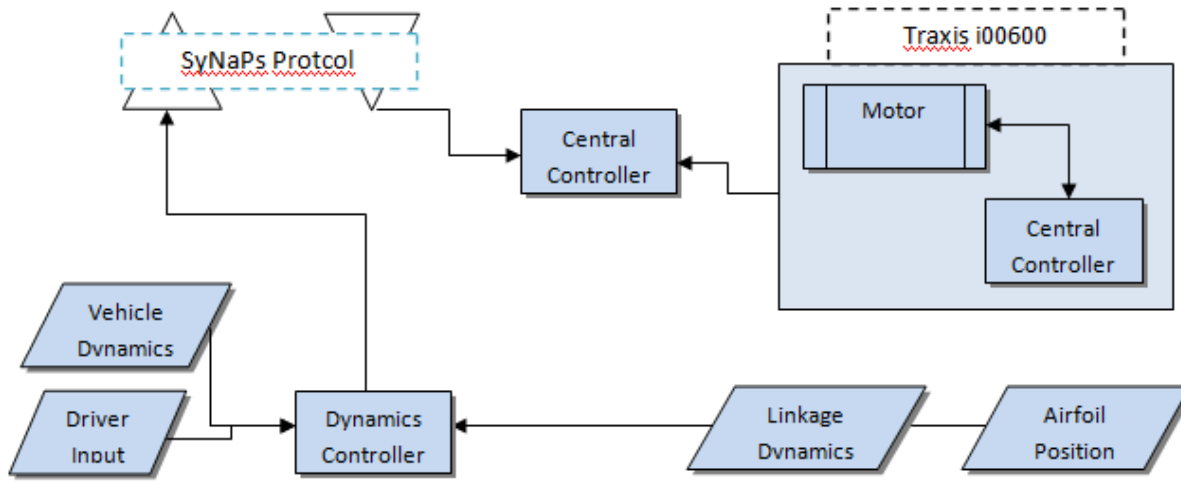


Figure 37. Updated System Layout – Feedback System [30].

2.4.2.3 Programmable Logic Unit

From the previous sections, the role of the SyNaPs protocol host to the system layout is clearly established, in that the PLU present in the design presented acts as a slave controller to the master nodal element. The master nodal element, in this case, would be the vehicle dynamics controller, which processes all of the input data. In consultation with the client [33], it was established that the overall role of the PLU for the design is to control the Actuation system, and accept feedback from the dynamics control via the SyNaPs protocol. This role differs greatly from what was initially anticipated, but provides a significant reduction in cost and complexity in the control system of the front wing, in that two entire feedback loops are eliminated. By allowing the controller to accept analog inputs, through a SyNaPs decoder, the overall system input requirements and data processing requirements are significantly decreased. Shown in Fig.38 is the Arduino board formally recommended for the project, the Arduino Uno.

The selected PLU device represents a powerful controller that runs at 16MHz and is capable of polling the required position from the SyNaPs protocol at 8000 samples per second



with a 10-bit resolution [35]. This resolution corresponds to a range of approximately 1000 possible position settings, over the 180 degree range of the motor rotation. When this capability is coupled with the feedback from the SyNaPs system, the remaining tasks for the PLU can be broken down into a functional flow-chart as shown below. The flowchart addresses the main processes that the PLU must perform, as well as a breakdown of the required logical functions of the PLU.

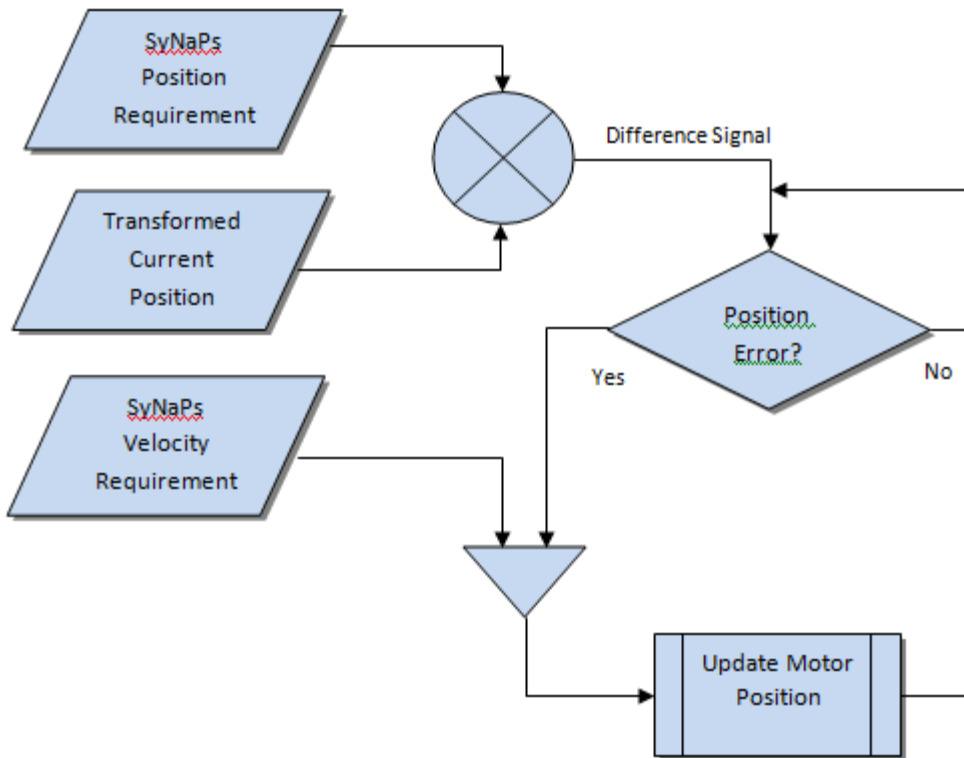


Figure 38. System Operation Flow Chart – Arduino Uno [30].

Based on the PLU choice, and the desired coding functionality, sample code was generated and is listed in the appendix. The sample code was written in the Arduino language. The coding captures this functionality, and accepts analog inputs for the position requirement, the current transformed position, and the velocity requirement. The output is the PWM signal required to drive the motor, with the output adjusting itself at the full sample capability of the Arduino on the input of the device.



The overall performance of the system is subjected to extensive testing and analysis to ensure that the system performs within the target spec, and this type of analysis is beyond the scope of the design report. A simple test was conducted using a sample servo library and is included in the appendix.

In summary, the PLU design presented for the front wing is a compact design that utilizes low weight and small size components to provide a highly repeatable closed loop control system for the design. Overall, a high performance solution is presented, which is in-line with the original design goals and the technical specifications for the control system.

2.4.3 Summary

The overall control system proposed for this design is one that is simple, and easily implementable. The design of the system was built around the idea that the electrical and computational load on the vehicle due to additional ancillary systems is as low as possible. The inclusion of complicated and higher order systems to control ancillary functionality on the vehicle is un-necessary and against the overall design initiative of the project. The SyNaPs system present on the car is an excellent example of this type of lean-electric design initiative, as it features a high level processor that is capable of controlling the entire car. The addition of one or more devices like this significantly lessens the computational burden on ancillary computational devices, and is therefore what the proposed design topology is based on as shown in Fig.39 . The overall layout shown uses the SyNaPs system to handle a significant amount of the computational load. This system takes the input of the driver, the vehicle dynamics, and the current airfoil position into account to control the actuation of the airfoil through the central controller for the airfoil. The amount of computational load ultimately led to the ability to use a low level control element, such as an Arduino Uno, for the airfoil control, as the overall control requirements were reduced to being well within the capability of the Arduino.

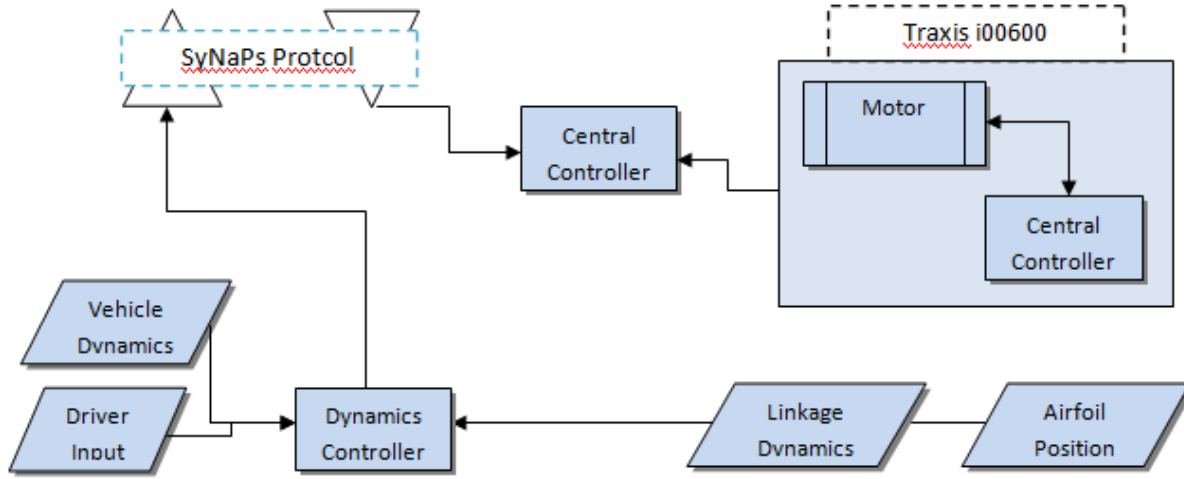


Figure 39. Finalized Overall System Layout [30].

The total system that was designed for the controls aspect required only 3 elements in total, all of which are purchasable and readily available. The overall system requires the following components: one Arduino Uno controller, two Traxis i00600 motors, and two Celesco SM-2 linear transducers. The nominal cost of this system, at the time of writing, is about \$800, which is a reasonable overall system cost. This cost will be greatly supplemented through the use of sponsorship, and is within the cost requirements of the client [33].

In summary, the system presents a solution for the control system that is compact, lightweight, and of reasonable cost. The design of the system is such that the capability exists for full automatic control, but as the client requested, the system can also provide manual control of the wings. It therefore meets all of the requirements of the client, and is within the implementation effort of the team.



3 Conclusion

The purpose of the project was to design an active aerodynamic front package in an effort to increase the performance of the UMSAE Formula Electric race car. The proposed aerodynamic design consists of a bi-plane wing arrangement, which allows adapting the angle of attack of the top wing for dynamic requirements of the race car while the bottom wing remains fixed at all times. Thereby, the performance envelope of the vehicle is increased in selected situations. The added performance of the proposed system outweighs the increased weight and complexity that such a system entails. Cost has been kept to a minimum to ensure economic feasibility of the proposed design.

The active airfoil can be rotated through angles of attack ranging from 28° to -28° . At a Reynolds number of 2.5×10^5 based on chord length, the airfoil exhibits several beneficial behaviors throughout this range of AoA. The performance increase associated with installing an active aerodynamic system on the UMSAE race car is estimated to improve steady-state cornering by 6% to 1.89g (active wing @ 13°). Alternatively, the car's straight-line braking could be improved by 8% to 2.04g (active wing @ 28°). Forces were calculated by means of simple hand calculations and validated by CFD software. The results show a delay in the stall of the airfoil with reduced ground clearance. The C_d of the stalled airfoil decreased with reduced ground clearance. As a result, the active wing was placed further up from the ground to ensure the maximum possible drag when the wing is stalled. This configuration is recommended to be used as an air brake supplementing the vehicle hydraulic brake system when necessary.

The control system design was addressed for proper implementation, without increasing the workload of the driver. However, driver input is still possible as the option to override the system is provided as well. Actuation system design as well as a cost analysis has also been performed to prove that further commitments to an active aerodynamic system are within the capabilities of the UMSAE Electric team.

A dynamic effect which was not covered by this project is dynamic stall. As previously mentioned, a rapid nose-down pitch motion of the chassis will increase the AoA at which stall



occurs for the active inverted airfoil. As the active aerodynamic system proposed for the UMSAE race car will alter the AoA rapidly, it may encounter this phenomenon. The effect of dynamic stall is beyond the scope of this project. It is recommended that extensive testing is performed prior to competition to ensure that the potential benefits of reduced lap-times are not at risk.



4 References

- [1] P. Labossiere, S. Young, F. Wheeler, P. Guerreiro, R. Lozowy (private communication), Sept. 16, 2011.
- [2] S. Young, (private communication), Sept. 16, 2011.
- [3] SolidWorks 2010. Vélizy, Ile-de: Dassault Systèmes SolidWorks Corp, 2010.
- [4] MATLAB version 7.13. Natick, Massachusetts: The MathWorks Inc., 2011.
- [5] N.Balakrishnan. (2011, Nov 30). *Mockup.sldasm*. Winnipeg, University of Manitoba.
- [6] T. D. Gillespie, Fundamentals of Vehicle Dynamics, Warrendale, PA: Society of Automotive Engineers, 1992.
- [7] SAE International. (2011, August 25) 2012 Formula HybridRules [Online]. Available: <http://www.formula-hybrid.org/pdf/Formula-Hybrid-2012-Rules.pdf> [October 2, 2011].
- [8] M. Alnouri (2011, Nov 21). “*Old cone.sldasm*”. Winnipeg, University of Manitoba.
- [9] M.Alnouri (2011, Nov 15). “*New cone.sldasm*”. Winnipeg, University of Manitoba.
- [10] M.Alnouri (2011, Nov 17). “*New cone_splitter_cowl.sldasm*”. Winnipeg, University of Manitoba.
- [11] M.Alnouri(2011, Nov 26). “*New cone_splitter.sldasm*”. Winnipeg, University of Manitoba.
- [12] X. Zhang. (2006). “Ground Effect Aerodynamics of Race Cars,” Applied Mechanics Review [Online], vol. 59 (1), pp. 33-50. Available: <http://scitation.aip.org.proxy1.lib.umanitoba.ca/journals/doc/ASMEDL-home/> [Oct 20, 2011].



- [13] J. Katz. (2006). "Aerodynamics of Race Cars," Annual Review of Fluid Mechanic [Online], vol. 38 (5), pp. 27-63. Available: <http://www.annualreviews.org/> [Oct 19, 2011].
- [14] D. J. Walter, "Study of Aerofoils at High Angle of Attack in Ground Effect," RMIT University, Melbourne, Australia, M.Eng. Thesis, September 2007.
- [15] M. S. Selig,J. J. Guglielmo, "High-Lift Low Reynolds Number Airfoil Design," JOURNAL OF AIRCRAFT, Vol.34, No 1, February, 1997.
- [16] M. S. Selig. UIUC Airfoil Data Site. [Online] Available: <http://www.ae.illinois.edu/m-selig/ads/afplots/s1210.gif>. [November 18, 2011].
- [17] "TH2G5.jpg" [Online] Available: http://www.centennialofflight.gov/essay/Theories_of_Flight/airplane/TH2G5.jpg [Dec. 2, 2011]
- [18] S.F. Hoerner, "Fluid-Dynamic Drag," Hoerner Fluid Dynamics, Vancouver, WA, 1965
- [19] M.Alnouri (2011, Nov 22). "*Low drag.sldasm*". Winnipeg, University of Manitoba.
- [20] M.Alnouri (2011, Nov 18). "*airbrake.sldasm*". Winnipeg, University of Manitoba.
- [21] M.Alnouri (2011, Nov 29). "*Max df.sldasm*". Winnipeg, University of Manitoba.
- [22] R. W. Fox, P. J. Pritchard, and A. T. McDonald, Introduction to Fluid Mechanics, 7th ed. Hoboken, NJ: John Wiley & Sons, INC., 2009.
- [23] F.Wheeler, S.Young, UMSAE Formula Electric, (Private Communication), Nov 29, 2011.
- [24] Maple~15 Programming Guide. Waterloo, ON: Maplesoft, 2011.



- [25] O. Vinogradov, Fundamentals of Kinematics and Dynamics of Machines and Mechanisms, 1st ed. Boca Raton, Florida: CRC Press, 2000.
- [26] M. Heiranian (2011, Nov 20). "*linkage.sldasm*". Winnipeg, University of Manitoba.
- [27] M. Heiranian (2011, Nov 15). "*Coupler angle.mw*". Winnipeg, University of Manitoba.
- [28] M. Heiranian (2011, Nov 26). "*Drag_velocity_crank angle.mw*". Winnipeg, University of Manitoba.
- [29] S. Young, F. Wheeler, (private communication), Nov.21, 2011.
- [30] N.Balakrishnan (2011, Nov 1) "*control topology.psd*". Winnipeg, University of Manitoba.
- [31] T. D. Gillespie, Fundamentals of Vehicle Dynamics, Warrendale, PA: Society of Automotive Engineers, 1992.
- [32] S.Gaudreau, UMSAE Formula Electric (2011, Nov 29). *Private Communication*.
- [33] G.Klassen, UMSAE Formula Electric (2011, Nov 29). *Private Communication*.
- [34] N.Balakrishnan. (2011, Nov 7). "*DSC_15159.jpg*". Winnipeg, University of Manitoba.
- [35] *The Arduino DAQ Chronicles - Measuring Stuff* [Online] Available: <https://sites.google.com/site/measuringstuff/the-arduino> [Nov.12, 2011].



UNIVERSITY
OF MANITOBA

5 Appendix

Nomenclature

AoA	angle of attack
$C\epsilon_1, C\epsilon_2$	k- ϵ turbulence-model coefficients
C_μ	k- ϵ turbulence-model coefficient
k	turbulence kinetic energy per unit mass (m^2/s^2)
P_k	turbulence production due to viscous
ϵ	turbulence dissipation rate (m^2/s^3)
ρ	density (kg/m^3)
μ	dynamic viscosity ($kg/(m \cdot s)$)
μ_t	eddy viscosity ($kg/(m \cdot s)$)
σ_k	turbulence model constant for the k equation

Table of Contents

1	Concept Search Phase.....	70
1.1	External Search	71
1.1.1	Literature Search.....	71
1.1.2	Racing Implementations and Competing Designs Search.....	73
1.2	Internal Search	77
2	Concept Analysis & Selection.....	80
2.1	Generation of Down Force.....	80
2.1.1	Concept Generation.....	81
2.1.2	Concept Screening	84
2.1.3	Concept Scoring	86
2.2	Control Systems	87
2.2.1	Technical Background	87
2.2.2	Concept Generation.....	89
2.2.3	Concept Screening	91
2.2.4	Concept Scoring	93
2.3	Actuation Mechanisms	95
2.3.1	Technical Background	95
2.3.2	Concept Generation.....	96
2.3.3	Concept Screening	99

2.3.1	Concept Scoring	100
3	Summary and Conclusion of Concept Analysis.....	102
4	Discussion.....	103
4.1	CFD Analysis	104
4.1.1	CFD Setup	104
4.1.2	CFD Results.....	107
5	Cost and Manufacturing	109
6	Lift and Drag Characteristics of S1223 Airfoil	111
7	Relevant Competition Rules.....	113
8	Coding for Main Control Elements.....	116
8.1	Class Wrapper for Servo Library	117
9	References	119

List of Figures

Figure 1. End Plate on a Formula Race Car	72
Figure 2. Example of an Under Body Diffuser	73
Figure 3. Lotus 49B.....	73
Figure 4. Minimal Drag Mode - The yellow Colour represents the Airflow of the blocked Passage	75
Figure 5. 2011 Sooner Racing Team Car with the active Aero Wings.....	76
Figure 6. Sketch 1 - Generation of Down Force	81
Figure 7. Sketch 2 - Generation of Down Force	82
Figure 8. Example of 32-bit Processor.....	88
Figure 9. Concept Generation Sketch - Control Systems	89
Figure 10. Concept Generation Sketch - Actuation Mechanism.....	98
Figure 11. Mesh Overview of CFD Analysis	105
Figure 12. Detail view of critical Mesh Refinement Area.	105
Figure 13. Velocity Plot for High Down Force Configuration.....	107
Figure 14. Velocity Plot for Low Drag Configuration	108
Figure 15. Velocity Plot for Airbrake Configuration	108
Figure 16. Lift Characteristics for the S1223 airfoil at $Re = 2 \times 10^5$	111
Figure 17. Drag Polar for the S1223 airfoil.....	112

List of Tables

TABLE I: METHODS USED FOR SEARCHING	70
TABLE II: TRIZ EVALUATION	77
TABLE III: TRIZ PARAMETERS.....	78
TABLE IV: TRI-STROMING RESULTS	79
TABLE V: INITIAL CONCEPTS - GENERATION OF DOWNFORCE	82
TABLE VI: CONCEPT SCREENING MATRIX - GENERATION OF DOWN FORCE	85
TABLE VII: WEIGHTED DECISION MATRIX – GENERATION OF DOWN FORCE	86
TABLE VIII: METHOD OF EVALUATING GENERATION OF DOWN FORCE CONCEPTS.	86
TABLE IX: INITIAL CONCEPTS - CONTROL SYSTEM.....	90
TABLE X: CONCEPT SCREENING MATRIX - CONTROL SYSTEM.....	92
TABLE XI: ANALOG/DIGITAL COMPARISON.....	93
TABLE XII: WEIGHTED DECISION MATRIX – CONTROL SYSTEM	94
TABLE XIII: THE METHOD OF EVALUATING CONTROL SYSTEMS CONCEPTS.....	94
TABLE XIV: INITIAL CONCEPTS - ACTUATION MECHANISM	96
TABLE XV: CONCEPT SCREENING MATRIX - ACTUATION MECHANISM	100
TABLE XVI: WEIGHED DECISION MATRIX – ACTUATION MECHANISM	101
TABLE XVII: THE METHOD OF EVALUATING ACTUATION MECHANISM CONCEPTS.	101
TABLE XVIII: MATERIAL AND FABRICATION COST OF THE DESIGN.....	110

The appendix is used to supplement the information presented in the body of the report. Herein, the concepts which were considered in the development of the final design and the associated selection criteria & analysis are presented. Furthermore, a detailed discussion of how the design meets the requirements, including a technical analysis and simulation to verify its strength and performance, are offered.

In order to facilitate the implementation of the proposed design, recommended assembly and manufacturing principles as well as a detailed cost analysis are also specified. The first section addresses the concept search phase as follows.

1 Concept Search Phase

The first step of the process of concept generation was to search for solutions from external sources. For example, implementations of similar concepts done by other teams participating in Formula SAE competitions were investigated as well as similar designs from racing applications. The client was also interviewed for any ideas or information regarding the problem. Other external sources, such as journal articles and patents were utilized. After completing the external search, an internal search was conducted, which consisted of using the Theory of Inventive Problem Solving (TRIZ) and brainstorming to generate possible design concepts. TABLE I tabulates the methods used in the concept search phase.

TABLE I: METHODS USED FOR SEARCHING

Type of Search	Methods	Sources
External	Patent Search	Google patents, USPO
	Literature Review	Compendex, Google Scholar, and ENGbase.net
	Client Interview	UMSAE Formula Electric Team
	Racing Implementations Search	Technical articles
	Competing SAE Teams Concept Search	FSAE.com discussion forums, Videos, Pictures
Internal	TRIZ	Team
	Brainstorming	Team

1.1 External Search

The section of the report dedicated to external searches is broken down into two further sub sections. The first subsection addresses findings from the performed literature search which is followed by a presentation of the search results from former and current racing implementations and competitors' designs.

1.1.1 Literature Search

Today's race cars are enhanced by incorporating aerodynamic features into their designs, thereby optimizing the ratio of down force to drag. However, before such a feature can be implemented, the characteristics of the air flow over the race car must first be obtained. This characterization of the flow is mostly done by means computational fluid dynamics, wind tunnel testing and track testing. Several methods of producing down force have been suggested, such as the addition of aerodynamic wings to the car, modifying vehicle's body aerodynamic shape, etc. [1].

One common method to create down force is to add aerodynamic wings to either the front or rear of the car. Engineers and designers first attempted to utilize the airplane wings on the race cars. However, this attempt was found to be unsuccessful due to several differences between the aerodynamic nature of cars and airplanes.

The first point is that the race car wings, especially the front wings, are very close to the ground as opposed to airplane wings. Basically, the effect of viscosity near the ground generates a boundary layer flow, which is termed the ground effect. The ground effect increases the amount of down force, which is favourable in race car designs. However, designers also account for the ground clearance and the fact that ground effect increases drag to an extent.

The second point is that the aspect ratio, defined as wing span divided by the chord length, is really small in the case of race cars. A small aspect ratio results in relatively high drag which is undesirable. Therefore, large plates are being attached to the end of race car wings in

order to reduce the effect of drag and increase the lift-drag ratio. Figure 1 shows an end plate on a formula race car.

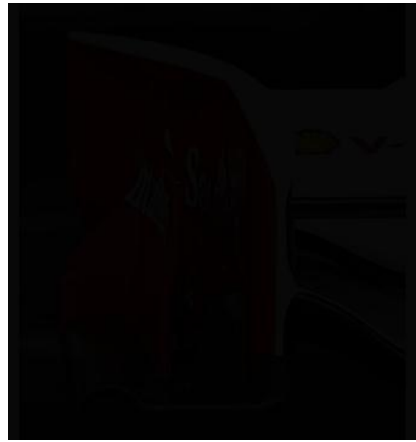


Figure 1. End Plate on a Formula Race Car [2] Permission pending.

The third difference between airplanes and race cars that has helped engineers to design better race cars is the level interaction between the wing and the vehicle's body. For example, the down force due to a rear wing increases as the wing is moved backward [1], [3].

Another method of producing down force in race cars is to enhance the aerodynamic shape of vehicle's body so that it generates more downward force. The only method that is allowed based on race car competition rules is employing an under body diffuser beneath the side pods of a race car, which is shown in Figure 2. The amount of down force increases as the ground clearance decreases. Basically, the under body diffuser is analogous to a situation where the air under the car is sucked by a set of fans which reduce the air pressure and result in high amount of down force [1].

The general methods of generating down force have been examined in the preceding discussion. In the following section of the report, the different formula car designs will be addressed. The aerodynamic features of each design will be examined in order to aid with the concept development for the UMSAE Electric vehicle. Features proven to be beneficial for similar applications will be considered further.



Figure 2. Example of an Under Body Diffuser [4]. Permission pending.

1.1.2 Racing Implementations and Competing Designs Search

Teams in Formula 1 have incorporated aerodynamic elements in their car designs since the late 1960s [5]. The first car to include a front wing for aerodynamic purposes is the Lotus 49B in 1968, shown in Figure 3. A generic airfoil shape was mounted on both sides of the front nose on the car [5].



Figure 3. Lotus 49B [9]. Permission pending.

In the 1970s, all of the teams were implementing aerodynamic elements on their cars [5]. At this point, some teams started experimenting with adjustable aerodynamics [5]. Ideas such as ground effect fans, and levitating wings were implemented [5]. Due to safety hazards and team budget control regulations, rules were put into place preventing actuated or powered aerodynamic elements in Formula 1 cars [5]. Therefore, teams had to be creative in developing designs that produce high amounts of down force with minimal drag effect on straightaways [5].

In 1997, Scuderia Ferrari implemented a concept that involved flexible wings [7]. The front wing of the car would deflect depending on the velocity of the airflow. At high speeds the front wing would flex and bend towards the ground, producing ground effect, which resulted in higher down force while producing minimal drag on straightaways. The present Formula 1 regulation stated that the front wing had to be a certain height above the ground [7]. This design was essentially a work around for producing higher down force while still remaining within the regulations.

The SAE Formula Electric competition rules do not dictate the height of the front wing with respect to the ground. Therefore, the team would not have to resort to such a design. But the idea of flexible wings is interesting, and could be incorporated in various ways. For example, the front wing's shape could be manipulated by an actuated mechanism using cables. The manipulation would produce a high down force shape when cornering, and a flatter shape on straightaways, resulting in minimal drag.

In 2010, McLaren developed a concept popularly known as the F-duct. The F-duct reduced drag effects of the rear wing at high speeds [8]. The design comprised an airflow passage that the driver blocks by covering it with his forearm. This motion would result in directing air towards the rear wing of the car, thereby disrupting the airflow, which otherwise passes through the driver's compartment. The concept in low-drag mode is shown in Figure 4.

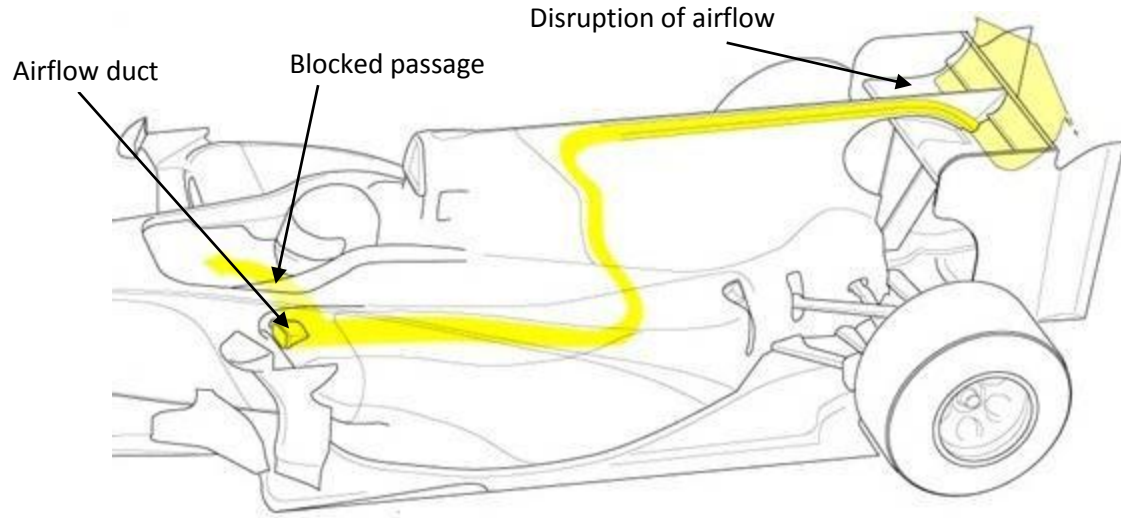


Figure 4. Minimal Drag Mode - The yellow Colour represents the Airflow of the blocked Passage [9]. Used with Permission.

When cornering, the driver would not block the passage; consequently, air would vent into the cockpit, and the rear wing's airflow would not be disrupted, thus generating down force due to the wings shape. The technique allows the driver to minimize drag effect when down force is not needed. Similar to the flexible wings concept, this was developed to bypass the stringent Formula 1 regulations governing active aerodynamic devices. The concept of redirecting air by passages to produce variable down force effects may present a suitable solution for the UMSAE Electric vehicle.

The NACA duct design, one of the concepts developed as part of this report, is derived from same principles as the F-duct concept. It redirects air through a passage at the nose of the car. When the passage is open, it directs air from the front upper surface of the car towards the underbody creating a ground effect, thus resulting in down force. At high speeds this passage would be blocked by a driver controlled plate, which would eliminate any drag effects. This design incorporates the main design principles of the F-duct, but the addition of the driver controlled plate results in a design that is much more adjustable when compared to the F-duct concept.

Another method that was employed during concept generation is searching for implementations of other SAE competitors. However, any documentation related to SAE teams'

designs is hard to obtain. Attempts made in contacting teams regarding any documentation on their designs went unanswered. Information had to be gathered from pictures, videos, and online forum discussions as our sources instead.

Teams participating in SAE formula competitions have been focusing increasingly on implementing aerodynamic packages in their cars. Most of these implementations are non-adjustable systems. The University of Oklahoma's Formula SAE team, Sooner Racing Team, implemented an aerodynamic system that incorporated adjustable front and rear wings in their 2011 car [10]. The car is shown in Fig. 6.



Figure 5. 2011 Sooner Racing Team Car with the active Aero Wings [11]. Permission pending.

Based on observation of a video showing this design in operation, the major elements of their design were determined [10]. The system uses segmented curvilinear airfoils for the front and rear wings to generate down force [10]. Based on intuition and observation, the system most likely utilizes an electric motor for actuation, and is controlled digitally based on vehicle dynamics parameters such as steering input, suspension travel, etc. The various elements of the system were considered during the concept development for this project.

1.2 Internal Search

Several contradicting elements were faced when dealing with needs of our client. The most prominent contradiction is to generate down force when cornering while having minimal drag when on a straightaway. The Theory of inventive Problem Solving (TRIZ) was utilized to gain insight on possible solutions.

TRIZ is a method used for finding possible solutions when encountering contradictions in satisfying the requirements of a design [12]. It is a matrix that consists of 40 rows and 40 columns. The columns are the improving feature, and the rows being the worsening feature. An improving feature of a design would be matched by its worsening feature. The cross linked cell shows possible design principles that can be used to overcome the problem.

For example, the contradiction of high down force and low drag are plugged in as TRIZ parameters. Force is the improving feature while loss of energy is the worsening feature. The cross linked cell shows TRIZ principles, curvature and dynamics as possible solutions to the contradiction [13]. The use of curvature when designing an airfoil can reduce the compromise between down force and drag to an extent [14]. The other proposed TRIZ principle is the use of dynamics. Several concepts have been developed which are dynamically adjustable for high down force when cornering and low drag on straightaways.

Another TRIZ principle that was utilized is segmentation. It deals with contradictions related to adjustability and complexity of control. TABLE II shows the design contradictions we faced and the corresponding TRIZ solutions.

TABLE II: TRIZ EVALUATION

Contradiction	TRIZ Principle	
<i>Improving Feature</i>	<i>Worsening Feature</i>	
Force	Loss of energy	Curvature, dynamics
Adjustability	Complexity of control	Segmentation
Stability of Object	Weight of moving Object	Taking out, skipping, parameters changes, inert atmosphere
Ease of manufacture	Complexity of System	Segmentation, copying, cheap short-living objects

Detailed descriptions of the TRIZ principles are provided below. After familiarization with the contradictions and their possible TRIZ solutions, the team went on to the process of generating ideas by tri-storming.

TABLE III: TRIZ PARAMETERS [12]

TRIZ Principle	Description
1 Segmentation	Divide an object into independent parts.
2 Taking Out	Separate an interfering part or property from an object.
14 Curvature	Instead of using rectilinear parts, surfaces, or forms, use curvilinear ones.
15 Dynamics	Design the characteristics of an object, external environment, or process to change to be optimal or to find an optimal operating condition.
21 Skipping	Conduct a process or certain stages at high speed.
26 Copying	Instead of an unavailable, expensive fragile object, use simpler and inexpensive copies.
27 Cheap Short-Living Objects	Replace an inexpensive object with a multiple of inexpensive objects, comprising certain qualities.
35 Parameter Changes	Changes an object's physical state.
39 Inert Atmosphere	Add neutral parts, or inert additives to an object.

Several ideas and concept designs were conceived in order to collect a list of methods to implement the front aerodynamic system. The tri-storming process started by dividing the design into three different major components, namely generation of down force, control systems and actuation mechanisms. Each of these design components was separately discussed by the team and different ideas that could possibly satisfy the design requirements were generated for each component. Table V outlines the outcomes of the tri-storming process. The detailed sketches of these concepts are provided in the respective section addressing each component. As seen in TABLE IV, some of the concepts for the generation of down force were further expanded into more concept designs. For example, the general idea of producing down force using a rotating cylinder itself embraces three expanded concept designs namely a typical cylinder, variable diameter and a drawstring bridge rotating cylinder. The next section of the report will address the analysis of concepts to select a final one.

TABLE IV: TRI-STROMING RESULTS [16]

Main Component	Generated Concept Title	Expanded Concept Title
Generation of Down Force	Solid Airfoil	Tail Rotation
		Center Rotation
		Path Motion
		Micro Motion
		A-Arm
		Out of Plane
		Fabric
		Flexible
		N-Part Structure
		Segmented
		Telescoping
	Rotating Cylinder	Typical
		Variable Diameter
		Drawstring Bridge
Control Systems	Splitter	None
	Profile Modification Nose Cone	None
	NACA Duct FCD Wing	None
	Resonance	None
	Active Airfoil Channel	None
	Air Suction	None
	Digital	None
	Analog	None
	Driver Controlled (Variable)	None
	Driver Controlled (Instantaneous)	None
Actuation Mechanism	Passive Mechanical (Sensing)	None
	Active Mechanical (Driven)	None
	Pneumatics	None
	Electric Motors	None
	Hydraulics	None
	Elastic	None
	Pulley	None
	Linear Actuator	None
	Electromagnetic	None
	Shape Memory Alloy	None

2 Concept Analysis & Selection

The attributes of a front aerodynamic system were divided into several sub-categories in order to focus the concept generation on the most critical needs of the customer. These sub-categories are generation of down force, control systems, and actuation mechanisms. Several concepts with the desired attributes emerged for each of the sub-categories as a result of the internal and external searches.

The concepts were put through a sequential refinement process, which is documented in the following sections. Step 1 of the refinement process consisted of a simplified technical & cost analysis, where each concept was assessed for its technical and economic feasibility with respect to the allotted resources. Concepts with potential for further development were selected in step 2 by screening and scoring matrices based on a set of criteria, which reflects the customer's needs. Finally, the results of a sensitivity analysis were paired in an attempt to integrate and fuse the most promising characteristics of the remaining concepts in step 3. A summary of the refinement process is given at the end of this section.

2.1 Generation of Down Force

The primary component of the aerodynamic system design is the method of down force generation. The method used to generate down force plays a fundamental role in how the system operates, as it largely dictates how the overall design is laid out and how it performs. Normally the process of concept generation, screening, and analysis is only performed on full featured concepts, but in the case of this project an iterative approach was used. By breaking the problem down into the sub-systems, the design problem can be decoupled such that each individual aspect can undergo a rigorous concept development without expanding the scope of the design excessively. To start this process, the main concepts for the method of down force generation will be discussed.

2.1.1 Concept Generation

The first major component of the design is the generation of down force, which addresses the key aerodynamic aspect of the design. Initially, the team developed seven different concepts, which are shown in TABLE V. Sketches of these concepts are provided below.

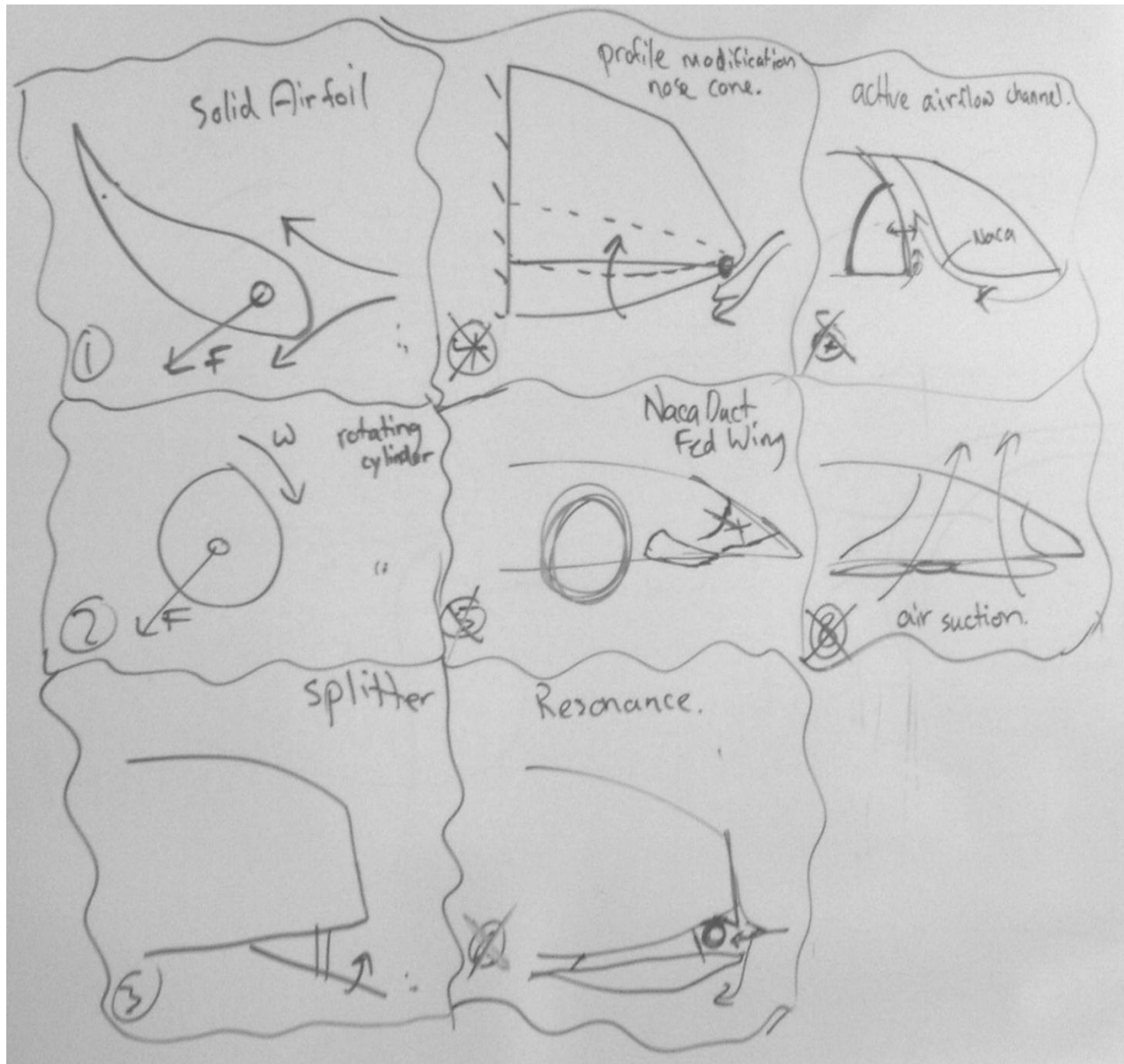


Figure 6. Sketch 1 - Generation of Down Force [16]

TABLE V: INITIAL CONCEPTS - GENERATION OF DOWNFORCE [16]

Generation of Down Force: Concepts Ideas

- 1 Solid Airfoil
- 2 Rotating Cylinder
- 3 Splitter
- 4 Profile Modification to Nose Cone
- 5 NACA Duct fed Wing
- 6 Resonance
- 7 Active Airflow Channel
- 8 Air Suction

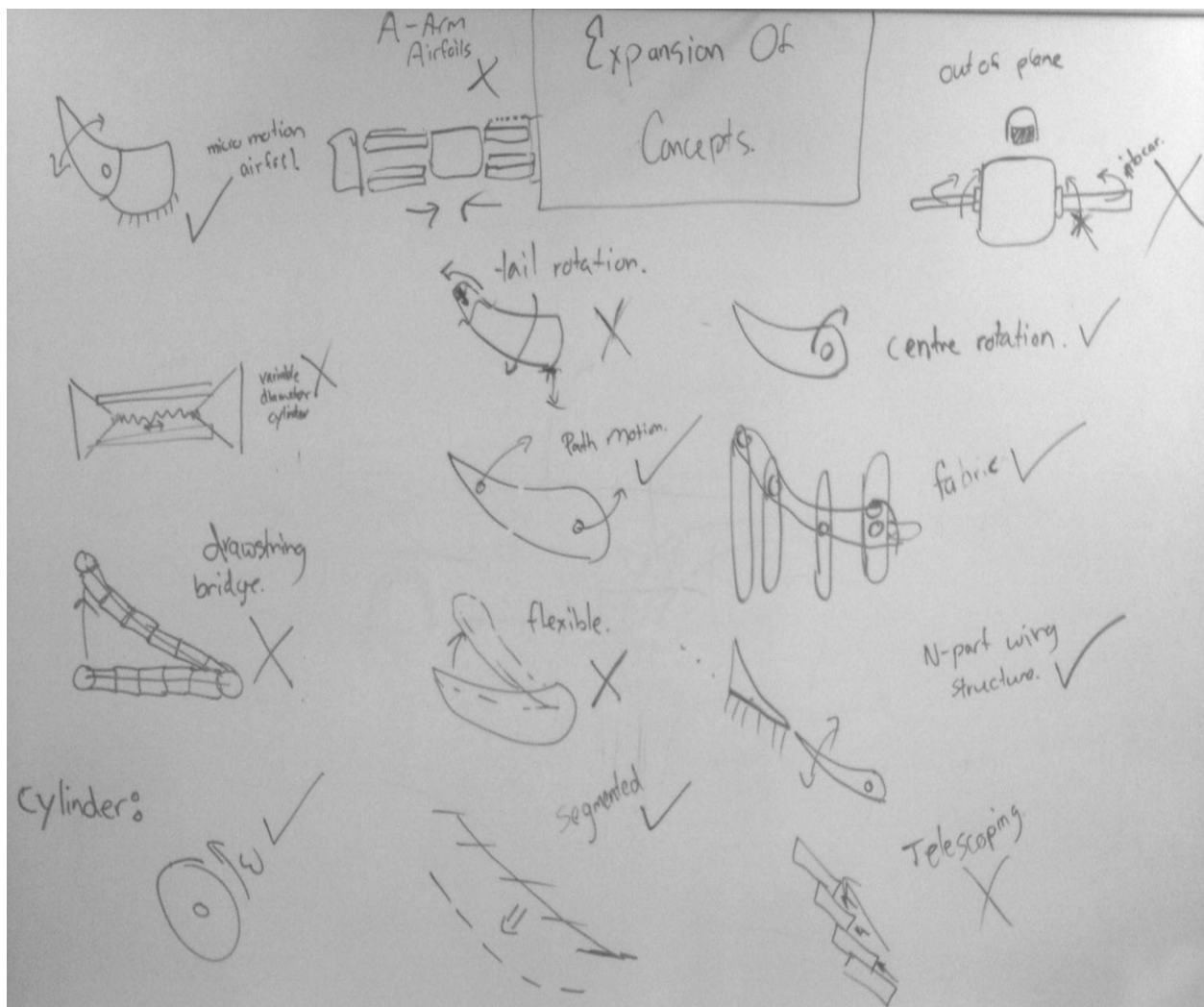


Figure 7. Sketch 2 - Generation of Down Force [16]

Prior to screening the concepts and ranking them, a preliminary analysis was performed on all of the concepts listed. This preliminary analysis was a feasibility study and involved basic calculations to look at the feasibility of all of the concepts. The preliminary analysis was considered an important part of the concept generation process, since the design that will ultimately be chosen has a stringent manufacturing and implementation criterion. The design must be implementable by the Formula Electric team within a reasonable timeframe and cost. Based on the analysis, the concepts that were eliminated were concepts 3, 5, and 6.

Concept 3 was eliminated for the distraction it may cause to the driver. Furthermore, it can potentially have high margins of error in terms of timing of actuation. Concept 5 was eliminated for its inflexibility in terms of function. Added value features, such as an air-brake cannot be implemented. Ambient conditions and high speed manoeuvring can lead to inaccuracies that potentially make the system obsolete. Concept 6 was eliminated based on the high complexity associated with designing the system. Mechanical interlocks would have to be implemented to start/stop the actuation. Additionally, approximating the required down force based on the wheel speed alone would lead to highly inaccurate actuation of the system.

2.1.2 Concept Screening

The first step of the screening phase was to define a stringent set of evaluation criteria. These criteria form the basis of the concept screening and evaluation sections, and therefore control the outcome of the project to a great extent. In order to satisfy the client's needs, the evaluation was drawn from the needs and specifications. To complement this information, the main criteria for evaluation were not only approved by the client, but also by each member of the design team to assure that the needs and specifications set out by the client were met.

The quantification of the needs was done such that each concept could be weighed against a performance scale for each criterion and evaluated accordingly. For reliability, concepts that had few failure modes or redundancy were desired, and designs that were prone to catastrophic failure were ranked lower. Drag and performance were somewhat contrary criteria in most cases, but were separated for cases which posed a unique solution to the down force/drag problem. These cases were generally seen in ideas that used unconventional means to produce down force, and as a result these designs were favoured strongly. Designs that had high amounts of drag and low performance were ranked poorly. For the simplicity criterion, the main focus was to look at the number of moving components. The goal was to obtain a solution that was ultimately as simple as possible without sacrificing performance.

Designs that had many moving parts or were generally complicated were ranked very low for this category. On the other hand, designs that had few moving parts were ranked very high. Cost was based on the expected implementation cost of each concept, which included preliminary estimates of the material and labour cost associated with the designs. The purpose of this estimate was to help promote the screening of expensive and complicated concepts. Manufacturability was approached from the perspective of the estimated build time of each concept. Concepts that could be implemented easily in the 2012 car would be rated very high, whereas concepts that required excessive implementation effort would be weighted much lower. Adjustability was evaluated based on the capability of each concept to be readily adjustable. Concepts that provided infinite ranges of adjustability were weighted very high. Designs that only had a single setting were given very low rankings. Ruggedness was judged

primarily on the overall toughness that each design could be built to and incorporated the needs of endurance and strength that the client desired. Designs that would not handle the competition environment well were ranked very low and designs that could endure the impacts and collisions with competition obstacles like pylons were ranked very high. Added value was primarily a measure of how easily the design could implement features such as an air-brake, or how innovative a design is. This category was left open, and generally designs were ranked high if they were either strong performers or innovative.

TABLE VI: CONCEPT SCREENING MATRIX - GENERATION OF DOWN FORCE [17]

Criterion	Path Motion	Micro Motion	Rotation	Fabric	Segment	N-Part	Cylinder
Reliability	–	0	+	–	–	0	0
Drag	0	–	0	+	+	–	–
Performance	+	0	+	+	+	+	0
Simplicity	0	0	+	–	–	+	+
Cost	+	0	+	–	0	+	–
Manufacturability	+	0	+	–	–	+	0
Weight	0	0	–	+	–	+	–
Adjustability	+	0	+	+	–	0	–
Ruggedness	–	0	+	–	–	+	+
Added Value	+	0	0	+	+	0	+
Score	+3	-1	6	0	-3	5	-1
Decision	✓	✗	✓	✗	✗	✓	✗

2.1.3 Concept Scoring

From the screening processes performed, only the top concepts were taken and scored. This elimination ensured that the design process remains focused on a narrow range of possible concepts, each of which was carefully evaluated for suitability to the client's needs and specifications. A weighted decision matrix is shown in TABLE VII below, which assigns weights to the selection criteria from the previous section and facilitates the numerical comparison of the different concepts. The evaluation criteria used for these concepts are listed below.

TABLE VII: WEIGHTED DECISION MATRIX – GENERATION OF DOWN FORCE [17]

Criterion	Weight	N-part	Rotation	Path Motion
Drag	0.15	10	0	6
Performance	0.30	5	10	9
Simplicity	0.25	5	10	8
Weight	0.10	8	4	7*
Adjustability	0.20	10**	0	8*
Score		6.9	6.2	7.9
Rank		2	3	1
Decision		x	x	✓

TABLE VIII: THE METHOD OF EVALUATING GENERATION OF DOWN FORCE CONCEPTS FOR EACH CRITERION [17].

Numerical Evaluation	0 %	50 %	100 %
Criterion			
Performance	Lowest power-to-weight ratio	Middle power-to-weight ratio	Highest power-to-weight ratio
Drag	Multiple failure modes	Few failure modes	Back-up built in
Weight	Highest in options	Middle in options	Lowest in options
Simplicity	Highest amount of parts	Moderate amount of parts	Lowest amount of parts
Adjustability	Highest in options	Middle in options	Lowest in options

Example:

For performance, generation of down force is considered to have the highest lift-to-drag ratio which corresponds to 100 % or a value of 10. The lowest lift-to-drag ratio is evaluated to be zero. All other concepts are linearly interpolated.

What can be seen from this selection process is that the clear winner was the Path Motion concept. This is not surprising when the above criteria are taken into consideration, as the concept represents an overall well rounded concept. In terms of drag, the concept is not the best performing, but it scores consistently high across all criteria. Therefore, the lower score is acceptable. In terms of adjustability, the concept is bested only by the N-Part concept. The N-Part concept would provide a higher level of adjustability, but would come at great cost, poor reliability, and considerable implementation effort.

In summary, the Path Motion concept was chosen as the best concept after the assessment of all the alternatives was completed. The evaluation of the control system is presented in the following section.

2.2 Control Systems

The second major component of the design is the control system, which consists of the type of data needed to control the actuation mechanism, and how that data is transferred. A control infrastructure allows the design to vary the performance of the front aerodynamic system, as well as to optimize its performance for a specific situation. The adjustability satisfies both the primary need of changing aerodynamic performance between straight line and cornering situations and optimizing the wing performance for a specific event. In the technical analysis below, the various control methodologies are discussed to provide a background to the screening process.

2.2.1 Technical Background

Due to the myriad of ways in which a driver can interact with a vehicle, control systems play a powerful role in motorsports. Through control systems the driver interaction with the vehicle can be optimized. In past years, the vehicles that have been designed by the Formula Electric team have been predominantly driven with the aid of several control systems. These controls normally account for systems that do not require driver interaction, or cannot be efficiently controlled by the driver.

An example of such a system is the regenerative braking system whereby the brake force from the electric motors is gradually blended in with the brake force from the mechanical brakes. This example shows that the human control element would not be a very powerful one in some situations, due to the control capability and workflow of the driver. If the driver was given control of the individual brake force distribution, then controlling the regenerative break would become part of the driver's workflow every time the brake pedal is pressed. This situation is not ideal because the driver has to focus on handling the vehicle to the best of his abilities. The addition of another item into the driver's workflow would reduce the driver capabilities.

In the past, systems such as regenerative breaking were strongly limited by control capability, but modern controls, such as the ones shown in the Fig. 7 below, are easily capable of handling this complex task.



Figure 8. Example of 32-bit Processor [15]. Permission pending.

The addition of a small, discrete controller adds little in terms of weight, power requirements, and safety measures. In exchange, the controller allows a level of control higher than what has been used in the past for high end consumer electronics. As a comparison, the depicted 32-bit processor is more powerful than the engine computer in a 90's race car engine, yet is available at even a hobbyist level. Digital controls such as this are a powerful tool, and represent only one of the major control elements discussed in the concept generation section.

2.2.2 Concept Generation

Initially, the team agreed on six different concepts, which are shown in TABLE IX. Sketches of these concepts are provided below.

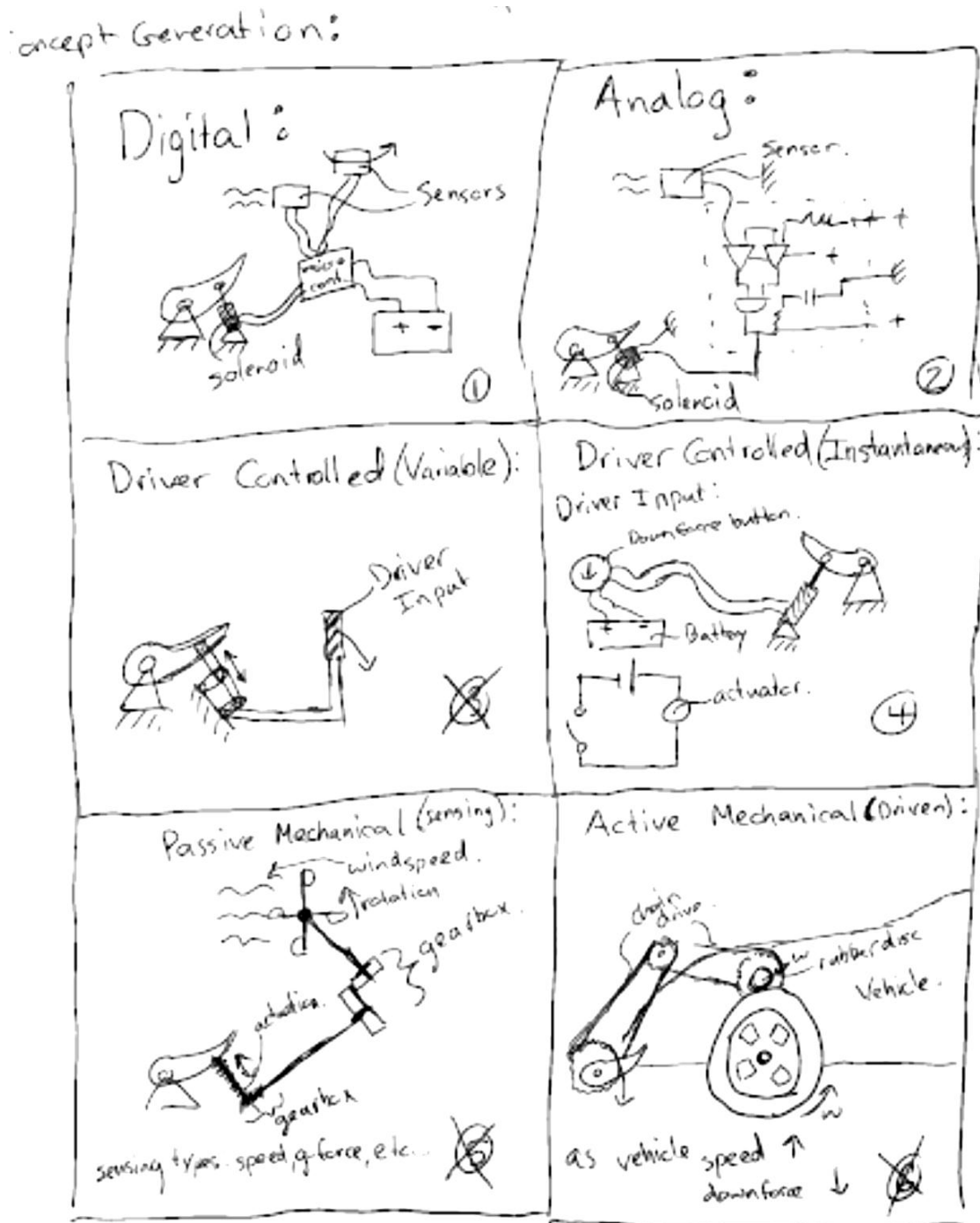


Figure 9. Concept Generation Sketch - Control Systems [16]

TABLE IX: INITIAL CONCEPTS - CONTROL SYSTEM [16]

#	Control Systems Concept
1	Digital
2	Analog
3	Driver Controlled (Variable)
4	Driver Controlled (Instantaneous)
5	Active Mechanical (Driven)
6	Passive Mechanical (Sensing)

Prior to the concept screening phase, a feasibility study was performed on all of these concepts. This study involved initial calculations and evaluations to determine if any/all of the concepts would be feasible ideas. This study was performed to keep the concept generation process as general as possible, but also to make sure that any ideas pushed to the concept scoring process were feasible ideas. As a result, the following concepts were removed and deemed unfeasible: 3, 5, and 6. Concept 3 was eliminated after consultation with the client, as it was deemed to be in conflict with the original design intent. The inclusion of manual proportional control in the driver workflow was deemed to be unacceptable. The ability for the driver to predictably control the system was suspect.

Concepts 5 and 6 were eliminated for similar reasons, as they both represent similar mechanical control schemes. Both designs would suffer from significant mechanical noise requiring isolators/damping to mitigate and have a slow mechanical response time to system changes. In addition, there would be difficulty in adjusting performance parameters, and the inability to respond differently to straight-line and cornering situations. This feasibility analysis left concepts 1, 2, and 4 as feasible design concepts, which were then pushed forward to the concept screening process.

2.2.3 Concept Screening

Once the initial design concepts were evaluated for feasibility, the concepts were further screened in order to select the best designs for full scale conceptual review. The concept selection level was increased such that a more detailed measure of concept performance could be attained. Selection criteria were established for the control systems aspect of the concept design, based on the needs outlined by the client. The criteria were performance of the system, reliability, driver ease, and adjustability.

These four criteria represent important aspects of the design to the client, and were therefore the main categories that the concepts were evaluated on. These criteria and the relative performance of the top concepts from the previous technical analysis are shown below in TABLE X.

Performance was a measure of the overall contribution of the concept to the performance of the system. This includes the ability to allow adaptive down force adjustment, system tuning, added value implementation capabilities, and system response capabilities. Reliability was a measure of how easy it was for the system to fail. Systems that had several modes of failure were ranked low, whereas systems that had redundancy and few failure modes were ranked high. Driver ease was another criterion, and was strongly based on the effect of the control system on the driver's workflow. Concepts that could easily be incorporated into the driver's workflow, or required little to no driver input scored high, whereas concepts that had a high level of driver input scored low. Finally, adjustability was taken into account, as the manual adjustability of the design was a critical need. Designs that could easily be manually adjustable were preferred in this case.

TABLE X: CONCEPT SCREENING MATRIX - CONTROL SYSTEM [17]

Criterion	Digital	Analog	Driver Controlled	(Instant)
Performance	+1	0	-1	
Reliability	+1	0	+1	
Driver Ease	+1	+1	-1	
Adjustability	+1	0	-1	
Score	+4	+1	-2	
Decision	✓	✓	✗	

As can be seen above, the overall screening process clearly favoured the analog and digital control system concepts over simple push-button approach. This was an expected outcome, as the push button concept can only provide limited performance due to single button actuation. In addition, it comes at the expense of interfering with the driver's workflow. This selection was further refined below by comparing the digital and analog systems in TABLE XI. This table looks at the different types of sensors that could be used with the two different control schemes. The types included speed sensors, G-force sensors, GPS technology, and Vehicle Dynamics.

Speed sensors would provide a measure of the forward speed of the vehicle from the mechanical wheel speed sensors on the car. G-force sensors were considered as the strain gauge sensors on the car, with the data about the lateral G-force extracted from the real-time data. GPS sensing would use a mobile GPS module to detect vehicle heading and location, and vehicle dynamics would take into account the various vehicle statistics available from onboard the vehicle such as acceleration and brake force required.

TABLE XI: ANALOG/DIGITAL COMPARISON [16]

Criterion	Digital	Analog
Speed	✓	✓
G-Force	✓	✓
GPS	✓	✗
Vehicle Dynamics	✓	✗
Score	4	2
Decision	✓	✗

In TABLE XI, the various sensing methods were compared for the two candidate screened concepts. The different sensing methods represented general concepts that could be used with a full electric control system, such as the two screened concepts. The sensing concepts are rather abstract at this level, such that the design is not constrained, but are included to provide a general direction for the detailed design phase. From the above comparison in TABLE XI, it is clear that the digital system can do everything that the analog system is capable of with additional capabilities. From this understanding, the analog system was replaced with the digital one before the concept scoring section, as there were no notable downsides to the digital system compared to the mechanical one that could be found.

2.2.4 Concept Scoring

From the concept screening above, only the top control system concepts were brought forward into the in-depth concept scoring process. This process represents a high level of concept analysis, where each concept is judged against a strict selection criterion through a weighted decision matrix, shown in Table XII below. The selection criteria itself was pulled forward from the screening section and the weighting for this criterion was done in conjunction with the client. The rubric used to evaluate the concepts with respect to each of these criteria can be found in TABLE XIII.

TABLE XII: WEIGHTED DECISION MATRIX – CONTROL SYSTEM [17]

Criterion	Weight	Digital	Digital GPS	Digital Vehicle	Digital G-
		Speed		Dynamics	Force
Cost	0.1	10	0	6	8
Performance	0.4	5	10	9	8
Adjustability	0.1	5	10	8	8
Reliability	0.3	8	4	7*	5
Implementation	0.1	10**	0	8*	5
Score		6.9	6.2	7.9	6.8
Rank		2	3	1	4
Decision		x	x	✓	x

TABLE XIII: THE METHOD OF EVALUATING CONTROL SYSTEMS CONCEPTS FOR EACH CRITERION [17].

Numerical Evaluation	0%	50%	100%
Criterion			
Cost	More than \$300	Between \$100 and \$300	Between \$0 and \$100
Performance	Does not accurately predict needed down force	Reasonably predicts needed down force	Accurately predicts needed down force
Adjustability	Cannot be adjusted	Can be adjusted manually	Self adjusted
Reliability	Likely to fail	Has few failure modes	Has backup modes
Implementation	Needs electrical and computer engineering expertise	Requires some effort to learn and implement	Can be implemented with ease

Example:

For performance, a digital GPS controlled system is expected to have great accuracy which corresponds to 100% or a value of 10, while a digital speed controlled system would reasonably predict down force needed, thus having a numerical value of 50% or a value of 5. All other concepts are linearly interpolated (digital vehicle dynamics = 8, digital g-force = 9).

What can be seen from this selection process is that the clear winner was the vehicle dynamics sensing technology with the digital control system. This is not surprising when the above criteria are taken into consideration, as the concept represents an overall well rounded concept. In terms of cost, the concept is not the cheapest, but considering the budget of this project is not heavily constrained, the lower score is acceptable. In terms of performance and

adjustability, the concept is bested only by the GPS based technology. GPS technology would provide a higher level of accuracy and depth of results, but would come at great cost, poor reliability, and considerable implementation effort. In terms of reliability and implementation effort, the vehicle dynamics concept is also the second best, only behind the speed sensor based approach. This is the key factor for this concept and the main reason for its high overall score, as the concept scores high in these sections. This high score is primarily due to the ability to reduce the implementation effort and failure modes of the system, as it has already been tested and implemented on the car. Existing instrumentation is an important factor to account for, as it represents the cost that the Formula Electric team has invested in the control system. It also represents the ability to utilize past work to improve the new design.

In overview, after generation, screening, and scoring was decided to be a digital control system with vehicle dynamics sensors.

2.3 Actuation Mechanisms

The final component of the design is the actuation system, which consists of subsystems that manipulate and modify the mechanism of creating down force. The actuation system allows the design to vary the performance of the front aerodynamic wing. It acts as an interface between the control system and the desired method of generating down force. To a large extent, it controls the way in which the design operates. The technical background for this section is discussed below.

2.3.1 Technical Background

Actuation systems have been around since the development of electric machines, and form the basis of industrial automation and motion. The principle use of electric machines was originally to simplify the human motions required to operate a mechanism, and as such actuators have been continually developed to meet these needs. An actuator, simply put, is a device that is capable of translating energy from a given form to kinetic energy. Common engineering energy inputs include hydraulic, electric, pneumatic, and potential energy storage methods. This stored energy can then be delivered as an output in the form of kinetic energy

through: rectilinear motion, curvilinear motion, rotary motion, or other types of motion. Of particular interest to this report is the topic of electric rotary actuators (motors) which can be obtained in many different configurations.

Electric rotary actuators are a very powerful type of actuator, in that they can be combined with linkages to perform a variety of motions. Through a linkage which can selectively constrain and control the rotary motion of the actuator, a rotary actuator can be used to provide almost any type of motion desired. In 3.1, the concept of linkages was introduced with the path motion concept, which was ultimately chosen as the desired method of generating down force. The path motion concept can also be applied to electric actuators in order to allow variable and adjustable motion profiles. With technologies like this, it is clear that the method of actuation is a decision that weighs heavily on the final design, and therefore the next section will look at proposed actuation method concepts.

2.3.2 Concept Generation

The team recognized eight different possible ways of implementing actuation mechanisms for the front aero package, and these concepts are named in TABLE XIV below.

TABLE XIV: INITIAL CONCEPTS - ACTUATION MECHANISM [16]

#	Actuation Mechanism Concept
1	Pneumatics
2	Electric Motors
3	Hydraulics
4	Elastic Actuator
5	Pulley
6	Linear Actuator
7	Electromagnetic
8	Shape Memory Alloy

As part of the concept generation stage, a feasibility study was performed on all of the major concepts before proceeding to the concept screening phase. Concept 3 represents a

powerful concept in many other applications, as hydraulics is one of best concepts available for minimizing weight and size of a system. These are all strong factors for front aerodynamic package design, but the dynamics of the actuation method were not deemed feasible for use. Through rough analysis, it was determined that the required response speed of the system far surpassed that of conventional light hydraulic systems; therefore, the concept was removed [6]. Concept 4 also presented an interesting idea, but the physics of the concept were deemed to be non-workable. The idea was based around the use of an elastic member that interacts with the down force generated by the wing to naturally allow the wing to change angle as the speed changed.

However, this type of motion is not possible to be performed by this concept, and therefore the concept was removed. Finally, shape memory alloy actuators (concept 8) were considered for an actuation mechanism, but were removed due to the inability for the actuators to handle the continual actuation required. Considering that the life cycle of many of the actuators considered was less than the actuation cycles required for a single endurance race, the concept was removed. With the initial feasibility analysis complete, the concept screening process was carried through on the remaining concepts.

Concept Generation:

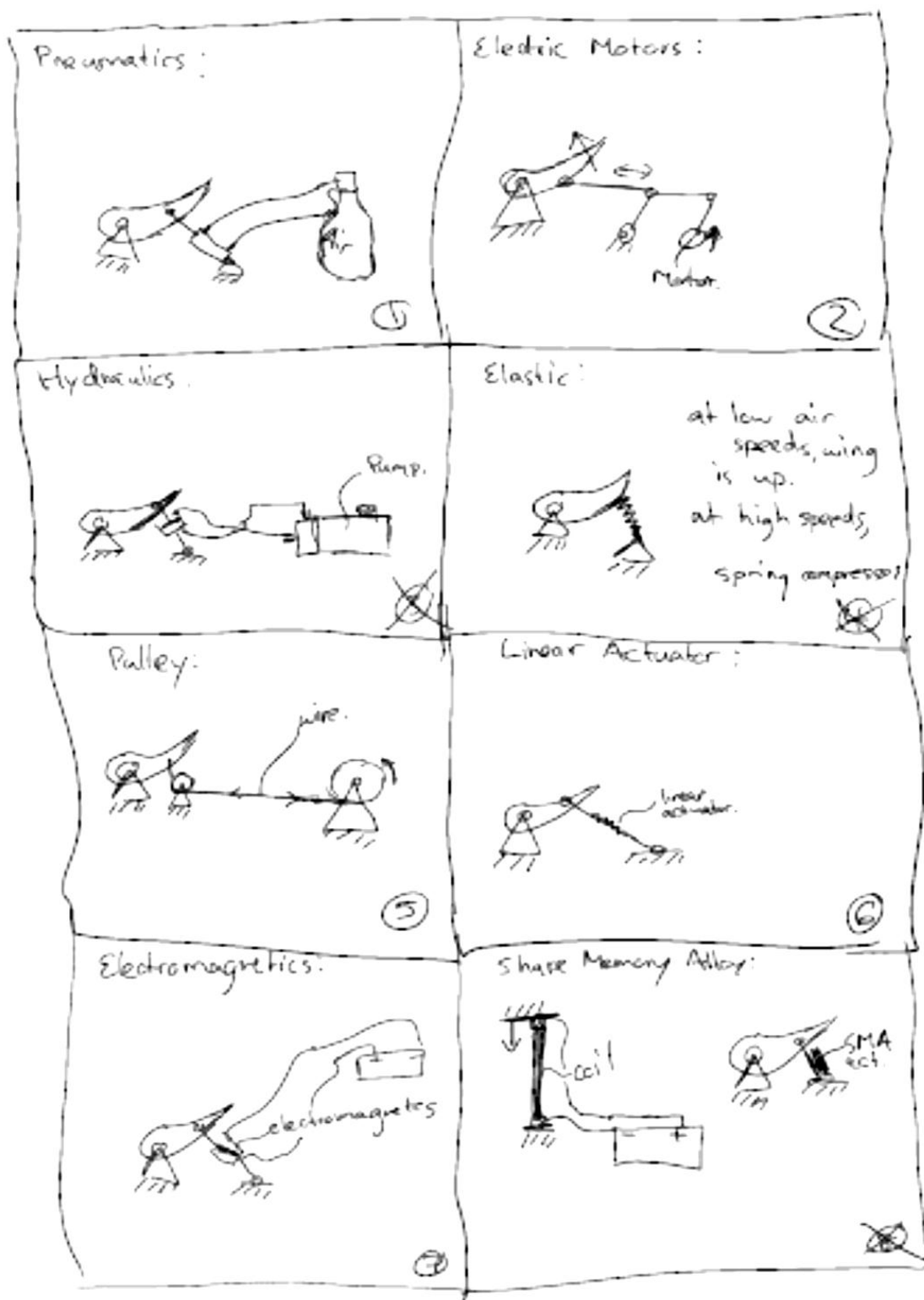


Figure 10. Concept Generation Sketch - Actuation Mechanism [16]

2.3.3 Concept Screening

Similar methodology as described in the preceding sections was applied to the concept screening of actuation mechanisms. The same criteria were used, namely system performance, reliability, weight, variable response ability, response speed.

These five criteria represent important aspects of the design to the client. Consequently, they were the main categories that the concepts were evaluated on. Performance was a measure of the overall contribution of the concept to the performance of the system. This contribution includes the ability for the actuators to receive the correct control signals and accurately control the amount of down force available to match the control input. Reliability was a measure of how easy it was for the system to fail. This criterion was evaluated in the same fashion as it was done in the previous sections. Weight was a large consideration for the overall design and was judged according to a strict rubric. Designs were ranked from lightest to heaviest, including the designs previously screened out, and designs that were lighter were judged accordingly in the selection process. The response criteria are both similar, but represent very distinct needs. The ability for the wing to have variable response by having intermediate down force settings was highly desirable, and was a strongly weighted need. The ability for the wing to respond quickly was also deemed an important characteristic. To address both of these needs, designs that would have fast and infinitely variable responses were desired. Designs that were slow and had non-variable responses were not favoured. Once the selection criteria were established, the concepts were compared based on the defined criteria. The results of the screening are outlined in TABLE XIV. As shown, the linear and electromagnetic actuators were eliminated since they failed to meet most of criteria. For example, electromagnetic actuators only satisfy the need for a reasonable fast response speed and exhibit poor responses to the rest of the criteria. Pneumatics, electric motors and pulley-type actuators worked out to have positive scores, and hence the team decided to continue with these three concepts

TABLE XV: CONCEPT SCREENING MATRIX - ACTUATION MECHANISM [17]

Criterion	Pneumatics	Electric Motors	Pulley	Linear	Electromagnetic
Performance	-1	+1	+1	0	-1
Reliability	+1	+1	0	0	-1
Weight	+1	0	0	-1	-1
Variable Response	-1	+1	+1	-1	-1
Response Speed	+1	0	0	-1	+1
Score	+1	+3	+2	-3	-3
Decision	✓	✓	✓	✗	✗

2.3.1 Concept Scoring

From the concept screening above, only the top actuation method concepts were brought forward into the in-depth concept scoring process. This process represents a high level concept analysis, where each concept is judged against strict selection criteria through a weighted decision matrix, shown in Table XV. The selection criteria itself was pulled forward from the screening section and the weighting for each criterion was done in conjunction with the client. The rubric used to evaluate the concepts with respect to each of these criteria can be found in Appendix A.3.

The three remaining concepts were evaluated according to a weighted method of scoring which has also been used for the preceding concept evaluation sections. The weight of each criterion was specified based on the UMSAE Formula Electric team's needs. For example, the overall performance of the design has the highest weight while the speed of actuation response only accounts for 10 percent of the total weight. The outcomes of this scoring evaluation are shown in Table XV. The electric motors exhibit the highest score among the three concepts; therefore, the electric motor based actuator was chosen as the team's final design for the actuation mechanism. What can be seen from the above analysis is that the electric motor concept was clearly shown to be the best concept design.

TABLE XVI: WEIGHED DECISION MATRIX – ACTUATION MECHANISM [17].

Criterion	Weight	Pneumatics	Electric Motors	Pulley
Performance	0.3	10	7	8
Reliability	0.2	5	10	7
Weight	0.2	8	10	5
Variable Response	0.2	0	8	5
Response Speed	0.1	10	6	5
Score		6.6	8.3	6.3
Rank		2	1	3
Decision		✗	✓	✗

TABLE XVII: THE METHOD OF EVALUATING ACTUATION MECHANISM CONCEPTS FOR EACH CRITERION [17].

Numerical Evaluation	0 %	50 %	100 %
Criterion			
Performance	Lowest power-to-weight ratio	Middle power-to-weight ratio	Highest power-to-weight ratio
Reliability	Multiple failure modes	Few failure modes	Back-up built in
Weight	Highest in options	Middle in options	Lowest in options
Variable response	No variability	Finite variability	Infinite variability
Response speed	Slow response	Reasonable response	Almost instant

Example:

For performance, pneumatics is considered to have the highest power-to-weight ratio which corresponds to 100 % or a value of 10. The lowest power-to-weight ratio is evaluated to be zero. All other concepts are linearly interpolated (pulley=8, electric motors=7).

This is not very surprising, as the motor design will have a tendency to have an equal performance in comparison to the pulley design, without having the deductions in complexity and reliability that come with the pulley wire and the springs required by that system. Once the weights of the various criteria were factored in, it became clear that a risky/non-adjustable design like the pneumatic one would not be favoured, even if it was the best performing and the quickest responding system. Overall, an electric motor was selected as the target actuation system.

3 Summary and Conclusion of Concept Analysis

In closing, this section serves as a summary for the conceptual design process that was used by KHAB Design & Engineering. The overall process was performed with the client's needs and requirements as the very top priority. Throughout the process the goal has been to produce a concept that is not only a simple yet reliable solution that the client can easily implement, but also to provide the client with an innovative design that meets their needs.

The previously developed set of needs and specifications was supplemented with research about the background of the problem and extensive work with the client to establish a solid base for the design process. Using the overall constraints, a series of external searches was performed, examining research databases, patents, competitor's designs, racing implementations to develop potential solutions. From the external search it was found that there were no existing designs that would be directly transferrable to address the needs of the client, and therefore a series of internal searches including tri-storming and TRIZ was used to search for concepts solutions. Using this knowledge, the design problem was broken down into its major subsystems: the method of generating down force, the control systems, and the actuation mechanisms for the front aerodynamic package. Concepts were developed for each subsystem, in an iterative process, and evaluated against the client's needs. It was decided to proceed with a digitally controlled four-bar link based wing design, actuated by electric motors, that uses vehicle dynamics and driver input as a primary method of adjustment.

Overall, the concept presented is a radical design that is innovative, but still meets all of the UMSAE Formula Electric Team's needs. The concept overall represents a reasonable and reliable method of having a variable front aerodynamic package, and has been designed with the teams capabilities and schedule in mind.

4 Discussion

The design of an intricate system such as a race car always demands that the designers make certain compromises to find the optimal solution. Previous studies have been dedicated to the aerodynamic limitations and requirements of a SAE race car [18], [19], [20]. The trade off between down force and drag has been deemed acceptable, as properly designed fixed wings offer an overall benefit to the performance of an SAE car. The potential performance benefit of using wings is further increased through mechanisms that allow for a variable **angle of attack (AoA)**. Such an active aerodynamic element offers numerous advantages, which the Formula Electric team intends to exploit in order to improve the performance of their vehicle at competition.

The wings on race cars typically consist of multi-element wings. A multi-element wing provides much higher lift in comparison with a single element wing of similar dimensions. The design presented in this report consists of a two-element structure. The design combines a fixed wing, placed at the bottom in close proximity to the ground, with an actively controlled wing that is elevated and placed further downstream. The mechanism to actively control a single wing is a lot simpler than that for several active elements. The implementation is therefore greatly facilitated on the Formula Electric vehicle. Moreover, the effective study of an active multi-element wing would require a lot more time due to the increased number of setup variables and complexity of the air flow. The essential benefit of the single element is the simplicity of the design while ensuring that the clients' requirement for down force is met.

The air flow over an open wheeled race car falls in the category of ground effect aerodynamics. For the most part, this area of study is still an experimental science. The reason for mandatory experiments is the lack of accuracy of numerical results as these methods are simply unable to accurately predict the complex fluid flows involved. Computational models can accurately describe flows over static objects. However, the suspension motion of the UMSAE vehicle, when it travels around the autocross track, leads to unsteady flow, which produces vortices and a turbulent wake as it travels over the vehicle and interacts with several components of the car and the ground boundary layer.

Nonetheless, CFD can be used to complement model scale experiments as it becomes more capable through further development. The complementary characteristics of CFD are especially applicable to flows around bodies such as a simple front wing. If the study is limited to the front wing separated from the rest of the vehicle, the flow could potentially stay attached over the majority of the aerodynamic surface making the obtained results more representative of the actual flow behaviour.

4.1 CFD Analysis

In order to verify the findings from the theoretical analysis, a CFD simulation was conducted on the front half of the car. The flow simulation tool within SolidWorks 2010 was utilized for this purpose, as it is known for its relative simplicity in setting up a CFD simulation. The results were mainly used to visually display various flow parameters and identify any occurring aerodynamic effects. It is acknowledged that the Flow Simulation add-in within SolidWorks is not accurate enough at low Reynolds numbers. Any numerical values obtained are subjected to large errors when compared to the theoretical analysis making them undependable. This section will document and discuss how the CFD was setup, in addition to providing the various plots gathered from the CFD simulation.

4.1.1 CFD Setup

Many approaches can be taken when setting up any form of computational analysis on an object, various factors can be accounted for, and different solution converging methods can be used. The details of the specific details of the CFD setup are presented in this section.

4.1.1.1 Computational Domain and Mesh Settings

Complex geometries on the car were simplified. Any components that have negligible aerodynamic effects such as suspension components were removed or replaced by smooth surfaces to minimize the possibility of any issues related to convergence to arise. The dimensions of the computational domain were chosen based on minimizing the run time required while maintaining accuracy. The mesh was set at a level of 2 out of 8 as the general

setting for mesh. A much finer mesh of 6 was used in areas with high aerodynamic effects such as the airfoils, inside faces of endplates, and nose cone as shown in Figure 11 and Figure 12.

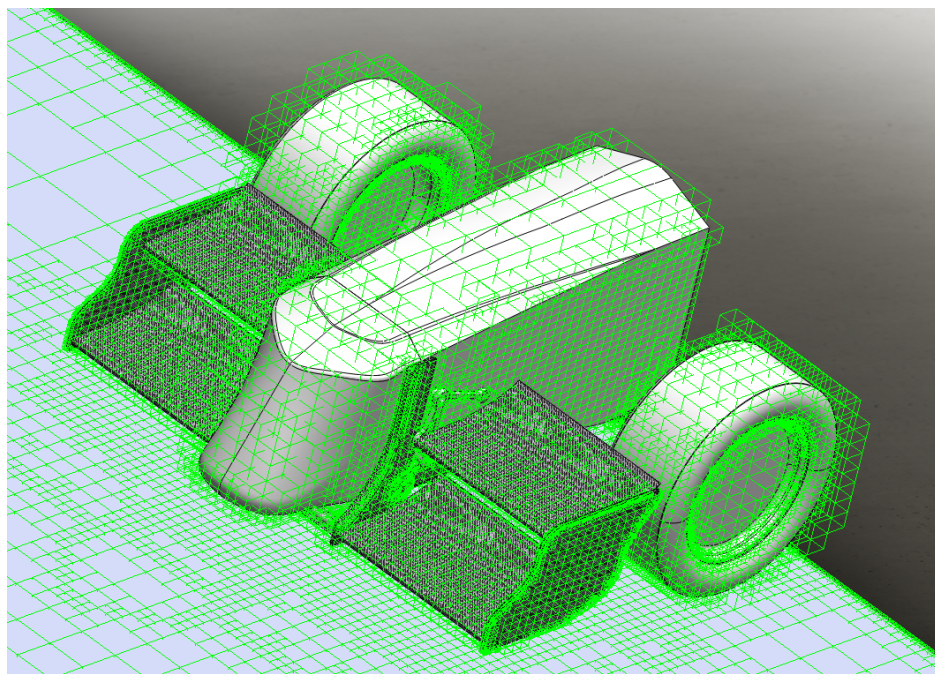


Figure 11. Mesh Overview of CFD Analysis [21].

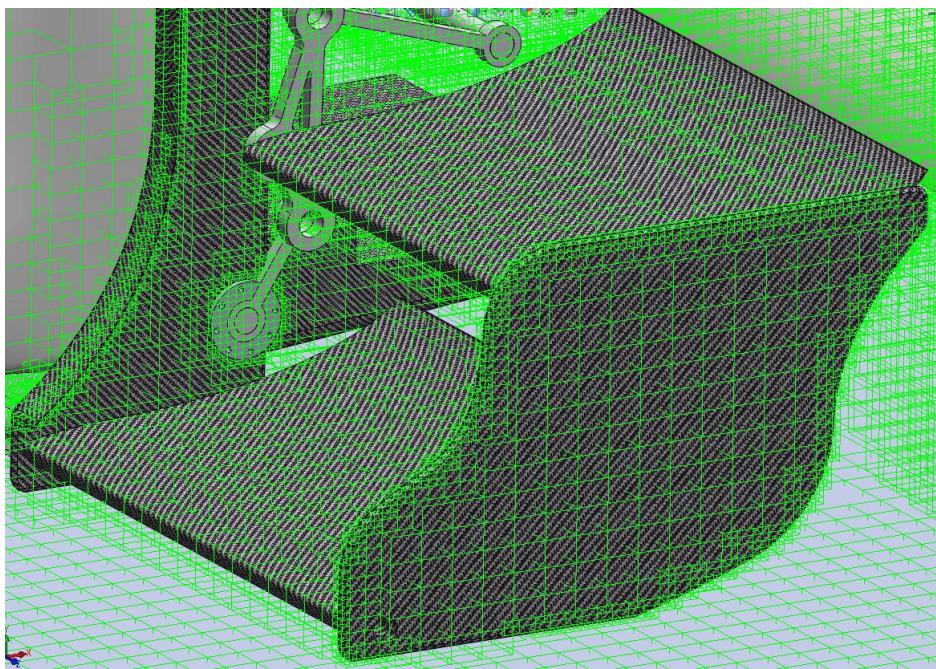


Figure 12. Detail view of critical Mesh Refinement Area [22].

4.1.1.2 Boundary Conditions

The analysis was setup as an external flow study with air at a relative humidity of 50% travelling at 13.89 m/s. The vehicle body was placed on a surface that serves as a road. The tire and road surfaces were both set as moving surfaces with velocities to account for their aerodynamic respective aerodynamic effects.

4.1.1.3 k- ε Turbulence Model

The standard k- ε turbulence model was used in the CFD, as it is the only option available in SolidWorks 2010 Flow Simulation. It is typically used for fully turbulent flows. The model is governed by the following equations:

$$\mu_t = C_\mu \rho \frac{k^2}{\varepsilon}$$

where k is the turbulent kinetic energy, ε is the dissipation, and C_μ is a constant [23]. The solutions for k and ε are derived from the following transport equations:

$$\mu_i \frac{\partial(\rho k)}{\partial x_i} = \frac{\partial}{\partial x_i} \left(\left(\mu + \frac{\mu_t}{\sigma_k} \right) \frac{\partial k}{\partial x_i} \right) + P_k - \rho \varepsilon$$

$$\mu_i \frac{\partial(\rho \varepsilon)}{\partial x_i} = \frac{\partial}{\partial x_i} \left(\left(\mu + \frac{\mu_t}{\sigma_k} \right) \frac{\partial \varepsilon}{\partial x_i} \right) + \frac{\varepsilon}{k} (C_{\varepsilon 1} P_k - C_{\varepsilon 2} \rho \varepsilon)$$

Where P_k , the turbulence production term is modeled using the following equation:

$$P_k = \mu_t \frac{\partial u_i}{\partial x_j} \left(\frac{\partial u_i}{\partial x_j} + \frac{\partial u_j}{\partial x_i} \right)$$

The standard constant values used by SolidWorks Flow Simulation are:

$$C_\mu = 0.09$$

$$C_{\varepsilon 1} = 1.44$$

$$C_{\varepsilon 2} = 1.92$$

$$\sigma_k = 1.0$$

4.1.2 CFD Results

The results in the form of velocity cutplots in of the three configurations are presented in this section.

4.1.2.1 Plots for High Down Force Configuration

Figure 13 shows the velocity plot over the wings in the high down force configuration for cornering. The top movable wing was set at an AoA of $\alpha = 13^\circ$. The velocity variation along the surface of the wings is illustrated by the colors. The channeling effect can be observed on the plot under the top wing.

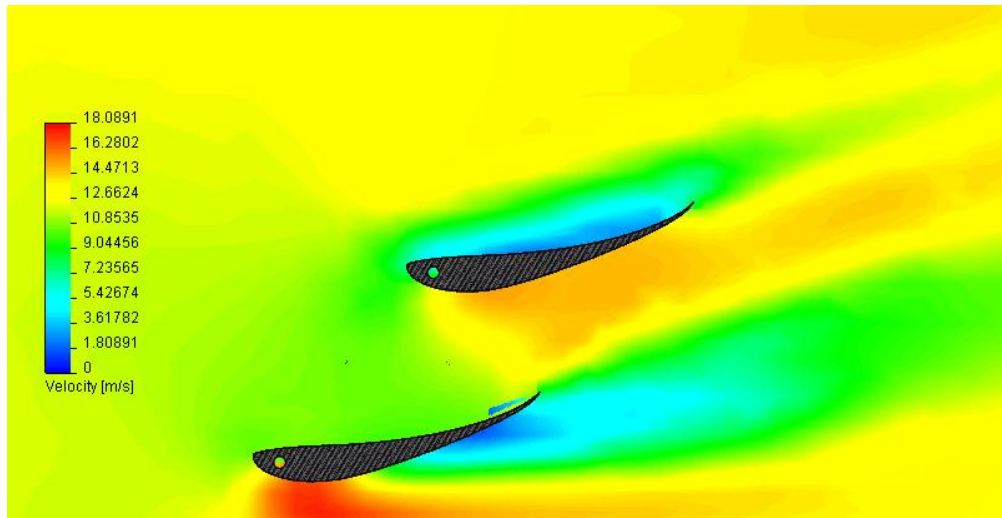


Figure 13. Velocity Plot for High Down Force Configuration [24]

4.1.2.2 Plots for Low Drag Configuration

Figure 14 shows the velocity plot over the wings in the minimal drag configuration for straightaways. The top movable wing is set at an AoA of $\alpha = +6^\circ$. The velocity variation along the surface of the wings is illustrated by the colors. The channeling effect is reduced greatly at this AoA, thus any drag effects due to down force are reduced. Additionally, the green region behind the fixed wing is reduced in area; hence less drag is occurring as the velocity reduction is less overall. The blue region above the top airfoil shows the flow separating from the surface. As previously mentioned, the Flow Simulation tool in SolidWorks can be inaccurate in some

aspects, as the airfoil at this angle according to the experimental data should not experience any separation [25].

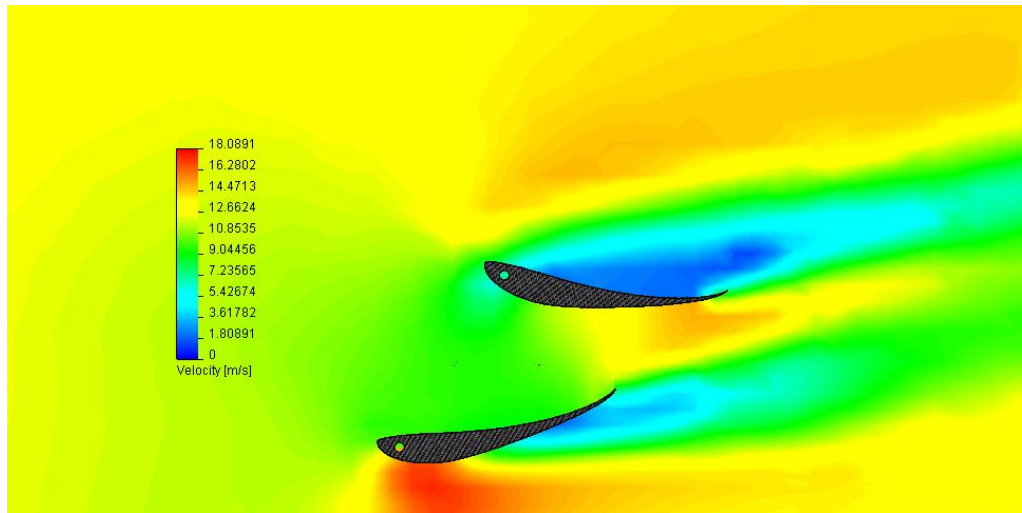


Figure 14. Velocity Plot for Low Drag Configuration [26]

4.1.2.3 Plots for Airbrake Configuration

Figure 15 shows the velocity plot over the wings in the airbrake configuration for braking. The top movable wing is set at an AoA of $\alpha = 28^\circ$. The velocity variation along the surface of the wings is illustrated by the colors. The big blue region behind the top airfoil signifies the vortices occurring resulting in substantial drag forces.

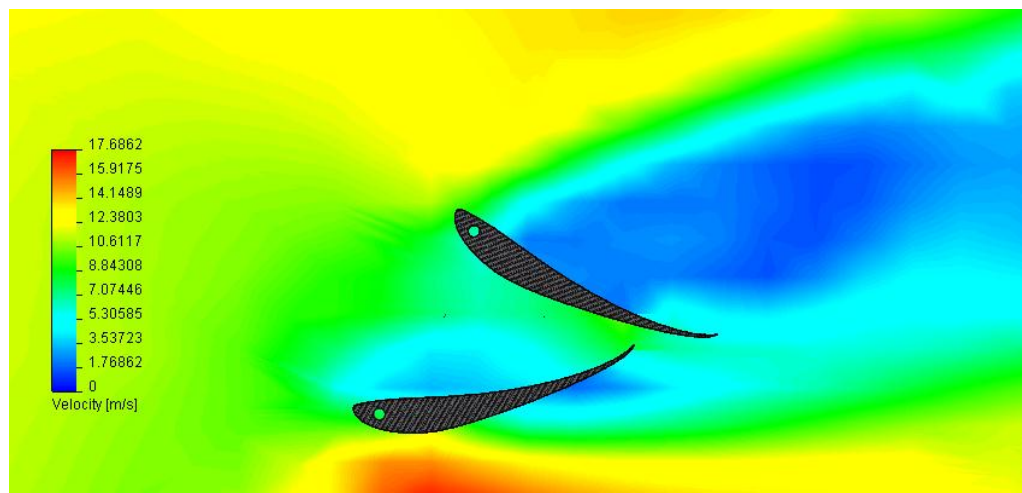


Figure 15. Velocity Plot for Airbrake Configuration [27]

5 Cost and Manufacturing

In this section of the report, the cost and manufacturability of the selected design are reviewed in order to assess demonstrate that the design is both economically feasible and easy to manufacture.

The manufacturing of the proposed system involves parts that are manufactured in-house such as the airfoil and linkages, and some components that are to be sourced commercially such as the electric motors and digital sensors. The airfoil can be manufactured from readily available materials to the UMSAE team such as fibre-glass, carbon-fibre, etc. The linkages for the control system are to be machined from aluminum. This process is relatively simple and achievable within the tools available to the UMSAE shop. The wiring for the sensors is within the client's capability. Moreover, electric motors for actuation are commonly available from suppliers. Finally, the linkage and the airfoil are to be coated in order to be protected against corrosion and erosion.

The fact that the 2011 front aero package design employed an unnecessarily complex manufacturing process led to a relatively expensive part. However, the design proposed in this report is expected to be manufactured in a simpler manner than the 2011 design, and hence the cost is anticipated to be less than or, in the worst case, equal to the cost of 2011 front aero package. The 2012 design is well within the allotted budget. Therefore, the selected concept design is predicted to be economically feasible. The detailed cost analysis will be discussed in the final design report.

The cost of fabrication of the design proposed by KHAB Engineering and Design team includes the three major design components: aerodynamic wing design, actuated four-bar linkage design and the control system. As mentioned in the manufacturing analysis, the wings are suggested to be made of carbon fibre which is a light and high strength material. However, carbon fibre is relatively expensive compared to other classes of fibre such as glass and plastic fibres. Basically, the material is itself inexpensive and costs about USD \$3 a pound. However, the processing requires energy sucking machines and involves a high amount of waste as high as 50 percent. Therefore, adding the cost of manufacturing process to the starting material, the

wing will cost about USD \$10 a pound [28]. The weight of all wings is expected to be around 15 pounds resulting in total cost of \$150 for wings.

The other component of the design is the actuated four-bar linkage which is to be made of Aluminum. The total length of all links is 1.3 ft so a commercial 2 ft long bar is recommended considering the waste. In the market, a $\frac{3}{4} \times \frac{3}{4}$ inch square and 2 ft long aluminium bar costs about USD \$9 [29]. In addition, the joints and pins between the bars will add to the cost but are negligible. The Aluminium machining is not an issue for the University of Manitoba SAE team as the needed machining tools are available in the team's shop. Therefore, the total cost of actuation system will be less than 20 USD \$.

The last component of the design is the electric motor that needs to be purchased. As stated in the report, the design uses a Torxis i00600 electric motor which costs USD \$ 289.99 [30]. Based on this initial cost analysis and estimate, the total expected cost of the design is about USD \$ 460. TABLE XVIII summarizes the cost of fabrication of the design.

TABLE XVIII: MATERIAL AND FABRICATION COST OF THE DESIGN [28], [29], [30].

	Wings	Actuation Linkage	Electric Motor	Total
Cost [USD \$]	150	20	290	460

6 Lift and Drag Characteristics of S1223 Airfoil

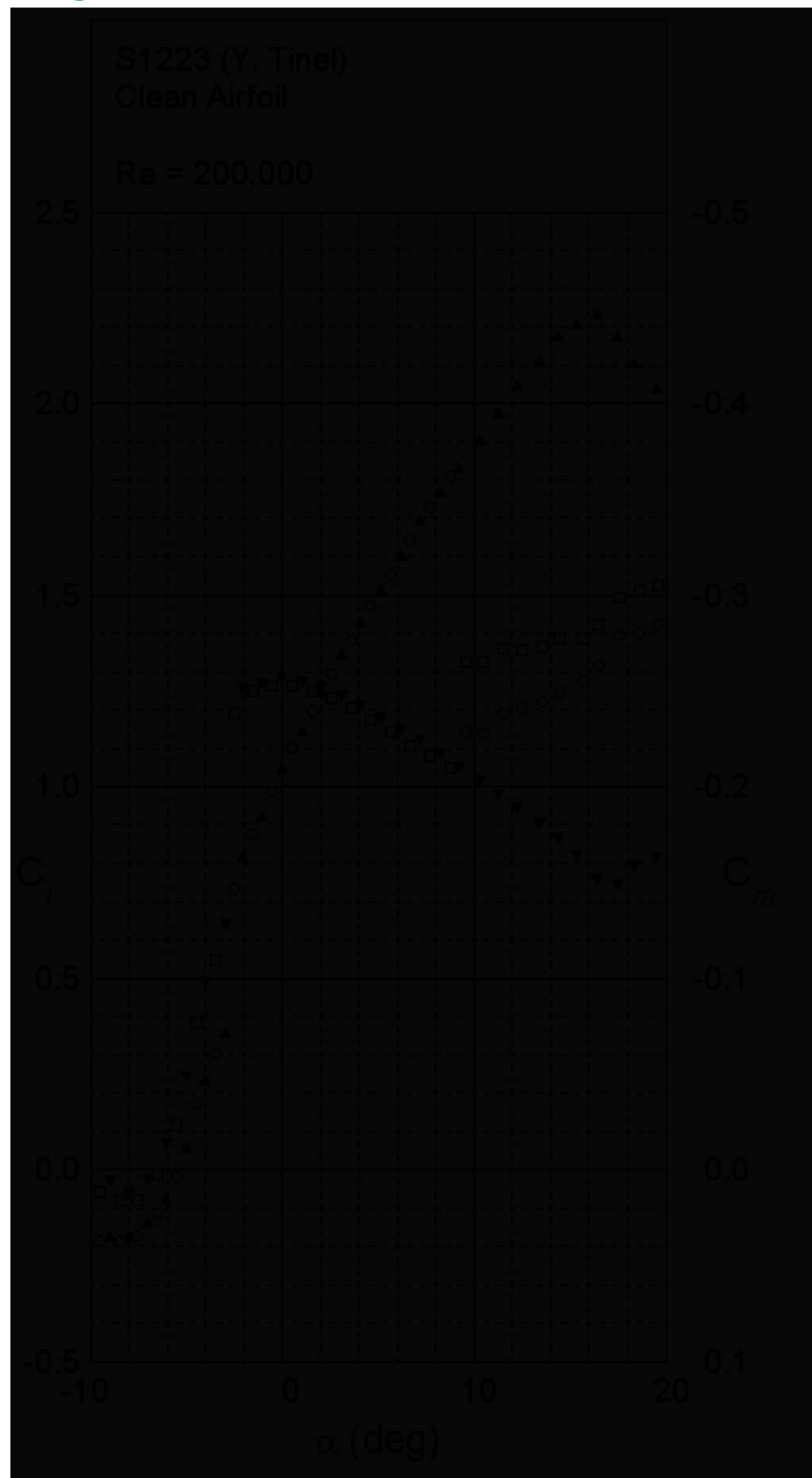


Figure 16. Lift Characteristics for the S1223 airfoil at $Re = 2 \times 10^5$ [31]. Permission pending.

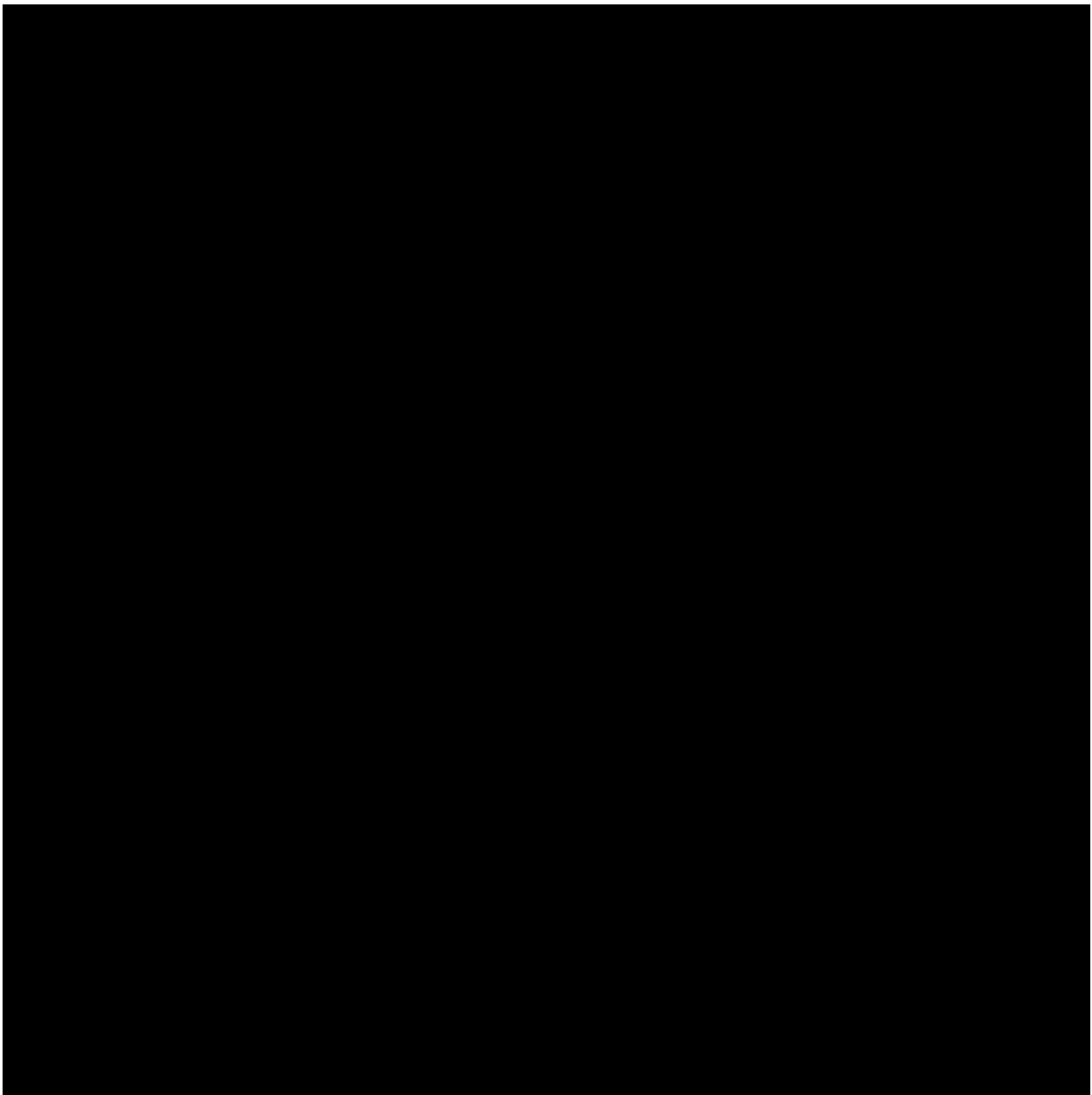


Figure 17. Drag Polar for the S1223 airfoil [31]. Pending permission.

7 Relevant Competition Rules

This list is an exact reproduction from the 2012 Formula Hybrid Rules [32].

3.1 General Design Requirements

3.1.1 Body and Styling

The vehicle must be open-wheeled and open-cockpit (a formula style body). There must be no openings through the bodywork into the driver compartment from the front of the vehicle back to the roll bar main hoop or firewall other than that required for the cockpit opening. Minimal openings around the front suspension components are allowed.

3.2 Chassis Rules

3.2.2 Ground Clearance

The ground clearance must be sufficient to prevent any portion of the car (other than tires) from touching the ground during track events, and with the driver aboard there must be a minimum of 25.4 mm (1 inch) of static ground clearance under the complete car at all times.

3.3.5 Frontal Impact Structure

Impact Attenuator

All teams must equip their vehicle with an impact attenuator that exhibits a constant, or near constant crush strength to provide a constant or near constant deceleration in the event of a collision²

The Impact Attenuator must be:

- a) Installed forward of the Front Bulkhead.
- b) At least 200 mm (7.8 in) long, with its length oriented along the fore/aft axis of the Frame.
- c) At least 100 mm (3.9 in) high and 200 mm (7.8 in) wide for a minimum distance of 200 mm (7.8 in) forward of the Front Bulkhead.
- d) Such that it cannot penetrate the Front Bulkhead in the event of an impact. If the Impact Attenuator is foam filled or honeycomb, a 1.5 mm (0.060 in) solid steel or 4.0 mm (0.157 in) solid aluminum metal

plate must be integrated into the Impact Attenuator. The metal plate must be the same size as the Front Bulkhead and bolted or welded to the Front Bulkhead.

e) Attached securely and directly to the Front Bulkhead and not by being part of non-structural bodywork. The attachment of the Impact Attenuator must be constructed to provide an adequate load path for transverse and vertical loads in the event of off-center and off-axis impacts. If not integral with the frame, i.e. welded, a minimum of four (4) 8 mm Grade 8.8 (5/16 inch Grade 5) bolts must attach the Impact Attenuator to the Front Bulkhead.

Alternative designs that do not comply with the minimum specifications given above require an approved “Structural Equivalency Form” per Section 3.3.2.

The attachment of the Impact Attenuator to a monocoque structure requires an approved Structural Equivalency Form per Section 3.3.2.

3.3.6 Front Bodywork

Sharp edges on the forward facing bodywork or other protruding components are prohibited. All forward facing edges on the bodywork that could impact people, e.g. the nose, must have forward facing radii of at least 38 mm (1.5 inches). This minimum radius must extend to at least 45 degrees (45°) relative to the forward direction, along the top, sides and bottom of all affected edges.

3.7.1 Aerodynamics and Ground Effects

All aerodynamic devices must satisfy the following requirements:

3.7.1.1 Location

In plan view, no part of any aerodynamic device, wing, undertray or splitter can be further forward than 460 mm (18 inches) forward of the fronts of the front tires, and no further rearward than the rear of the rear tires. No part of any such device can be wider than the outside of the front tires measured at the height of the front hubs.

3.7.1.2 Driver Egress Requirements

Egress from the vehicle within the time set in section 3.4.9 “Driver Egress,” must not require any movement of the wing or wings or their mountings. The wing or wings must be mounted in such

positions, and sturdily enough, that any accident is unlikely to deform the wings or their mountings in such a way to block the driver's egress.

3.7.1.3 Wing Edges - Minimum Radii

All wing leading edges must have a minimum radius 12.7 mm (0.5 inch). Wing leading edges must be as blunt or blunter than the required radii for an arc of plus or minus 45 degrees ($\pm 45^\circ$) centered on a plane parallel to the ground or similar reference plane for all incidence angles which lie within the range of adjustment of the wing or wing element. If leading edge slats or slots are used, both the fronts of the slats or slots and of the main body of the wings must meet the minimum radius rules.

3.7.1.4 Other Edge Radii Limitations

All wing edges, end plates, Gurney flaps, wicker bills, splitters undertrays and any other wing accessories must have minimum edge radii of at least 3 mm (1/8 inch) i.e., this means at least a 6 mm (1/4 inch) thick edge.

3.7.1.5 Wing Edge Restrictions

No small radius edges may be included anywhere on the wings in such a way that would violate the intent of these rules (e.g. vortex generators with thin edges, sharp square corners on end plates, etc.).

8 Coding for Main Control Elements

The body of the report covered the design of the control system for the active aero portion of the design. The overall design relied heavily on the SyNaPs protocol that the team is developing [33], and the coding of the design is featured below.

```
#include <Servo.h>

int pRead = A0;
int pFeed = A1;
int vRead = A2;
int pCurr = 0;
int pDes = 0;
int vDes = 0;
int pErr = 0;

Servo actuator1;
Servo actuator2;

void setup()
{
    Serial.begin(9600);
    actuator1.attach(5);
    actuator2.attach(6);
}

void loop() {
    pDes = analogRead(pRead);
    pCurr = analogRead(pFeed);
    vDes = analogRead(vRead);

    pErr = pDes - pCurr;
    Serial.println(pErr);

    vDes = map(vDes, 0, 1023, 10, 25); //1023 Vin val maps to 25ms.
    pDes = map(pDes, 0, 890, 0, 179); //890 Ain val maps to 180 degrees.
    actuator1.write(pDes);
    actuator2.write(pDes);

    delay(vDes);
}
```

8.1 Class Wrapper for Servo Library

As mentioned in the previous section, a class wrapper is used to handle the servo control library, and the applicable code from this is shown below. The code comprises of a software translation library that utilizes the built in PWM (Pulse Width Modulation) capabilities of the ATmega328, but allows the angle to be quickly set, while minimizing the programming required to use the servo. The attached class wrapper is to be used in cases where the development environment for the Uno is not available. As referenced above, the ideal solution would be to utilize the ATmega328 as a basis for a controller for only the aero portion, with a custom circuit board. This coding was taken from [34] and is a freely available class wrapper for use with the Arduino development environment

```
#ifndef Servo_h
#define Servo_h

#include <inttypes.h>

// Say which 16 bit timers can be used and in what order
#if defined(__AVR_ATmega1280__) || defined(__AVR_ATmega2560__)
#define _useTimer5
#define _useTimer1
#define _useTimer3
#define _useTimer4
typedef enum { _timer5, _timer1, _timer3, _timer4, _Nbr_16timers } timer16_Sequence_t;

#elif defined(__AVR_ATmega32U4__)
#define _useTimer3
#define _useTimer1
typedef enum { _timer3, _timer1, _Nbr_16timers } timer16_Sequence_t;

#elif defined(__AVR_AT90USB646__) || defined(__AVR_AT90USB1286__)
#define _useTimer3
#define _useTimer1
typedef enum { _timer3, _timer1, _Nbr_16timers } timer16_Sequence_t;

#elif defined(__AVR_ATmega128__)
||defined(__AVR_ATmega1281__)||defined(__AVR_ATmega2561__)
#define _useTimer3
#define _useTimer1
typedef enum { _timer3, _timer1, _Nbr_16timers } timer16_Sequence_t;

#else // everything else

```

```

#define _useTimer1
typedef enum { _timer1, _Nbr_16timers } timer16_Sequence_t ;
#endif

#define Servo_VERSION      2 // software version of this library

#define MIN_PULSE_WIDTH    544 // the shortest pulse sent to a servo
#define MAX_PULSE_WIDTH   2400 // the longest pulse sent to a servo
#define DEFAULT_PULSE_WIDTH 1500 // default pulse width when servo is attached
#define REFRESH_INTERVAL 20000 // minumim time to refresh servos in microseconds

#define SERVOS_PER_TIMER    12 // the maximum number of servos controlled by one timer
#define MAX_SERVOS (_Nbr_16timers * SERVOS_PER_TIMER)

#define INVALID_SERVO      255 // flag indicating an invalid servo index

typedef struct {
    uint8_t nbr    :6;        // a pin number from 0 to 63
    uint8_t isActive :1;      // true if this channel is enabled, pin not pulsed if false
} ServoPin_t ;

typedef struct {
    ServoPin_t Pin;
    unsigned int ticks;
} servo_t;

class Servo
{
public:
    Servo();
    uint8_t attach(int pin); // attach the given pin to the next free channel, sets pinMode,
returns channel number or 0 if failure
    uint8_t attach(int pin, int min, int max); // as above but also sets min and max values for writes.
    void detach();
    void write(int value); // if value is < 200 its treated as an angle, otherwise as pulse width in
microseconds
    void writeMicroseconds(int value); // Write pulse width in microseconds
    int read(); // returns current pulse width as an angle between 0 and 180 degrees
    int readMicroseconds(); // returns current pulse width in microseconds for this servo (was
read_us() in first release)
    bool attached(); // return true if this servo is attached, otherwise false
private:
    uint8_t servoIndex; // index into the channel data for this servo
    int8_t min; // minimum is this value times 4 added to MIN_PULSE_WIDTH
    int8_t max; // maximum is this value times 4 added to MAX_PULSE_WIDTH
};

#endif

```

9 References

- [1] J. Katz. (2006). "Aerodynamics of Race Cars," *Annual Review of Fluid Mechanics* [Online], vol. 38 (5), pp. 27-63. Available: <http://www.annualreviews.org/> [Oct. 19, 2011].
- [2] 20100826203100. (2010, Aug. 26). China Daily [Online]. Available: <http://www.china-daily.org/> [Oct 20, 2011].
- [3] X. Zhang. (2006). "Ground Effect Aerodynamics of Race Cars," Applied Mechanics Review [Online], vol. 59 (1), pp. 33-50. Available: <http://scitation.aip.org.proxy1.lib.umanitoba.ca/journals/doc/ASMEDL-home/> [Oct. 20, 2011].
- [4] d09mon2267. (2009, May. 25). F1 Technical: Formula One Uncovered [Online]. Available: <http://www.f1technical.net/forum/viewtopic.php?f=6&t=6321&start=420> [Oct 20, 2011].
- [5] "Race Car Aerodynamics," class notes for SG1102, Department of Mechanics, KTH Institute of Technology, 2010.
- [6] F. Burgmann. (2011, Mar. 2). "Lotus_49B," in *f1nest.com: New Regulations for the 2011 Season* [Online]. Available: <http://www.f1nest.com/2011/03/new-regulations-for-2011-season.html> [Oct. 20, 2011].
- [7] *The Grapevine - Rumours and speculation in the world of Formula One* [Online]. (1999, Mar. 3). Available: <http://www.atlasf1.com/99/aus/preview/grapevine.html> [Oct. 20, 2011].
- [8] C. Scarborough. (2010, Mar. 11). *McLaren Snorkel: How it works* « Scarbsf1's Blog [Online]. Available: <http://scarbsf1.wordpress.com/2010/03/11/235/> [Oct. 21, 2011].
- [9] C. Scarborough. (2010, Mar. 25). "sauber_f_duct," in *Sauber: F-Duct detail* « Scarbsf1's Blog [Online]. Available: <http://scarbsf1.wordpress.com/2010/03/25/sauber-f-duct-detail/> [Oct. 21, 2011].
- [10] "Sooner Racing Team Gives You Wings! (That Move)," *YouTube*.n.d. [Online] Available: <http://www.youtube.com/watch?v=7wozSqFXitY> [Oct. 21, 2011].
- [11] Formula SAE Sooner Racing Team. (2011) "206730_10150152628028022_1701282630_21_6856064_3164230_n," in *Photos of Formula SAE Sooner Racing Team* [Online]. Available:

<http://www.facebook.com/photo.php?fbid=10150152628028022&set=pu.170128263021&type=1&theater> [Oct. 21, 2010].

- [12] Triz Journal. (2004). *Triz 40 Principles* [Online]. Available: http://www.triz40.com/aff_Principles.htm [Sept. 29, 2011].
- [13] Triz Journal. (2004). *Triz 40 Principles* [Online]. Available: http://www.triz40.com/aff_Matrix.htm [Sept. 29, 2011].
- [14] R. W. Fox, P. J. Pritchard, and A. T. McDonald, *Introduction to Fluid Mechanics*, 7th ed. Hoboken, NJ: John Wiley & Sons, INC., 2009.
- [15] Atmel Corporation. (2010, Oct. 24). “banner_AVR_1,” in *Atmel Corporation - Atmel AVR 8- and 32-bit Microcontrollers - AVR Xplain* [Online]. Available: http://www.atmel.com/products/AVR/xplain.asp?category_id=163&family_id=607&source=redirect [Oct. 27, 2011].
- [16] M. Heiranian, M. Alnouri, N. Balakrishnan, and W. Koos. *Conceptual Model* (2011, Oct.)
- [17] M. Heiranian, M. Alnouri, N. Balakrishnan, and W. Koos. Screening and Scoring Mtrices (2011, Oct.).
- [18] Jawad, B.A, Longnecker, M.M, “Aerodynamic Evaluation on Formula SAE Vehicles,” SAE 2001-01-1270, Society of Automotive Engineers, Warrendale, USA, 2001
- [19] S. Wordley, J. Saunders, “Aerodynamics for Formula SAE: Initial Design and Perfomance Prediction,” SAE 2006-01-0806, Society of Automotive Engineers, Warrendale, USA, 2006
- [20] N. McKay, A. Gopalarathnam, “The Effects of Wing Aerodynamics on Race Vehicle Performance,” SAE 2002-01-3294, Society of Automotive Engineers, Warrendale, USA, 2002
- [21] M. Alnouri (2011, Nov 29). “*Mesh Overview.sldasm*”. Winnipeg, University of Manitoba.
- [22] M. Alnouri (2011, Nov 21). “*Critical Mesh.sldasm*”. Winnipeg, University of Manitoba.

- [23] R. J. Lozowy, A. M. El-Shaboury, H. M. Soliman, S. J. Ormiston, "Simulation and performance enhancement of the air cooling system in the valve halls of a DC/AC power converter station", *Build Simulation*, Vol. 3, Issue 3 pp 233-244, September, 2010
- [24] M. Alnouri (2011, Nov 21). "*max df.sldasm*". Winnipeg, University of Manitoba.
- [25] D. Balli, "Design and Construction of an Aerodynamic Airfoil for the SAE Formula Car," University of Manitoba, Winnipeg, Canada, B.Sc. Thesis 1998.
- [26] M. Alnouri (2011, Nov 22). "*Low drag.sldasm*". Winnipeg, University of Manitoba.
- [27] M. Alnouri (2011, Nov 18). "*airbrake.sldasm*". Winnipeg, University of Manitoba.
- [28] *Why does carbon fibre cost so much? - explore magazine - Canada's Outdoor Magazine* [Online]. Available: <http://explore-mag.com/article/gear/why-does-carbon-fibre-cost-so-much/> [Dec 1, 2011]
- [29] *Metals Depot Shopping* [Online]. Available: [http://www.metalsdepot.com/Cart3/viewCart1.phtml?LimAcc=\\$LimAcc&aident=](http://www.metalsdepot.com/Cart3/viewCart1.phtml?LimAcc=$LimAcc&aident=) [Dec 1, 2011]
- [30] *Torxis i00600 12V High Torque Servo Motor – RobotShop* [Online]. Available: <http://www.robotshop.com/ProductInfo.aspx?pc=RB-Ins-01> [Dec 1, 2011]
- [31] M. S. Selig, J. J. Guglielmo, "High-Lift Low Reynolds Number Airfoil Design," *JOURNAL OF AIRCRAFT*, Vol.34, No 1, February, 1997.
- [32] SAE International. (2011, August 25) *2012 Formula Hybrid Rules* [Online]. Available: <http://www.formula-hybrid.org/pdf/Formula-Hybrid-2012-Rules.pdf> [Oct. 2, 2011].
- [33] G. Klassen, UMSAE Formula Electric (2011, Nov 29). *Private Communication*.
- [34] *The Arduino DAQ Chronicles - Measuring Stuff* [Online] Available: <https://sites.google.com/site/measuringstuff/the-arduino> [Nov. 12, 2011].

Pre-Stall Calculations - Fixed Bottom Wing

Constants																
Density [kg/m^3]	Span [m]	Chord [m]	e	Wing Area [m^2]	Height of Endplate [m]	AR	AR_effective	CM	μ	Phi	AoA, L=0 [dgrees]	h_bw	a [per degree]			
1.225	0.4064	0.3018	0.7	0.12265152	0.4206	1.346587	3.994499669	-0.152	0.0000184	0.897106294	-6	0.075	0.067733322			
Angle of Attack		-6														
Velocity [m/s]	Re	Csf	a [per degree]	CL (finite)	Cdmin	Cdi	CD (finite)	Downforce [N]	Drag [N]	Moment [N.m]	L/D	Resultant Force Magnitude	Resultant Force Direction			
13.9	279288	0.005026	0.067733	0	0.018947	0	0.02397313	0	0.3479632	N/A	0	0.347963242	0			
Angle of Attack		13														
Velocity [m/s]	Re	Csf	a_ground effect	CL (finite)	Cdmin	Cdi	CD (finite)	Downforce [N]	Drag [N]	Moment [N.m]	L/D	Resultant Force Magnitude	Resultant Force Direction			
0.1	2009.266	0.059253	0.125129	2.377446063	0.018947	1.908706	1.790512121	-0.00178603	0.0013451	-3.44621E-05	-1.327802273	0.002235895	-53.01571249			
0.2	4018.533	0.041898	0.125129	2.377446063	0.018947	1.908706	1.77315736	-0.00714414	0.0053283	-0.000137848	-1.340798125	0.008912303	-53.28352464			
0.3	6027.799	0.03421	0.125129	2.377446063	0.018947	1.908706	1.765468916	-0.01607431	0.0119366	-0.000310159	-1.34663717	0.020021647	-53.40277039			
0.4	8037.065	0.029626	0.125129	2.377446063	0.018947	1.908706	1.760885691	-0.02857654	0.0211656	-0.000551394	-1.35014219	0.035561223	-53.47403085			
0.5	10046.33	0.026499	0.125129	2.377446063	0.018947	1.908706	1.757757945	-0.04465085	0.0330125	-0.000861553	-1.352544626	0.055529468	-53.52273687			
0.6	12055.6	0.02419	0.125129	2.377446063	0.018947	1.908706	1.75544914	-0.06429722	0.0474755	-0.001240636	-1.354323523	0.079925328	-53.55872948			
0.7	14064.86	0.022395	0.125129	2.377446063	0.018947	1.908706	1.753654737	-0.08751566	0.0645534	-0.001688643	-1.355709316	0.10874803	-53.586726			
0.8	16074.13	0.020949	0.125129	2.377446063	0.018947	1.908706	1.75220831	-0.11430617	0.0842451	-0.002205575	-1.356828437	0.141996973	-53.60930805			
0.9	18083.4	0.019751	0.125129	2.377446063	0.018947	1.908706	1.751010214	-0.14466875	0.1065498	-0.002791431	-1.357756822	0.179671675	-53.62802303			
1	20092.66	0.018737	0.125129	2.377446063	0.018947	1.908706	1.74999666	-0.17860339	0.1314668	-0.003446211	-1.3585432	0.221771737	-53.64386238			
1.1	22101.93	0.017865	0.125129	2.377446063	0.018947	1.908706	1.74912467	-0.2161101	0.1589956	-0.004169915	-1.359220474	0.268296821	-53.65749459			
1.2	24111.2	0.017105	0.125129	2.377446063	0.018947	1.908706	1.748364088	-0.25718888	0.1891357	-0.004962544	-1.359811769	0.319246638	-53.66938902			
1.3	26120.46	0.016434	0.125129	2.377446063	0.018947	1.908706	1.747693047	-0.30183973	0.2218865	-0.005824096	-1.360333388	0.374620935	-53.67988616			
1.4	28129.73	0.015836	0.125129	2.377446063	0.018947	1.908706	1.747095254	-0.35006265	0.2572478	-0.006754573	-1.360799337	0.434419488	-53.68923988			
1.5	30138.99	0.015299	0.125129	2.377446063	0.018947	1.908706	1.746558283	-0.40185763	0.2952192	-0.007753975	-1.361217708	0.498642099	-53.6976438			
1.6	32148.26	0.014813	0.125129	2.377446063	0.018947	1.908706	1.746072476	-0.45722468	0.3358004	-0.0088223	-1.361596438	0.56728859	-53.70524855			
1.7	34157.53	0.014371	0.125129	2.377446063	0.018947	1.908706	1.74563019	-0.5161638	0.3789912	-0.009959549	-1.361941422	0.640358799	-53.71217331			
1.8	36166.79	0.013966	0.125129	2.377446063	0.018947	1.908706	1.745225294	-0.57867499	0.4247912	-0.01165723	-1.362257396	0.717852579	-53.71851375			
1.9	38176.06	0.013594	0.125129	2.377446063	0.018947	1.908706	1.744852799	-0.64475824	0.4732003	-0.012440821	-1.362548213	0.799769797	-53.72434771			
2	40185.33	0.013249	0.125129	2.377446063	0.018947	1.908706	1.744508603	-0.71441356	0.5242182	-0.013784844	-1.362817047	0.886110328	-53.72973924			
2.1	42194.59	0.01293	0.125129	2.377446063	0.018947	1.908706	1.744189295	-0.78764096	0.5778448	-0.01519779	-1.363066538	0.976874058	-53.73474158			
2.2	44203.86	0.012633	0.125129	2.377446063	0.018947	1.908706	1.743892013	-0.86444041	0.6340799	-0.016679661	-1.3632989	1.072060881	-53.73939943			
2.3	46213.13	0.012355	0.125129	2.377446063	0.018947	1.908706	1.743614336	-0.94481194	0.6929232	-0.018230456	-1.36351601	1.171670698	-53.74375061			
2.4	48222.39	0.012095	0.125129	2.377446063	0.018947	1.908706	1.7433542	-1.02875553	0.7543748	-0.019850175	-1.363719469	1.275703418	-53.74782737			
2.5	50231.66	0.011851	0.125129	2.377446063	0.018947	1.908706	1.743109833	-1.1162712	0.8184343	-0.021538818	-1.363910649	1.384158954	-53.75165739			
2.6	52240.92	0.01162	0.125129	2.377446063	0.018947	1.908706	1.742879703	-1.20735892	0.8851016	-0.023296386	-1.36409074	1.497037224	-53.75526461			
2.7	54250.19	0.011403	0.125129	2.377446063	0.018947	1.908706	1.742662479	-1.30201872	0.9543767	-0.025122877	-1.364260775	1.614338153	-53.75866984			
2.8	56259.46	0.011198	0.125129	2.377446063	0.018947	1.908706	1.742456999	-1.40025059	1.0262594	-0.027018293	-1.364421656	1.736061669	-53.76189124			

2.9	58268.72	0.011003	0.125129	2.377446063	0.018947	1.908706	1.742262241	-1.50205452	1.1007496	-0.028982634	-1.364574177	1.862207703		-53.7649448
3	60277.99	0.010818	0.125129	2.377446063	0.018947	1.908706	1.742077303	-1.60743052	1.1778472	-0.031015898	-1.364719039	1.99277619		-53.76784459
3.1	62287.26	0.010642	0.125129	2.377446063	0.018947	1.908706	1.741901389	-1.71637859	1.2575521	-0.033118087	-1.364856862	2.12776707		-53.77060312
3.2	64296.52	0.010475	0.125129	2.377446063	0.018947	1.908706	1.741733785	-1.82889873	1.3398641	-0.0352892	-1.364988199	2.267180283		-53.77323149
3.3	66305.79	0.010315	0.125129	2.377446063	0.018947	1.908706	1.74157386	-1.94499093	1.4247833	-0.037529237	-1.365113544	2.411015775		-53.77573963
3.4	68315.05	0.010162	0.125129	2.377446063	0.018947	1.908706	1.741421042	-2.0646552	1.5123094	-0.039838198	-1.365233339	2.559273492		-53.77813644
3.5	70324.32	0.010016	0.125129	2.377446063	0.018947	1.908706	1.741274822	-2.18789154	1.6024424	-0.042216083	-1.365347981	2.711953383		-53.78042991
3.6	72333.59	0.009875	0.125129	2.377446063	0.018947	1.908706	1.741134737	-2.31469995	1.6951823	-0.044662893	-1.365457832	2.869055401		-53.78262727
3.7	74342.85	0.009741	0.125129	2.377446063	0.018947	1.908706	1.741000371	-2.44508043	1.7905289	-0.047178627	-1.365563215	3.030579498		-53.78473506
3.8	76352.12	0.009612	0.125129	2.377446063	0.018947	1.908706	1.740871344	-2.57903297	1.8884822	-0.049763285	-1.365664425	3.19652563		-53.78675919
3.9	78361.39	0.009488	0.125129	2.377446063	0.018947	1.908706	1.740747312	-2.71655758	1.9890421	-0.052416868	-1.365761732	3.366893754		-53.78870506
4	80370.65	0.009369	0.125129	2.377446063	0.018947	1.908706	1.74062796	-2.85765426	2.0922085	-0.055139374	-1.365855379	3.54168383		-53.79057759
4.1	82379.92	0.009254	0.125129	2.377446063	0.018947	1.908706	1.740513003	-3.00232301	2.1979814	-0.057930805	-1.365945592	3.720895816		-53.79238127
4.2	84389.18	0.009143	0.125129	2.377446063	0.018947	1.908706	1.740402175	-3.15056382	2.3063607	-0.060791116	-1.366032574	3.904529676		-53.79412023
4.3	86398.45	0.009036	0.125129	2.377446063	0.018947	1.908706	1.740295237	-3.3023767	2.4173463	-0.063720439	-1.366116514	4.092585373		-53.79579823
4.4	88407.72	0.008933	0.125129	2.377446063	0.018947	1.908706	1.740191965	-3.45776165	2.5309382	-0.066718643	-1.366197587	4.28506287		-53.79741878
4.5	90416.98	0.008833	0.125129	2.377446063	0.018947	1.908706	1.740092156	-3.61671867	2.6471363	-0.069785771	-1.36627595	4.481962134		-53.79898506
4.6	92426.25	0.008736	0.125129	2.377446063	0.018947	1.908706	1.739995618	-3.77924776	2.7659406	-0.072921823	-1.366351753	4.683283132		-53.80050004
4.7	94435.52	0.008643	0.125129	2.377446063	0.018947	1.908706	1.739902179	-3.94534891	2.887351	-0.076126799	-1.366425132	4.889025832		-53.80196647
4.8	96444.78	0.008552	0.125129	2.377446063	0.018947	1.908706	1.739811674	-4.11502213	3.0113674	-0.079400699	-1.366496212	5.099190202		-53.80338689
4.9	98454.05	0.008465	0.125129	2.377446063	0.018947	1.908706	1.739723955	-4.28826742	3.1379898	-0.082743524	-1.366565113	5.313776213		-53.80476364
5	100463.3	0.00838	0.125129	2.377446063	0.018947	1.908706	1.739638881	-4.46508478	3.2672182	-0.086155272	-1.366631943	5.532783836		-53.80609893
5.1	102472.6	0.008297	0.125129	2.377446063	0.018947	1.908706	1.739556321	-4.64547421	3.3990525	-0.089635945	-1.366696804	5.756213041		-53.8073948
5.2	104481.8	0.008217	0.125129	2.377446063	0.018947	1.908706	1.739476154	-4.8294357	3.5334927	-0.093185543	-1.36675979	5.984063803		-53.80865314
5.3	106491.1	0.008139	0.125129	2.377446063	0.018947	1.908706	1.739398267	-5.01696926	3.6705386	-0.096804064	-1.366820991	6.216336094		-53.80987574
5.4	108500.4	0.008063	0.125129	2.377446063	0.018947	1.908706	1.739322554	-5.20807489	3.8101904	-0.10049151	-1.366880489	6.453029889		-53.81106426
5.5	110509.6	0.00799	0.125129	2.377446063	0.018947	1.908706	1.739248915	-5.40275258	3.9524478	-0.10424788	-1.366938362	6.694145162		-53.81222024
5.6	112518.9	0.007918	0.125129	2.377446063	0.018947	1.908706	1.739177257	-5.60100235	4.097311	-0.108073174	-1.366994683	6.939681888		-53.81334516
5.7	114528.2	0.007848	0.125129	2.377446063	0.018947	1.908706	1.739107494	-5.80282418	4.2447798	-0.111967392	-1.367049519	7.189640046		-53.81444037
5.8	116537.4	0.00778	0.125129	2.377446063	0.018947	1.908706	1.739039542	-6.00821808	4.3948542	-0.115930535	-1.367102936	7.44401961		-53.81550717
5.9	118546.7	0.007714	0.125129	2.377446063	0.018947	1.908706	1.738973326	-6.21718405	4.5475342	-0.119962601	-1.367154992	7.702820558		-53.81654675
6	120556	0.00765	0.125129	2.377446063	0.018947	1.908706	1.738908772	-6.42972208	4.7028197	-0.124063592	-1.367205745	7.96604287		-53.81756026
6.1	122565.2	0.007587	0.125129	2.377446063	0.018947	1.908706	1.738845812	-6.64583219	4.8607107	-0.128233507	-1.367255249	8.233686522		-53.81854877
6.2	124574.5	0.007525	0.125129	2.377446063	0.018947	1.908706	1.738784381	-6.86551436	5.0212071	-0.132472347	-1.367303553	8.505751495		-53.81951329
6.3	126583.8	0.007465	0.125129	2.377446063	0.018947	1.908706	1.738724419	-7.0887686	5.184309	-0.13678011	-1.367350707	8.782237767		-53.82045478
6.4	128593	0.007407	0.125129	2.377446063	0.018947	1.908706	1.738665868	-7.3155949	5.3500163	-0.141156798	-1.367396753	9.06314532		-53.82137414
6.5	130602.3	0.007349	0.125129	2.377446063	0.018947	1.908706	1.738608673	-7.54599328	5.5183289	-0.14560241	-1.367441736	9.348474133		-53.82227222
6.6	132611.6	0.007294	0.125129	2.377446063	0.018947	1.908706	1.738552784	-7.77996372	5.6892469	-0.150116947	-1.367485696	9.638224187		-53.82314983
6.7	134620.8	0.007239	0.125129	2.377446063	0.018947	1.908706	1.73849815	-8.01750623	5.8627701	-0.154700407	-1.367528671	9.932395465		-53.82400773
6.8	136630.1	0.007185	0.125129	2.377446063	0.018947	1.908706	1.738444725	-8.25862081	6.0388986	-0.159352792	-1.367570696	10.23098795		-53.82484666
6.9	138639.4	0.007133	0.125129	2.377446063	0.018947	1.908706	1.738392467	-8.50330746	6.2176324	-0.164074101	-1.367611807	10.53400162		-53.82566731
7	140648.6	0.007082	0.125129	2.377446063	0.018947	1.908706	1.738341332	-8.75156617	6.3989713	-0.168864334	-1.367652037	10.84143646		-53.82647032
7.1	142657.9	0.007032	0.125129	2.377446063	0.018947	1.908706	1.738291281	-9.00339695	6.5829155	-0.173723491	-1.367691416	11.15329245		-53.82725632
7.2	144667.2	0.006983	0.125129	2.377446063	0.018947	1.908706	1.738242277	-9.2587998	6.7694647	-0.178651573	-1.367729973	11.46956958		-53.8280259
7.3	146676.4	0.006935	0.125129	2.377446063	0.018947	1.908706	1.738194283	-9.51777472	6.9586191	-0.183648579	-1.367767738	11.79026783		-53.82877963
7.4	148685.7	0.006888	0.125129	2.377446063	0.018947	1.908706	1.738147266	-9.7803217	7.1503786	-0.188714509	-1.367804737	12.11538718		-53.82951805
7.5	150695	0.006842	0.125129	2.377446063	0.018947	1.908706	1.738101192	-10.0464408	7.3447431	-0.193849363	-1.367840995	12.44492762		-53.83024166
7.6	152704.2	0.006797	0.125129	2.377446063	0.018947	1.908706	1.73805603	-10.3161319	7.5417127	-0.199053141	-1.367876537	12.77888914		-53.83095095
7.7	154713.5	0.006752	0.125129	2.377446063	0.018947	1.908706	1.738011751	-10.5893951	7.7412873	-0.204325844	-1.367911386	13.11727171		-53.83164644

7.8	156722.8	0.006709	0.125129	2.377446063	0.018947	1.908706	1.737968326	-10.8662303	7.9434669	-0.209667471	-1.367945565	13.46007533	-53.83232844
7.9	158732	0.006666	0.125129	2.377446063	0.018947	1.908706	1.737925728	-11.1466376	8.1482515	-0.215078022	-1.367979094	13.80729997	-53.8329975
8	160741.3	0.006625	0.125129	2.377446063	0.018947	1.908706	1.737883932	-11.430617	8.3556409	-0.220557497	-1.368011994	14.15894564	-53.83365398
8.1	162750.6	0.006584	0.125129	2.377446063	0.018947	1.908706	1.737842912	-11.7181685	8.5656354	-0.226105897	-1.368044285	14.5150123	-53.83429828
8.2	164759.8	0.006543	0.125129	2.377446063	0.018947	1.908706	1.737802644	-12.009292	8.7782347	-0.231723221	-1.368075984	14.87549995	-53.83493077
8.3	166769.1	0.006504	0.125129	2.377446063	0.018947	1.908706	1.737763107	-12.3039876	8.9934388	-0.237409469	-1.368107111	15.24040857	-53.83555181
8.4	168778.4	0.006465	0.125129	2.377446063	0.018947	1.908706	1.737724278	-12.6022553	9.2112479	-0.243164641	-1.368137681	15.60973816	-53.83616173
8.5	170787.6	0.006427	0.125129	2.377446063	0.018947	1.908706	1.737686136	-12.904095	9.4316617	-0.248988737	-1.368167711	15.98348869	-53.83676086
8.6	172796.9	0.006389	0.125129	2.377446063	0.018947	1.908706	1.737648661	-13.2095068	9.6546804	-0.254881758	-1.368197218	16.36166016	-53.83734952
8.7	174806.2	0.006353	0.125129	2.377446063	0.018947	1.908706	1.737611834	-13.5184907	9.8803038	-0.260843703	-1.368226215	16.74425255	-53.83792802
8.8	176815.4	0.006316	0.125129	2.377446063	0.018947	1.908706	1.737575637	-13.8310466	10.108532	-0.266874572	-1.368254718	17.13126586	-53.83849663
8.9	178824.7	0.006281	0.125129	2.377446063	0.018947	1.908706	1.737540051	-14.1471746	10.339365	-0.272974365	-1.368282741	17.52270006	-53.83905564
9	180834	0.006246	0.125129	2.377446063	0.018947	1.908706	1.737505061	-14.4668747	10.572803	-0.279143083	-1.368310296	17.91855515	-53.83960531
9.1	182843.2	0.006211	0.125129	2.377446063	0.018947	1.908706	1.737470648	-14.7901468	10.808845	-0.285380724	-1.368337397	18.31883111	-53.84014591
9.2	184852.5	0.006178	0.125129	2.377446063	0.018947	1.908706	1.737436798	-15.116991	11.047492	-0.29168729	-1.368364055	18.72352794	-53.84067767
9.3	186861.8	0.006144	0.125129	2.377446063	0.018947	1.908706	1.737403496	-15.4474073	11.288744	-0.29806278	-1.368390284	19.13264562	-53.84120085
9.4	188871	0.006111	0.125129	2.377446063	0.018947	1.908706	1.737370727	-15.7813956	11.5326	-0.304507195	-1.368416094	19.54618415	-53.84171566
9.5	190880.3	0.006079	0.125129	2.377446063	0.018947	1.908706	1.737338476	-16.1189561	11.779061	-0.311020533	-1.368441496	19.9641435	-53.84222232
9.6	192889.6	0.006047	0.125129	2.377446063	0.018947	1.908706	1.73730673	-16.4600885	12.028127	-0.317602796	-1.368466502	20.38652368	-53.84272105
9.7	194898.8	0.006016	0.125129	2.377446063	0.018947	1.908706	1.737275477	-16.8047931	12.279797	-0.324253983	-1.36849112	20.81332466	-53.84321206
9.8	196908.1	0.005985	0.125129	2.377446063	0.018947	1.908706	1.737244703	-17.1530697	12.534072	-0.330974094	-1.368515362	21.24454645	-53.84369554
9.9	198917.4	0.005955	0.125129	2.377446063	0.018947	1.908706	1.737214397	-17.5049184	12.790951	-0.33776313	-1.368539236	21.68018902	-53.84417168
10	200926.6	0.005925	0.125129	2.377446063	0.018947	1.908706	1.737184547	-17.8603391	13.050435	-0.34462109	-1.368562752	22.12025237	-53.84464067
10.1	202935.9	0.005896	0.125129	2.377446063	0.018947	1.908706	1.737155141	-18.2193319	13.312523	-0.351547973	-1.368585918	22.56473649	-53.84510268
10.2	204945.2	0.005867	0.125129	2.377446063	0.018947	1.908706	1.737126168	-18.5818968	13.577216	-0.358543782	-1.368608744	23.01364138	-53.84555788
10.3	206954.4	0.005838	0.125129	2.377446063	0.018947	1.908706	1.737097618	-18.9480338	13.844514	-0.365608514	-1.368631238	23.46696701	-53.84600644
10.4	208963.7	0.00581	0.125129	2.377446063	0.018947	1.908706	1.737069482	-19.3177428	14.114415	-0.37274217	-1.368653407	23.92471338	-53.84644853
10.5	210973	0.005782	0.125129	2.377446063	0.018947	1.908706	1.737041748	-19.6910239	14.386922	-0.379944751	-1.368675259	24.38688048	-53.84688428
10.6	212982.2	0.005755	0.125129	2.377446063	0.018947	1.908706	1.737014407	-20.067877	14.662033	-0.387216256	-1.368696802	24.8534683	-53.84731387
10.7	214991.5	0.005728	0.125129	2.377446063	0.018947	1.908706	1.736987451	-20.4483023	14.939748	-0.394556685	-1.368718042	25.32447684	-53.84773742
10.8	217000.8	0.005702	0.125129	2.377446063	0.018947	1.908706	1.73696087	-20.8322995	15.220067	-0.401966039	-1.368738988	25.79990608	-53.84815507
10.9	219010	0.005675	0.125129	2.377446063	0.018947	1.908706	1.736934655	-21.2198689	15.502991	-0.409444316	-1.368759646	26.27975602	-53.84856697
11	221019.3	0.00565	0.125129	2.377446063	0.018947	1.908706	1.736908799	-21.6110103	15.78852	-0.416991518	-1.368780021	26.76402664	-53.84897325
11.1	223028.6	0.005624	0.125129	2.377446063	0.018947	1.908706	1.736883293	-22.0057238	16.076652	-0.424607644	-1.368800122	27.25271794	-53.84937403
11.2	225037.8	0.005599	0.125129	2.377446063	0.018947	1.908706	1.73685813	-22.4040094	16.36739	-0.432292695	-1.368819953	27.74582991	-53.84976943
11.3	227047.1	0.005574	0.125129	2.377446063	0.018947	1.908706	1.736833301	-22.805867	16.660731	-0.440046669	-1.368839521	28.24336254	-53.85015957
11.4	229056.4	0.00555	0.125129	2.377446063	0.018947	1.908706	1.736808799	-23.2112967	16.956677	-0.447869568	-1.368858831	28.74531583	-53.85054458
11.5	231065.6	0.005525	0.125129	2.377446063	0.018947	1.908706	1.736784618	-23.6202985	17.255227	-0.455761391	-1.36887789	29.25168975	-53.85092455
11.6	233074.9	0.005501	0.125129	2.377446063	0.018947	1.908706	1.736760751	-24.0328723	17.556381	-0.463722138	-1.368896702	29.76248432	-53.85129961
11.7	235084.2	0.005478	0.125129	2.377446063	0.018947	1.908706	1.73673719	-24.4490182	17.86014	-0.471751809	-1.368915273	30.27769951	-53.85166985
11.8	237093.4	0.005455	0.125129	2.377446063	0.018947	1.908706	1.736713929	-24.8687362	18.166503	-0.479850405	-1.368933607	30.79733533	-53.85203537
11.9	239102.7	0.005432	0.125129	2.377446063	0.018947	1.908706	1.736690961	-25.2920262	18.47547	-0.488017925	-1.368951711	31.32139175	-53.85239628
12	241112	0.005409	0.125129	2.377446063	0.018947	1.908706	1.736668282	-25.7188883	18.787041	-0.496254369	-1.368969589	31.84986879	-53.85275268
12.1	243121.2	0.005387	0.125129	2.377446063	0.018947	1.908706	1.736645884	-26.1493225	19.101217	-0.504559737	-1.368987244	32.38276642	-53.85310465
12.2	245130.5	0.005365	0.125129	2.377446063	0.018947	1.908706	1.736623763	-26.5833287	19.417997	-0.51293403	-1.369004683	32.92008464	-53.85345229
12.3	247139.8	0.005343	0.125129	2.377446063	0.018947	1.908706	1.736601911	-27.0209071	19.737381	-0.521377246	-1.369021909	33.46182344	-53.85379568
12.4	249149	0.005321	0.125129	2.377446063	0.018947	1.908706	1.736580325	-27.4620574	20.059369	-0.529889387	-1.369038927	34.00798282	-53.85413491
12.5	251158.3	0.0053	0.125129	2.377446063	0.018947	1.908706	1.736558998	-27.9067799	20.383962	-0.538470452	-1.36905574	34.55856277	-53.85447007
12.6	253167.6	0.005279	0.125129	2.377446063	0.018947	1.908706	1.736537925	-28.3550744	20.711158	-0.547120442	-1.369072353	35.11356328	-53.85480123

12.7	255176.8	0.005258	0.125129	2.377446063	0.018947	1.908706	1.736517102	-28.806941	21.040959	-0.555839355	-1.36908877	35.67298435	-53.85512848
12.8	257186.1	0.005237	0.125129	2.377446063	0.018947	1.908706	1.736496523	-29.2623796	21.373364	-0.564627193	-1.369104995	36.23682596	-53.85545188
12.9	259195.4	0.005217	0.125129	2.377446063	0.018947	1.908706	1.736476184	-29.7213903	21.708373	-0.573483955	-1.369121031	36.80508812	-53.85577152
13	261204.6	0.005197	0.125129	2.377446063	0.018947	1.908706	1.73645608	-30.1839731	22.045986	-0.582409641	-1.369136882	37.37777081	-53.85608747
13.1	263213.9	0.005177	0.125129	2.377446063	0.018947	1.908706	1.736436207	-30.650128	22.386204	-0.591404252	-1.369152551	37.95487402	-53.85639979
13.2	265223.2	0.005157	0.125129	2.377446063	0.018947	1.908706	1.73641656	-31.1198549	22.729025	-0.600467786	-1.369168043	38.53639776	-53.85670857
13.3	267232.4	0.005138	0.125129	2.377446063	0.018947	1.908706	1.736397135	-31.5931539	23.074451	-0.609600245	-1.36918336	39.12234201	-53.85701385
13.4	269241.7	0.005119	0.125129	2.377446063	0.018947	1.908706	1.736377928	-32.0700249	23.42248	-0.618801628	-1.369198505	39.71270677	-53.85731572
13.5	271251	0.0051	0.125129	2.377446063	0.018947	1.908706	1.736358935	-32.550468	23.773114	-0.628071936	-1.369213482	40.30749203	-53.85761422
13.6	273260.2	0.005081	0.125129	2.377446063	0.018947	1.908706	1.736340151	-33.0344832	24.126352	-0.637411167	-1.369228294	40.90669779	-53.85790943
13.7	275269.5	0.005062	0.125129	2.377446063	0.018947	1.908706	1.736321574	-33.5220705	24.482193	-0.646819323	-1.369242944	41.51032404	-53.8582014
13.8	277278.8	0.005044	0.125129	2.377446063	0.018947	1.908706	1.736303199	-34.0132298	24.840639	-0.656296403	-1.369257434	42.11837077	-53.8584902
13.9	279288	0.005026	0.125129	2.377446063	0.018947	1.908706	1.736285023	-34.5079612	25.201689	-0.665842407	-1.369271768	42.73083797	-53.85877588

Pre-Stall Calculations - Active Top Wing

Constants														
Density [kg/m^3]	Span [m]	Chord [m]	e	Wing Area [m^2]	Height of Endplate [m]	AR	AR_effective	CM	μ	Phi	AoA, [ddegrees]	L=0	h_bw	a [per degree]
1.225	0.4064	0.3018	0.7	0.12265152	0.4206	1.346587	3.994499669	-0.152	0.0000184	0.979822457	-6	0.177	0.067733322	
Angle of Attack	-6													
Velocity [m/s]	Re	Csf	a [per degree]	CL (finite)	Cdmin	Cdi	CD (finite)	Downforce [N]	Drag [N]	Moment [N.m]	L/D	Resultant Force Magnitude	Resultant Force Direction	
13.9	279288	0.005026	0.067733	0	0.018947	0	0.02397313	0	0.3479632	N/A	0	0.347963242	0	
Angle of Attack	13													
Velocity [m/s]	Re	Csf	a_ground effect	CL (finite)	Cdmin	Cdi	CD (finite)	Downforce [N]	Drag [N]	Moment [N.m]	L/D	Resultant Force Magnitude	Resultant Force Direction	
0.1	2009.266	0.059253	0.078754	1.49633412	0.018947	0.756092	0.819036385	-0.00112411	0.0006153	-3.44621E-05	-1.8269	0.001281484	-61.30538021	
0.2	4018.533	0.041898	0.078754	1.49633412	0.018947	0.756092	0.801681624	-0.00449643	0.002409	-0.000137848	-1.8665	0.005101103	-61.81920648	
0.3	6027.799	0.03421	0.078754	1.49633412	0.018947	0.756092	0.79399318	-0.01011696	0.0053683	-0.000310159	-1.8846	0.011453024	-62.0484342	
0.4	8037.065	0.029626	0.078754	1.49633412	0.018947	0.756092	0.789409955	-0.01798571	0.0094886	-0.000551394	-1.8955	0.020335169	-62.18554616	
0.5	10046.33	0.026499	0.078754	1.49633412	0.018947	0.756092	0.78628221	-0.02810267	0.0147672	-0.000861553	-1.903	0.031746334	-62.27931521	
0.6	12055.6	0.02419	0.078754	1.49633412	0.018947	0.756092	0.783973404	-0.04046785	0.0212023	-0.001240636	-1.9087	0.045685709	-62.34863629	
0.7	14064.86	0.022395	0.078754	1.49633412	0.018947	0.756092	0.782179001	-0.05508124	0.0287926	-0.001688643	-1.913	0.062152699	-62.40257338	
0.8	16074.13	0.020949	0.078754	1.49633412	0.018947	0.756092	0.780732575	-0.07194284	0.0375372	-0.002205575	-1.9166	0.081146842	-62.4460895	
0.9	18083.4	0.019751	0.078754	1.49633412	0.018947	0.756092	0.779534479	-0.09105266	0.0474351	-0.002791431	-1.9195	0.102667768	-62.48216067	
1	20092.66	0.018737	0.078754	1.49633412	0.018947	0.756092	0.778520925	-0.11241069	0.0584856	-0.003446211	-1.922	0.126715169	-62.51269429	
1.1	22101.93	0.017865	0.078754	1.49633412	0.018947	0.756092	0.777648935	-0.13601693	0.0706884	-0.004169915	-1.9242	0.153288786	-62.53897683	
1.2	24111.2	0.017105	0.078754	1.49633412	0.018947	0.756092	0.776888353	-0.16187139	0.0840427	-0.004962544	-1.9261	0.182388396	-62.56191166	
1.3	26120.46	0.016434	0.078754	1.49633412	0.018947	0.756092	0.776217312	-0.18997406	0.0985483	-0.005824096	-1.9277	0.214013804	-62.58215436	
1.4	28129.73	0.015836	0.078754	1.49633412	0.018947	0.756092	0.775619518	-0.22032495	0.1142047	-0.006754573	-1.9292	0.24816484	-62.60019373	
1.5	30138.99	0.015299	0.078754	1.49633412	0.018947	0.756092	0.775082548	-0.25292405	0.1310115	-0.007753975	-1.9305	0.284841349	-62.61640268	
1.6	32148.26	0.014813	0.078754	1.49633412	0.018947	0.756092	0.77459674	-0.28777136	0.1489686	-0.0088223	-1.9318	0.324043195	-62.63107133	
1.7	34157.53	0.014371	0.078754	1.49633412	0.018947	0.756092	0.774154455	-0.32486689	0.1680755	-0.009959549	-1.9329	0.365770255	-62.64442924	
1.8	36166.79	0.013966	0.078754	1.49633412	0.018947	0.756092	0.773749558	-0.36421063	0.1883321	-0.011165723	-1.9339	0.410022414	-62.65666075	
1.9	38176.06	0.013594	0.078754	1.49633412	0.018947	0.756092	0.773377064	-0.40580258	0.2097382	-0.012440821	-1.9348	0.456799569	-62.66791582	
2	40185.33	0.013249	0.078754	1.49633412	0.018947	0.756092	0.773032868	-0.44964275	0.2322935	-0.013784844	-1.9357	0.506101626	-62.67831787	
2.1	42194.59	0.01293	0.078754	1.49633412	0.018947	0.756092	0.772713559	-0.49573114	0.2559978	-0.01519779	-1.9365	0.557928496	-62.68796952	
2.2	44203.86	0.012633	0.078754	1.49633412	0.018947	0.756092	0.772416277	-0.54406773	0.2808509	-0.016679661	-1.9372	0.612280099	-62.6969569	
2.3	46213.13	0.012355	0.078754	1.49633412	0.018947	0.756092	0.772138601	-0.59465254	0.3068527	-0.018230456	-1.9379	0.669156357	-62.7053529	
2.4	48222.39	0.012095	0.078754	1.49633412	0.018947	0.756092	0.771878465	-0.64748556	0.3340031	-0.019850175	-1.9386	0.728557201	-62.71321967	
2.5	50231.66	0.011851	0.078754	1.49633412	0.018947	0.756092	0.771634097	-0.7025668	0.3623018	-0.021538818	-1.9392	0.790482563	-62.7206106	
2.6	52240.92	0.01162	0.078754	1.49633412	0.018947	0.756092	0.771403967	-0.75989625	0.3917487	-0.023296386	-1.9398	0.854932382	-62.72757182	
2.7	54250.19	0.011403	0.078754	1.49633412	0.018947	0.756092	0.771186743	-0.81947392	0.4223438	-0.025122877	-1.9403	0.921906599	-62.73414343	
2.8	56259.46	0.011198	0.078754	1.49633412	0.018947	0.756092	0.770981263	-0.8812998	0.4540868	-0.027018293	-1.9408	0.991405158	-62.74036049	
2.9	58268.72	0.011003	0.078754	1.49633412	0.018947	0.756092	0.770786505	-0.94537389	0.4869778	-0.028982634	-1.9413	1.063428006	-62.74625377	

3	60277.99	0.010818	0.078754	1.49633412	0.018947	0.756092	0.770601568	-1.01169619	0.5210164	-0.031015898	-1.9418	1.137975095	-62.75185046
3.1	62287.26	0.010642	0.078754	1.49633412	0.018947	0.756092	0.770425653	-1.08026671	0.5562028	-0.033118087	-1.9422	1.215046377	-62.75717464
3.2	64296.52	0.010475	0.078754	1.49633412	0.018947	0.756092	0.77025805	-1.15108545	0.5925367	-0.0352892	-1.9426	1.294641807	-62.76224772
3.3	66305.79	0.010315	0.078754	1.49633412	0.018947	0.756092	0.770098124	-1.22415239	0.630018	-0.037529237	-1.943	1.376761342	-62.76708886
3.4	68315.05	0.010162	0.078754	1.49633412	0.018947	0.756092	0.769945307	-1.29946756	0.6686467	-0.039838198	-1.9434	1.461404942	-62.7717152
3.5	70324.32	0.010016	0.078754	1.49633412	0.018947	0.756092	0.769799087	-1.37703093	0.7084228	-0.042216083	-1.9438	1.548572567	-62.7761422
3.6	72333.59	0.009875	0.078754	1.49633412	0.018947	0.756092	0.769659002	-1.45684252	0.749346	-0.044662893	-1.9442	1.638264181	-62.78038376
3.7	74342.85	0.009741	0.078754	1.49633412	0.018947	0.756092	0.769524635	-1.53890232	0.7914163	-0.047178627	-1.9445	1.730479747	-62.78445248
3.8	76352.12	0.009612	0.078754	1.49633412	0.018947	0.756092	0.769395608	-1.62321034	0.8346337	-0.049763285	-1.9448	1.825219231	-62.7883598
3.9	78361.39	0.009488	0.078754	1.49633412	0.018947	0.756092	0.769271576	-1.70976657	0.8789981	-0.052416868	-1.9451	1.9224826	-62.79211612
4	80370.65	0.009369	0.078754	1.49633412	0.018947	0.756092	0.769152225	-1.79857101	0.9245094	-0.055139374	-1.9454	2.022269823	-62.79573092
4.1	82379.92	0.009254	0.078754	1.49633412	0.018947	0.756092	0.769037267	-1.88962367	0.9711675	-0.057930805	-1.9457	2.124580868	-62.79921287
4.2	84389.18	0.009143	0.078754	1.49633412	0.018947	0.756092	0.76892644	-1.98292454	1.0189724	-0.06079116	-1.946	2.229415708	-62.80256992
4.3	86398.45	0.009036	0.078754	1.49633412	0.018947	0.756092	0.768819502	-2.07847363	1.067924	-0.063720439	-1.9463	2.336774313	-62.80580936
4.4	88407.72	0.008933	0.078754	1.49633412	0.018947	0.756092	0.76871623	-2.17627092	1.1180222	-0.066718643	-1.9465	2.446656657	-62.80893791
4.5	90416.98	0.008833	0.078754	1.49633412	0.018947	0.756092	0.76861642	-2.27631644	1.1692671	-0.069785771	-1.9468	2.559062712	-62.81196175
4.6	92426.25	0.008736	0.078754	1.49633412	0.018947	0.756092	0.768519883	-2.37861016	1.2216584	-0.072921823	-1.947	2.673992454	-62.81488661
4.7	94435.52	0.008643	0.078754	1.49633412	0.018947	0.756092	0.768426443	-2.4831521	1.2751963	-0.076126799	-1.9473	2.791445858	-62.81771775
4.8	96444.78	0.008552	0.078754	1.49633412	0.018947	0.756092	0.768335939	-2.58994226	1.3298806	-0.079400699	-1.9475	2.911422899	-62.8204601
4.9	98454.05	0.008465	0.078754	1.49633412	0.018947	0.756092	0.768248219	-2.69898062	1.3857113	-0.082743524	-1.9477	3.033923556	-62.82311819
5	100463.3	0.00838	0.078754	1.49633412	0.018947	0.756092	0.768163145	-2.81026721	1.4426883	-0.086155272	-1.9479	3.158947805	-62.82569625
5.1	102472.6	0.008297	0.078754	1.49633412	0.018947	0.756092	0.768080585	-2.923802	1.5008116	-0.089635945	-1.9481	3.286495625	-62.82819823
5.2	104481.8	0.008217	0.078754	1.49633412	0.018947	0.756092	0.768000418	-3.03958501	1.5600811	-0.093185543	-1.9484	3.416566994	-62.83062778
5.3	106491.1	0.008139	0.078754	1.49633412	0.018947	0.756092	0.767922531	-3.15761623	1.6204968	-0.096804064	-1.9485	3.549161893	-62.83298835
5.4	108500.4	0.008063	0.078754	1.49633412	0.018947	0.756092	0.767846818	-3.27789567	1.6820587	-0.10049151	-1.9487	3.684280301	-62.83528314
5.5	110509.6	0.00799	0.078754	1.49633412	0.018947	0.756092	0.767773179	-3.40042332	1.7447666	-0.10424788	-1.9489	3.821922199	-62.83751515
5.6	112518.9	0.007918	0.078754	1.49633412	0.018947	0.756092	0.767701522	-3.52519918	1.8086206	-0.108073174	-1.9491	3.962087569	-62.83968718
5.7	114528.2	0.007848	0.078754	1.49633412	0.018947	0.756092	0.767631758	-3.65222326	1.8736207	-0.111967392	-1.9493	4.104776392	-62.84180188
5.8	116537.4	0.00778	0.078754	1.49633412	0.018947	0.756092	0.767563807	-3.78149555	1.9397667	-0.115930535	-1.9495	4.249988649	-62.84386173
5.9	118546.7	0.007714	0.078754	1.49633412	0.018947	0.756092	0.767497591	-3.91301606	2.0070587	-0.119962601	-1.9496	4.397724325	-62.84586906
6	120556	0.00765	0.078754	1.49633412	0.018947	0.756092	0.767433037	-4.04678478	2.0754966	-0.124063592	-1.9498	4.547983402	-62.84782607
6.1	122565.2	0.007587	0.078754	1.49633412	0.018947	0.756092	0.767370077	-4.18280171	2.1450803	-0.128233507	-1.95	4.700765863	-62.84973482
6.2	124574.5	0.007525	0.078754	1.49633412	0.018947	0.756092	0.767308646	-4.32106686	2.2158099	-0.132472347	-1.9501	4.856071693	-62.85159726
6.3	126583.8	0.007465	0.078754	1.49633412	0.018947	0.756092	0.767248684	-4.46158022	2.2876853	-0.13678011	-1.9503	5.013900875	-62.85341524
6.4	128593	0.007407	0.078754	1.49633412	0.018947	0.756092	0.767190133	-4.60434179	2.3607064	-0.141156798	-1.9504	5.174253395	-62.85519051
6.5	130602.3	0.007349	0.078754	1.49633412	0.018947	0.756092	0.767132938	-4.74935158	2.4348733	-0.14560241	-1.9506	5.337129238	-62.8569247
6.6	132611.6	0.007294	0.078754	1.49633412	0.018947	0.756092	0.767077048	-4.89660958	2.5101859	-0.150116947	-1.9507	5.502528388	-62.85861937
6.7	134620.8	0.007239	0.078754	1.49633412	0.018947	0.756092	0.767022414	-5.04611579	2.5866442	-0.154700407	-1.9508	5.6	

8	160741.3	0.006625	0.078754	1.49633412	0.018947	0.756092	0.766408196	-7.19428405	3.6848443	-0.220557497	-1.9524	8.083056383	-62.8789041
8.1	162750.6	0.006584	0.078754	1.49633412	0.018947	0.756092	0.766367176	-7.37526525	3.777339	-0.226105897	-1.9525	8.286303602	-62.88014838
8.2	164759.8	0.006543	0.078754	1.49633412	0.018947	0.756092	0.766326909	-7.55849468	3.8709789	-0.231723221	-1.9526	8.492073934	-62.88136986
8.3	166769.1	0.006504	0.078754	1.49633412	0.018947	0.756092	0.766287372	-7.74397231	3.9657641	-0.237409469	-1.9527	8.700367368	-62.88256922
8.4	168778.4	0.006465	0.078754	1.49633412	0.018947	0.756092	0.766248542	-7.93169816	4.0616946	-0.243164641	-1.9528	8.911183895	-62.88374712
8.5	170787.6	0.006427	0.078754	1.49633412	0.018947	0.756092	0.7662104	-8.12167222	4.1587702	-0.248988737	-1.9529	9.124523504	-62.8849042
8.6	172796.9	0.006389	0.078754	1.49633412	0.018947	0.756092	0.766172925	-8.3138945	4.256991	-0.254881758	-1.953	9.340386185	-62.88604107
8.7	174806.2	0.006353	0.078754	1.49633412	0.018947	0.756092	0.766136099	-8.50836499	4.356357	-0.260843703	-1.9531	9.55877193	-62.8871583
8.8	176815.4	0.006316	0.078754	1.49633412	0.018947	0.756092	0.766099901	-8.7050837	4.4568681	-0.266874572	-1.9532	9.779680728	-62.88825645
8.9	178824.7	0.006281	0.078754	1.49633412	0.018947	0.756092	0.766064316	-8.90405061	4.5585243	-0.272974365	-1.9533	10.00311257	-62.88933606
9	180834	0.006246	0.078754	1.49633412	0.018947	0.756092	0.766029325	-9.10526575	4.6613256	-0.279143083	-1.9534	10.22906745	-62.89039765
9.1	182843.2	0.006211	0.078754	1.49633412	0.018947	0.756092	0.765994913	-9.30872909	4.765272	-0.285380724	-1.9535	10.45754535	-62.89144171
9.2	184852.5	0.006178	0.078754	1.49633412	0.018947	0.756092	0.765961063	-9.51444065	4.8703635	-0.29168729	-1.9535	10.68854628	-62.89246872
9.3	186861.8	0.006144	0.078754	1.49633412	0.018947	0.756092	0.765927761	-9.72240042	4.9766	-0.29806278	-1.9536	10.92207021	-62.89347914
9.4	188871	0.006111	0.078754	1.49633412	0.018947	0.756092	0.765894991	-9.93260841	5.0839815	-0.304507195	-1.9537	11.15811714	-62.89447341
9.5	190880.3	0.006079	0.078754	1.49633412	0.018947	0.756092	0.76586274	-10.1450646	5.1925081	-0.311020533	-1.9538	11.39668706	-62.89545196
9.6	192889.6	0.006047	0.078754	1.49633412	0.018947	0.756092	0.765830995	-10.359769	5.3021796	-0.317602796	-1.9539	11.63777997	-62.89641519
9.7	194898.8	0.006016	0.078754	1.49633412	0.018947	0.756092	0.765799742	-10.5767217	5.4129961	-0.324253983	-1.9539	11.88139585	-62.89736351
9.8	196908.1	0.005985	0.078754	1.49633412	0.018947	0.756092	0.765768968	-10.7959225	5.5249575	-0.330974094	-1.954	12.1275347	-62.89829729
9.9	198917.4	0.005955	0.078754	1.49633412	0.018947	0.756092	0.765738662	-11.0173716	5.6380639	-0.33776313	-1.9541	12.37619652	-62.8992169
10	200926.6	0.005925	0.078754	1.49633412	0.018947	0.756092	0.765708811	-11.2410688	5.7523152	-0.34462109	-1.9542	12.62738128	-62.9001227
10.1	202935.9	0.005896	0.078754	1.49633412	0.018947	0.756092	0.765679405	-11.4670143	5.8677113	-0.351547973	-1.9543	12.88108899	-62.90101502
10.2	204945.2	0.005867	0.078754	1.49633412	0.018947	0.756092	0.765650433	-11.695208	5.9842524	-0.358543782	-1.9543	13.13731963	-62.90189421
10.3	206954.4	0.005838	0.078754	1.49633412	0.018947	0.756092	0.765621883	-11.9256499	6.1019383	-0.365608514	-1.9544	13.39607321	-62.90276057
10.4	208963.7	0.00581	0.078754	1.49633412	0.018947	0.756092	0.765593746	-12.15834	6.2207691	-0.37274217	-1.9545	13.65734971	-62.90361442
10.5	210973	0.005782	0.078754	1.49633412	0.018947	0.756092	0.765566012	-12.3932784	6.3407447	-0.379944751	-1.9545	13.92114912	-62.90445606
10.6	212982.2	0.005755	0.078754	1.49633412	0.018947	0.756092	0.765538672	-12.6304649	6.4618652	-0.387216256	-1.9546	14.18747144	-62.90528577
10.7	214991.5	0.005728	0.078754	1.49633412	0.018947	0.756092	0.765511715	-12.8698997	6.5841304	-0.394556685	-1.9547	14.45631666	-62.90610383
10.8	217000.8	0.005702	0.078754	1.49633412	0.018947	0.756092	0.765485134	-13.1115827	6.7075404	-0.401966039	-1.9548	14.72768478	-62.90691051
10.9	219010	0.005675	0.078754	1.49633412	0.018947	0.756092	0.76545892	-13.3555139	6.8320952	-0.409444316	-1.9548	15.00157579	-62.90770609
11	221019.3	0.00565	0.078754	1.49633412	0.018947	0.756092	0.765433064	-13.6016933	6.9577948	-0.416991518	-1.9549	15.27798967	-62.90849079
11.1	223028.6	0.005624	0.078754	1.49633412	0.018947	0.756092	0.765407558	-13.8501209	7.0846391	-0.424607644	-1.955	15.55692643	-62.90926489
11.2	225037.8	0.005599	0.078754	1.49633412	0.018947	0.756092	0.765382394	-14.1007967	7.2126281	-0.432292695	-1.955	15.83838606	-62.9100286
11.3	227047.1	0.005574	0.078754	1.49633412	0.018947	0.756092	0.765357565	-14.3537208	7.3417619	-0.440046669	-1.9551	16.12236855	-62.91078216
11.4	229056.4	0.00555	0.078754	1.49633412	0.018947	0.756092	0.765333064	-14.608893	7.4720403	-0.447869568	-1.9551	16.40887389	-62.91152579
11.5	231065.6	0.005525	0.078754	1.49633412	0.018947	0.756092	0.765308883	-14.8663135	7.6034635	-0.455761391	-1.9552	16.69790208	-62.91225971
11.6	233074.9	0.005501	0.078754	1.49633412	0.018947	0.756092	0.765285015	-15.1259822	7.7360313	-0.463722138	-1.9553	16.98945312	-62.91298413
11.7	235084.2	0.005478	0.078754	1.49633412	0.018947	0.756092	0.765261454	-15.3878991	7.8697437	-0.471751809	-1.9553		

13	261204.6	0.005197	0.078754	1.49633412	0.018947	0.756092	0.764980345	-18.9974063	9.712164	-0.582409641	-1.956	21.33606282		-62.92223215
13.1	263213.9	0.005177	0.078754	1.49633412	0.018947	0.756092	0.764960472	-19.2907982	9.8619004	-0.591404252	-1.9561	21.66545581		-62.92283543
13.2	265223.2	0.005157	0.078754	1.49633412	0.018947	0.756092	0.764940825	-19.5864383	10.012781	-0.600467786	-1.9561	21.99737155		-62.92343186
13.3	267232.4	0.005138	0.078754	1.49633412	0.018947	0.756092	0.7649214	-19.8843266	10.164807	-0.609600245	-1.9562	22.33181004		-62.92402155
13.4	269241.7	0.005119	0.078754	1.49633412	0.018947	0.756092	0.764902193	-20.1844632	10.317976	-0.618801628	-1.9562	22.66877127		-62.92460464
13.5	271251	0.0051	0.078754	1.49633412	0.018947	0.756092	0.764883199	-20.4868479	10.472291	-0.628071936	-1.9563	23.00825524		-62.92518124
13.6	273260.2	0.005081	0.078754	1.49633412	0.018947	0.756092	0.764864416	-20.7914809	10.627749	-0.637411167	-1.9563	23.35026194		-62.92575147
13.7	275269.5	0.005062	0.078754	1.49633412	0.018947	0.756092	0.764845839	-21.0983621	10.784352	-0.646819323	-1.9564	23.69479138		-62.92631545
13.8	277278.8	0.005044	0.078754	1.49633412	0.018947	0.756092	0.764827464	-21.4074915	10.9421	-0.656296403	-1.9564	24.04184354		-62.9268733
13.9	279288	0.005026	0.078754	1.49633412	0.018947	0.756092	0.764809287	-21.7188691	11.100992	-0.665842407	-1.9565	24.39141842		-62.92742513

Initial Data

restart

Accuracy and approximation: five significant numbers

Digits := 5 :

The following data were used to simulate the four bar linkage mechanism:

$$r1 := 0.26249 = 0.26249$$

$$r2 := 0.081 = 0.081$$

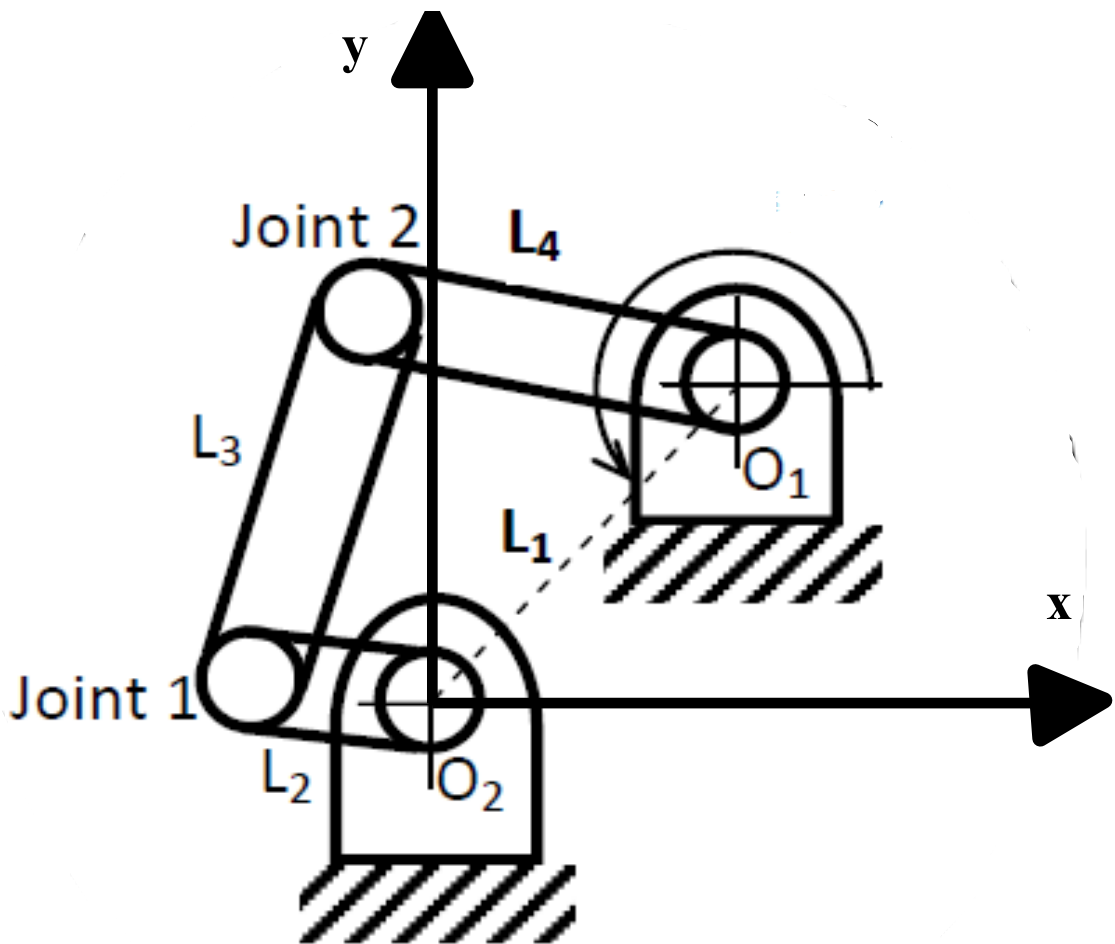
$$r3 := 0.150 = 0.150$$

$$r4 := 0.1605 = 0.1605$$

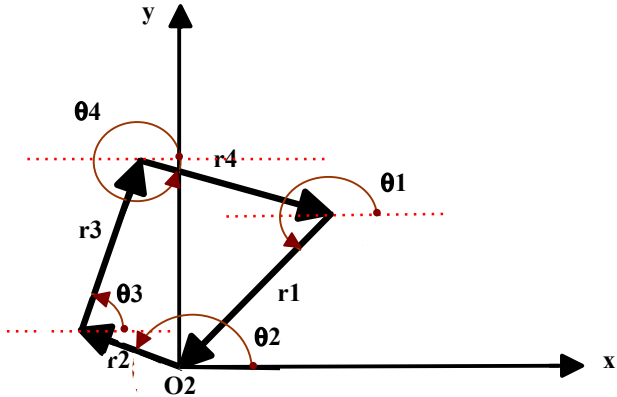
$$\theta1 := \text{evalf}\left(\frac{3}{2} \cdot \pi - \frac{49.635 \cdot \pi}{180}\right) = 3.8459$$

r1, r2, r3 and r4 are the lengths of the links in meters. Rather, r1 is the frame length, r2 is the crank length, r3 is the coupler length and r4 is the rocker length.

theta1 is the angle of the frame with respect to the x-direction. This angle is in radians.



Basically, r_2 is denoted as the vector describing the driving link with the magnitude of 81 mm, r_3 and r_4 are denoted as the vectors describing the connecting links 3 and 4 with the magnitude of 150 and 160.5 mm respectively. And finally, the constant distance of 269.42 mm is described by vector r_1 . The assumption regarding the directions of the vectors is such that all the vectors are drawn in a head to tail fashion producing a closed loop. The angles associated with each vector are drawn with respect to the positive x-axis as shown below (Note that the dotted lines are parallel to the x-axis):



The mathematical representation above requires that sum of all vectors in the closed loop must be zero:

$$\sum_{i=1}^4 \mathbf{r}_i = \mathbf{r}_1 + \mathbf{r}_2 + \mathbf{r}_3 + \mathbf{r}_4 = \mathbf{0}$$

$$r_1(\cos \theta_1, \sin \theta_1)^T + r_2(\cos \theta_2, \sin \theta_2)^T \\ r_3(\cos \theta_3, \sin \theta_3)^T + r_4(\cos \theta_4, \sin \theta_4)^T =$$

In this case, the magnitude of all vectors are known; in addition, θ_1 is given and θ_2 is the input angle. Therefore, the angles θ_3

and θ_4 are unknown. This case corresponds to the case 4 of loop closure equation of the OV. Now the all known vectors are

moved to the right hand side of the equation:

$$r_3(\cos \theta_3, \sin \theta_3)^T + r_4(\cos \theta_4, \sin \theta_4)^T = \\ -r_1(\cos \theta_1, \sin \theta_1)^T - r_2(\cos \theta_2, \sin \theta_2)^T$$

Where θ_i and θ_j are unkowns

$$r_i(\cos \theta_i, \sin \theta_i)^T + r_j(\cos \theta_j, \sin \theta_j)^T = b (\cos \alpha, \sin \alpha)^T$$

▼ Loop-closure equation 1

Here the vectors of R1,R2,R3, and R4 are obtained from their magnitudes and directions.

R1 := r1·⟨cos(θ1), sin(θ1)⟩ :

R2 := r2·⟨cos(θ2), sin(θ2)⟩ :

R3 := r3·⟨cos(θ3), sin(θ3)⟩ :

R4 := r4·⟨cos(θ4), sin(θ4)⟩ :

Fundamentals of vectors require that the sum of the vectors must be equal to zero (loop-Closure equation)

loop1 := R1 + R2 + R3 + R4 = 0 :

All the known vectors are moved to the right hand side of the loop closure equation

loop1 := R3 + R4 = -(R1 + R2) :

Given: $r_1, r_2, r_3, r_4, \theta_1, \theta_2$

Unknown: $\theta_3, \theta_4 \Rightarrow$ 4th Case in the OV book

▼ Calculation of vector b

Define vector b as the sum of the known vectors on the right hand side of the loop closure equation (loop1):

$$b := -(R1 + R2) :$$

The x and y components of vector b are computed as follows:

$$b1x := b[1] :$$

$$b1y := b[2] :$$

$$b1 := \sqrt{b1x^2 + b1y^2} :$$

$$\alpha1 := \arctan(b1y, b1x) :$$

▼ Calculation of unknowns θ_3, θ_4

$$ri := r3 :$$

$$rj := r4 :$$

$$\theta_i := \theta_3 :$$

$$A := \frac{(b1^2 - ri^2 + rj^2)}{2 b1 \cdot rj} :$$

$$B := \frac{(b1 - rj \cdot A)}{ri} :$$

$$C1 := \frac{rj}{ri} \sqrt{1 - A^2} :$$

$$C2 := -\frac{rj}{ri} \sqrt{1 - A^2} :$$

Note that two possible configurations are possible (See O.V book, whether we use $C1$ or $C2$):

$$\theta_i := \alpha1 - \arctan(C1, B) :$$

$$\theta_i := \alpha1 - \arctan(C2, B) :$$

$$\theta_3 := \theta_i :$$

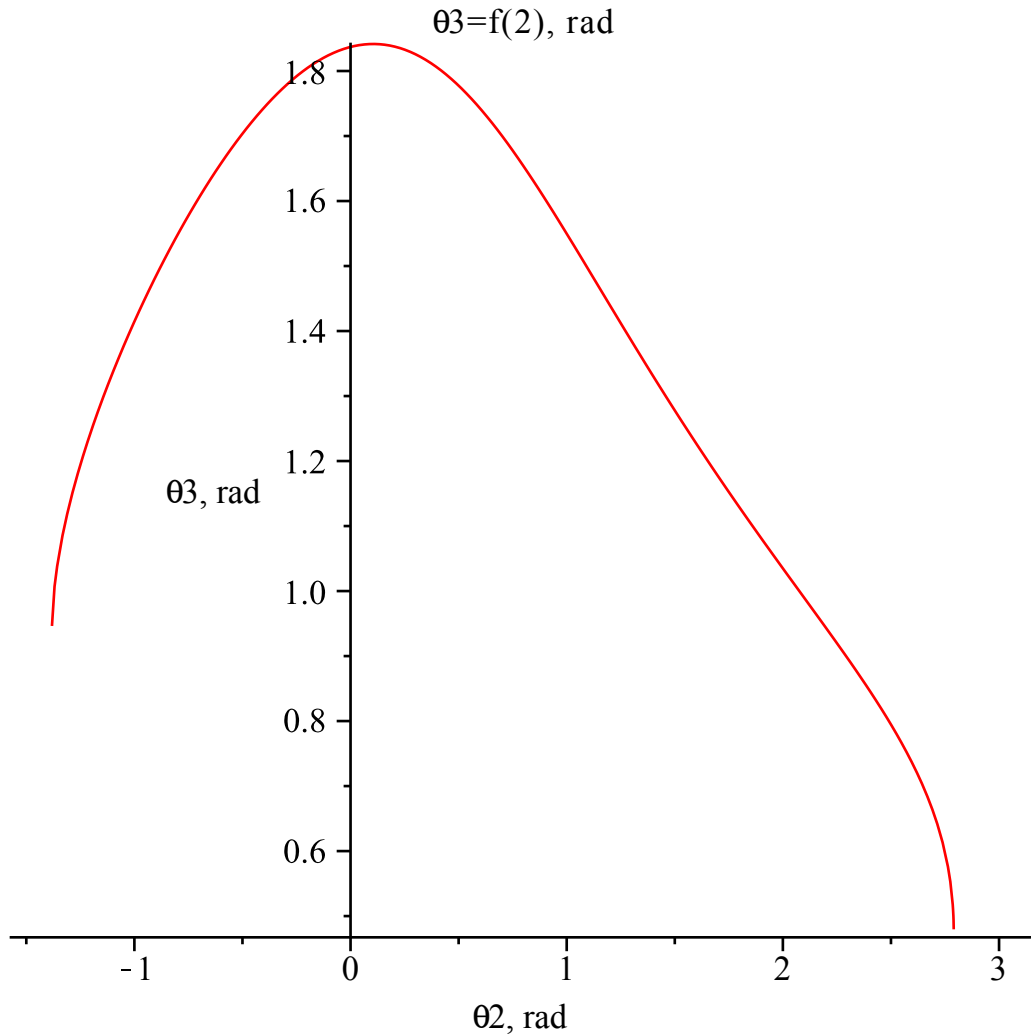
$$\cos \alpha \theta j := \frac{(b1 - ri \cdot \cos(\alpha1 - \theta_i))}{rj} :$$

$$\begin{aligned}
 \sin\alpha\theta_j &:= -\frac{\mathbf{r}_i \cdot \sin(\alpha_1 - \theta_i)}{\mathbf{r}_j} : \\
 \theta_j &:= \alpha_1 - \arctan(\sin\alpha\theta_j, \cos\alpha\theta_j) : \\
 \theta_4 &:= \theta_j :
 \end{aligned} \tag{4.1}$$

Plots

The plot of coupler angle in terms of the crank angle is shown below:

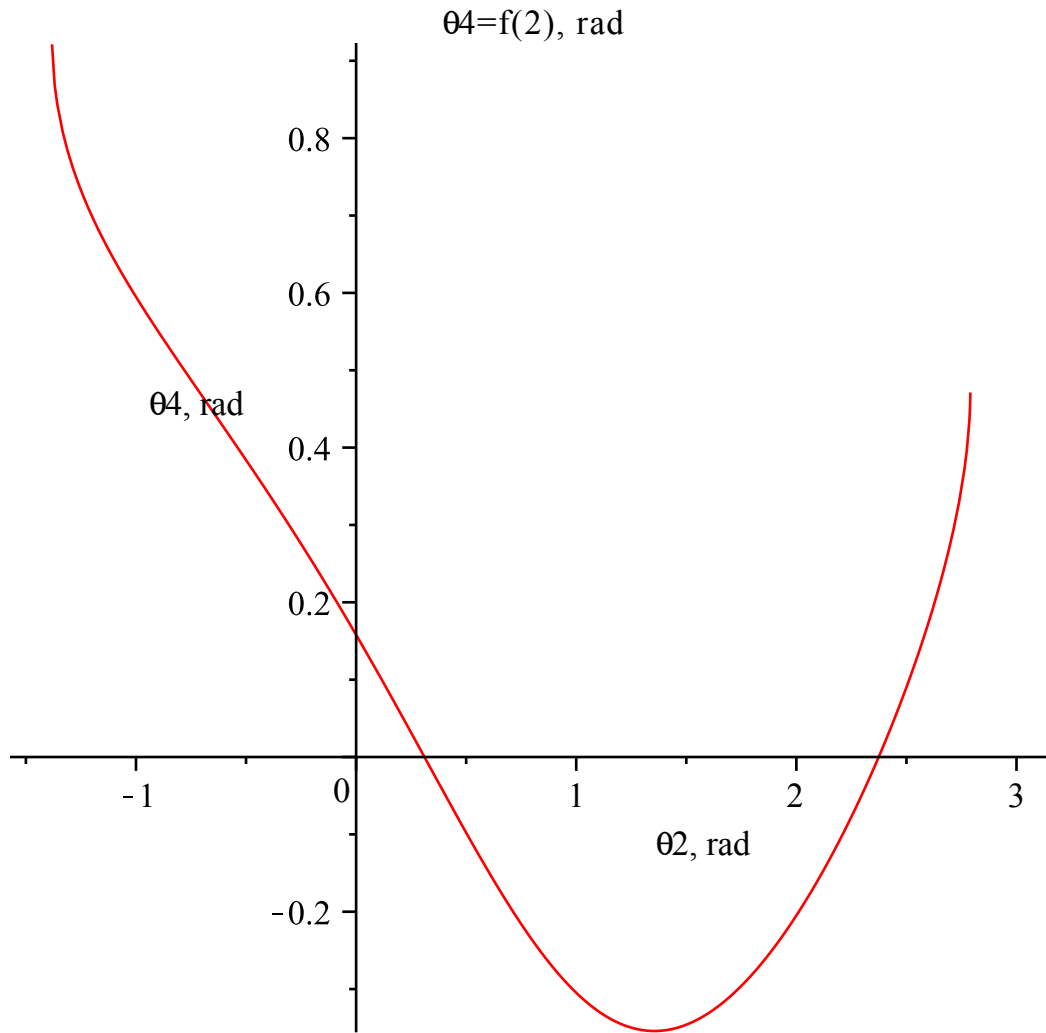
$$\text{plot}\left(\theta_3, \theta_2 = -\frac{\pi}{2} .. \pi, \text{labels} = ["\theta_2, \text{rad}", "\theta_3, \text{rad}"], \text{title} = "\theta_3=f(\theta_2), \text{rad}"\right)$$



It is easy to probe this plot and get theta2(input) for any theta3(output or wing)

The plot of rocker angle as a function crank (input) angle is shown below:

$$\text{plot}\left(\theta_4, \theta_2 = -\frac{\pi}{2} \dots \pi, \text{labels} = ["\theta_2, \text{rad}", "\theta_4, \text{rad}"], \text{title} = "\theta_4=f(\theta_2), \text{rad}"\right)$$



The sum of R2 and R3 would give us the vector from the joint 2 to the joint 3 and then its magnitude is calculated as shown:

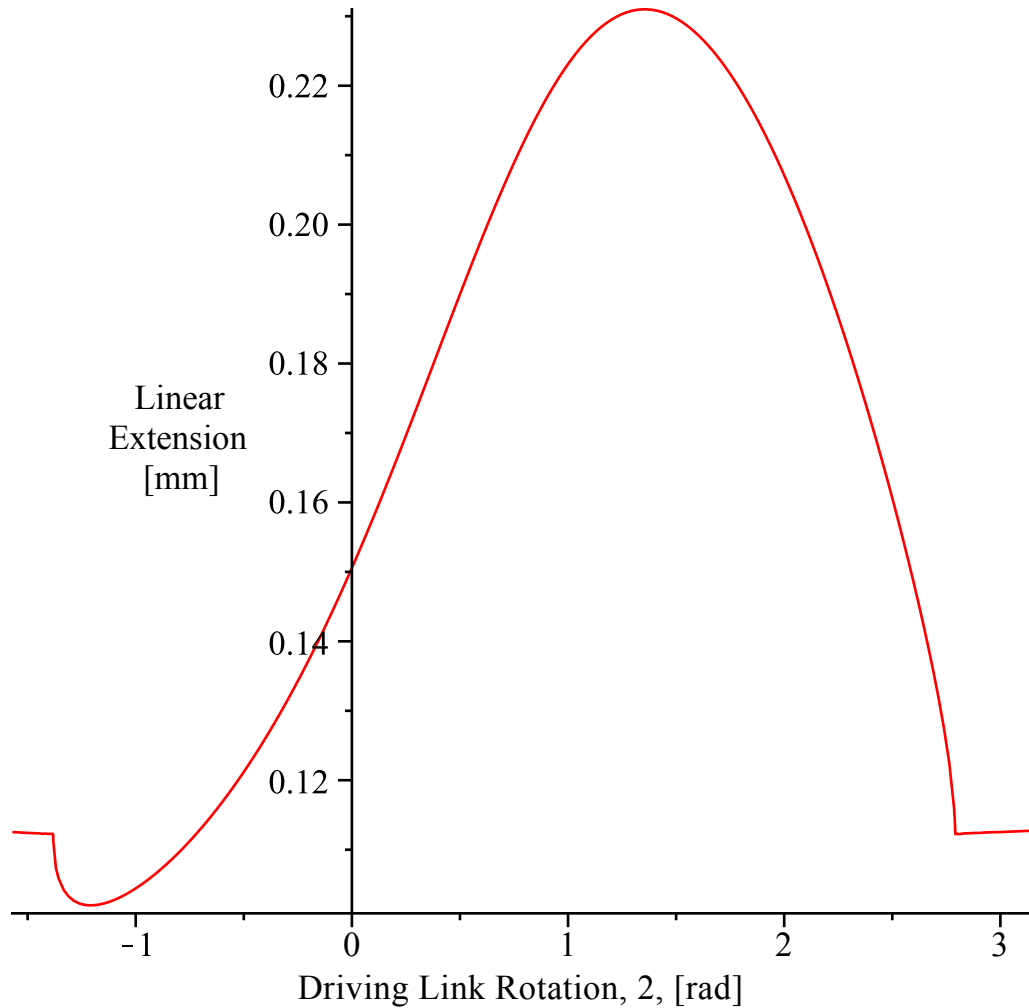
$$R_{23x} := R_2 + R_3 :$$

$$r_{23x} := \sqrt(R_{23x} \cdot R_{23x}) :$$

➤ The plot of the magnitude of r23 as a function of theta2 (input) is

shown (used in control analysis):

```
plot(r23x, theta2 = -pi/2 .. pi, labels = [ "theta2, rad", "r23, m" ], title = "r23=f(theta2), m")
```



Animation

Note: J23 - joint between links 2 and 3;
J34 - joint between links 3 and 4;
O2J23 - line connecting points O2 and Joint23;
J23J34 - line connecting Joint23 and Joint34;
J34O1 - line connecting Joint34 and point O1;

```
with(plots) :  
with(geometry) :  
with(plottools) :
```

```

pointO2 := <0, 0> :
J23 := R2 :
J34 := R2 + R3 :
pointO1 := R2 + R3 + R4 :

```

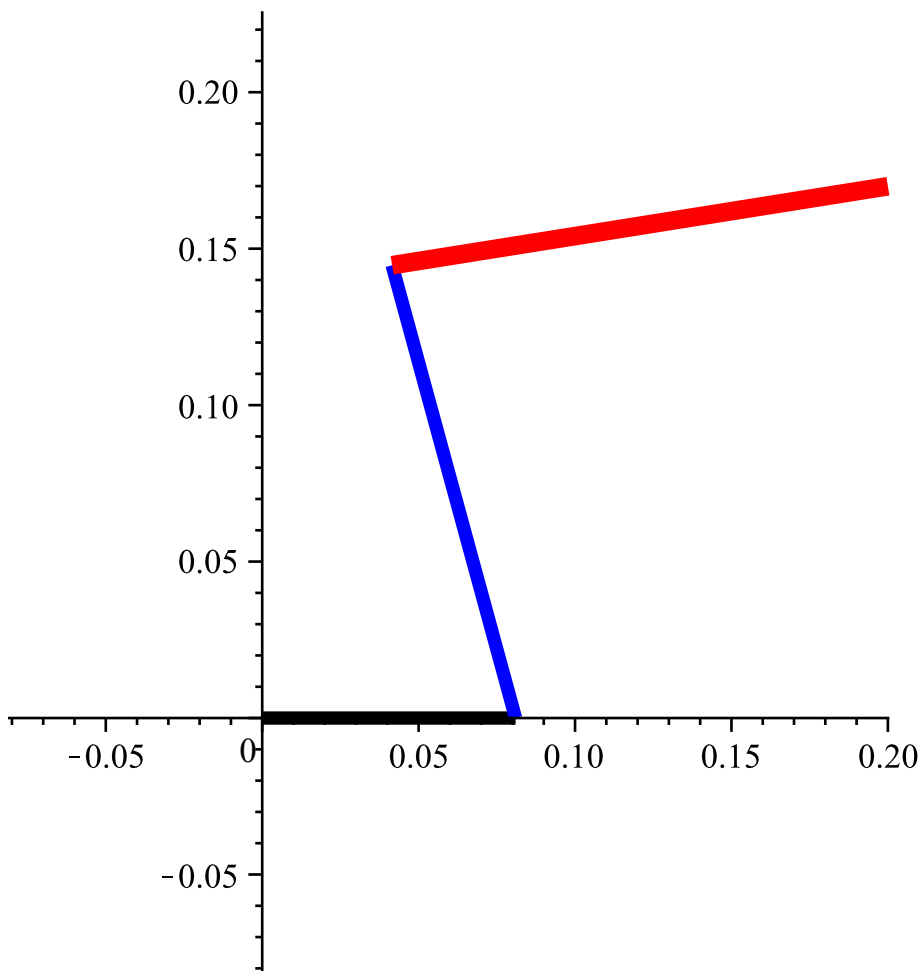
```

MechLoop1 :=proc(input)
global θ2, r1, r2, r3, r4;
local x1, y1, x2, y2, x3, y3, x4, y4, O2J23, J23J34, J34O1;
θ2 := input;
x1 := pointO2[1];
y1 := pointO2[2];
x2 := J23[1];
y2 := J23[2];
x3 := J34[1];
y3 := J34[2];
x4 := pointO1[1];
y4 := pointO1[2];
O2J23 := plottools[line]([x1, y1], [x2, y2], color = black,
thickness = 5);
J23J34 := plottools[line]([x2, y2], [x3, y3], color = blue,
thickness = 5);
J34O1 := plottools[line]([x3, y3], [x4, y4], color = red, thickness
= 7);
plots[display](O2J23, J23J34, J34O1);
end proc:

animate(MechLoop1, [θ2], θ2 = 0 .. 2 π, frames = 50, trace = 0,
scaling = constrained, )
it just works over a range of input theta2

```

$$\theta_2 = 0.$$



$\theta_2 := '02':$

Velocity Analysis:

Analysis:

This loop refers to the fourth case of mechanism according to the O. V. textbook. Using equations 2.84 and 2.85 we will have:

$$\omega_i r_i \sin(\theta_j - \theta_i) = -\dot{r}_i \cos(\theta_j - \theta_i) - \dot{r}_j + \dot{b}_x \cos \theta_j + \dot{b}_y \sin \theta_j \quad (2.84)$$

$$\omega_j r_j \sin(\theta_i - \theta_j) = -\dot{r}_j \cos(\theta_i - \theta_j) - \dot{r}_i + \dot{b}_x \cos \theta_i + \dot{b}_y \sin \theta_i \quad (2.85)$$

We can solve for ω_3 and ω_4 in equations 2.84 and 2.85 which leads us to equations 2.99 and 2.100 in O.V Textbook.

$$\omega_3 = \omega_2 \frac{r_2 \sin(\theta_2 - \theta_4)}{r_3 \sin(\theta_4 - \theta_3)} \quad (2.99)$$

$$\omega_4 = \omega_2 \frac{r_2 \sin(\theta_2 - \theta_3)}{r_4 \sin(\theta_3 - \theta_4)} \quad (2.100)$$

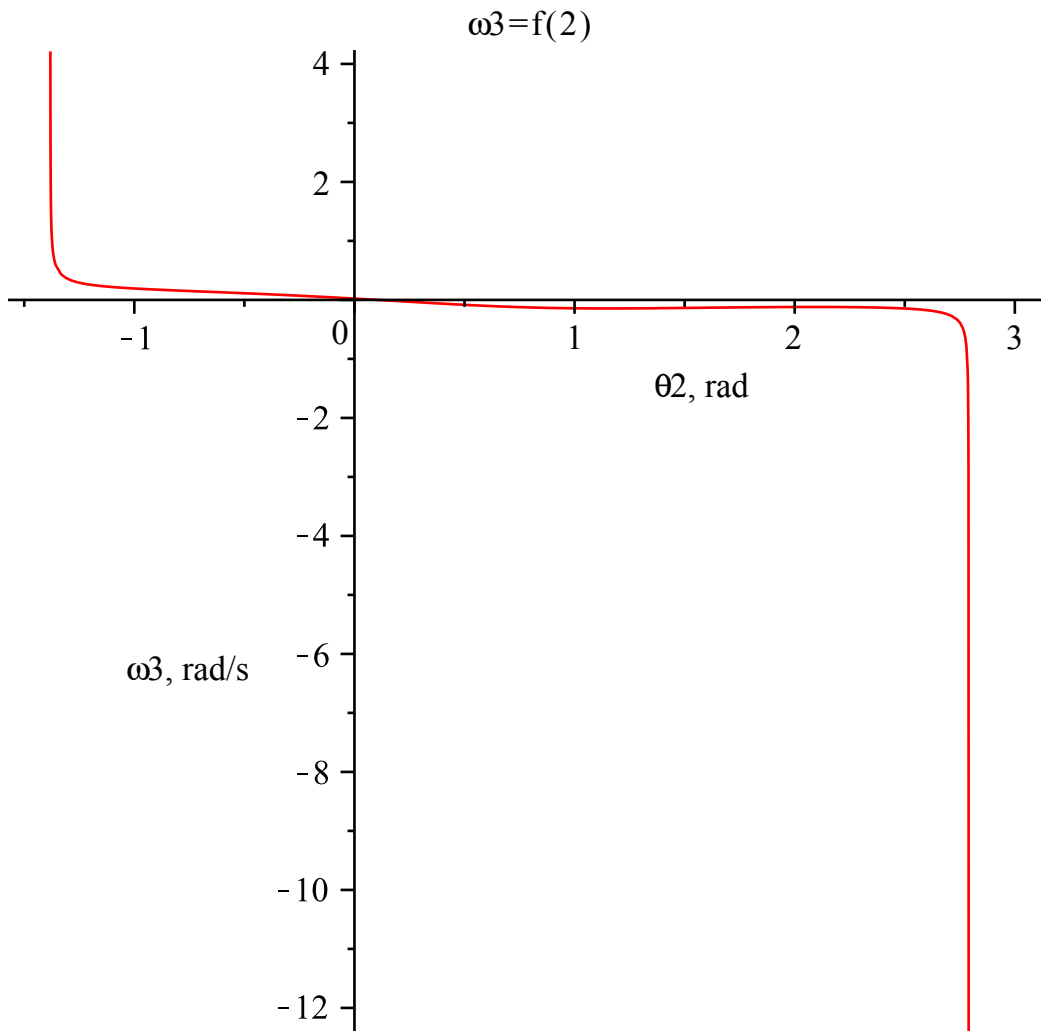
$$\omega_2 := \frac{\pi}{12} :$$

$$\omega_3 := \omega_2 \cdot \left(\frac{r_2 \cdot \sin(\theta_2 - \theta_4)}{r_3 \cdot \sin(\theta_4 - \theta_3)} \right) :$$

$$\omega_4 := \omega_2 \cdot \left(\frac{r_2 \cdot \sin(\theta_2 - \theta_3)}{r_3 \cdot \sin(\theta_3 - \theta_4)} \right) :$$

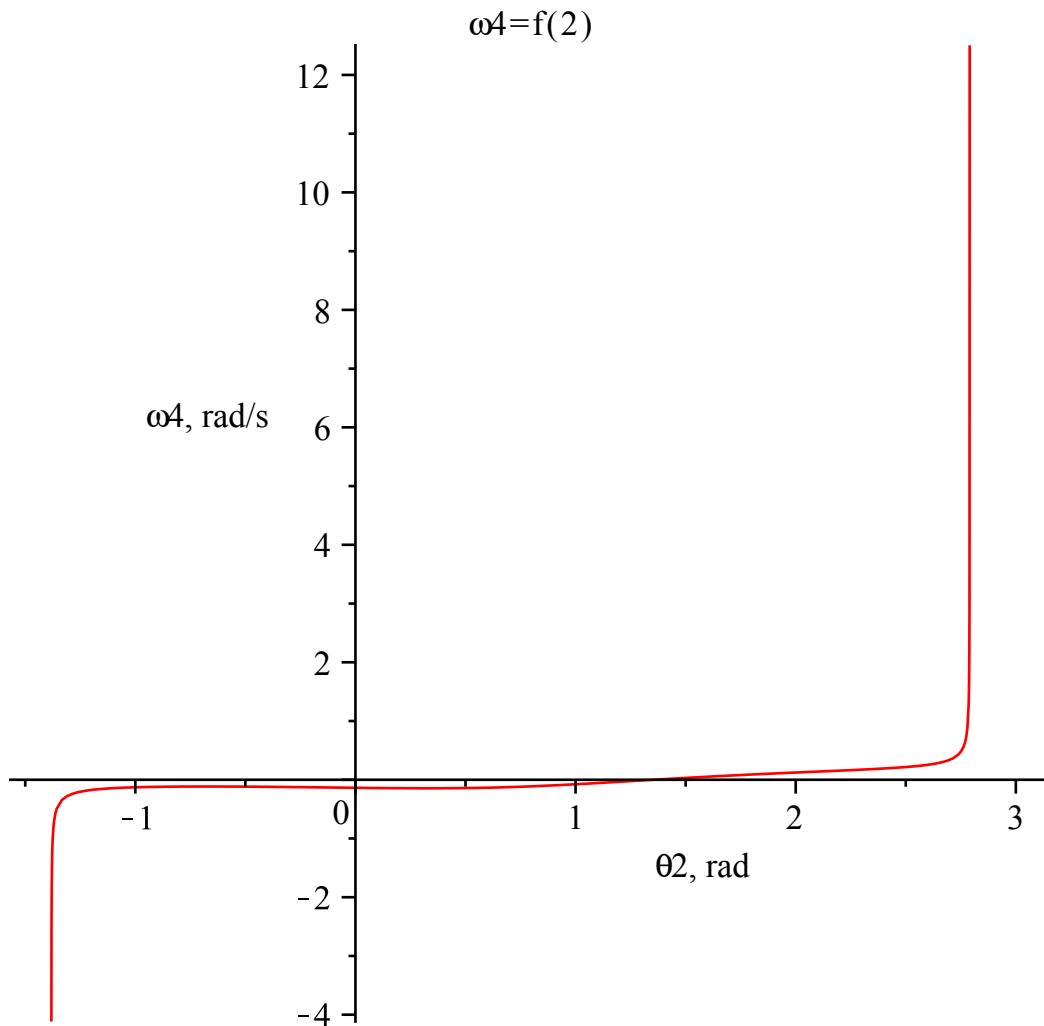
Plots

$$\text{plot}\left(\omega_3, \theta_2 = -\frac{\pi}{2} .. \pi, \text{labels} = ["\theta_2, \text{rad}", "\omega_3, \text{rad/s}"], \text{title} = "\omega_3=f(\theta_2)"\right)$$



This suggests that the variation of angular velocity of the wing is not significant, so for the constant crank velocity we would have approximately constant wing angular velocity. The extreme points where we have vertical asymptotes indicate the boundaries of the system. The linkage will not move beyond the boundaries.

$$\text{plot}\left(\omega_4, \theta_2 = -\frac{\pi}{2} .. \pi, \text{labels} = ["\theta_2, \text{rad}", "\omega_4, \text{rad/s}"], \text{title} = "\omega_4=f(\theta_2)"\right)$$



Acceleration

As the mechanism corresponds to the fourth case we use equations 2.141 and 142 to solve for unkowns:

$$\alpha_3 = \frac{-r_3\omega_3(\omega_4 - \omega_3)\cos(\theta_4 - \theta_3) + r_2\alpha_2\sin(\theta_2 - \theta_4) + r_2\omega_2(\omega_2 - \omega_4)\cos(\theta_2 - \theta_4)}{r_3\sin(\theta_4 - \theta_3)} \quad (2.141)$$

Analysis:

$\alpha_2 := 0 :$

$$\alpha_3 := \frac{1}{r_3\sin(\theta_4 - \theta_3)} (-r_3 \cdot \omega_3 \cdot (\omega_4 - \omega_3) \cdot \cos(\theta_4 - \theta_3) + r_2 \cdot \alpha_2)$$

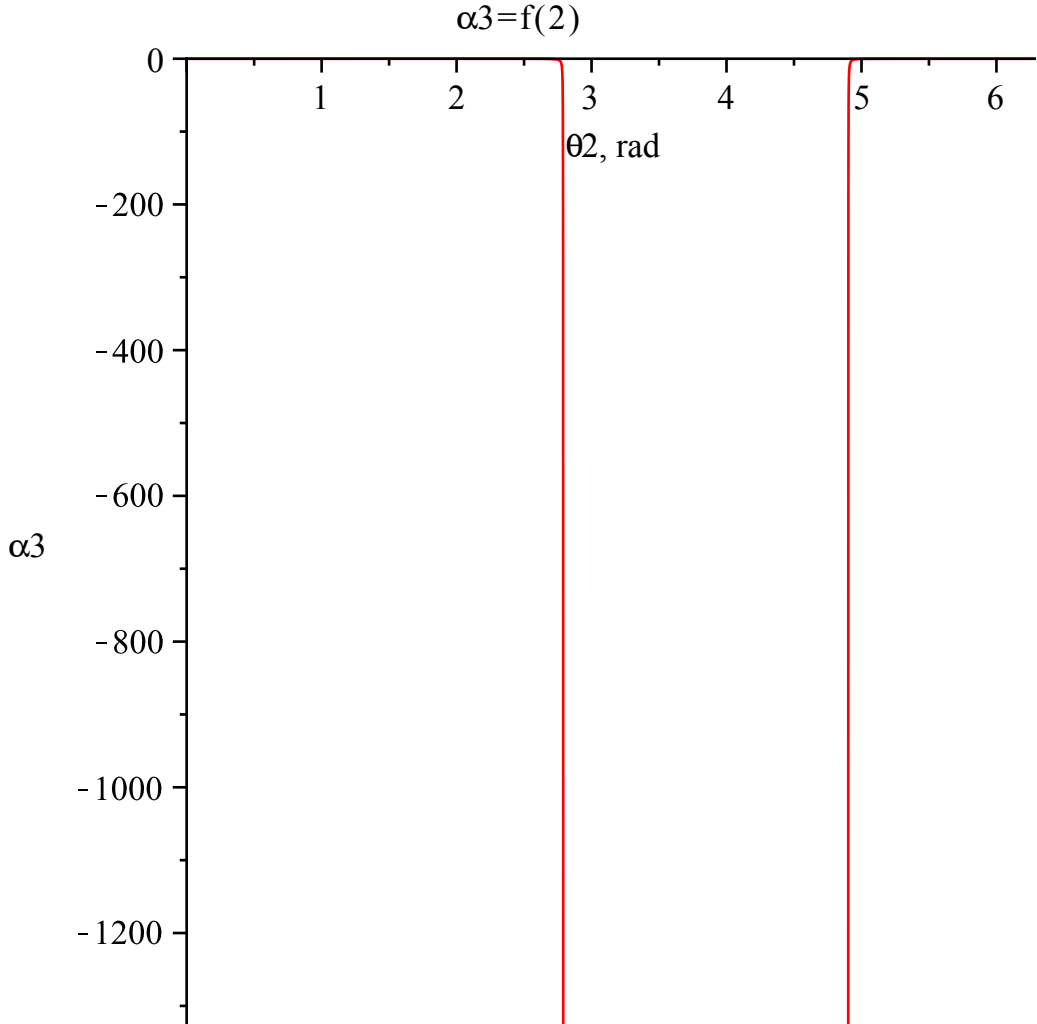
```

.sin(θ2 - θ4) + r2.ω2.(ω2 - ω4).cos(θ2 - θ4)) :
α4 :=  $\frac{1}{r4.\sin(\theta3 - \theta4)}(-r4 \cdot \omega4.(\omega3 - \omega4).\cos(\theta3 - \theta4) + r2.\alpha2$ 
.sin(θ2 - θ3) + r2.ω2.(ω2 - ω3).cos(θ2 - θ3)) :

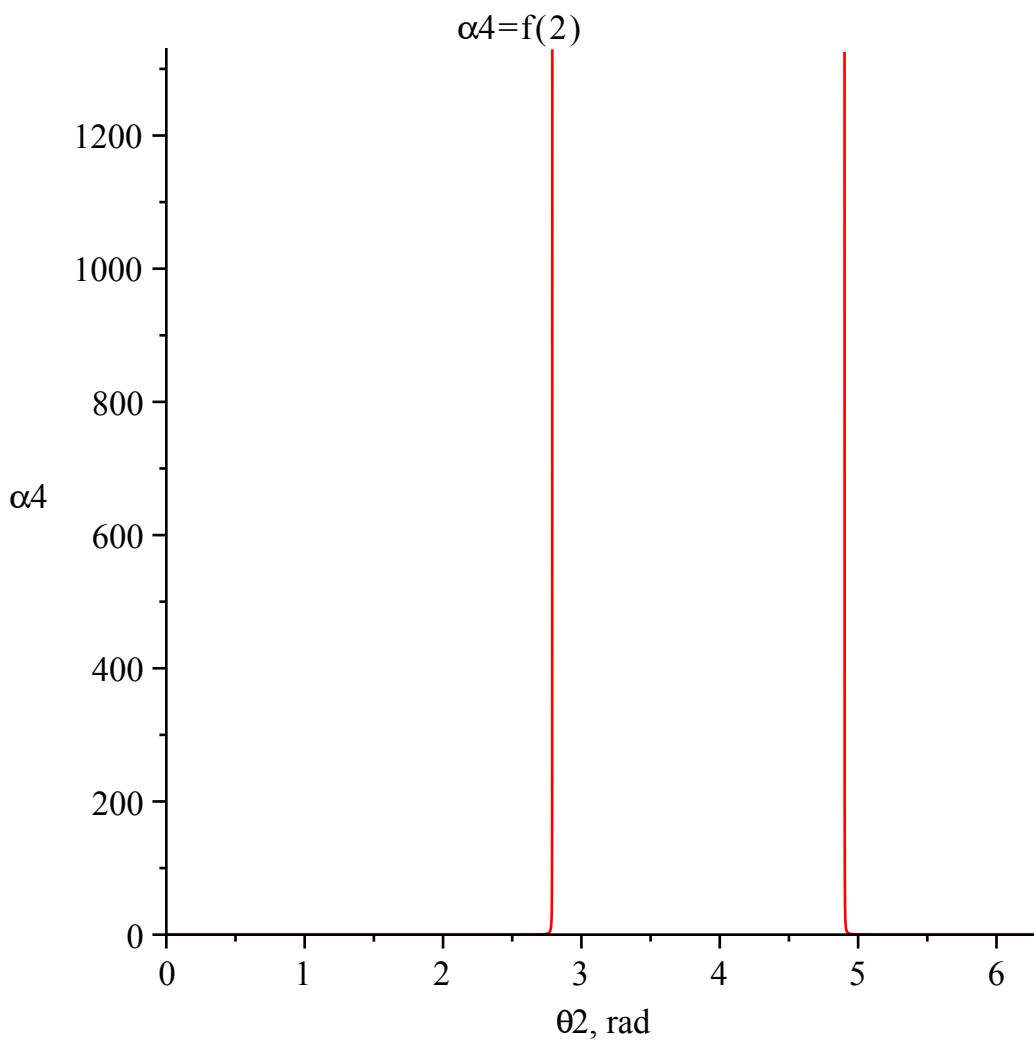
```

Plots

```
plot(α3, θ2 = 0 ..2·π, labels = [ "θ2, rad", "α3" ], title = "α3=f(θ2)" )
```



```
plot(α4, θ2 = 0 ..2·π, labels = [ "θ2, rad", "α4" ], title = "α4=f(θ2)" )
```



Force Analysis:

The angle of attack of the wing is geometrically related to the coupler angle:

$$\alpha := \left(\theta_3 - \frac{75.51}{180} \pi \right) :$$

From the aerodynamic analysis, the resultant aerodynamic force (drag+downforce). Basically, they depend on air density, car velocity, angle of attack and the size coefficient:

$$\text{ResultantF} := \left((0.472018 \cdot V^2 \cdot \alpha)^2 + (.00944 \cdot V^2 \cdot \alpha)^2 \right)^{0.5} : \quad (9.1)$$

The resultant force is revolved into x and y direction and the effect of wing's weight is incorporated into Fy:

$$\begin{aligned} r2x &:= r2 \cdot \cos(\theta2) : \\ r2y &:= r2 \cdot \sin(\theta2) : \\ Fx &:= \text{ResultantF} \cdot \cos(\alpha) : \\ Fy &:= \text{ResultantF} \cdot \sin(\alpha) + 14 : \end{aligned} \quad (9.2)$$

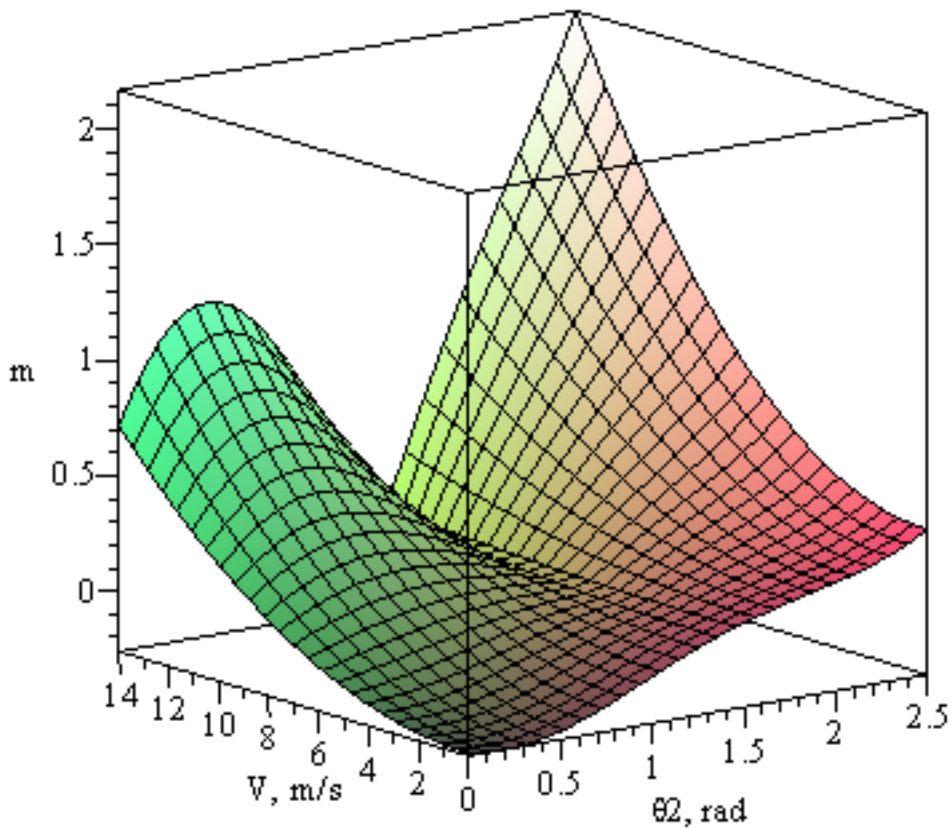
Applying the inverse dynamic method and ignoring the inertial forces, the torque by the crank can be obtained from:

$$T := r2x \cdot \left(\frac{Fy}{2} \right) + r2y \cdot \left(\frac{Fx}{2} \right) - \frac{\pi}{2} \cdot \alpha : \text{Moment equilibrium equation for link 2}$$

The 3D plot of torque as functions of input angle and car velocity is shown below:

```
plot3d(T, θ2 = 0 .. 2.5, V = 0 .. 14, labels = ["θ2, rad", "V, m/s", "T, N m"], title = "T=f(θ2,V)")
```

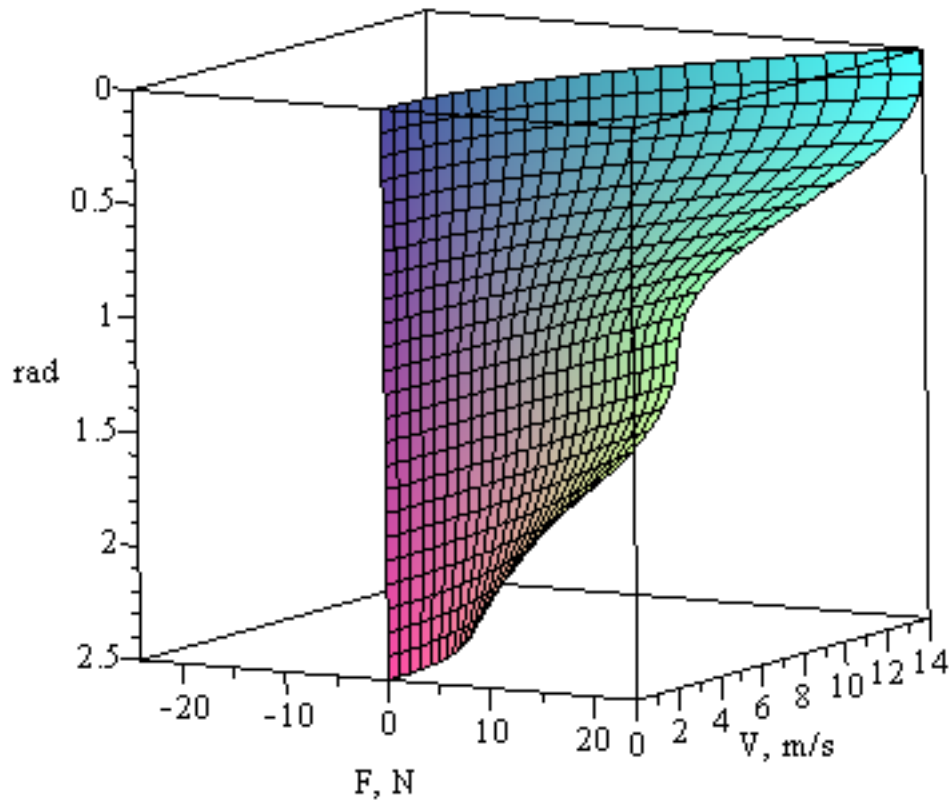
$$T=f(2, V)$$



The 3D plot of downforce as functions of input angle and car velocity is shown below:

```
plot3d(ResultantF·sin(α), θ2 = 0 .. 2.5, V = 0 ..14, labels = [ "θ2, rad",
"V, m/s", "F, N "], title = "F=f(θ2,V)")
```

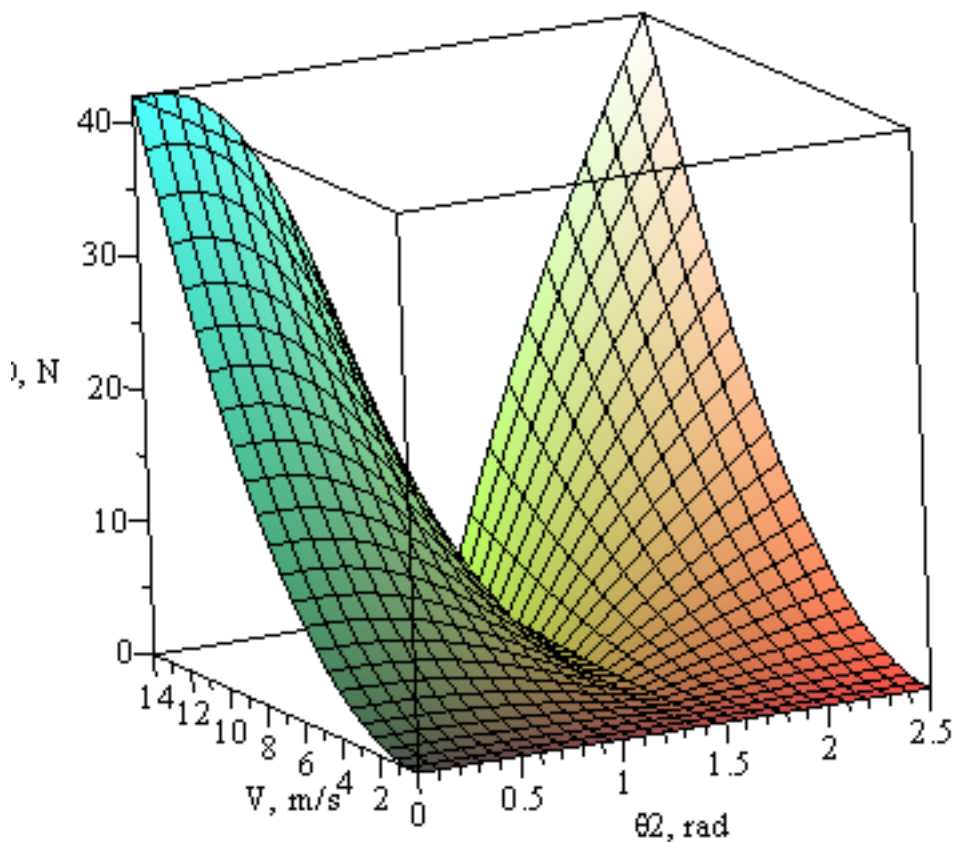
$$F=f(2, V)$$

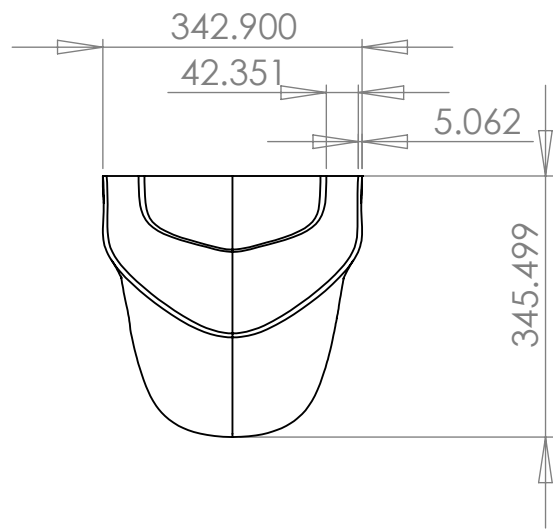
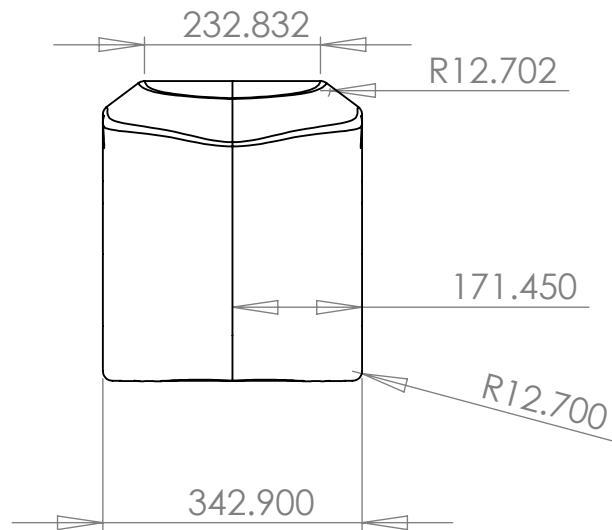


The 3D plot of drag as functions of input angle and car velocity is shown below:

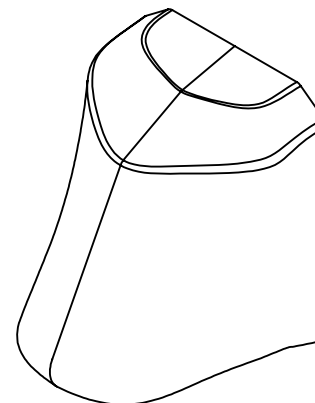
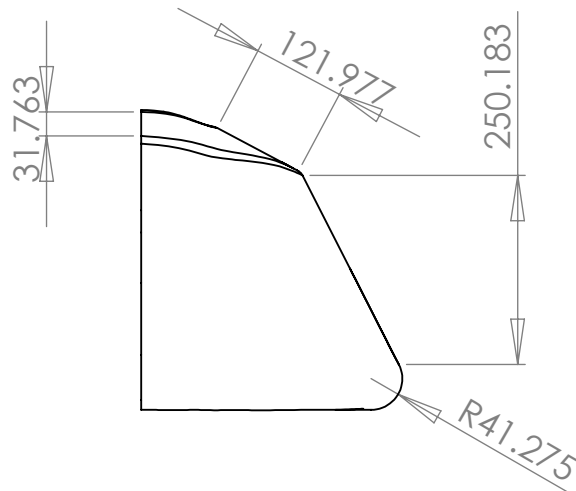
```
plot3d(Fx, θ2 = 0 .. 2.5, V = 0 ..14, labels = ["θ2, rad", "V, m/s", "D, N "], title  
= "D=f(θ2,V)")
```

$$D=f(2, V)$$



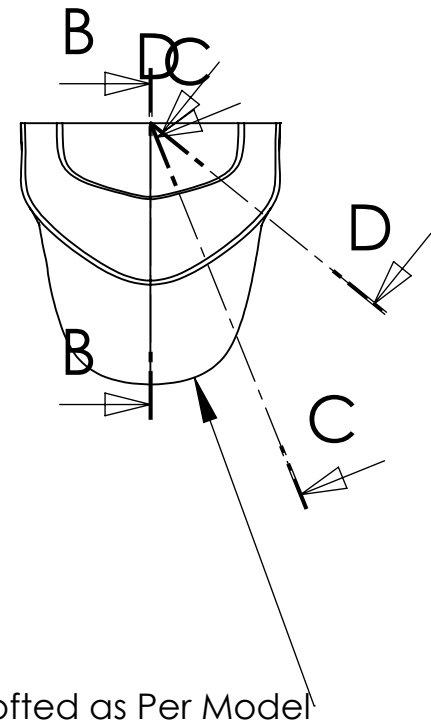
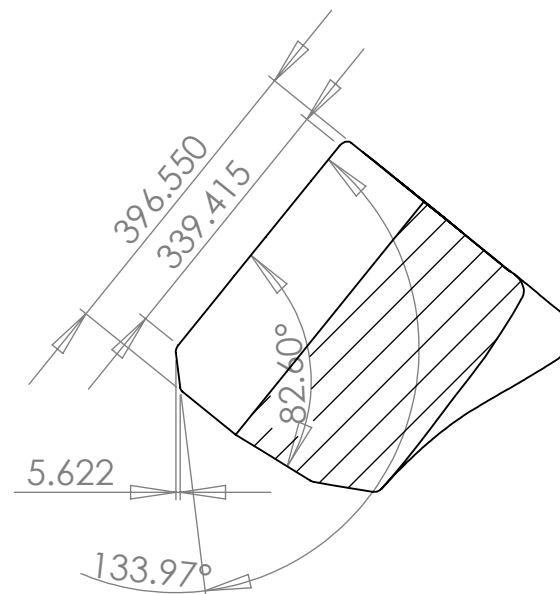
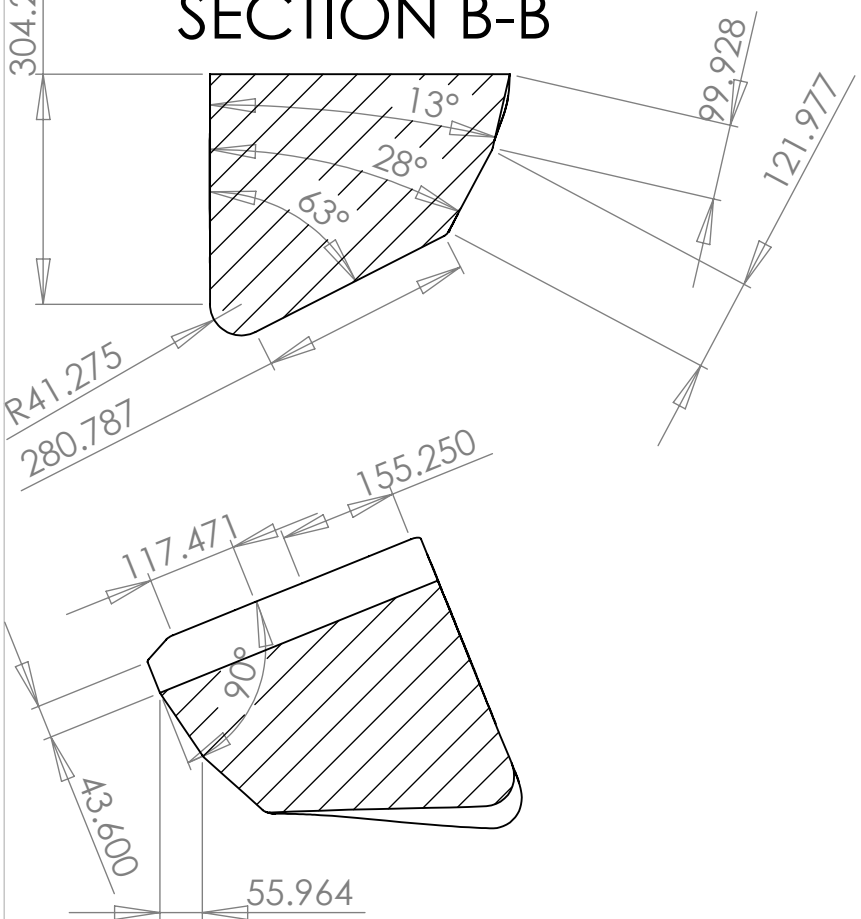


PROPRIETARY AND CONFIDENTIAL
THE INFORMATION CONTAINED IN THIS
DRAWING IS THE SOLE PROPERTY OF
KHAB ENGINEERING AND DESIGN. ANY
REPRODUCTION IN PART OR AS A WHOLE
WITHOUT THE WRITTEN PERMISSION OF
KHAB ENGINEERING AND DESIGN IS
PROHIBITED.



UNLESS OTHERWISE SPECIFIED:	KHAB ENGINEERING & DESIGN		
DIMENSIONS ARE IN INCHES TOLERANCES: ANGULAR: MACH \pm 0.1 TWO PLACE DECIMAL \pm 0.1 THREE PLACE DECIMAL \pm 0.01	TITLE: Nose Cone, FE-XX-12		
INTERPRET GEOMETRIC TOLERANCING PER: ASME Y14.5-2009			
MATERIAL Glass Fiber Reinforced Polymer	SIZE	DWG. NO.	REV
FINISH AS SHOWN	A	FE-12-AR-001	A
DO NOT SCALE DRAWING	SCALE: 1:10		SHEET 1 OF 15

SECTION B-B

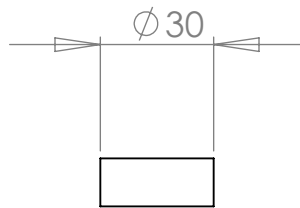
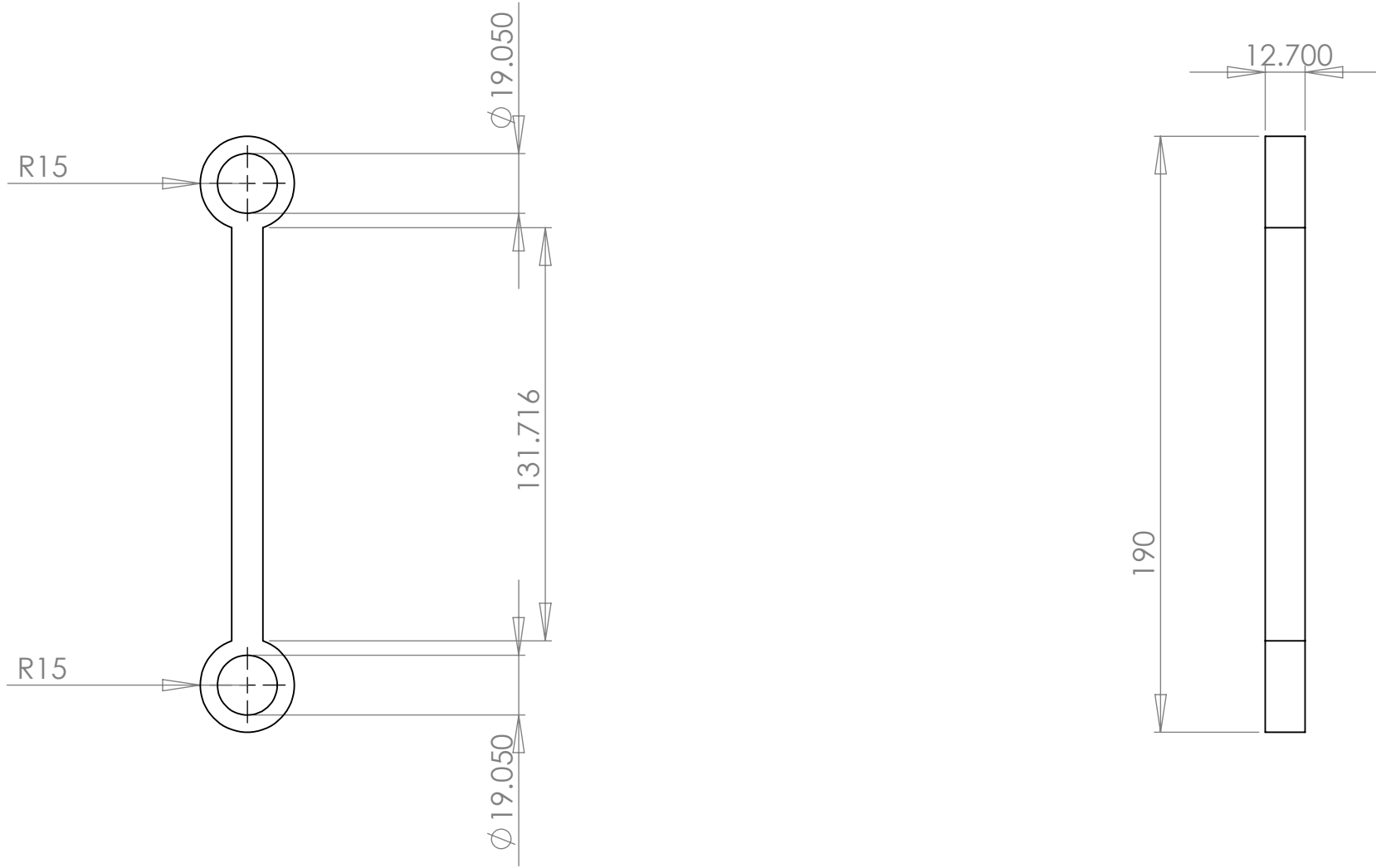


SECTION C-C

SECTION D-D

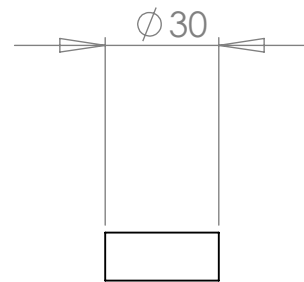
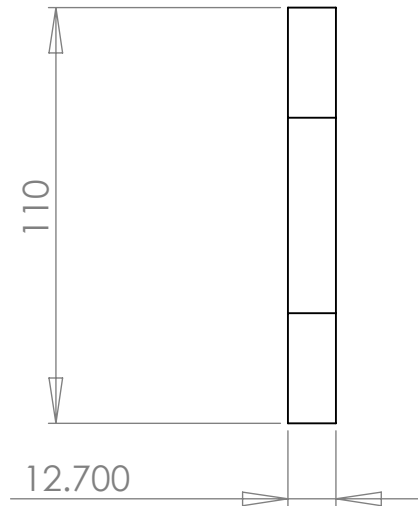
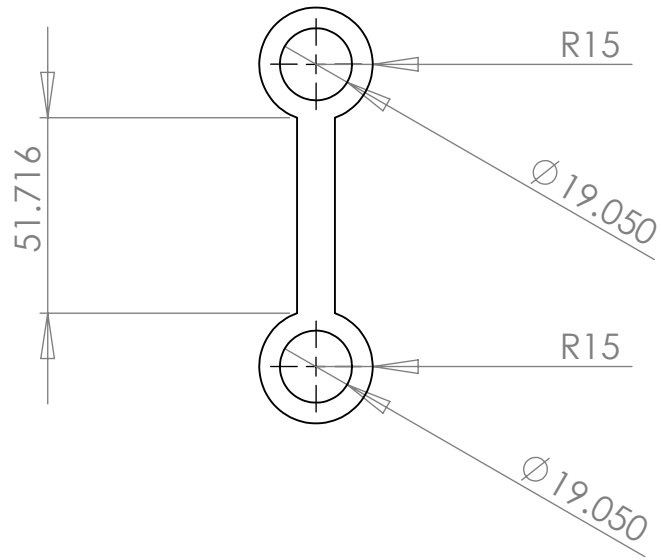
PROPRIETARY AND CONFIDENTIAL
THE INFORMATION CONTAINED IN THIS DRAWING IS THE SOLE PROPERTY OF Khab Engineering and Design. ANY REPRODUCTION IN PART OR AS A WHOLE WITHOUT THE WRITTEN PERMISSION OF Khab Engineering and Design IS PROHIBITED.

UNLESS OTHERWISE SPECIFIED:	Khab Engineering & Design		
DIMENSIONS ARE IN INCHES TOLERANCES: ANGULAR: MACH \pm 0.1 TWO PLACE DECIMAL \pm 0.1 THREE PLACE DECIMAL \pm 0.01	TITLE: Nose Cone, FE-XX-12		
INTERPRET GEOMETRIC TOLERANCING PER: ASME Y14.5-2009			
MATERIAL Glass Fiber Reinforced Polymer	SIZE	DWG. NO.	REV
FINISH AS SHOWN	A	FE-12-AR-001	A
DO NOT SCALE DRAWING	SCALE: 1:10 WEIGHT:		SHEET 2 OF 15



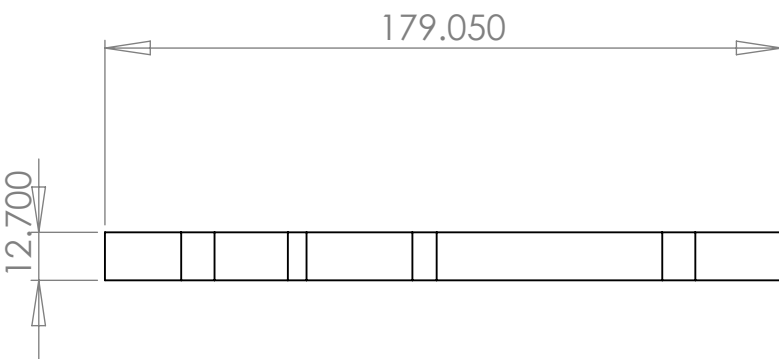
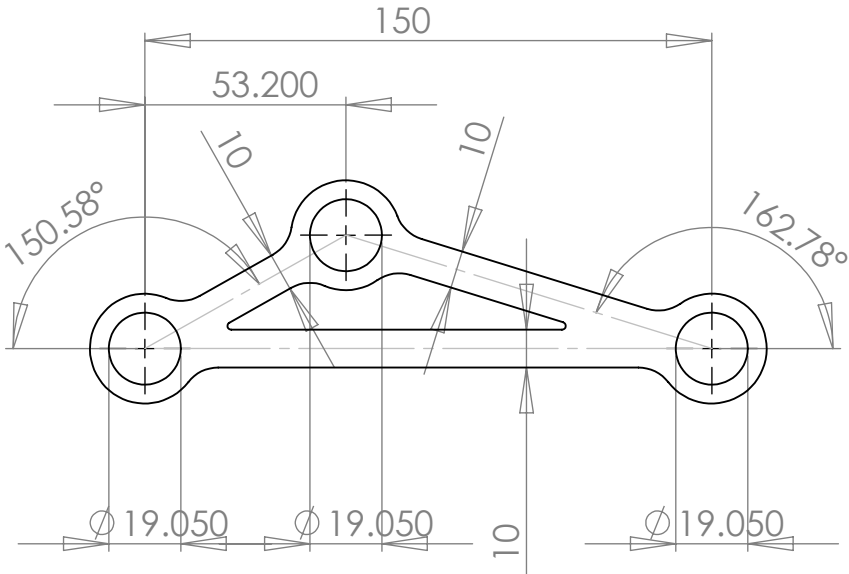
PROPRIETARY AND CONFIDENTIAL
THE INFORMATION CONTAINED IN THIS
DRAWING IS THE SOLE PROPERTY OF
KHAB ENGINEERING AND DESIGN. ANY
REPRODUCTION IN PART OR AS A WHOLE
WITHOUT THE WRITTEN PERMISSION OF
KHAB ENGINEERING AND DESIGN IS
PROHIBITED.

UNLESS OTHERWISE SPECIFIED:	KHAB ENGINEERING & DESIGN		
DIMENSIONS ARE IN INCHES TOLERANCES: ANGULAR: MACH \pm 0.1 TWO PLACE DECIMAL \pm 0.1 THREE PLACE DECIMAL \pm 0.01	TITLE: Rear Link, FE-XX-12		
INTERPRET GEOMETRIC TOLERANCING PER: ASME Y14.5-2009			
MATERIAL Glass Fiber Reinforced Polymer	SIZE	DWG. NO.	REV
FINISH AS SHOWN	A	FE-12-AR-002	A
DO NOT SCALE DRAWING	SCALE: 1:10 WEIGHT: SHEET 3 OF 15		

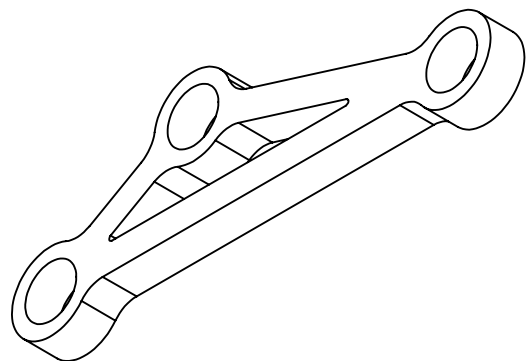
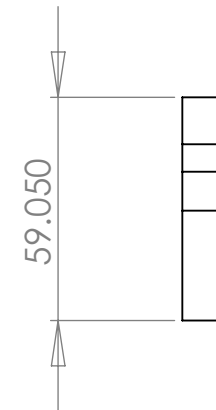


PROPRIETARY AND CONFIDENTIAL
THE INFORMATION CONTAINED IN THIS DRAWING IS THE SOLE PROPERTY OF Khab Engineering And Design, ANY REPRODUCTION IN PART OR AS A WHOLE WITHOUT THE WRITTEN PERMISSION OF Khab Engineering And Design IS PROHIBITED.

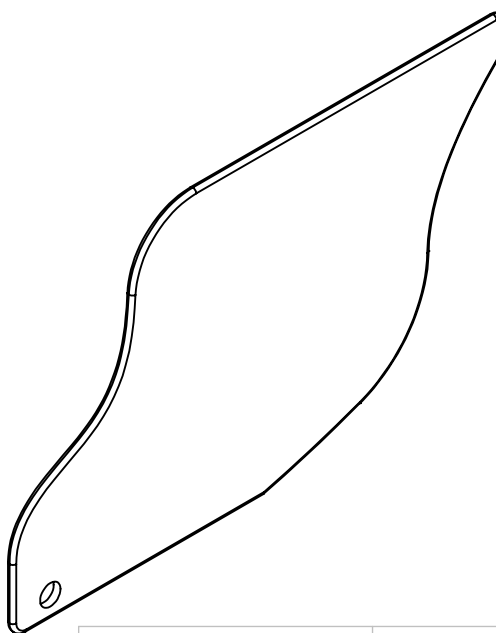
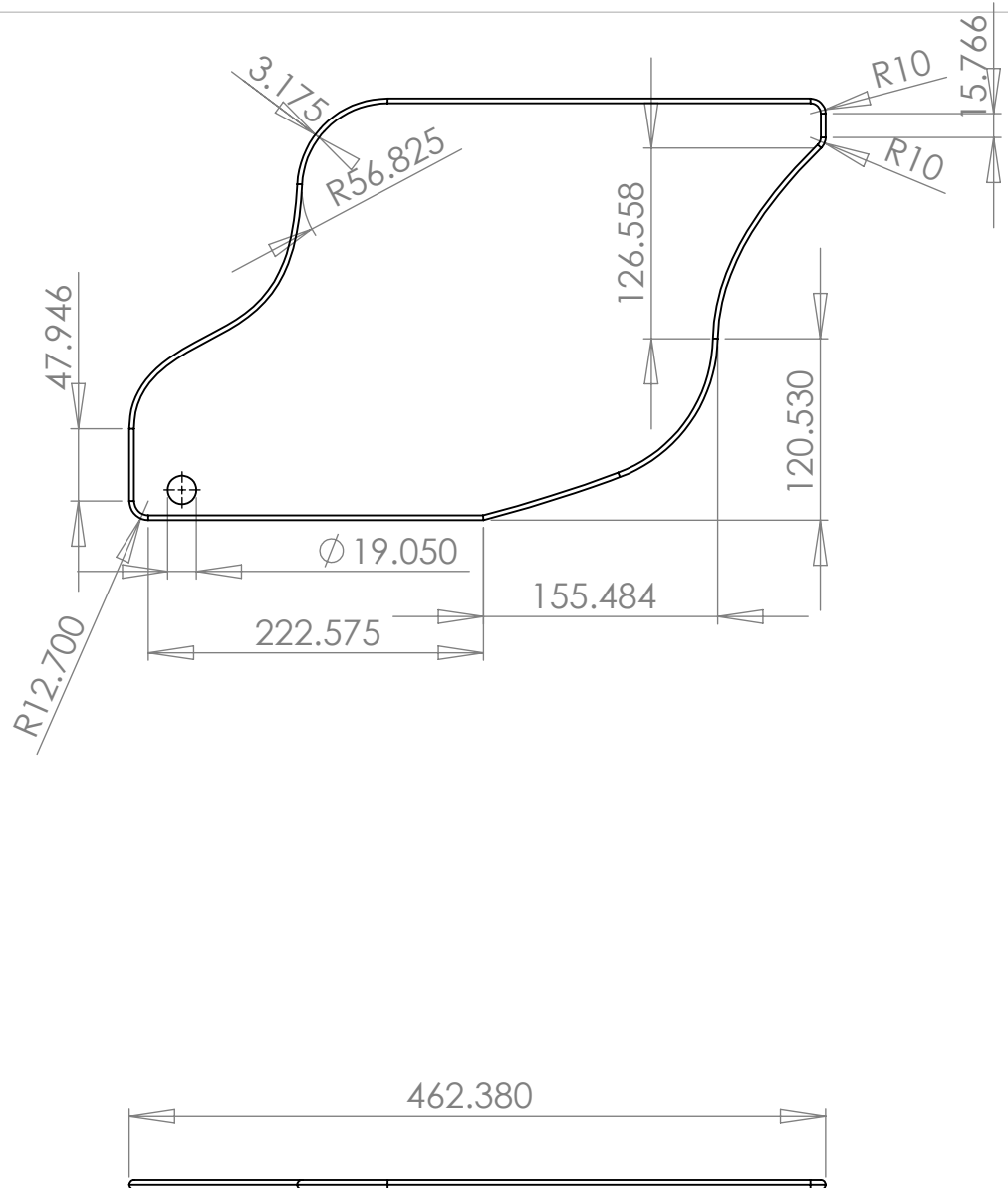
UNLESS OTHERWISE SPECIFIED:	Khab Engineering & Design		
DIMENSIONS ARE IN INCHES TOLERANCES: ANGULAR: MACH \pm 0.1 TWO PLACE DECIMAL \pm 0.1 THREE PLACE DECIMAL \pm 0.01	TITLE: Front Link, FE-XX-12		
INTERPRET GEOMETRIC TOLERANCING PER: ASME Y14.5-2009			
MATERIAL Glass Fiber Reinforced Polymer	SIZE	DWG. NO.	REV
FINISH AS SHOWN	A	FE-12-AR-003	A
DO NOT SCALE DRAWING	SCALE: 1:10		SHEET 4 OF 15



PROPRIETARY AND CONFIDENTIAL
THE INFORMATION CONTAINED IN THIS DRAWING IS THE SOLE PROPERTY OF Khab Engineering and Design, ANY REPRODUCTION IN PART OR AS A WHOLE WITHOUT THE WRITTEN PERMISSION OF Khab Engineering and Design IS PROHIBITED.



UNLESS OTHERWISE SPECIFIED:	Khab Engineering & Design		
DIMENSIONS ARE IN INCHES TOLERANCES: ANGULAR: MACH \pm 0.1 TWO PLACE DECIMAL \pm 0.1 THREE PLACE DECIMAL \pm 0.01	TITLE: Moving End Plate FE-XX-12		
INTERPRET GEOMETRIC TOLERANCING PER: ASME Y14.5-2009			
MATERIAL Glass Fiber Reinforced Polymer	SIZE	DWG. NO.	REV
FINISH AS SHOWN	A	FE-12-AR-004	A
DO NOT SCALE DRAWING	SCALE: 1:10 WEIGHT: SHEET 5 OF 15		



UNLESS OTHERWISE SPECIFIED:

DIMENSIONS ARE IN INCHES
TOLERANCES:
ANGULAR: MACH \pm 0.1
TWO PLACE DECIMAL \pm 0.1
THREE PLACE DECIMAL \pm 0.01

INTERPRET GEOMETRIC
TOLERANCING PER: ASME Y14.5-2009

MATERIAL
Glass Fiber Reinforced Polymer

FINISH
AS SHOWN
DO NOT SCALE DRAWING

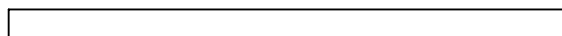
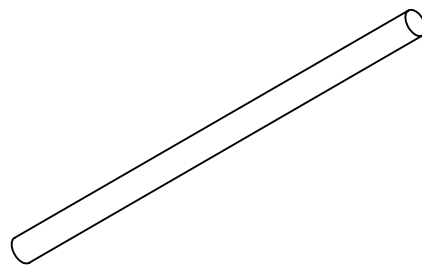
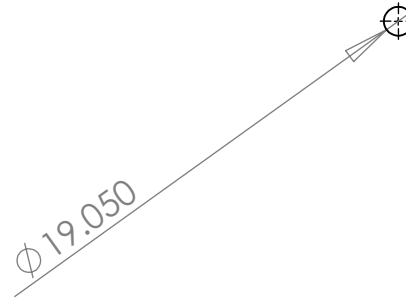
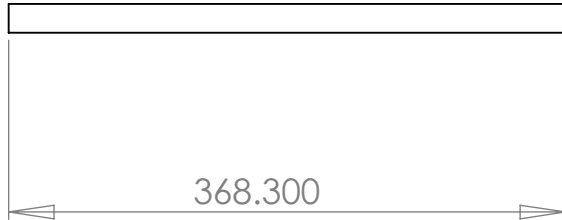
KHAB ENGINEERING & DESIGN

TITLE:
Outer End Plate
FE-XX-12

SIZE	DWG. NO.	REV
A	FE-12-AR-005	A
SCALE: 1:10 WEIGHT:		SHEET 6 OF 15

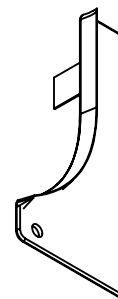
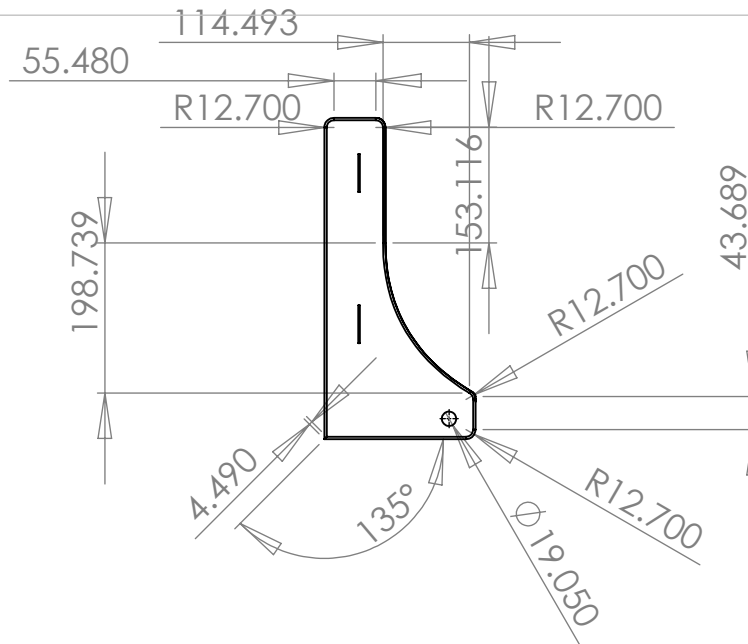
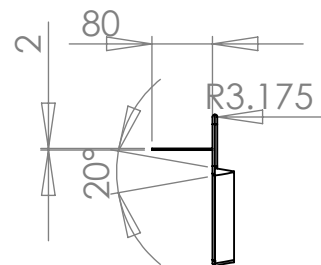
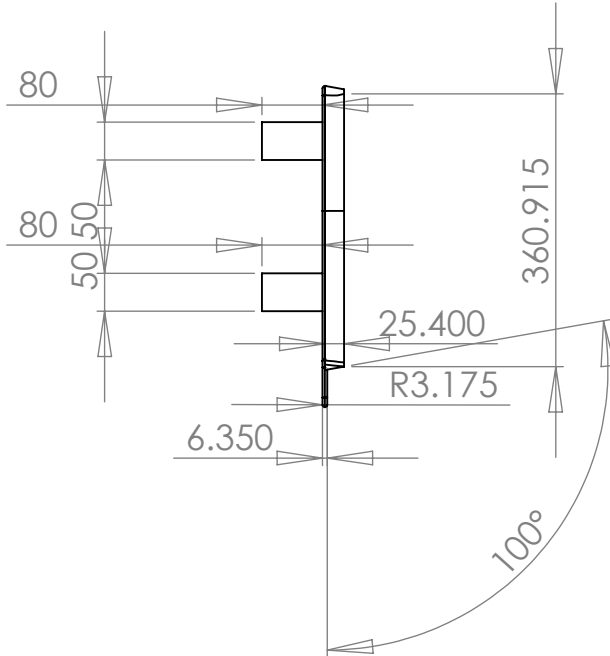
PROPRIETARY AND CONFIDENTIAL

THE INFORMATION CONTAINED IN THIS
DRAWING IS THE SOLE PROPERTY OF
KHAB ENGINEERING AND DESIGN. ANY
REPRODUCTION IN PART OR AS A WHOLE
WITHOUT THE WRITTEN PERMISSION OF
KHAB ENGINEERING AND DESIGN IS
PROHIBITED.

**PROPRIETARY AND CONFIDENTIAL**

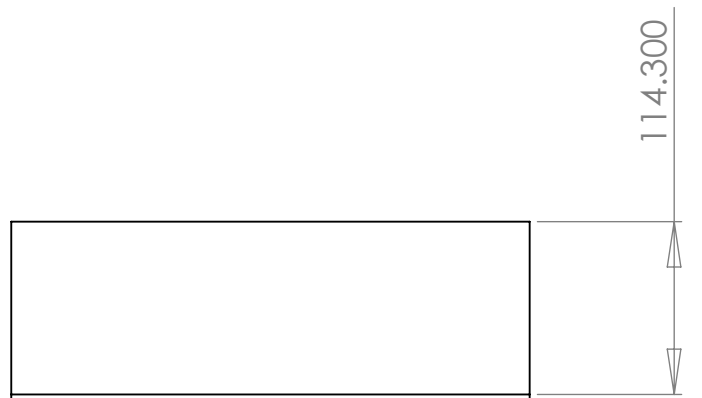
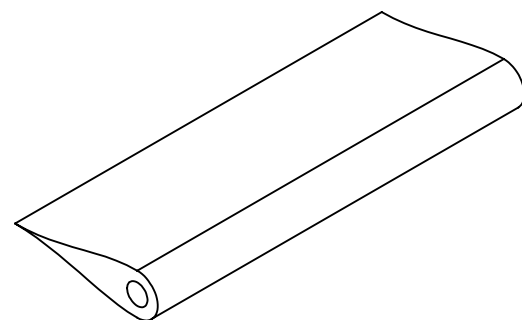
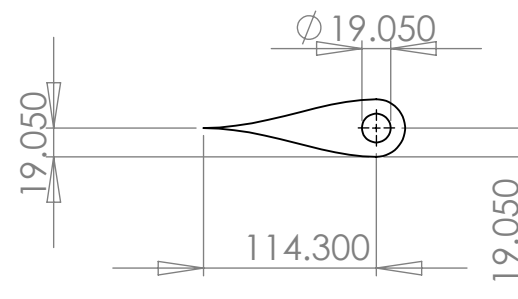
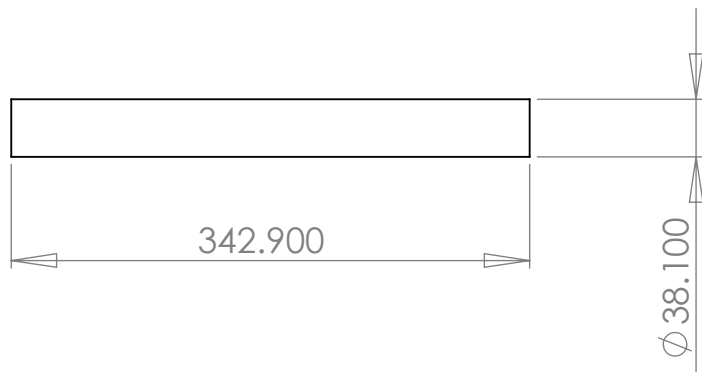
THE INFORMATION CONTAINED IN THIS DRAWING IS THE SOLE PROPERTY OF Khab Engineering And Design, ANY REPRODUCTION IN PART OR AS A WHOLE WITHOUT THE WRITTEN PERMISSION OF Khab Engineering And Design IS PROHIBITED.

UNLESS OTHERWISE SPECIFIED:	Khab Engineering & Design		
DIMENSIONS ARE IN INCHES TOLERANCES: ANGULAR: MACH \pm 0.1 TWO PLACE DECIMAL \pm 0.1 THREE PLACE DECIMAL \pm 0.01	TITLE: Control Rod FE-XX-12		
INTERPRET GEOMETRIC TOLERANCING PER: ASME Y14.5-2009			
MATERIAL Glass Fiber Reinforced Polymer	SIZE A	DWG. NO. FE-12-AR-006	REV A
FINISH AS SHOWN	DO NOT SCALE DRAWING	SCALE: 1:10	WEIGHT: SHEET 7 OF 15



PROPRIETARY AND CONFIDENTIAL
THE INFORMATION CONTAINED IN THIS DRAWING IS THE SOLE PROPERTY OF Khab Engineering and Design. ANY REPRODUCTION IN PART OR AS A WHOLE WITHOUT THE WRITTEN PERMISSION OF Khab Engineering and Design IS PROHIBITED.

UNLESS OTHERWISE SPECIFIED:	Khab Engineering & Design		
DIMENSIONS ARE IN INCHES TOLERANCES: ANGULAR: MACH \pm 0.1 TWO PLACE DECIMAL \pm 0.1 THREE PLACE DECIMAL \pm 0.01	TITLE: Inner Plate FE-XX-12		
INTERPRET GEOMETRIC TOLERANCING PER: ASME Y14.5-2009			
MATERIAL Glass Fiber Reinforced Polymer	SIZE	DWG. NO.	REV
FINISH AS SHOWN	A	FE-12-AR-007	A
DO NOT SCALE DRAWING	SCALE: 1:10 WEIGHT: SHEET 8 OF 15		



PROPRIETARY AND CONFIDENTIAL

THE INFORMATION CONTAINED IN THIS DRAWING IS THE SOLE PROPERTY OF Khab Engineering and Design, ANY REPRODUCTION IN PART OR AS A WHOLE WITHOUT THE WRITTEN PERMISSION OF Khab Engineering and Design IS PROHIBITED.

UNLESS OTHERWISE SPECIFIED:

DIMENSIONS ARE IN INCHES
TOLERANCES:
ANGULAR: MACH \pm 0.1
TWO PLACE DECIMAL \pm 0.1
THREE PLACE DECIMAL \pm 0.01

INTERPRET GEOMETRIC
TOLERANCING PER: ASME Y14.5-2009

MATERIAL
Glass Fiber Reinforced Polymer

FINISH

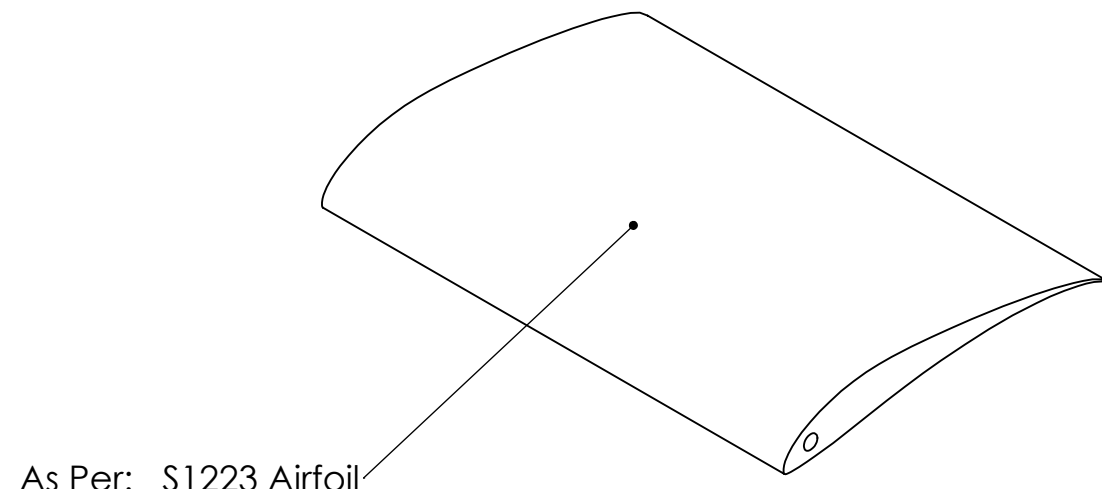
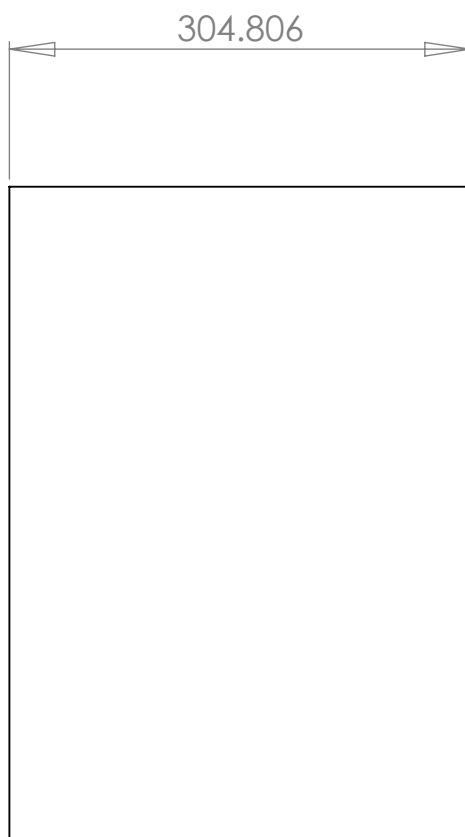
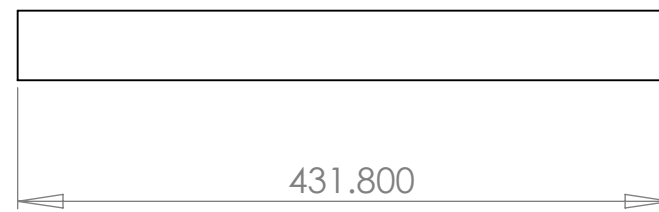
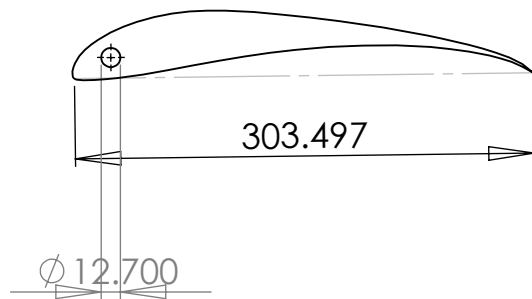
AS SHOWN

DO NOT SCALE DRAWING

Khab Engineering & Design
TITLE:
**Symmetric Airfoil
FE-XX-12**

SIZE	DWG. NO.	REV
A	FE-12-AR-008	A

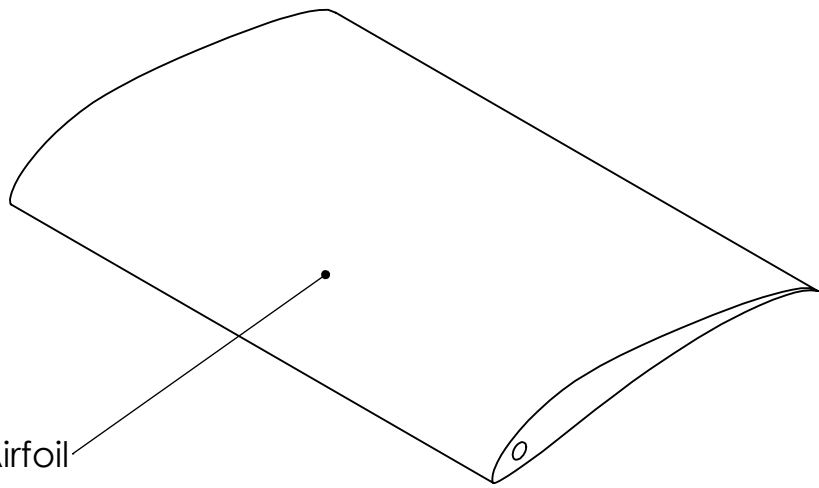
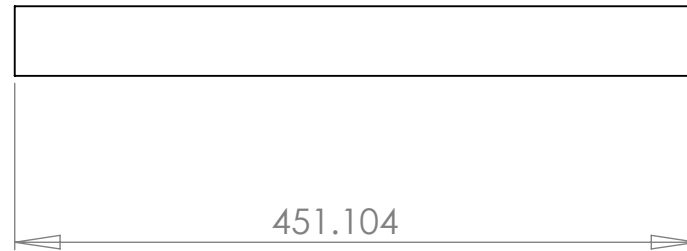
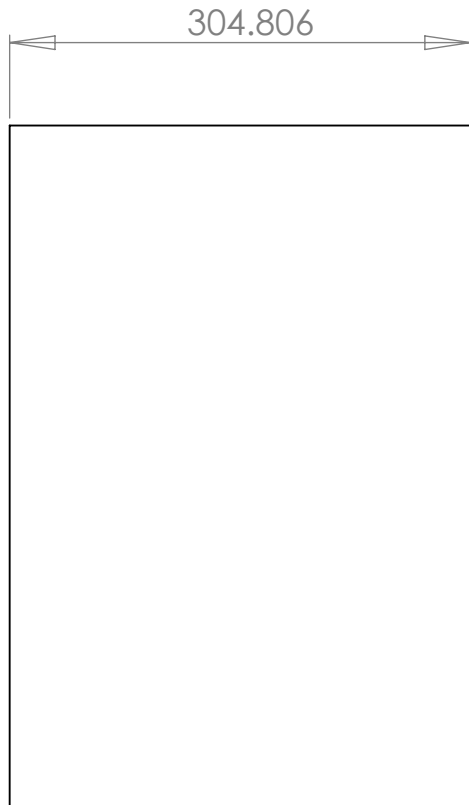
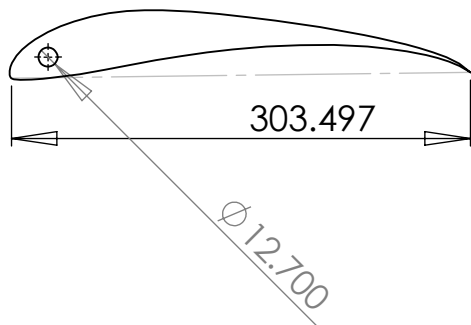
SCALE: 1:10	WEIGHT:	SHEET 9 OF 15
-------------	---------	---------------



As Per: S1223 Airfoil

PROPRIETARY AND CONFIDENTIAL
THE INFORMATION CONTAINED IN THIS DRAWING IS THE SOLE PROPERTY OF Khab Engineering And Design, ANY REPRODUCTION IN PART OR AS A WHOLE WITHOUT THE WRITTEN PERMISSION OF Khab Engineering And Design IS PROHIBITED.

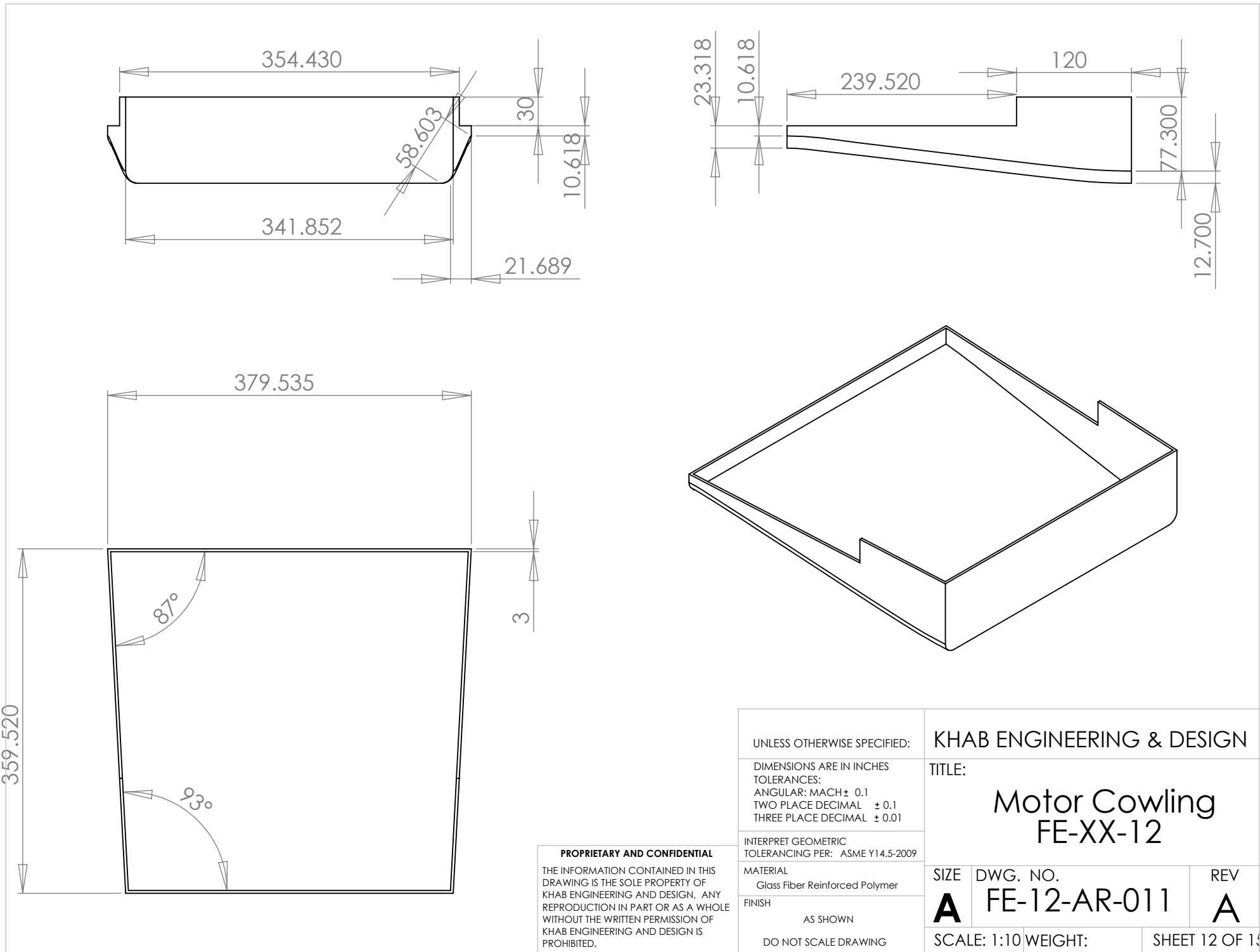
UNLESS OTHERWISE SPECIFIED:	Khab Engineering & Design		
DIMENSIONS ARE IN INCHES TOLERANCES: ANGULAR: MACH \pm 0.1 TWO PLACE DECIMAL \pm 0.1 THREE PLACE DECIMAL \pm 0.01	TITLE: S1223 Upper Airfoil FE-XX-12		
INTERPRET GEOMETRIC TOLERANCING PER: ASME Y14.5-2009			
MATERIAL Glass Fiber Reinforced Polymer	SIZE	DWG. NO.	REV
FINISH AS SHOWN	A	FE-12-AR-009	A
DO NOT SCALE DRAWING	SCALE: 1:10		WEIGHT: SHEET 10 OF 15

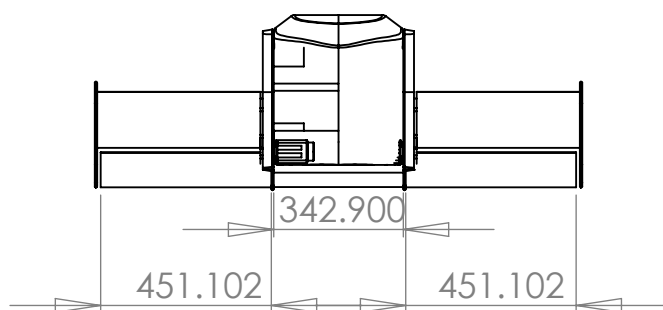
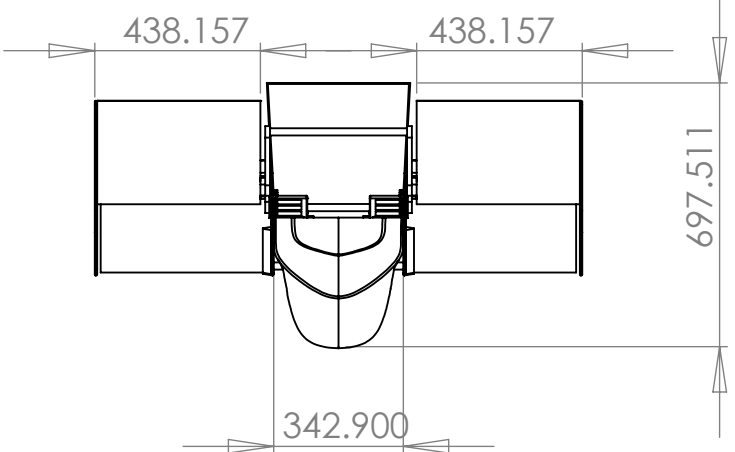
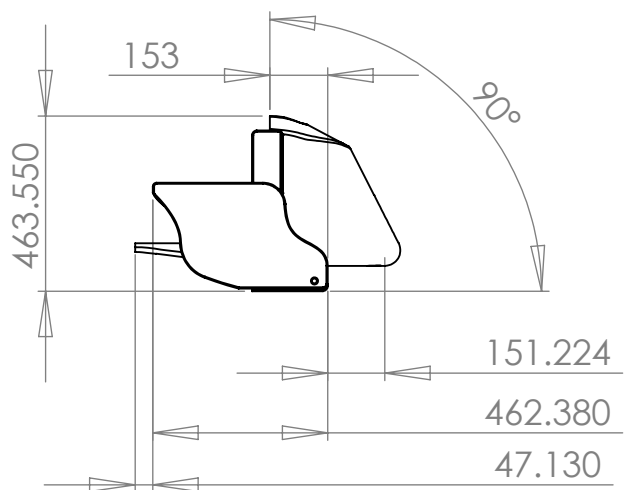
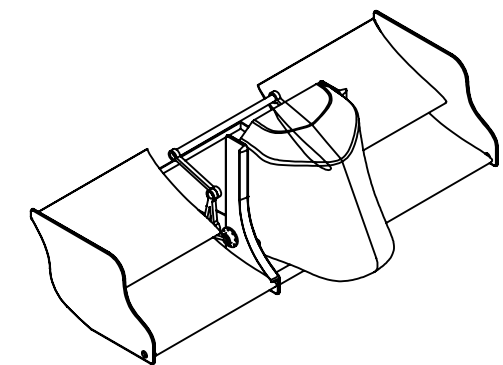


As Per: S1223 Airfoil

PROPRIETARY AND CONFIDENTIAL
THE INFORMATION CONTAINED IN THIS DRAWING IS THE SOLE PROPERTY OF Khab Engineering And Design, ANY REPRODUCTION IN PART OR AS A WHOLE WITHOUT THE WRITTEN PERMISSION OF Khab Engineering And Design IS PROHIBITED.

UNLESS OTHERWISE SPECIFIED:	Khab Engineering & Design		
DIMENSIONS ARE IN INCHES TOLERANCES: ANGULAR: MACH \pm 0.1 TWO PLACE DECIMAL \pm 0.1 THREE PLACE DECIMAL \pm 0.01	TITLE: S1223 Lower Airfoil FE-XX-12		
INTERPRET GEOMETRIC TOLERANCING PER: ASME Y14.5-2009			
MATERIAL Glass Fiber Reinforced Polymer	SIZE	DWG. NO.	REV
FINISH AS SHOWN	A	FE-12-AR-010	A
DO NOT SCALE DRAWING	SCALE: 1:10		SHEET 11 OF 15

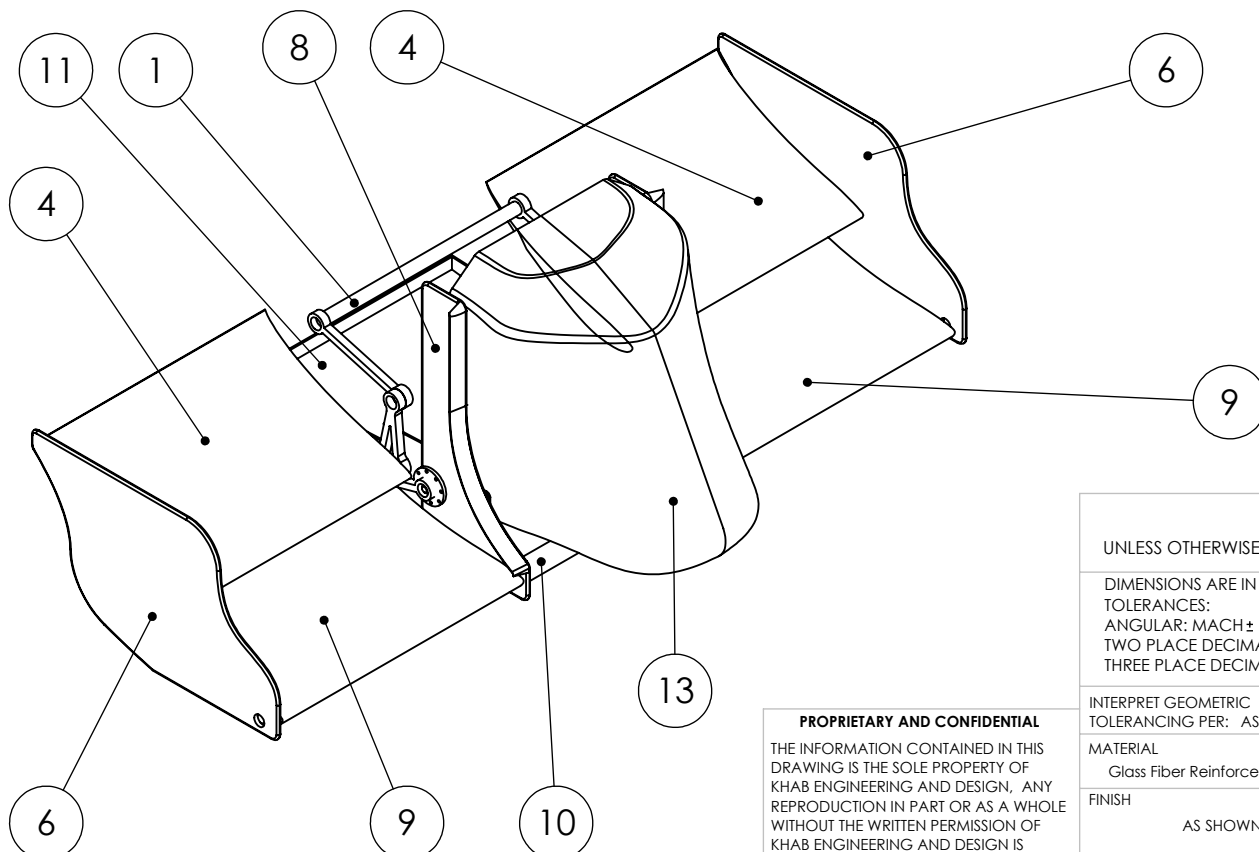




PROPRIETARY AND CONFIDENTIAL
THE INFORMATION CONTAINED IN THIS DRAWING IS THE SOLE PROPERTY OF Khab Engineering and Design. ANY REPRODUCTION IN PART OR AS A WHOLE WITHOUT THE WRITTEN PERMISSION OF Khab Engineering and Design IS PROHIBITED.

UNLESS OTHERWISE SPECIFIED:	Khab Engineering & Design		
DIMENSIONS ARE IN INCHES TOLERANCES: ANGULAR: MACH \pm 0.1 TWO PLACE DECIMAL \pm 0.1 THREE PLACE DECIMAL \pm 0.01	TITLE: Master Assembly FE-XX-12		
INTERPRET GEOMETRIC TOLERANCING PER: ASME Y14.5-2009			
MATERIAL Glass Fiber Reinforced Polymer	SIZE	DWG. NO.	REV
FINISH AS SHOWN	A	FE-12-AR-100	A
DO NOT SCALE DRAWING	SCALE: 1:10		SHEET 13 OF 15

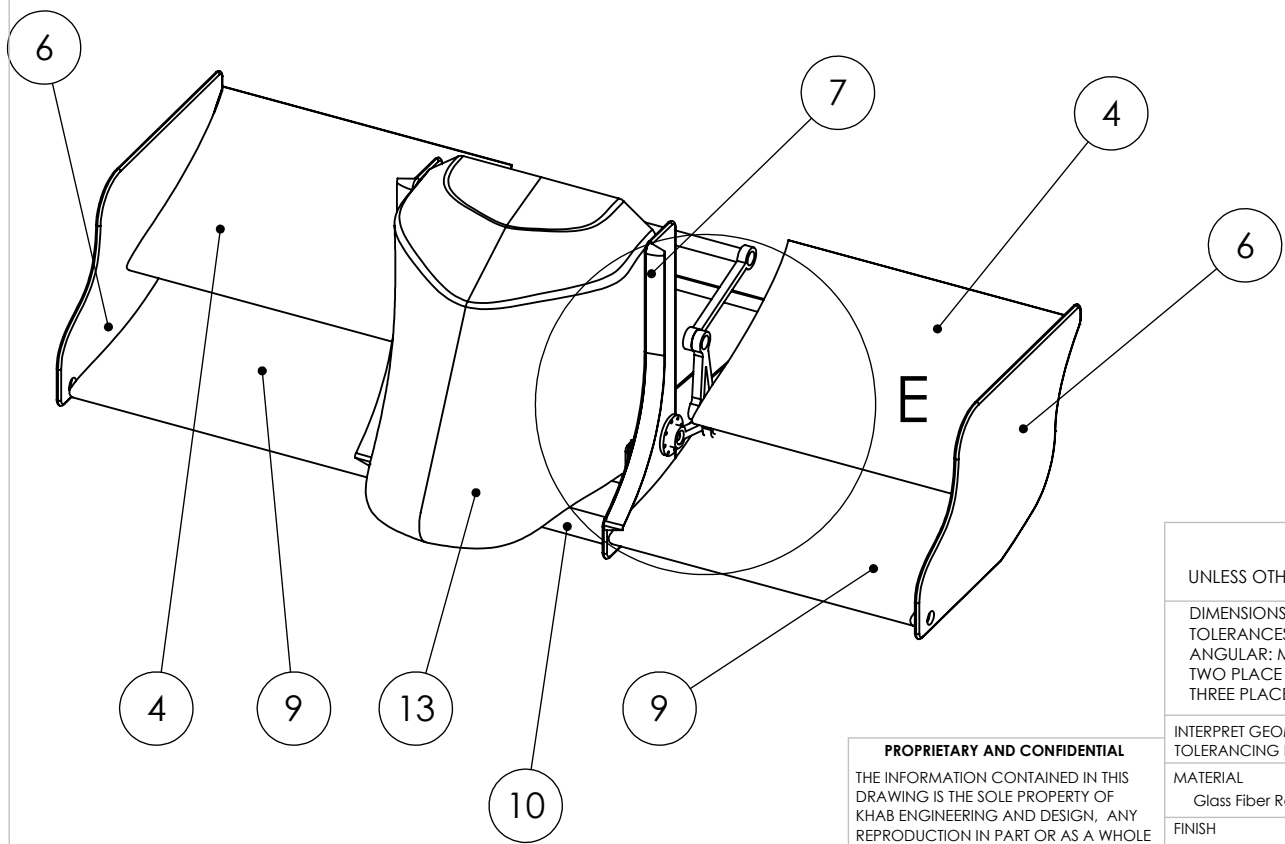
ITEM	PART NUMBER	DESCRIPTION	Default (1)/QTY.
1	FE-12-AR-006	Control Rod	3
2	FE-12-AR-003	Front Link	2
3	FE-12-AR-002	Rear Link	2
4	FE-12-AR-009	S1223 Upper	2
5	FE-12-AR-004	Moving End Plate	2
6	FE-12-AR-005	Outer End Plate	2
7	FE-12-AR-007A	Inner End Plate	1
8	FE-12-AR-007B	Innter End Plate	1
9	FE-12-AR-010	S1223 Lower	2
10	FE-12-AR-008	Symmetric Airfoil	1
11	FE-12-AR-011	Motor Cowling	1
12	FE-12-AR-012	Servo Actuator	2
13	FE-12-AR-001	Nose Cone	1



PROPRIETARY AND CONFIDENTIAL
THE INFORMATION CONTAINED IN THIS DRAWING IS THE SOLE PROPERTY OF Khab Engineering and Design, ANY REPRODUCTION IN PART OR AS A WHOLE WITHOUT THE WRITTEN PERMISSION OF Khab Engineering and Design IS PROHIBITED.

UNLESS OTHERWISE SPECIFIED:	Khab Engineering & Design		
DIMENSIONS ARE IN INCHES TOLERANCES: ANGULAR: MACH \pm 0.1 TWO PLACE DECIMAL \pm 0.1 THREE PLACE DECIMAL \pm 0.01	TITLE: Master Assembly FE-XX-12		
INTERPRET GEOMETRIC TOLERANCING PER: ASME Y14.5-2009	MATERIAL Glass Fiber Reinforced Polymer		
MATERIAL Glass Fiber Reinforced Polymer	SIZE A	DWG. NO. FE-12-AR-100	REV A
FINISH AS SHOWN	DO NOT SCALE DRAWING		
SCALE: 1:10		WEIGHT:	SHEET 14 OF 15

ITEM	PART NUMBER	DESCRIPTION	Default (1)/QTY.
1	FE-12-AR-006	Control Rod	3
2	FE-12-AR-003	Front Link	2
3	FE-12-AR-002	Rear Link	2
4	FE-12-AR-009	S1223 Upper	2
5	FE-12-AR-004	Moving End Plate	2
6	FE-12-AR-005	Outer End Plate	2
7	FE-12-AR-007A	Inner End Plate	1
8	FE-12-AR-007B	Inner End Plate	1
9	FE-12-AR-010	S1223 Lower	2
10	FE-12-AR-008	Symmetric Airfoil	1
11	FE-12-AR-011	Motor Cowling	1
12	FE-12-AR-012	Servo Actuator	2
13	FE-12-AR-001	Nose Cone	1



PROPRIETARY AND CONFIDENTIAL
THE INFORMATION CONTAINED IN THIS
DRAWING IS THE SOLE PROPERTY OF
KHAB ENGINEERING AND DESIGN, ANY
REPRODUCTION IN PART OR AS A WHOLE
WITHOUT THE WRITTEN PERMISSION OF
KHAB ENGINEERING AND DESIGN IS
PROHIBITED.

UNLESS OTHERWISE SPECIFIED:

DIMENSIONS ARE IN INCHES
TOLERANCES:
ANGULAR: MACH \pm 0.1
TWO PLACE DECIMAL \pm 0.1
THREE PLACE DECIMAL \pm 0.01

INTERPRET GEOMETRIC
TOLERANCING PER: ASME Y14.5-2009

MATERIAL
Glass Fiber Reinforced Polymer

FINISH
AS SHOWN

DO NOT SCALE DRAWING

KHAB ENGINEERING & DESIGN

TITLE:

Master Assembly
FE-XX-12

SIZE	DWG. NO.	REV
A	FE-12-AR-100	A

SCALE: 1:10 WEIGHT: SHEET 15 OF 15